HIGHLY POROUS POLY (HIPE) MATERIALS: SYNTHESIS AND CHARACTERIZATION

A Thesis submitted to the

UNIVERSITY OF PUNE

For the Degree of

DOCTOR OF PHILOSOPHY

In

CHEMISTRY

By

ABDUL WASIF ABDUL LATEEF SHAIKH

Research Guide

DR. S. PONRATHNAM

POLYMER SCIENCE AND ENGINEERING DIVISION,
NATIONAL CHEMICAL LABORATORY,
PUNE-411008, INDIA

NOVEMBER 2012

राष्ट्रीय रासायनिक प्रयोगशाला
(वैज्ञानिक तथा औद्योगिक अनुसंधान परिषद)
डॉ. होमी भाभा मार्ग, पुणे - 411 008. भारत
NATIONAL CHEMICAL LABORATORY
(Council of Scientific & Industrial Research)
Dr. Homi Bhabha Road, Pune - 411 008. India.

1950-2010 Celebrating Sixty Years of Science
हीरक जयन्ती वर्ष 2009-10

CERTIFICATE

Certified that the work incorporated in this thesis entitled "**Highly Porous Poly (HIPE) Materials: Synthesis and Characterization**" submitted by **Abdul Wasif Abdul Lateef Shaikh** was carried out by the candidate at National Chemical Laboratory, Pune- 411008, under my supervision. Such material as obtained from other sources has been duly acknowledged in this thesis.

November 2012
Pune

Dr. S. Ponrathnam
(Research Guide)

Dr. N. N. Chavan
(Co-Guide)

DECLARATION

I hereby declare that the thesis entitled **"Highly Porous Poly (HIPE) Materials: Synthesis and Characterization"** submitted for Ph.D degree to the University of Pune has been carried out at National Chemical Laboratory, Pune, India, under the supervision of Dr. S. Ponrathnam, Polymer Science and Engineering Division, National Chemical Laboratory, Pune-411008. The work is original and has not been submitted in part or full by me for any degree or diploma to this or any other university.

November 2012 **(Abdul Wasif Abdul Lateef Shaikh)**

Pune

Dedicated to,

My Family

(Abba, Ammi, Farhat Apa, Nikhat and Tauseef)

Acknowledgement

"Gratitude and affection sometimes cannot be expressed by mere words or sentences".

All praise to ***Almighty*** *the source of knowledge and wisdom within and beyond our comprehension and WHO bestowed His continuous boundless bounty upon me, blessed with courage of facing problems and obstacles, determination, and strength to complete this work.*

I feel very happy to express my sincere gratitude and appreciation to all the people whose direct or indirect contribution helped me during my research career.

My deepest gratitude goes first to my research guide ***Dr. S. Ponrathnam****. I am indebted to him for his guidance, encouragement, motivation, inspiration, support and patience like a guardian. Your insight and high standards are truly unforgettable. You shall definitely continue to be a source of motivation for my future work. I am extremely grateful to my co-guide,* ***Dr. N. N. Chavan*** *for all his support and encouragement throughout my research period.*

I would like to extend my thanks to ***Dr. Sourav Pal, Director, NCL*** *for allowing me to carry out research and extending all possible infrastructural facilities and permitting me to present this work in the form of a Ph.D. thesis*

My deepest and sincere thanks go to ***Dr. C. R. Rajan****. He was always there for me. I learnt a lot from him. His meticulous approach to a problem was splendid. Working with him was always a pleasure. I thank* ***Dr. D. R. Saini*** *and* ***Dr. M. S. Qureshi*** *for all their valuable discussions and support. I am thankful to* ***Dr. S. S. Tambe*** *for helping me with all his expertise in modeling the kinetics data. I thank* ***Dr. Smita Mule*** *for her constant support. I feel very happy to say thanks to* ***Mr. Sunil Bhongale*** *for his fruitful discussions and help in GC analysis and for being a very good friend. My sincere gratitude extends to* ***Dr. Steve Merrigan (P&G, USA)*** *for his enlighten discussion and joyful company.*

I am extremely indebted and thankful to my Masters supervisor ***Dr. Prof. S. V. Lonikar*** *for his support and helpful discussion throughout the time spent with him during my Masters course and thesis work. I like to thank* ***Dr. N. N. Maldar*** *for his constant support during my Masters course. I am extremely thankful to* ***Dr. R. A. Kulkarni*** *who was very generous and kind to me during my initial years at NCL. More than a supervisor, he helped me a lot by his constant support and friendship. Sir, thank you for everything. I would like to extend my thanks to* ***Dr. (Mrs.) A. N. Bote*** *and* ***Mrs. D. A. Dhoble*** *for their invaluable support.*

I am very lucky to accompany and work with some of the people who are such a wonderful colleagues and friends too. To begin with, I am sincerely indebted and thankful to ***Sarika Deokar*** *for her invaluable support and companionship extended to me at every stage of my research and thesis. I am extremely thankful to* ***Dr. R. Harikrishna*** *for his support and*

companionship extended to me throughout my research career. I feel very happy to thank ***Dr. Ganesh Ingavle*** *and* ***Dr. N. S. Pujari*** *for their friendship, support and help to extend my research career. I am thankful to* ***Khudbuddin Mulani***, ***Ravi Ghorpade*** *and* ***Mohasin Momin*** *for being a very good colleagues and friends as well. I also extend my thanks to* ***Mr. John Aruldoss***, *for all his support during the project and sharing good companionship. I really enjoyed the company of* ***Mr. Abhijit Jadhav***, *who is such a wonderful friend and a nice colleague too. I like to thank* ***Mr. Sunny Scaria*** *and* ***Mr. Timothy Ponrathnam***, *I miss all the great time spent with them. I also extend my sincere thanks to* ***Mr. S.N. Sathe*** *and* ***Mr. Lalan Giri*** *for helping me technically and personally during my thesis work.*

I like to thank ***Mr. Punitharasu***, ***Mr. Bhupesh Rajurkar*** *and* ***Mr. Samarth Vaidya*** *for their help in kinetics and modeling studies.*

I would like to extend my thanks to my colleagues ***Mr. Kishore Rajdeo***, ***Ms. Sonali Bhosale***, ***Mrs. Archana***, ***Mr. Sachin Mane***, *for their help and cooperation.*

My sincere thank goes to all my friends, one of the biggest assets of life. I always enjoyed their company and all were there for me at every stage. I would like to thank ***Samir Chikkali***, ***Tanveer Shaikh***, ***Amit Kulkarni***, ***Suleman Inamdar***, ***Mahesh Kulkarni***, ***Ravi Potrekar***, ***Mohan Wadikar, Jabeen and Imtiaz Tamboli***, ***Shahed Parvez***, ***Gaffar Mulla***, ***Ilyas Shaikh, Imran Khan and Javed Shaikh***. *I would also like to thank* ***Sandeep Kothawade***, ***Hamid Shaikh***, ***Chandrashekhar Kulkarni***, ***Abhijit Purude***, ***Vivek Kothgire***, ***Rakesh Singh, Harshad Chavan and Yogesh Karade*** *whose company also I enjoyed a lot.*

*Last, but not least, I thank my family. I thank my father****, Mr. Abdul Lateef*** *and my* ***mother***, *for being such a wonderful parents. They have been always the source of inspiration and the biggest gift to me from* ***Almighty***. *I thank them for all their love, support, educating me with aspects from both social and personal life with all the difficulties, for unconditional support to pursue my interests, for patience and for believing in me. I am extremely lucky to I have sisters like* ***Farhat Apa*** *and* ***Nikhat*** *and brother* ***Tauseef.*** *I thank all for their love, immense support and constant encouragement and believing in me. I would like to thank my Uncle,* ***Mr. Jabbar Shaikh***, *who has been constantly supporting me since my childhood, encouraged me to pursue my career in a better way. I feel lucky to have elder brother like* ***Manzoor Ahmed*** *who was always with me with all his love and has been a source of inspiration for me. I would like to thank him for constantly supporting me and extending lots of love and friendship to me. I extend my love to my cousin* ***Noaman*** *and niece* ***Saba;*** *their presence and love always made my life enjoyable. I extend my thanks to all the relatives and friends for their love and support.*

I would also like to acknowledge the financial support received from CSIR in the form of Senior Research Fellowship, without which this research would not have been possible.

CONTENTS

Sr. No. **Chapter - IV** **Page No.**

Synthesis and morphological studies of styrene based polyHIPEs

Sr. No.	**Chapter - VI**	**Page No.**
	Summary and conclusions	

List of Figures

Figure No.	**Chapter - V**	

List of Tables

Abbreviations

HIPE	High internal phase emulsion
HLB	Hydrophile-lipophile balance
PIT	Phase inversion temperature
Tg	Glass transition temperature
CLD	Crosslink density
LCST	Lower critical solution temperature
RDH	rhomboidal dodecahedral
TKDH	tetrakaidecahedral
O/W	Oil in water
W/O	Water in oil
O/O	Oil in oil
Arquad 2HT-75	di(hydrogenated tallow alkyl) dimethyl ammonium chloride
Span 80	Sorbitan monooleate
Span 85	Sorbitan trioleate
Span 20	Sorbitan monolaurate
Tween 20	Polyoxyethylene sorbitan monolaurate
Tween 80	Polyoxyethylene sorbitan monooleate
Brij 30	Polyoxyethylene (4) lauryl ether

Brij 35	Polyoxyethylene (23) lauryl ether
AOT	Aerosol-OT
CTAB	Cetyl trimethylammonium bromide
Triton X-405	Polyoxyethylene (40) isooctyl phenyl ether
EHA	2-Ethylhexyl acrylate
EHMA	2-Ethylhexyl methacrylate
EGDMA	Ethylene dimethacrylate
STY	Styrene
DVB	Divinyl benzene
AN	Acrylonitrile
HEMA	Hydroxylethyl methacrylate
HEA	Hydroxyethyl acrylate
GMA	Glycidyl methacrylate
APS	Ammonium persulphate
KPS	Potassium persulphate
NaPS	Sodium persulphate
ASA	Ascorbic acid
AIBN	Azobis-isobutronitrile
NaCl	Sodium chloride
$CaCl_2$	Calcium chloride
$CdCl_2$	cadmium chloride

CdS	cadmium sulphide
Cr (VI)	Chromium (VI)
MEHQ	monomethyl ether hydroquinone
PTZ	Phenothiazine
LM	Levenberg Marquadt
MATLAB	MATrix LABoratory
RK	Runge-Kutta
IR	Infra red
SEM	Scanning electron microscopy
OM	Optical microscopy
BET	Brunner Emmet Teller
EDX	Energy dispersive spectroscopy
GC	Gas chromatography
XRD	X-Ray Diffraction
DMA	Dynamic mechanical analyzer
UV	Ultra-violet
k_d	Dissociation constant
$t_{1/2}$	Half life
k_p	Rate constant
R_p	Rate of polymerization
Ea	Energy of activation

A	Pre-exponential factor
R	Universal gas constant
T	Absolute temperature

Highly Porous Poly (HIPE) Materials: Synthesis and Characterization

Abstract

This study investigated the synthesis of various porous polyHIPE materials based on monomers like acrylate, methacrylate, styrene and acrylonitrile. The thesis work has been divided into six chapters covering all the aspects of the synthesis of various polyHIPEs, morphological studies, polymerization kinetics and utilization of some polyHIPEs for their efficiency to adsorb metal ions and summary and conclusions.

A high internal phase emulsion (HIPE) is an emulsion in which the dispersed phase occupies more than 74% of the volume of the emulsion. A continuous monomer phase can be polymerized to yield a low-density foam, a polyHIPE, following the removal of the dispersed phase. An outstanding feature of polyHIPEs is their high void fraction in combination with an open and accessible macroporosity resulting from the use of high internal phase emulsions (HIPEs) as templates. Oil-in-water (O/W) as well as water-in-oil (W/O) emulsion systems for the preparation of polyHIPEs have been described (the first phase mentioned refers to the continuous phase and the second phase is known as the internal (or droplet) phase). Polymerization of the continuous phase of the emulsion in the presence of a crosslinking agent allows to freeze its structure and to remove the droplet phase without structural collapse. The dried material shows open interconnecting porous morphology with increased pore volume even though surface areas usually tend to be moderate due to the large size of the voids. PolyHIPEs with open-cell morphology have demonstrated advantageous structural properties and liquid absorbency, prompting their use as absorbents, in ion exchange systems, tissue scaffolds and as heat resistant structural foams.

Morphological properties of acrylate based polyHIPEs were investigated and the effect of comonomers on the stabilization of HIPE emulsions were studied. The effect of type and concentration of initiator, salt and porogen on the formation and stability of HIPE were noted. Increase in salt concentration and presence of water soluble polymers

in the aqueous discontinuous phase leads to the formation of soft and elastic polymers. Interplay of compositions resulted in variations in yield stress values.

The effect of pH, temperature, concentration of initiator and inhibitor on the rate of HIPE polymerization was noted and a kinetics protocol was established. A general trend of increase in rate of polymerization with increase in concentration of initiator was observed. A phenomenological model was proposed for analyzing the kinetics of polymerization carried out at varying concentration of initiator and inhibitor at three different temperatures. From the phenomenological model, the rate parameters as well as activation energy were calculated using Runge-Kutta method. The modeled data had high proximity towards experimental data.

PolyHIPEs were prepared with Arquad 2HT-75, Span 20 and Span 80 as surfactant with oil: water ratio above 1: 15. Least stability of HIPE formation was observed below oil: water ratios of 1: 5 as observable from the morphology of the prepared polyHIPEs. More open cell structure was obtained in polyHIPEs synthesized using oil: water ration above 1: 10. The pores generated can be used as templates for synthesis of cadmium sulphide particles. Styrene-divinylbenzene(DVB) polyHIPEs containing cadmium chloride monoliths using high internal phase emulsion methodology were prepared using two different strategies. $CdCl_2$ was embedded in the polyHIPE matrix by both ways before and after polymerization. The cadmium chloride was then converted into cadmium sulphide by treating it with sodium hydroxide followed by sodium sulphide. XRD patters provide insight into the presence of CdS particle in the matrix.

Functional group present in the polymer is the basic requirement for the polymer to be hydrophobic or hydrophilic in nature. Acrylonitrile-divinylbenzene (AN-DVB) porous polymers were synthesized using HIPE templating. Formation stable copolymeric polyHIPEs were studied using various classes of non-ionic surfactants and the variations in stability and morphology were investigated. The nitrile group present was converted to amidoxime functionality and the modified amidximated polyHIPEs were evaluated for chelation Cr(VI) metal ion at various conditions.

CHAPTER - I

Introduction

1.1 Porous polymers

Porous materials are currently of great scientific as well as technological interest. Classically porous materials are in the form of organic materials, inorganic materials, polymeric foams, porous polymers etc. A large number of porous materials have been developed for insulation, cushioning, impact protection, catalysis, membranes, construction materials etc. Materials having different pore sizes (from nanometer to millimeter) have been developed. The order of the pores in the material is either regular or irregular depending upon the method of formation. Different preparative approaches have been employed to synthesize different types of porous structures such as suspension, high internal phase emulsion, foaming, phase separation, imprinting or templating methods.

Porous polymers are attracting much interest as a result of their applications (both real and potential) in many areas of advanced materials science. The applications include as low dielectric constant substrates for use in the microelectronics industry,[1] scaffold for tissue engineering,[2] 3D cell culture,[3-5] supports for catalysts,[6] polymers for separation processes, and as templates for the production of porous inorganic materials. Porous polymers come in many formats, including particles (often known as beads), membranes, films and monoliths. Non-particulate formats can be prepared using a wide variety of methods, which can nominally be separated into templating[7] and non-templating approaches. Typical porous polymers in various forms are depicted in Figure 1.1.

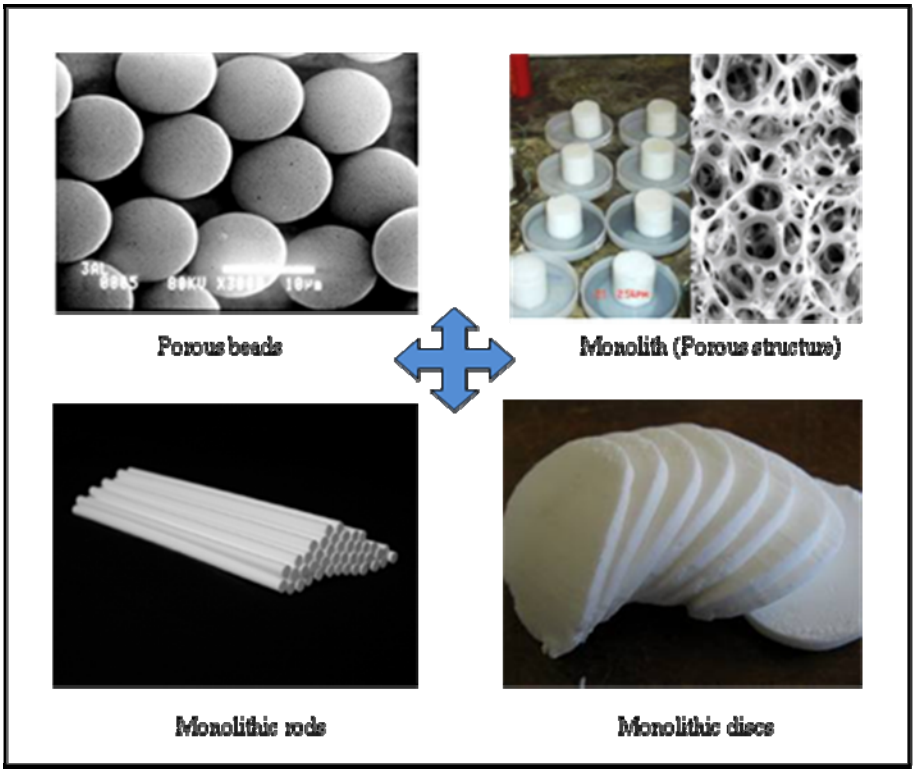

Figure 1.1 : Porous polymers in beads and monolithic form

The present thesis covers the work focusing on the synthesis of porous polymeric monoliths using novel high internal phase emulsion (HIPE) templating approach. Synthesis of polymeric monoliths based on various monomeric systems was carried out and the studies were conducted on their morphological properties, polymerization kinetics and post modification of functional groups present in the polymer matrix.

1.1.1 Porous polymers using templates

A modern approach that is increasingly employed to prepare highly porous and well-defined porous polymers is emulsion templating. Here the droplets (dispersed phase) of the emulsions are used to create pores in a solid material by curing or polymerization of the emulsion continuous phase resulting in the formation of porous polymer structures. Depending upon the nature of emulsion composition employed, the

characteristic domain size of the porous network can range from few nanometers to hundreds of micrometers.

1.2 Templating methods

Templating methods involve solidifying a two-phase mixture of porogen (the template) and polymer precursor, then removing the porogen to leave behind pores.[8] Specific examples of this so called 'endo-templating' approach include salt crystal and other particulate leaching, microemulsion and emulsion templating. On the other hand, a non-templating process begins with a single phase liquid system that undergoes phase separation at some point, yielding a solid matrix and a fluidic 'porogen'. Removal of the porogen leaves behind a porous material. Examples of non-templating methods for the preparation of porous polymers include thermally induced phase separation (TIPS), phase separation during crosslinking, gas blowing and directional freezing.

1.2.1 Emulsion templating

Emulsion templating methods represent an attractive route to highly porous polymeric materials termed as "monoliths" with well-defined porosity and pore structure. The process has been known since 1960s[9] was further developed extensively by workers at Unilever in the 1980s[10] and in recent years has seen increased interest from both academia and industry.

1.2.1.1 *Emulsions*

Emulsions are colloidal systems made of liquid droplets dispersed in another liquid phase. They are produced by shearing these two immiscible liquids, which

provides necessary energy to reach a metastable state through fragmentation of one phase into other.[11] An emulsion is often described as either oil-in-water (O/W) or water-in-oil (W/O) where the first phase mentioned refers to the internal (or dispersed) phase. At the early stages in the field of emulsion the volume fractions of oil and water were not so important, and that the emulsion type and stability were determined primarily by the nature of the surfactant. There is an important cornerstone guiding practical emulsion formulation: the Bancroft rule,[12] which states that the liquid in which the surfactant is predominantly dissolved would form the external or continuous phase. Generally, emulsions have average droplet sizes of at least several micrometers and the droplets have a rather broad size distribution unless special procedures are adopted (e.g. fractionation of the emulsion). Emulsions have been investigated extensively for decades and are used in a range of common practical applications in many industries, such as pharmaceutical, cosmetic, papermaking, food and agriculture. The definition of emulsion varies in literature depending on its application. However, Becher[13] defined emulsion as; "an emulsion is a heterogeneous system, consisting of at least one immiscible liquid intimately dispersed in another in the form of droplets, whose diameters, in general exceed 0.1 microns. Such systems possess a minimal stability, which may be accentuated by additives such as surface-active agents and finely divided soils."

The minimal stability of the emulsion system is attributed to an increased surface free energy, which accompanies the emulsification process. The surface-active agents, which are added to an emulsion to increase its stability by lowering the interfacial tension at the interface are known as surfactants. There is also a distinction between the

types of emulsions based on rheological properties. An emulsion, which is transparent, thermodynamically stable, and has a small particle size (5-100 nm), is known as micro-emulsion, whereas an opaque and kinetically stable emulsion with a larger particle size (200-10000 nm) is termed a macro-emulsion or simply an emulsion. Micro-emulsion has a much longer shelf life than macro-emulsion because of their thermodynamic stability. The stability is dependent on the interfacial tension at the interface, more the interfacial tension less is the stability and vice versa. The formation of emulsions is caused by the dispersion of droplets of the two immiscible liquids into one another. This leads to increase in interfacial tension and the accompanying free energy make the system thermodynamically unstable. The presence of the surfactant helps to stabilize the emulsion by reducing the interfacial tension at the interface of both the liquids. It also reduces the rate of coalescence of the dispersed liquid droplets by forming mechanical, steric and/or electrical barriers around them. The steric and electrical barriers prevent the droplets from getting too close enough to coalesce. The mechanical barrier increases the resistance to coalescence up on shock or shear.[14]

1.2.1.2 *Surfactant and HLB value*

Surfactant is an abbreviation for surface-active agents, which literally means active at a surface. In other words, a surfactant is characterized by its tendency to adsorb at the surface and interfaces. The term interface denotes a boundary between any two immiscible phases; the term surface indicates that one of the phases is a gas, usually air. Surfactant molecules adsorb and orient themselves in different ways depending upon the environment. Figure 1.2 shows few possible orientations of surfactant molecules at the interface.

Surfactants are known by their characteristic physical property i.e. termed as the hydrophile-lypophile balance (HLB). HLB is a relative ratio of polar and non-polar groups in the surfactant.[15] The HLB system for selecting suitable surfactants to stabilize emulsions has been in use now for many decades. It developed initially from observations by Griffin[16-18] that the efficiency of blends of hydrophilic and lipophilic non-ionic surfactants as emulsifiers for particular oil was at a maximum when the blends contained similar weight percentages of hydrophilic material. It was concluded that, "HLB value is a function of the weight percentage of the hydrophilic portion of the molecule of a nonionic surfactant". Several analytical procedures have been proposed for determining the HLB of surfactants and their blends. However, they all suffer from the disadvantage that the surfactants are examined in isolation from the practical environment so that the data are of dubious value.

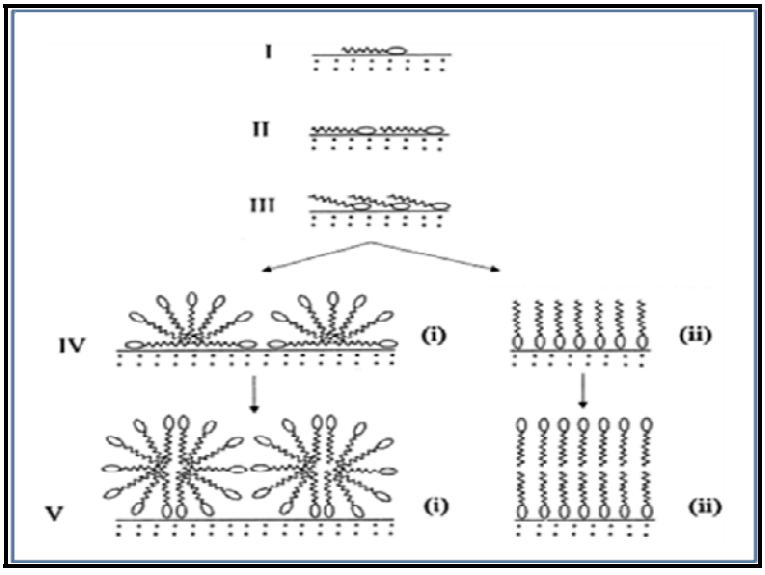

Figure 1.2 : Adsorption of non-ionic surfactants and orientation at the interface on hydrophilic adsorbents: (I) initial interaction of surfactant molecule with the surface; (II) monolayer coverage by the surfactant; (III) displacement of hydrophobic group of surfactant; (IV) (i) hemi-micelle adsorption, (ii) vertical adsorption of the surfactant; and (V) (i) micelle adsorption, (ii) bilayer adsorption. [19]

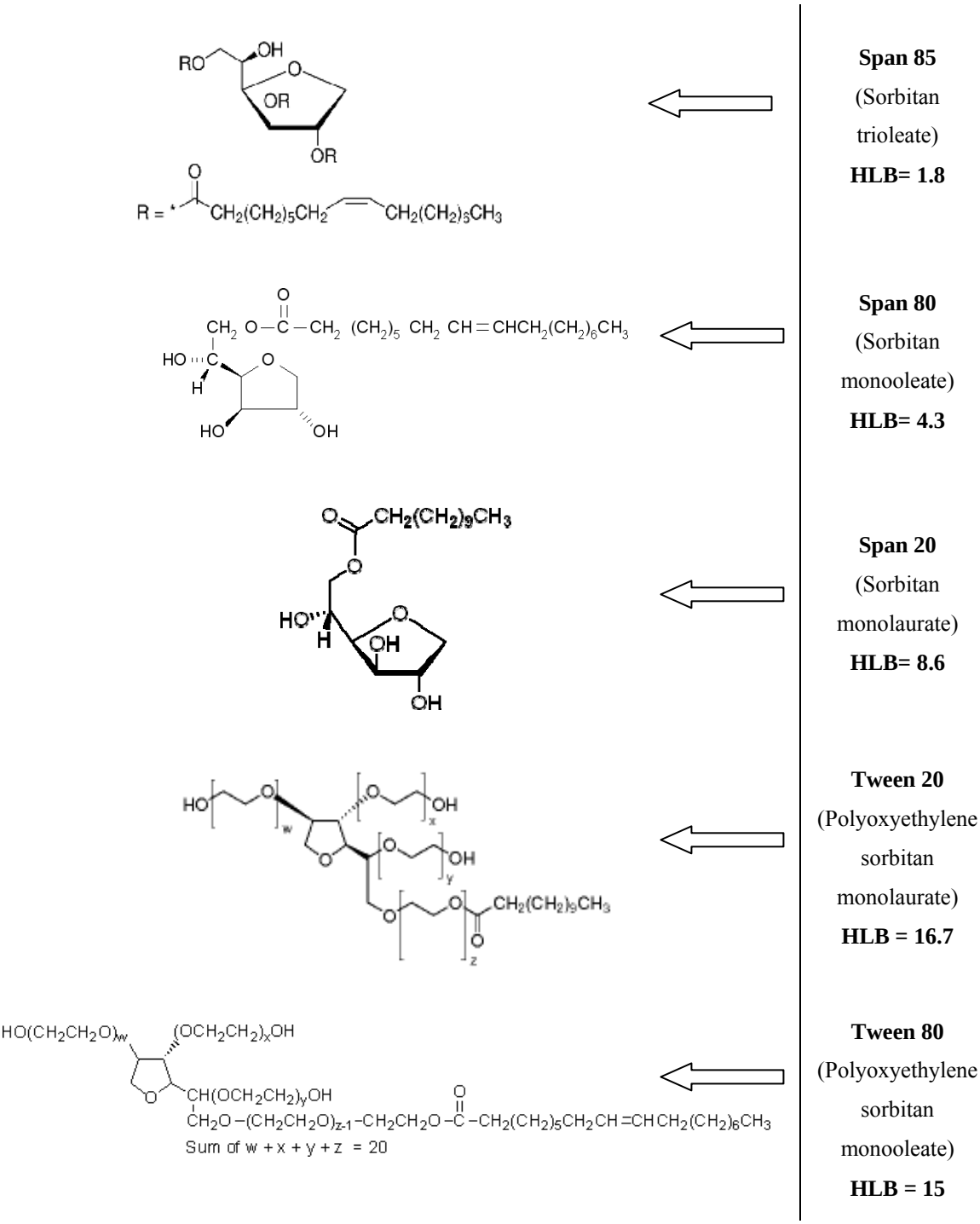

Figure 1.3 : Non-ionic surfactants with different HLB values

Shinoda[20] highlighted the difficulties in evaluating meaningful HLB's when he pointed out that this concept depends upon the balance of emulsifier at the oil-water

interface, and in addition, HLB would depend on the nature of the oil phase and on the additives in both the phases. Temperature is also important since it would influence the interaction between the aqueous phase and the hydrophilic groups of the emulsifiers, and between the oil phase and the lipophile groups. Figure 1.3 shows the structure of few non-ionic surfactants with their HLB values.

Griffin proposed a theory that emulsifying agents contain oil-loving (hydrophobic) and water-loving (hydrophilic) groups. It is the balance of the size and the strength of these groups that is referred to as HLB. An emulsifier or surfactant that is hydrophobic in character is assigned a low HLB value (below 9) and one that is hydrophilic is assigned a high HLB value (above 11). Those in the range of 9-11 are intermediates. The HLB of a surfactant or blend of surfactants is an excellent indication of what the surfactant system will do whether it will form an oil-in-water emulsion or a water-in-oil emulsion or even act as a solubilizer for some oil.

The efficiency of the surfactant is related to the chemical structure that can be related to the chemical structure of the material to be emulsified. The HLB value allows blending of two surfactants in order to achieve the exact HLB needed. The blend can be adjusted to suit the oil or other active ingredients. The most stable emulsion system usually consists of blends of two or more surfactants where one has lipophilic tendencies and the other has hydrophilic tendency. The chemical type is related to the chemical family of the surfactant. For example, a polyoxyethylene sorbitan oleate ester type of blend (Tween 80) with its unsaturated lipophilic oleate “tail” in the oil is compatible with oils having unsaturated bonds. Tween 60 (stearate), Tween 20 (laurate) and Tween 40 (palmitate) are all more compatible with oils having saturated bonds. Although both

oils might require the same HLB which these types of surfactants have, the emulsifier which attracts the oil will be more effective.

This classification system completely disregards the interaction of the surfactant with the oil and only considers water solubility.[21] Surfactants with low HLB are more oil soluble and are thus suitable for preparing water-in-oil (W/O) emulsion whereas those surfactants with high HLB values have good water solubility thereby rendering them suitable for preparation of oil-in-water (O/W) emulsions. Among non-ionic surfactants comprised of ethylene oxide segments, the larger the portion of ethylene oxide units (hydrophilic part of the surfactant molecule), more water soluble will be the surfactant. The hydrophobic part of the surfactant embeds itself in the oil droplet and the hydrophilic ethylene oxide part interacts with the water to surround the oil droplet and form an emulsion. Surfactant must remain in solution to perform their function. In contrast to salts, which dissolve more readily in hot water, the solubility of non-ionic surfactant has a temperature limit termed as cloud point. At this temperature, the surfactant drops out of solution and causes the solution to become turbid. Surfactant activity and performance are usually at an optimum below the cloud point. The deficiency in the HLB scheme prompted the development of the PIT (phase inversion temperature) system by Shinoda, which provides information about the types of oils, phase volume relationships and surfactant concentration. It was established on the idea that the HLB of a non-ionic surfactant changes with temperature and that the inversion of emulsion type occurs when the hydrophile and lipophile tendencies of the surfactant are just balanced. No emulsion would form at this temperature. Emulsions stabilized

with non-ionic surfactants are oil-in-water types at low temperatures and invert to water-in-oil types at higher temperature.

1.2.2 Microemulsion templating

1.2.2.1 *Microemulsions*

Microemulsions are an intermediate state between micellar solutions and emulsions and can be interpreted as swollen micellar systems. They are one-phase, transparent and thermodynamically stable systems with domain sizes between 10 and 250 nm (some definitions limit the size of the domains to approximately 100 nm). The term "microemulsion" was first used by Hoar and Schulman in 1943.[22]

Microemulsions consist of at least three components, namely water, oil and surfactant. The composition of a microemulsion can be figured as a ternary phase with the fractions of water, oil and surfactant. A microemulsion system will form either oil-in-water (O/W) phase or water-in-oil (W/O) phase. The bicontinuous (sometimes called middle) phase exists as an intermediate state in which oil and water domains are randomly dispersed with the two phases. By changing the ratio of components, a microemulsion undergoes a phase inversion. Considering the small domain size in a globular microemulsion and the number of domains, the surface to be stabilized by a surfactant is relatively high. Therefore, a high amount of surfactant usually has to be used as high as 1:1 weight ratio in relation to the total amount of monomer. High surfactant demands can be a drawback when using a microemulsion as a precursor for polymeric materials since some surfactants are expensive and can be difficult to remove after polymerization.

1.2.2.2 *Porous polymers from microemulsion templates*

Porous polymers can also be obtained by polymerization of the microemulsions. Several porous polymers have been synthesized using microemulsion templating. The polymers are synthesized by using both polymerizable surfactants and non-polymerizable surfactants. Microemulsion derived porous polymers have found use in the field of separation methods. Stationary phases for capillary electro chromatography have been prepared from bicontinuous microemulsions such as butyl methacrylate (BMA) / Ethylene glycol dimethacrylate (EGDMA) / water (W) using sodium dodecyl sulphate (SDS) as surfactant.[23-24] Microemulsions were used to prepare porous polymer supports for catalysts.[25] The researchers synthesized a monomer with phosphonic acid moieties, which was copolymerized with styrene in a microemulsion formulation using Aerosol-OT (AOT) as surfactant.

1.2.3 Water droplet templating

In an article published in *Nature* in 1994, Widawaski et. al.[26] demonstrated an elegant method that employs water droplets to create a honeycomb like regular array of pores in polymer films. A drop of a solution of either star polystyrene or poly (styrene-*b*-paraphenylene) in carbon disulfide (CS_2) was deposited onto a flat surface and dried in a stream of moist air. The resulting polymer film was observed to possess a regular, hexagonal array of micrometer-sized holes as seen in Figure 1.4.

Regular morphologies were not observed with linear polystyrenes in the absence of moisture or in methanol saturated conditions; the diameter of the pores increased with the molecular weight of the arms of star polystyrene, although regularity was lost at Mn

> 50k; regularity increased with the number of arms. The process by which porosity is created is a result of so called "breathe figures," that is, the formation of water droplets that condense on the surface of an evaporating polymer solution, which undergoes significant cooling as solvent is removed.[27] Such breathe figure patterns have two important features that result in the formation of the observed porous morphology. They form a hexagonal, close-packed pattern of droplets on the surface, and the droplets do not coalesce on contact since they are separated by a film of solution.

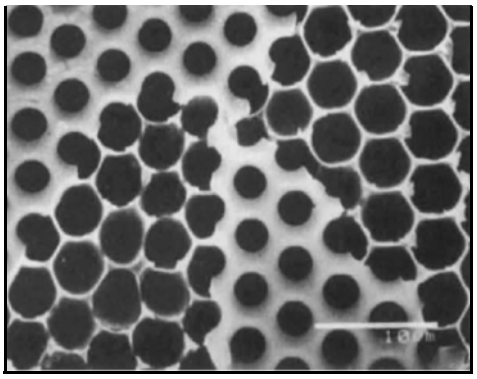

Figure 1.4 : Honeycomb film prepared from star polystyrene *[Widawaski[26]]*

However, subsequent studies have shown that honeycomb like porous films can in fact be formed from a wide variety of polymer architectures, including random-coil linear polymers with[28,29] or without[30] polar end groups, rigid-rod polymers,[31] random[32] and block copolymers[33] and star microgels.[34] Porous films produced by the breathe pattern method can be processed post formation to give structures with interesting novel morphologies. One application of highly porous polymers in general is as substrates for the culture of cells in three dimensions, either for *in vitro* purposes or for tissue engineering. Honeycomb polymer films have been studied in this regard. The ability of porous films prepared from a polypyrrole amphiphilic copolymer blend to support the

growth of mouse fibroblasts was investigated.[35] The surfaces were found to produce a relatively nontoxic cellular response, and cell attachment and growth were optimal (i.e., the same as with tissue culture polystyrene) when the pore diameter was less than 1 μm.

1.2.4 High internal phase emulsion (HIPE) templating

Large varieties of porous polymers have been synthesized using high internal phase emulsions (HIPEs) as templates generally known as polymerized HIPEs or polyHIPEs or polyHIPE monoliths.[36] The polymerization of HIPEs provides a direct synthetic route to a variety of novel porous monoliths having interconnected pore structure. Hydrophobic as well as hydrophilic monomers can be polymerized (using free radical polymerization) by water-in-oil (W/O) and oil-in-water (O/W) emulsions respectively.

1.3 High internal phase emulsions (HIPEs)

1.3.1 Introduction

High internal phase emulsions (HIPEs) are concentrated, highly viscous and paste like emulsions. A well known example is mayonnaise in which the major phase is vegetable oil emulsified in the minor phase vinegar using the lecithin in egg yolk as the surfactant. Lissant was one of the first to describe the structure and properties of the non-Newtonian, thixotropic Bingham fluids that were termed as high internal phase emulsions (or high internal phase ratio emulsions, HIPREs).[37-39] These emulsions have also been referred to as concentrated emulsions,[40-42] gel emulsions,[43-45] and hydrocarbon gels.[46] HIPEs were originally investigated as a method for entrapping volatile, toxic

solvents in non-Newtonian formulations for applications such as cleaning wax or sulfur from oil and gas wells and as a method for transporting bulk solids.[47-50]

Lissant classified high internal phase emulsions (HIPEs) as emulsions with internal phase contents of 70% or more.[51] More recent definition of HIPE refers to internal phase contents of 74% or more (volume fraction as 0.74) in either water-in- oil (W/O) or oil-in-water (O/W) type emulsions. The maximum volume occupied by a number of uniform spheres or the maximum packing fraction is 74%, which results in deformation of the dispersed phase droplets into polyhedra separated by thin films of continuous phase. For applications, where porosity is to be maximized, internal phase contents of around 90% are typical. It depends critically on the nature of the surfactant/emulsifier used, which must be soluble in the continuous phase otherwise, phase inversion will occur. The porous polymers obtained by this method have well defined cellular morphology, which is different from the foams formed by other methods such as gas blowing. The morphological features such as cell size,[52] interconnecting hole size[53] and porosity can be efficiently controlled,[54] which makes polyHIPE a superior product than the gas blown foams. Their structure, which is analogous to conventional gas-liquid foam of low liquid content, gives rise to a number of peculiar and fascinating properties such as high viscosity.

1.3.2 Structure of HIPE

High internal phase emulsions are kinetically stable heterogeneous systems formed by two immiscible liquids with the surfactant at the interface of both the liquids. The dispersed phase droplets must either be non-uniform i.e. polydisperse or deformed

into non-spherical, polyhedral cells. In the theoretical treatment of the geometry of HIPEs, Lissant showed that the dispersed phase droplets for a monodispersed system would assume a rhomboidal dodecahedral (RDH) packing from 74% to 94% internal phase volume, with increasing deformation into polyhedra. Above 94%, the packing changes to tetrakaidecahedral (TKDH) (truncated octahedral) as shown in Figure 1.5 (a) and (b). Later work indicated that pentagonal dodecahedra should be formed at dispersed phase contents above 96%.[55,56] Initial investigations of polystyrene based polyHIPEs showed that the voids were relatively monodisperse and were polyhedral in shape.[39] Subsequent work with other polyHIPEs has shown that spherical polydisperse systems are also common.

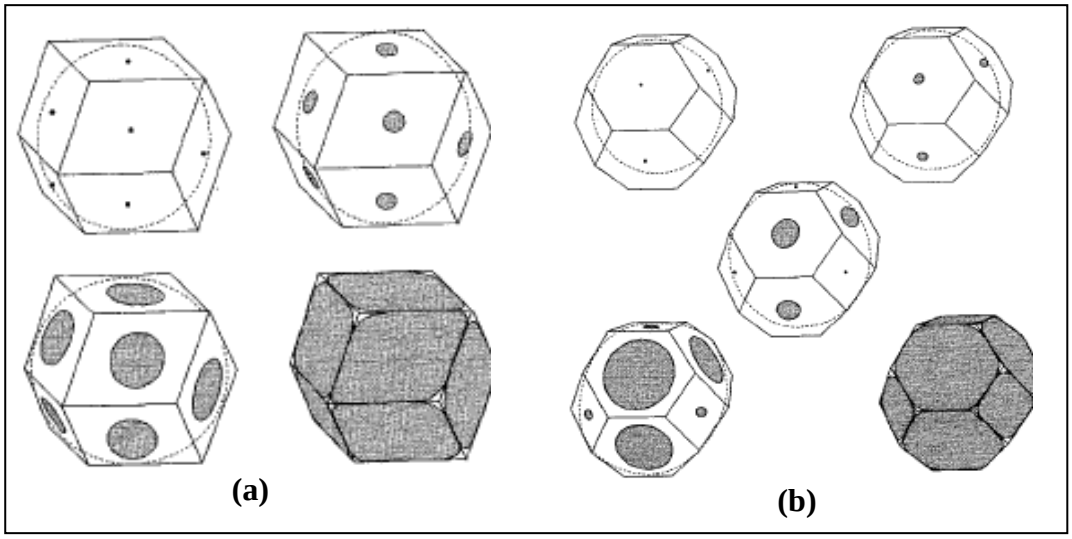

Figure 1.5 : Transition from sphere to polyhedra: (a) rhomboidal dodecahedron and (b) tetrakaidecahedron [36]

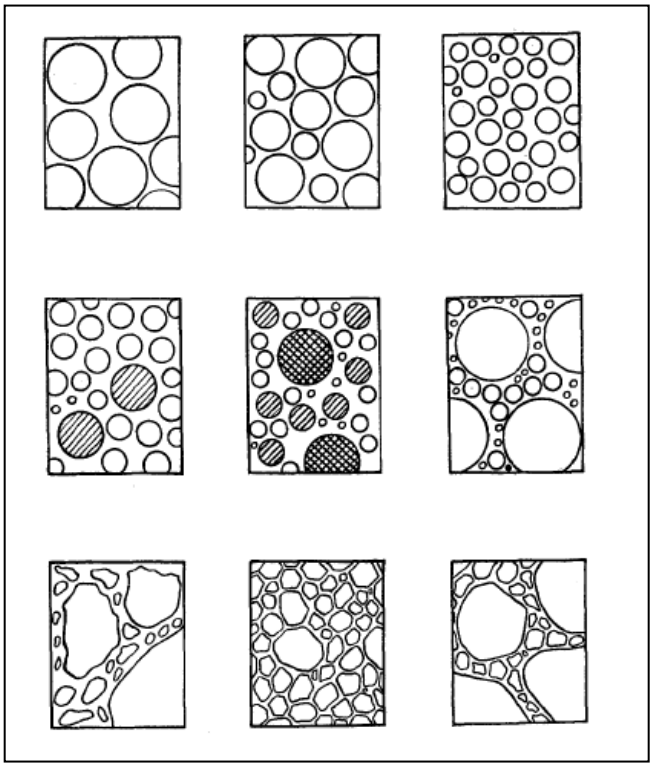

Figure 1.6 : Different geometries of dispersed droplets in concentrated emulsion[36]

The different geometries of dispersed droplets formed during the high internal phase emulsion preparation are shown in Figure 1.6. These are influenced by different parameters such as water to oil ratio, stirring speed, surfactant types and concentration etc. It has been known that if a monodisperse system of rigid spheres is packed in the most advantageous manner, the spheres will occupy a little over 74% of the total volume of the system. However, a higher density can be achieved by carefully arranging the spheres. Start with a layer of spheres in a hexagonal lattice, then put the next layer of spheres in the lowest points you can find above the first layer, and so on as shown in the Figure 1.7. This natural method of stacking the spheres creates one of two similar patterns called cubic closed packing and hexagonal close packing. Each of these two arrangements has an average density of ~74%. The Kepler conjecture says that this is

the best that can be done; no other arrangement of spheres has a higher average density than this.

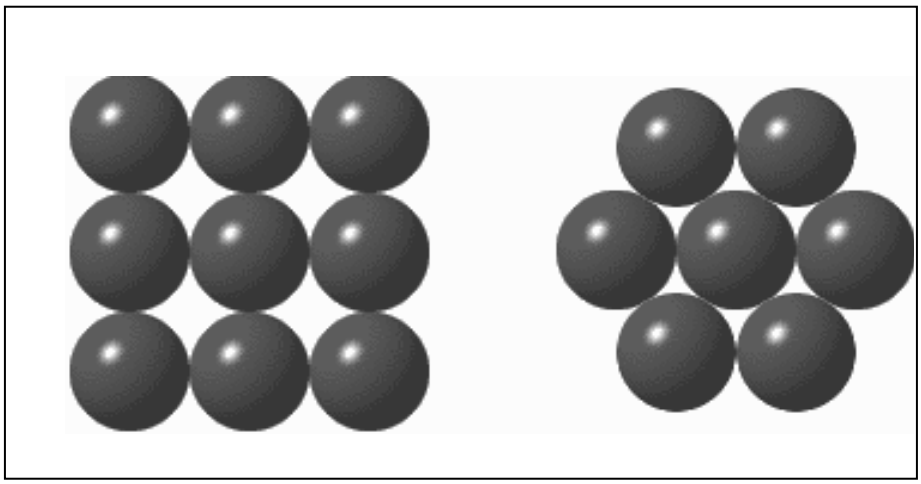

Figure 1.7 : Highest possible volume occupied by solid spheres

1.3.3 Formation of HIPE

High internal phase emulsions (HIPEs) are formed by mixing two immiscible liquids in the presence of an emulsifier, usually a surfactant. One of the liquids is almost always an aqueous solution and the other is usually hydrophobic. The major phase is usually added slowly under constant agitation to a solution consisting of the minor phase and the surfactant. HIPEs can also be formed by applying a centrifugal field to an emulsion.[57,58] This "creaming" process separates the excess continuous phase from the emulsion, concentrating the dispersed phase into a HIPE. The optical microscopic images of a typical HIPE are depicted in Figure 1.8. Emulsions which are not thermodynamically stable systems and tend to coalesce, can also undergo creaming as they phase separate.

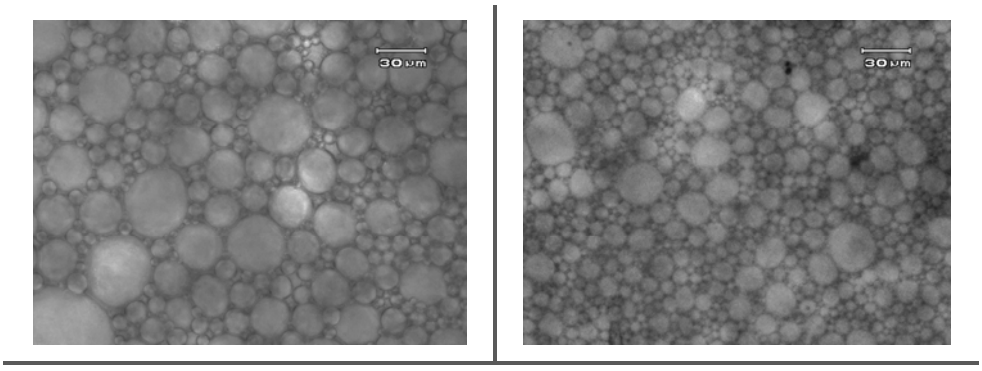

Figure 1.8 : Optical microscopy images of high internal phase emulsion (HIPE)

1.3.4 Stability of HIPE

HIPE stability is influenced by a number of factors including the molecular structures of the components comprising the phases and of the surfactant, the surfactant content, presence of stabilizing salts, dispersed phase content and temperature.

1.3.4.1 *Effect of surfactant*

The first criterion for the formation of a stable HIPE is the presence of two immiscible liquids, one of which is aqueous. The nature of the organic or oil phase can vary to a considerable extent, although the most stable HIPEs are generally produced with more hydrophobic liquids. The nature of the surfactant employed to stabilize HIPE ultimately facilitates its formation. Above a certain critical limit of internal phase volume, an emulsion will tend to invert to the opposite type i.e. an oil-in-water (O/W) emulsion will become the water-in-oil (W/O) type and vice versa. This can be prevented from occurring by careful choice of surfactant, such that it is completely insoluble in the dispersed phase of the emulsion. The molecular geometry of the surfactant is also an important factor. The assembly of surfactant molecules at the interface should enhance

convex interface curvature within the minor phase. A nonionic surfactant with a low hydrophilic lipophilic balance (HLB), such as sorbitan monooleate (Span 80) with HLB of 4.3 is needed to form a stable W/O HIPE. The effects of the nature of the surfactant, surfactant concentration and presence of cosurfactants in a HIPE of styrene (S) and divinylbenzene (DVB) were investigated.[59-62] The stability of such HIPEs appeared to vary inversely with the cosurfactant HLB. To achieve a stable HIPE, the surfactant must lower the interfacial tension between the phases, must form a rigid interfacial film and must rapidly adsorb at the interface.[63] The stability of a HIPE is kinetic in nature and depends on the repulsion generated between the droplets of the internal phase. Ionic surfactants stabilize HIPEs through electrostatic repulsion while nonionic surfactants stabilize HIPEs through steric repulsion. The higher the interfacial tension between the phases, greater is the tendency of the surfactant to concentrate at the interface and form a strong interfacial film. The tendency toward coalescence decreases with the increasing strength of the interfacial film. The strength of the interfacial film is enhanced by the ability of the surfactant to pack closely and a surfactant blend is often able to pack more effectively. The presence of a salt can also enhance the ability of the surfactant head groups to pack into an ordered structure.

1.3.4.2 *Effect of salt*

The addition of sodium chloride (NaCl) was found to enhance the rigidity of the interfacial film in W/O HIPE, raising its elastic modulus and apparent yield stress and enhancing the stability.[64] Various salts are used to stabilize HIPEs, including calcium chloride hydrate and potassium sulfate. The nature of the salt is an important factor.[44] Salts that reduce the interaction of nonionic surfactants with the aqueous phase, thereby

increasing surfactant-surfactant interaction and the formation of a more ordered interface, were more effective at enhancing HIPE stability.[65] The salts can also enhance stability by inhibiting Ostwald ripening, a process by which large droplets grow at the expense of smaller ones. They reduce the solubility of the aqueous phase in the oil phase, thus reducing the attractive forces between the droplets.[66] The stability of HIPE has been correlated with the water/oil interfacial tension for both W/O and O/W systems. The lesser the interfacial tension, the greater is the HIPE stability and the greater is the amount of internal phase that can be incorporated.[67-68]

1.3.4.3 *Other factors affecting HIPE stability*

The polarity of the organic component in a W/O HIPE also affects the stability. In general, the greater the hydrophobicity of the oil phase and the greater the hydrophilicity of the aqueous phase, the greater is the interfacial tension and the greater is the stability of the HIPE.[67] Relatively polar organic components require more hydrophobic surfactants, whereas relatively hydrophobic organic components require more hydrophilic surfactants. Thus it was found to be easier to form HIPEs with aliphatic organics than with aromatic organics.[45] When the oil phase in an O/W emulsion contained aromatic or halogenated organics it was difficult to form a HIPE using a nonionic surfactant due to the interactions between the surfactant and the dispersed phase.[68] The amount of organic phase that could be added to an O/W HIPE increased with increasing surfactant concentration.[69] Partial polymerization of the monomers in the dispersed phase was also found to enhance the stability of the HIPE.[70] Increasing the viscosity of the continuous phase reduces the amount of dispersed phase that could be incorporated.[68] Increasing the temperature enhances the coalescence of the

dispersed droplets and reduces emulsion stability.[43,45] Poly(butylene oxide) /poly(ethylene oxide) block copolymers were developed, that could stabilize HIPEs at concentrations as low as 0.12 wt% of the organic phase without the need for a salt stabilizer.[71] The stability of a HIPE whether W/O or O/W, is usually related to the presence of relatively large amounts of a surfactant that is highly soluble in the external phase (typically around 20% of the external phase) is highly insoluble in the internal phase, is easy to pack on the outside of a sphere, but is difficult to pack on the inside of a sphere. There can be exceptions to this rule of thumb. A water soluble ionic surfactant like cetyltrimethylammonium bromide (CTAB), has been used to form a stable W/O HIPE with S/DVB in the external phase through vigorous stirring.[72]

1.3.5 Polymerized HIPEs or polyHIPEs

Polymer materials can easily be prepared from HIPEs if one or the other (or both) phases of the emulsion contain monomeric species. The term "polyHIPE" is a Unilever trade name, which describes a material produced by polymerization in the external phase of a HIPE in 1982 by Barby and Haq.[73] The external (non-droplet) phase is converted into a solid polymer and the emulsion droplets are removed yielding (in most cases) a highly interconnected network of micron sized pores of quite well defined diameter. This process yields a range of products with widely differing properties. Additionally, as the concentrated emulsion acts as a scaffold or template, the microstructure of the resultant material is determined by the emulsion structure immediately prior to polymerization. A continuous monomer phase is polymerized to yield low density polyHIPE following the removal of the dispersed phase. A typical HIPE and subsequent polyHIPE preparation is depicted in Figure 1.9.

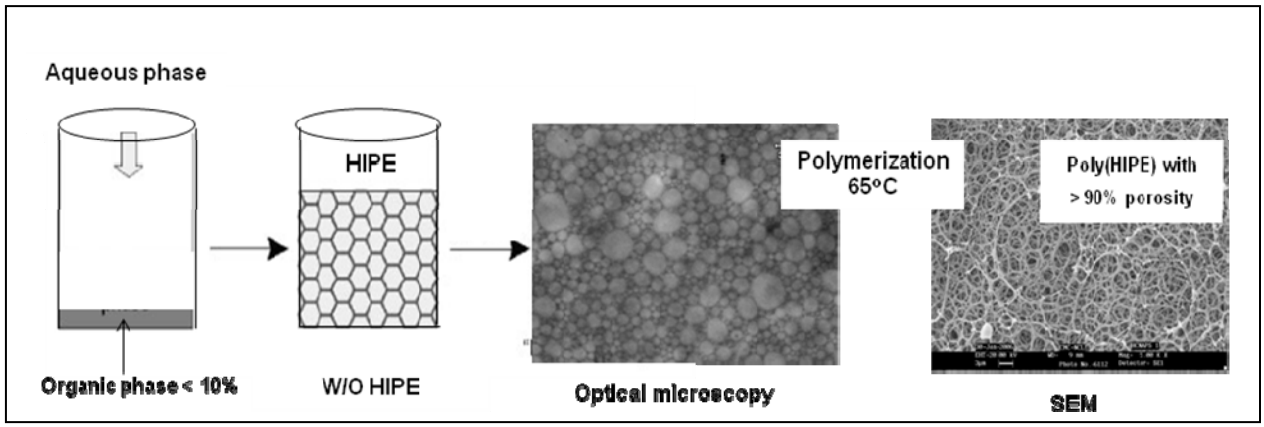

Figure 1.9 : Preparation of HIPE and subsequent polyHIPE

1.3.5.1 *Formation of W/O polyHIPEs*

Water-in-oil (W/O) polyHIPEs have been successfully synthesized by free radical polymerization of monomers such as styrene, acrylates and methacrylates. PolyHIPEs are usually crosslinked using a crosslinking comonomer to prevent collapse or disintegration under the capillary stresses generated during drying. Divinylbenzene (DVB) is commonly used as a crosslinking comonomer for W/O polyHIPEs. The W/O polyHIPEs most commonly investigated are based on styrene and divinylbenzene, the polymer described in the original patent by Barby and Haq.[73] The W/O HIPE is formed by adding the aqueous phase to a solution of oil phase (monomer and surfactants) as illustrated schematically in Fig. 1.9. Surfactant with HLB range of 2-6 is needed to prepare a stable styrene based W/O HIPE. The surfactant usually chosen for such HIPEs is sorbitan monooleate with an HLB of 4.3. At least 4% surfactant (based on the total mass of the external phase) is usually needed to form an open-cell polyHIPE structure. The optimal surfactant contents are usually 20-50% of the external phase. Surfactant

contents greater than 80% of the external phase can yield a closed-cell structure.[59-62] Block copolymer surfactants have also been used to synthesize styrene based polyHIPEs.[74] The initiator can be added to the organic phase (e.g. 2,2′-azobisisobutyronitrile (AIBN) or benzoyl peroxide (BPO)) or to the aqueous phase (e.g. potassium persulfate (KPS)). Polymerization is usually allowed to take place for around 24 h at elevated temperatures (between 50°C and 80°C). The result is a water-filled, crosslinked monolith in the shape of the reaction vessel. The typical W/O, low-density, brittle, highly porous acrylonitrile-divinylbenzene (AN-DVB) polyHIPE monolith and its corresponding interconnecting morphology are shown in Figure 1.10 (a) and (b) respectively.

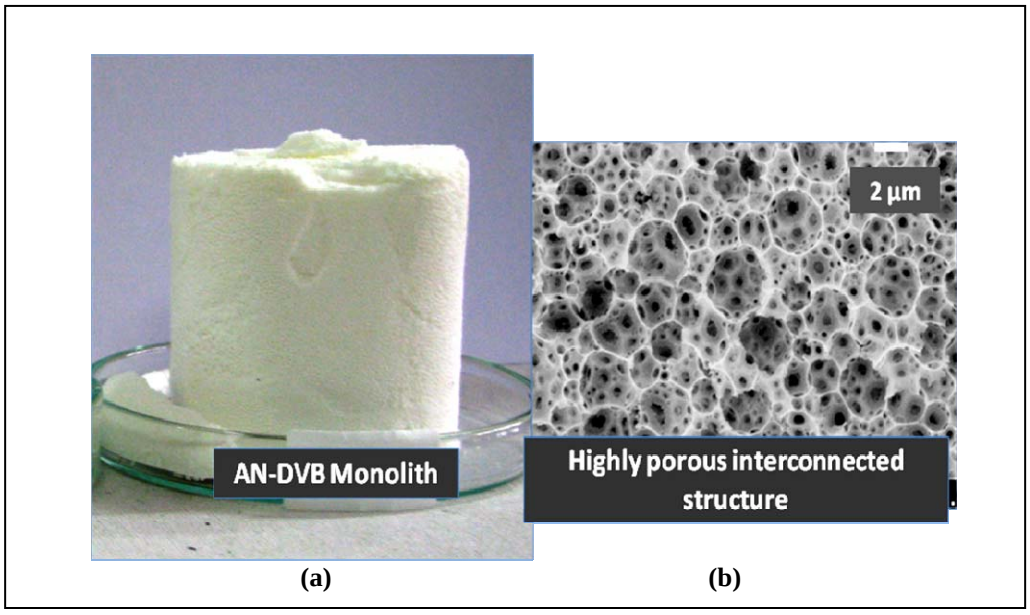

Figure 1.10 : AN-DVB polyHIPE; (a) monolith having the shape of the reaction vessel and (b) SEM image showing interconnected morphology

Removing the dispersed phase droplets leaves spherical voids between 5 and 15 µm. The void walls in Figure 1.10 (b) contain numerous interconnecting holes between 0.1 and 2 µm where the thin polymer envelope has ruptured. The mechanical behavior

of polyHIPEs was varied from rubbery to glassy through copolymerization in styrene/acrylate copolymers.[75] In addition, polyHIPEs with high glass transition temperatures (T_gs) were synthesized through copolymerization of styrene with maleimides.[76,77] Initiation takes place within the monomer when the initiator is dissolved in the external phase but takes place at the interface when the initiator is dissolved in the internal phase. The locus of initiation has been shown to be extremely important in determining the molecular structure, the porous structure, and the properties.[78] This is especially true when the monomer and the crosslinking comonomer have different interfacial activities. An initiator located at the interface promotes the reaction of the monomer that is found in excess at the interface while an initiator located in the bulk promotes a more random reaction. PolyHIPEs with open-cell morphology have demonstrated advantageous structural properties and liquid absorbency, prompting their use as absorbents, in ion exchange systems and as heat resistant structural foams. PolyHIPE made of styrene-divinyl benzene was extensively studied in the initial stages of the discovery of the system, however this has opened a vast area of research that can be applied to a series of monomers of various types including acrylates, methacrylates etc. The range of monomers which can be employed, is largely dictated by the physical chemistry of the emulsion system. For instance, monomers must be sufficiently hydrophobic to allow the formation of stable W/O HIPEs

1.3.5.2 *Formation of O/W polyHIPEs*

For the preparation of porous polymers from water soluble or miscible monomers, oil-in-water (O/W) HIPEs must be used. Most of the reports on O/W HIPEs mention difficulties in achieving a sufficiently stable emulsion. Whereas in W/O HIPEs,

surfactants with low HLB values are used. O/W HIPEs require surfactants that are soluble in the aqueous phase and have generally high HLB values. Various amounts of surfactant stabilized the emulsions well enough to obtain polyHIPEs of polyacrylamide where cavity and interconnecting pore sizes depended on the amount of surfactant used. Similar attempts of preparing polyHIPEs based on acrylic acid were unsuccessful. Work on acrylic acid polyHIPEs has resulted in the preparation of stable monoliths of polyacrylic acid using toluene as the internal phase and Triton X-405 as the surfactant, leading to open porous structures with cavities between 4 and 8 μm and interconnecting pores between 0.4 and 1 μm.[79] In this case, the initiator was shown to influence the morphological features of the prepared monoliths. Furthermore, the pH value of the aqueous phase and the degree of crosslinking [N, N′-methylene bis(acrylamide) crosslinker] influenced the final structure. O/W polyHIPEs were synthesized based on monomers such as acrylic acid (AA), acrylamide, N-isopropylacrylamide (NiPAAm), 2-hydroxyethyl methacrylate (HEMA) and hydroxyethyl acrylate (HEA).[79-82]

PolyHIPE materials have also been prepared by polycondensation in high internal phase emulsions.[83] Thus a resorcinol-formaldehyde porous copolymer was synthesised from an O/W HIPE of cyclohexane in an aqueous solution of resorcinol, formaldehyde and surfactant. The addition of acid catalyst to an emulsion, followed by heating resulted in copolymerization. Other systems prepared included urea-formaldehyde, phenolformaldehyde, melamine-formaldehyde and polysiloxane-based elastomeric species.[83]

The resorcinol-formaldehyde polymers have been used to prepare highly porous carbon materials by controlled pyrolysis in an inert atmosphere.[84,85] The microstructure

of the carbon is an exact copy of the porous polymer precursor. Poly(methacrylonitrile) polyHIPE polymers have also been used for this purpose. These monolithic highly porous carbons are potentially useful in electrochemical applications particularly re-chargeable batteries and super-capacitors. Open-cell polyHIPE materials have also been prepared from hydrophilic methacrylates which on hydrolysis yield hydrophilic poly (methacrylic acid) based species. Stable HIPEs containing high levels of glycidyl methacrylate (GMA) can also be formed from which porous polymers can be made. These have considerable potential for further exploitation due to the reactive epoxide group.

1.3.5.3 *Formation of non-aqueous polyHIPEs*

Non-aqueous or oil in oil (O/O) emulsions are emulsions where the phases are two immiscible organic liquids. Riess and coworkers[86-87] have studied the stabilization of waterless systems with block and graft copolymers, where one of the liquids is a good solvent for one of the blocks and a non-solvent for the other and vice versa. Sharma has published a considerable volume of work on non-aqueous emulsions involving ethylene glycol as the polar organic phase and either benzene[88] or chlorobenzene[89] as the non-polar organic phase. The surfactants used were anionic or nonionic, low molecular weight materials. More recently, attention is focused on the formation of non-aqueous microemulsions,[90] usually with formamide as the polar organic phase, and the first example of liposome formation in a non-aqueous solvent was reported.[91] The above emulsions were not highly concentrated. Highly concentrated non-aqueous HIPE emulsions are used as safety fuels in military applications.[92] Here the emulsifier system used was a blend of two nonionics, with an optimal HLB value of 12. One of the most

important factors was the solubility of the emulsifier in the continuous (formamide) phase. Thus, higher the surfactant solubility, the more stable will be the emulsion. The emulsifier concentration was also important. The stability increased to a maximum and then decreased with an increase in surfactant concentration. Surprisingly, the HLB number did not appear to have much effect on the stability of the emulsions over the range studied (11 to 14). This was attributed to the high concentration of emulsifier in the continuous phase, although the narrow HLB value range is probably also a factor. The non-aqueous HIPEs showed similar properties to their water-containing counterparts. Examination by optical microscopy revealed a polyhedral, polydisperse microstructure.

1.3.5.4 *Formation of dispersed phase polyHIPEs*

The dispersed phase of HIPEs may also be used to prepare polymeric materials. In this case, conversion of monomer dispersed droplets to polymer results in latexes or particulates. Lissant[93] prepared polymer particles by polymerization of HIPEs of vinyl chloride monomer in water. Concentrated emulsions with high phase volume ratios (above 0.9) gave agglomerates of particles with a relatively monodisperse size distribution. The particles themselves appeared to be hollow. The explanation given for this was that poly(vinyl chloride) is considerably denser than vinyl chloride monomer. Since polymerization is probably initiated on the surface of the droplets, by a water soluble initiator, polymer will grow until the surface is covered. This resulted in a rigid sphere encapsulating unreacted monomer. Polymerization will continue inside the shell with concomitant shrinkage until all the monomer is consumed resulting in hollow spheres. The presence of the rigid shell prevents additional initiator from reaching

unreacted monomer resulting in the formation of a high molecular weight polymer. Using this method, synthesis of monodispersed polystyrene latexes are reported.[94,95] Copolymer particles can also be prepared from HIPEs.[96] Other latexes which have been produced by this method include poly(butyl methacrylate), poly(butyl acrylate) and poly(styrene/DVB).[97] Dispersed phase polymerization of HIPEs has also been used to prepare polymer supported quaternary onium phase transfer catalysts.[98]

Polyurethane / polypyrro-composites,[99] poly(methyl-ethacrylate) / polypyrrole-composite,[100] polypyrrole / poly(ethylene-co-vinyl acetate), polyaniline / polystyrene[101] and polyaniline / poly(alkyl methacrylate)[102] composites were synthesized. A rubber-like copolymer/carbon fibre composite material has also been prepared.[103] Rubber-toughened polystyrene composites were obtained by polymerizing the dispersed phase of a styrene/styrene-butadiene-styrene solution of O/W HIPE.[104] Kim and Ruckenstein[105] reported the preparation of polyacrylamide particles from a HIPE of aqueous acrylamide solution in a non-polar organic solvent. Crosslinked polyacrylamide latexes encapsulating microparticles of silica and alumina have also been prepared by this method.[106]

1.3.5.5 *Formation of bicontinuous polyHIPEs*

If both continuous and dispersed phases of highly concentrated emulsions contain monomeric species, it is possible to obtain hydrophilic/hydrophobic polymer composite materials. Polyacrylamide/polystyrene composites have been prepared in this manner[107] from both W/O and O/W HIPEs containing aqueous acrylamide and a solution of styrene in an organic solvent. The composite materials have been used to

form selective membranes for the separation of liquid mixtures.[108] Other hydrophilic/hydrophobic membranes have been generated from HIPEs of aqueous sodium acrylate solution in divinylbenzene.[109] The emulsions were more stable than corresponding styrene containing systems leading to more favourable membrane preparation. The mechanical properties of these membranes were improved by including a crosslinker, methylene bisacrylamide, in the aqueous phase, and by using a styrene/butyl acrylate mixture as the continuous phase.[110] The styrene/butyl acrylate mixture had to be prepolymerized to low conversion to allow HIPE formation. The permeation rate of the membrane was improved by including a porogen (hexane) in the organic phase, generating a permanent porous structure.[111] Gelatin-poly(methyl methacrylate) composite materials can also be prepared through HIPE pathway.[112] Concentrated emulsions of methyl methacrylate in aqueous gelatin/surfactant solutions on polymerization at 50°C yielded composite membrane materials. A comb-like polymer, possessing hydrophilic and hydrophobic side chains anchored to an amphiphilic backbone was prepared.[113] A quaternary ammonium and quaternary phosphonium monomers were copolymerized and used for this purpose.

1.3.5.6 *Formation of pickering polyHIPEs*

Pickering emulsions are stabilized by solid particles at the interface rather than by surfactants.[114] Recent work has shown that emulsions with 40% external phase can be stabilized by nanoparticles such as carbon nanotubes through the formation of Pickering emulsions.[115] Very low loadings of titania nanoparticles functionalized with oleic acid yielded stable W/O HIPEs and these HIPEs were used to synthesize PS based polyHIPEs.[116]

1.3.6 Functionalization of polyHIPEs

Number of reactions have been investigated for the surface functionalization of polyHIPEs.[117] PolyHIPE surfaces have been functionalized by using 4-vinylbenzyl chloride (VBC) as a comonomer or by using surfactant molecules soluble in the monomer possessing an allyl or an acryloyl group.[118-121] Functionalization has also proceeded via pendent unreacted DVB vinyl groups in poly(S-*co*-DVB) polyHIPEs.[122-125] Glycidyl methacrylate (GMA) has also been used as a functional monomer.[126] Reactive acrylates such as 4- nitrophenyl acrylate, 2,4,6-trichlorophenyl acrylate, and even *t*-butyl acrylate were also used to enhance functionalization.[127-129] ATRP was used to graft polymethacrylates to a polyHIPE surface functionalized using a bromo ester comonomer.[130]A ruthenium catalyst was also attached to polyHIPEs for alkylidene exchange reactions.[131] Stimuli responsive peptide side-chain polymers prepared by reversible addition fragmentation (RAFT) chain transfer polymerization were attached to the C=C bonds of residual crosslinker in polyHIPEs based on poly(ethylene glycol) (PEG), leading to materials that were capable of reversible assembly with complementary molecules in solution.[132]

1.3.7 Morphology of polyHIPEs

It is now well understood that a phase separation during the formation of the network is mainly responsible for the formation of porous structures in a dried state. Major factors effecting formation of pores include effect of diluent, crosslinker, temperature and initiator.[133] In order to obtain macroporous structures, a phase separation must occur during the course of the crosslinking process so that the two-

phase structure is fixed by the formation of additional crosslinks.[134] Depending on the synthesis parameters, phase separation takes place on a macro scale (macrosyneresis) or on a micro scale (microsyneresis). Macroporous networks usually have a broad pore size distribution ranging from 10-104Å. In general, macroporous copolymers refer to materials prepared in the presence of a pore forming agent and having a dry porosity, characterized by a lower density of the network due to the voids than that of the matrix polymer.[135] Another problem with the definition of macroporosity arises from the variation of the pore structure of the networks depending on their post treatment process.[136] A macroporous copolymer may become nonporous if it is first swollen in a good solvent and then dried at an elevated temperature. Subsequently the loss of porosity can be recovered by a solvent exchange procedure and the original swollen state porosity called maximum porosity can be preserved in the dried state. Because only the maximum porosity is a characteristic property for a given material, it is appropriate to define the macroporosity with respect to the maximum porosity.[133] IUPAC classification of pores based on the pore width[137] as (a) micropores have widths of up to 20 Å (b) mesopores have widths in the range 20-500 Å (c) macropores have widths greater than 500 Å.

A typical pore size distribution of a styrene-divinylbenzene copolymer network prepared in the presence of a non-solvating diluent shows pores from a few tens of angstroms up to several thousands of angstroms in radius exist inside the macroporous material. Agglomerates of particles of various sizes inside the porous copolymer are responsible for this broad size distribution of pores. The pores are in fact, irregular voids between agglomerates which are typically interconnected.[138] The formation process of

the porous structure can be divided into three stages.[139] The smaller particles called nuclei are about 102 Å in diameter. The nuclei are nonporous and constitute the highly crosslinked regions of the network. Micropores defined with widths of up to 20 Å appear between the nuclei. The agglomerations of nuclei are called microspheres and they are about 103 Å in diameter. Mesopores constitute the interstices between the microspheres. Microspheres are agglomerated again into larger irregular moieties of 2500-10,000 Å inside the polymer material. Meso and macropores appear between the agglomerates of the microspheres.[140]

Williams[141] discovered that the surfactant level had a profound effect on the cellular structure of polyHIPE materials. Below a surfactant concentration of 5%, the polymers produced had a closed-cell structure. The aqueous phase in this material remained trapped inside the structure, resulting in a high density polymer. Above a surfactant concentration of 7%, open-cell foam was produced with an entirely interconnected microstructure. The aqueous phase could easily be removed yielding a dry, low-density polymer matrix. Surprisingly, the surfactant concentration was found to be more important than the phase volume in determining the final cellular structure. A material prepared from a HIPE of as much as 97% internal phase volume and 5% surfactant still gave a closed-cell polyHIPE.

Williams and coworkers[142] investigated the effect of variation of the DVB content of the monomer phase on the cellular structure of the resulting foam. The phase volume and surfactant and initiator concentrations were kept constant while the DVB content was increased from 0 to 100% which caused a drop in average cell size from 15 μm to 6 μm. Sherrington and coworkers[143] produced polyHIPE materials with an

additional porous structure within the walls of the macro cells. It was observed that an increase in high internal phase volume with chlorobenzene as porogen resulted in a decrease in surface area.[144] The internal phase volume ratio can have a profound influence on the surface area.[145,146]

1.3.8 Properties of polyHIPEs

PolyHIPE materials possess novel properties as a result of their unique cellular structure. Referring specifically to open-cell polymers, they are characterized by a very low dry bulk density, typically less than 0.1 g/cm^3, due to their highly porous and interconnected structure. The cell sizes can range from 5 to 100 μm, surface areas of less than 10 m^2 g^{-1}. The addition of porogen can lead to high surface area and will possess low bulk density (< 0.1 g/cm^3) and very high pore volumes which can go even above 90%.[144] Another important property of open-cell polyHIPE materials is their ability to absorb large quantities of solvent by capillary action.[147] Simply immersing a piece of the material in the liquid causes absorption with displacement of the air from inside the matrix. This occurs until all voids are filled.

1.3.8.1 *Surface area*

PolyHIPEs exhibit modest surface areas around 5-20 m^2/g, since the voids in polyHIPEs are tens of micrometers in diameter and the walls are solid. Surface areas of hundreds of square meters per gram have been achieved by adding a porogen to the external phase. Adding a porogen creates a second family of pores due to phase separation within the developing polymer matrix, resulting in surface areas up to 700 m^2/g and reducing the density by over a factor of two.[148-151] While typical polyHIPE

densities are around 0.1 g/cm^3, polyHIPEs with densities as low as 0.0126 g/cm^3 have been synthesized through variations in the surfactant type, the surfactant content and the porogen content.[152] The use of a porogen often affects the structure of the wall. This structure seems to reflect the formation and the phase separation of porogen-swollen microgel particles during polymerization. Eventually the microgel particles aggregate and react to form the walls of the polyHIPE. This "particle assembly" wall structure is also seen for hydrophilic polyHIPEs synthesized from aqueous solutions of monomers with water acting as the swelling porogen. Recent work indicates that the porosity of a swollen polyHIPE can be significantly greater than that of a dried polyHIPE.[153] PolyHIPEs can also be "fixed" in the swollen state through hypercrosslinking generating extremely high surface areas (up to 1200 m^2/g).[154]

1.3.8.2 *Liquid absorption*

PolyHIPEs are able to absorb large quantities of liquid through capillary action.[10] Absorption begins when the polyHIPE is immersed in the liquid and can continue until the air has been displaced and the voids are filled with liquid. The tendency of a particular polyHIPE to absorb a particular liquid depends on the interfacial tension between the two, specifically on the contact angle. A polystyrene (PS) based polyHIPE will readily absorb toluene and the walls will swell. Methanol will be absorbed to a lesser extent and water will not be absorbed at all. The presence of residual surfactant in a PS-based polyHIPE, however will lower the contact angle and significant amounts of water can be absorbed. Hydrogel polyHIPEs will absorb water readily and will undergo extensive swelling. Liquids that are readily absorbed can be easily pumped through polyHIPEs. The back pressures generated by pumping will be relatively low owing to

the relatively large pore size. The ability to pump liquids is of importance for many potential applications including catalysis, liquid chromatography, separation and tissue engineering.

1.3.8.3 *Mechanical properties*

PolyHIPEs generally exhibit compressive stress-strain curves typical of foams. These curves contain three distinct regions: a linear elastic stress-strain region as shown in Figure 1.11 at low strains. The modulus and the yield stress plateau decrease with decreasing density, reflecting the volumetric replacement of solid polymer with air. The modulus of a polyHIPE is also dependent upon the modulus of the wall material.

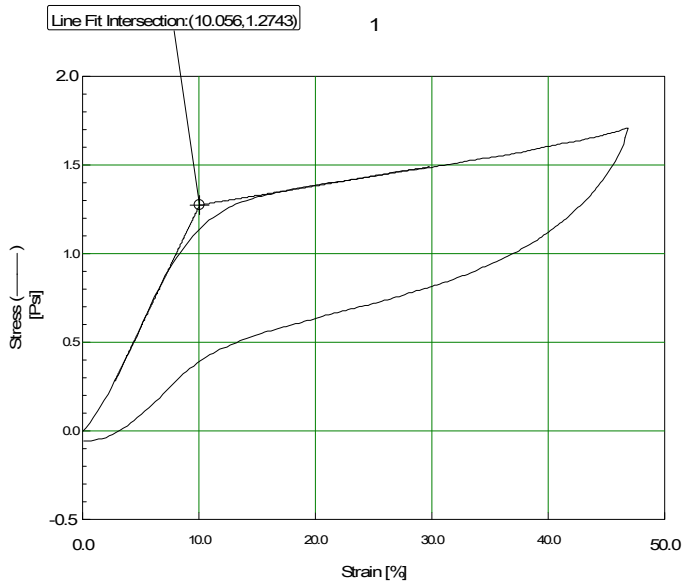

Figure 1.11 : Typical stress-strain behaviour of PolyHIPE

1.3.9 Applications of polyHIPEs

The scientific and patent literature reveals wide variety of potential applications for polyHIPEs. PolyHIPEs find applications in formation of silver film on the interior of polyHIPE polymers, with a view to produce materials with good thermal insulation.

PolyHIPEs have found use in high energy physics experiments such as inertially confined fusion.[62] Deuterated polystyrene based polyHIPEs were used for thermal nuclear fusion targets.[155] The majority of applications take advantage of the porous structure and the relative ease with which liquids can be pumped through polyHIPEs. A large proportion of applications involve using polyHIPEs or more often functionalized poly-HIPEs as a support material. Examples of polyHIPE applications include supports for solid-phase peptide synthesis,[156] carriers for flavin in column reactors with high flow rates,[157] supports for biocatalyst systems using quaternary ammonium groups,[158] carriers for transporting hazardous or flammable liquids,[10] and matrices for the immobilization of cells and enzymes.[159-161] Poly(glycidyl methacrylate) based polyHIPEs have been functionalized and used as chromatographic columns for protein separation and the flow properties studied.[162,163] Many applications use the water absorption capabilities of polyHIPEs. Polyvinylpyridine was grafted to poly(S-*co*-VBC) polyHIPEs for the separation of heavy metals from water.[164] Sulfonation of a polyHIPE was used to produce an ion exchange resin.[165] Immobilized catalyst supports were produced by sulfonating poly(S-*co*-DVB), by functionalizing poly(DVB-*co*-VBC) or poly(S-*co*-DVB), or by using a functional acrylate comonomer.[166-172] A poly N-isopropylacrylamide (NiPAAm) based hydrogel polyHIPE was used as a particle pump through which organic matter in the internal phase was released on contraction of the hydrogel at the lower critical solution temperature (LCST) in water.[173] Halo-organic contaminants were removed from water using polyHIPEs.[174] A rapid and reversible clathrate hydrate hydrogen storage system was produced by adding a tetrahydrofuran (THF)-water system to a PS-based polyHIPE.[175]

The porous structure, ability to absorb water and well-defined porous morphology make polyHIPEs into materials of interest for biomedical applications. PolyHIPEs have been shown to have potential as scaffolds for in vitro 3D cell culture[176-178] and this has led over the last few years to investigations into biodegradable polyHIPEs as potential scaffolds for tissue engineering.[179,180] PolyHIPEs with 50 wt% of biodegradable (vinyl-terminated) polycaprolactone (PCL) and 50 wt% EHA with respect to the total monomer content were observed to degrade completely within 10 weeks in a sodium hydroxide solution, although it should be noted that these polyHIPEs possessed a very inhomogeneous, phase separated initial morphology.[181] Other W/O biodegradable polyHIPEs include those based on poly(propylene fumarate) (PPF).[180] It was shown that the stability of the precursor emulsion for these materials has a direct impact on the degree of interconnectivity of the polyHIPE.

The relatively large surface area of polyHIPEs compared to nonporous materials makes conducting polyHIPEs of interest for sensing applications. PolyHIPEs were coated with polythiophene, polypyrrole, and polyaniline to synthesize conductive porous polymers for applications such as electromagnetic interference shielding and sensors.[182] In other work, nickel was deposited onto the internal surface of a polyHIPE. Functionalized polyHIPEs with or without graphite particles were used for selective electrochemical sensing.[183] PolyHIPEs coated with a conducting polymer were also used as sensors for organic vapors.[184] Alternative electrodes for lead–acid battery applications were produced through the deposition of PbO_2 on polyHIPEs.[185] PolyHIPEs have also been used as templates for the synthesis of porous inorganic monoliths. The pyrolysis of polyHIPEs has been used to produce porous carbon monoliths for a variety of

applications.[186] The calcinations of hybrid polyHIPEs was used to prepare polyHIPE-templated inorganic monoliths.[187] Emulsion templated porous materials have been investigated as potential water purification materials.[188]

1.4 References

[1] Svec, F.; Tennikova T. B.; Deyl Z. *Monolithic Materials: Preparation, Properties and Applications* Elsevier, Amsterdam **2003**, 173.

[2] Bokhari M.; Carnachan R. J.; Cameron N. R.; Przyborski S. A. *Biochem. Biophys. Res. Commun.* **2007**, *354*, 1095.

[3] Abbott A. *Nature* **2003**, *424*, 870.

[4] Justice, B. A.; Badr, N. A.; Felder, R. A. *Drug Discovery Today* **2009**, *14*, 102.

[5] Cukierman, E.; Pankov R.; Stevens, D. R.; Yamada, K. M. *Science* **2001**, *294*, 1708.

[6] (i) Schoo, H. F. M.; Challa, G.; Rowatt, B.; Sherrington, D. C. *React. Polym.* **1992**, *16*, 125. (ii) Krajnc, P.; Leber, N.; Stefanec, D.; Kontrec, S.; Podgornik, A. *J. Chrom. A* **2005**, *69*, 1065.

[7] Silverstein, M. S.; Cameron, N.R.; Hillmyer, M. A. *Porous Polymers* John Wiley & Sons **2011.**

[8] Thomas, A.; Goettmann, F.; Antonietti, M.; *Chem. Mater***. 2008**, *20*, 738.

[9] Bartl, H.; Bonin, W. Von *Makromol. Chem*. **1962**, *57*, 74.

[10] Barby, D.; Haq, Z. *Patent EP060138* **1982**.

[11] Myers, D.; *Surfaces, Interfaces, and Colloids: Principles and Applications*, Wiley- VCH, 2nd Edn. **1999**.

[12] Bancroft, W.D. *J. Phys. Chem*. **1913**, *17*, 501-519.

[13] Becher, P. *Emulsions, Theory and Practice,* Reinhold Publishing Co., New York **1965**, 2.

[14] *The HLB System - a time saving guide to emulsifier selection*. May **1992**, Delaware: ICI Surfactants.

[15] Griffin, W. C. *J. Soc. Cosmet. Chem.* **1949**, *1*, 311.

[16] Griffin, W. C. *J. Soc. Cosmet. Chem.* **1954**, *5*, 249.

[17] Griffin, W. C. *Off. Dig. Fed. Paint Varn. Prod. Clubs* **1956**, *28*, 446.

[18] Sherman, P. *"Emulsion Science"*, Academic Press, New York, **1968**, Chapter 3.

[19] Kuckam P.; Rossi, S.; *Adv. Colloid. Interf. Sci.* **1999**, *82*, 43.

[20] Shinoda, k.; *Proc. Int. Congr. Surface Activ. 5th* **1969**, *2*, 275.

[21] Prince, L. H. *Microemulsions: Theory and Practice*, Academic Press, New York**, 1977**.

[22] Hoar, T. P.; Schulman, J. H.; *Nature* **1943**, *152*, 102.

[23] Cameron, N. R.; Flook, K. J.; Wren, S. A. C. *Chromatographia* **2003**, *57*, 203.

[24] Flook, K. J.; Cameron N. R.; Wren S. A. C. *J. Chromat. A* **2004**, *1044*, 245.

[25] Sundell, M. J.; Pajunen, E. O.; Hormi, O. E. O.; Nasman, J. H. *Chem. Mater*. **1993**, *5*, 372.

[26] Widawaski, G.; Rawiso, M.; Francoise B. *Nature* **1994**, *369*, 387.

[27] Pitois, O.; Francoise. B.; *Eur. Phys. J.- B 1999*, *8*, 225.

[28] Srinivasarao, M.; Colling, D.; Philips, A.; Patel, S. *Science* **2001**, *292*, 79-83.

[29] Bolognesi, A.; Mercogliano, C.; Yunus, S.; Civardi, M.; Comoretto, D.; Turturro, A. *Langmuir* **2005**, *21*, 3480.

[30] Peng, J.; Han, Y.C.; Fu, J.; Yang, Y. M.; Li, B. *Macromol. Chem. Phys*. **2003**, *204*, 125.

[31] Song, L.; Bly, R. K.; Wilson, J. N.; Bakbak, S.; Park, J. O.; Sirinivasarao, M.; Bunz, U. H. F. *Adv. Mater*. **2004**, *16*, 115.

[32] Zhao, B.; Li, C. X.; Lu, Y.; Wang, X. D.; Liu, Z. L.; Zhang, B. H. *Polymer* **2005**, *46*, 9508.

[33] Karthaus, O.; Maruyama, N.; Cieren, X.; Shimomura, M.; Hasegawa, H.; Hashimoto, T. *Langmuir* **2000**, *16*, 6071.

[34] Connal, L.; Gurr, P. A.; Qiao, G. G.; Solomon, D. H. *J. Mater. Chem*. **2005**, *15*, 1286.

[35] Beattie, D.; Wong, K. H., Williams, C.; Poole-Warren, L. A.; Savis, T. P.; Barner Kowollik, C.; Stenzel, M. H. *Biomacromolecules* **2006**, *7*, 1072.

[36] Cameron, N. R.; Sherrington, D.C. *Adv Polym Sci*. **1996**, *126*, 163-214.

[37] Lissant, K. J.; *J. Colloid. Interf. Sci.* **1966**, *22*, 462.

[38] Lissant, K. J.; Pearce; B. W.; Wu, S. H.; Mayhan, K. G. *J. Colloid Interf. Sci.* **1974**, *47*, 416.

[39] Lissant, K. J.; Mayhan, K. G.; *J. Colloid Interf. Sci*. **1973**, *42*, 201.

[40] Kim, K. J.; Ruckenstein, E. *Makromol. Chem. Rapid Commun*. **1988**, *9*, 285.

[41] Ruckenstein, E.; Kim, K. J. *J. Appl. Polym. Sci*. **1988**, *36*, 907.

[42] Ruckenstein, E.; Park, J. S.; *J. Polym. Sci.-C Polym. Lett*. **1988**, *26*, 529.

[43] Kuneida, H.; Evans, D. F.; Solans, N.; Yoshida, M.; *Colloids Surf*. **1990**, *47*, 35.

[44] Kuneida, H.; Yano, N.; Solans, C. *Colloid Surf*. **1989**, *36*, 313.

[45] Kuneida, H.; Solans, C.; Shida, N.; Parra, J. L.; *Colloids Surf*. **1987**, *24*, 225.

[46] Ebert, G.; Platz, G.; Rehange, H. *Phys. Chem. Chem. Phys*. **1988,** *92*, 1158.

[47] Lissant, K. J. *US 3732166*, **1973**.

[48] Lissant, K. J. *US 3700594*, **1972**.

[49] Lissant, K. J. *US 3617095*, **1971**.

[50] Lissant, K. J. *US 3523826*, **1970**.

[51] Lissant, K. J., *Emulsions and Emulsion Technology, Part 1, Marcel Dekker, New York,* **1974**, Chapter-1.

[52] Barbetta, A.; Cameron, N. R.; Cooper, S. J. *Chem. Commun.* **2000**, *3*, 221.

[53] Gregory, M.; Sharples, I.; Tucker, M. *European Patent 299762,* **1989**.

[54] Cameron, N.R. *Polymer* **2005**, *46*, 1439.

[55] Princen, H. M.; Kiss, A. D. *Langmuir* **1987**, *3*, 36-41.

[56] Princen, H. M. *Langmuir* **1986**, *2*, 519-524.

[57] Princen, H. M.; Aronson, M. P.; Moser, J. C. *J. Colloid Interf. Sci.* **1980**, *75*, 246-270.

[58] Princen, H. M. *J. Colloid Interf. Sci.* **1979**, *71*, 55-66.

[59] Williams, J. M. *Langmuir* **1991**, *7*, 1370–1377.

[60] Williams, J. M.; Gray, A. J.; Wilkerson, M. H. *Langmuir* **1990**, *6*, 437.

[61] Williams, J. M.; Wrobleski, D. A. *Langmuir* **1988**, *4*, 656–662.

[62] Williams, J. M. *Langmuir* **1988**, *4*, 44-49.

[63] Ford, R. E.; Furmidge, C. G. L. *J. Colloid Interf. Sci.* **1966**, *22*, 331-334.

[64] Pons, R.; Solans, C.; Stebe, M. J.; Erra, P.; Ravey, J. C. *Prog. Colloid Polym. Sci.* **1992**, *89*, 110–113.

[65] Rajagopalan, V.; Solans, C.; Kunieda, H. *Colloid Polym. Sci.* **1994**, *272*, 1166–1173

[66] Kizling, J.; Kronberg, B. *Colloids Surf.* **1990**, *50*, 131-140.

[67] Chen, H. H.; Ruckenstein, E. *J. Colloid Interf. Sci.* **1990**, *138*, 473-479.

[68] Chen, H. H.; Ruckenstein, E. *J. Colloid Interf. Sci.* **1991**, *145*, 260-269.

[69] Ruckenstein, E.; Ebert, G.; Platz, G. *J Colloid Interf. Sci.* **1989**, *133*, 432-441.

[70] Ruckenstein, E.; Sun, F. *J Appl. Polymer Sci.* **1992**, *46*, 1271-1277.

[71] Mork, S. W.; Rose, G. D.; Green, D. P. *J. Surfact. Deterg.* **2001**, *4*, 127-134.

[72] Zhang, S.; Chen, J. *Polymer* **2007**, *48*, 3021-3025.

[73] Barby, D.; Haq, Z. *EP 60138*, **1982**.

[74] Litt, M. H.; Hsieh, B. R.; Krieger, I. M.; Chen, T. T.; Lu, H. L. *J. Colloid Interf. Sci.* **1987**, *115*, 312-329.

[75] Cameron, N. R.; Sherrington, D. C. *J. Mater. Chem.* **1997**, *7*, 2209-2212

[76] Duke, J. R.; Hoisington, M. A.; Langlois, D. A.; Benicewicz, B. C. *Polymer* **1998**, *39*, 4369-4378.

[77] Hoisington, M. A.; Duke, J. R.; Apen, P. G. *Polymer* **1997**, *38*, 3347-3357.

[78] Livshin, S.; Silverstein, M. S. *Soft Matter* **2008**, *4*, 1630-1638.

[79] Zhang, H.; Cooper, A. I. *Chem Mater* **2002**, *14*, 4017-4020.

[80] Krajnc, P.; Stefanec, D.; Pulko, I. *Macromol Rapid Commun.* **2005**, *26*, 1289-1293.

[81] Kovacic, S.; Stefanec, D.; Krajnc, P. *Macromolecules* **2007**, *40*, 8056-8060.

[82] Kulygin, O.; Silverstein, M. S. *Soft Matter* **2007**, *3*, 1525-1529.

[83] Elmes, A. R.; Hammond, K.; Sherrington, D. C. *European Patent Appl. 0289238;* **1988**.

[84] Even Jr. W. R.; Gregory, D. P. *MRS Bull.* **1994**, *19*, 29.

[85] Edwards C. J. C.; Hitchen D. A.; Sharpies, M. *U.S. Patent 4755655,* **1988**.

[86] Periard, J.; Branderet, A.; Riess, G. *J. Polym. Sci. Polym. Lett.* **1970**, *8*, 109.

[87] Riess, G. *Makromol. Chem. Suppl.* **1985**, *13*, 157.

[88] Sharma M. K. *Prog. Coll. Polym. Sci.* **1978**, *63*, 75.

[89] Sharma, M. K. *Prog. Coll. Polym. Sci.* **1978,** *63*, 87.

[90] Dorfler, H. D.; Swaboda, C.; *Coll. Polym. Sci.* **1993,** *271*, 586.

[91] Meliani, A.; Perez, E, Rico, I.; Lattes, A.; Moisand, A. *New J. Chem.* **1991**, *15*, 871.

[92] Beerbower, A.; Nixon, J.; Wallace, T. J. *J. Aircraft* **1968**, *5*, 367.

[93] Lissant, K. J.; Pearce, B.W.; Wu S. H.; Mayhan K. G. *J. Coll. Interf. Sci.* **1974**, *47*, 416.

[94] E. Ruckenstein, K.J. Kim., *J. Appl. Polym. Sci.* **1988**, 36, 907.

[95] Sun, F.; Ruckenstein, E. *J. Appl. Polym. Sci.* **1993**, *48*, 1279.

[96] Ruckenstein, E.; Kim, K. J. *J. Polym. Sci. Pt. A. Polym. Chem.* **1989**, *27*, 4375.

[97] Ruckenstein, E.; Park, J. S. *Polymer* **1990**, *31*, 2397.

[98] Hong, L.; Ruckenstein, E. *Polymer* **1992**, *33*, 1968.

[99] Ruckenstein, E.; Chen, J. H. *Polymer* **1991**, *32*, 1230.

[100] Ruckenstein, E.; Yang, S. *Polymer* **1993**, *34*, 4655.

[101] Ruckenstein, E.; Yang, S. *Synth. Metals* **1993**, *53*, 283.

[102] Yang, S.; Ruckenstein, E. *Synth. Metals* **1993**, *59*, 1.

[103] Ruckenstein, E. L; Hong *J. Appl. Polym. Sci.* **1994**, *53*, 923.

[104] Li, H.; Ruckenstein, E. *J. Appl. Polym. Sci.* **1994**, *52*, 1949.

[105] Kim, K. J.; Ruckenstein, E. *Macromol. Chem. Rapid Commun*. **1988**, *9*, 285.

[106] Park, J. S.; Ruckenstein, E. *Polymer* **1990**, *31*, 175.

[107] Ruckenstein, E., Park, J.S. *J. Polym. Sci. Polym. Lett.* **1988**, *26*, 529.

[108] Ruckenstein E.; *Coll. Polym. Sci.* **1989**, *267*, 792.

[109] Chen H. H.; Ruckenstein, E. *J. Appl. Polym. Sci.* **1991**, *42*, 2429.

[110] Sun, F.; Ruckenstein, E. *J. Memb. Sci.* **1993**, *81*, 191.

[111] Sun, F.; Ruckenstein. E. *J. Memb. Sci.* **1993**, *85*, 59.

[112] Xu, G.; Ruckenstein E. *J. Appl. Polym. Sci.* **1992**, *46*, 683.

[113] Ruckenstein, E.; Hong, L. *Macromol.* **1993**, *26*, 1363.

[114] Pickering, S. U. *J. Chem. Soc.* **1907**, *91*, 2001-2021.

[115] Menner, A.; Verdejo, R.; Shaffer, M.; Bismarck, A. *Langmuir* **2007**, *23*, 2398-2403.

[116] Menner, A.; Ikem, V.; Salgueiro, M.; Shaffer, M. S. P.; Bismarck, A. *Chem Commun.* **2007**, 4274-4276.

[117] Cameron, N. R. *Polymer* **2005**, *46*, 1439-1449.

[118] Ruckenstein, E.; Hong, L. *Chem. Mater.* **1992**, *4*, 122-127.

[119] Barbetta, A.; Cameron, N. R.; Cooper, S. J. *Chem. Commun.* **2000**, 221-222.

[120] Krajnc, P.; Brown, J. F.; Cameron, N. R. *Organic Lett.* **2002**, *4*, 2497-2500.

[121] Leber, N.; Fay, J. D. B.; Cameron, N. R.; Krajnc, P. *J Polym Sci A Polym Chem* **2007**, *45*, 4043-4053.

[122] Mercier, A.; Deleuze, H.; Mondain-Monval, O. *React Funct Polym* **2000**, *46*, 67-79.

[123] Mercier, A.; Kuroki, S.; Ando, I.; Deleuze, H.; Mondain-Monval, O *J. Polym. Sci. B Polym. Phys.* **2001**, *39*, 956-963.

[124] Mercier, A.; Deleuze, H.; Mondain-Monval, O. *Macromol Chem. Phys.* **2001**, *202*,2672-2680.

[125] Deleuze, H.; Maillard, B.; Mondain-Monval, O. *Bioorg Med. Chem. Lett.* **2002**, *12*,1877-1880.

[126] Krajnc, P.; Leber, N.; Stefanec, D.; Kontrec, S.; Podgornik, A. *J. Chromatogr A* **2005**,*1065*, 69-73.

[127] Stefanec, D.; Krajnc, P. *Polym Int.* **2007**, *56*, 1313-1319.

[128] Pulko, I.; Kolar, M.; Krajnc, P. *Sci Total Environ* **2007**, *386*, 114-123.

[129] Livshin, S.; Silverstein, M. S. *J. Polym. Sci. A Polym. Chem.* **2009**, *47*, 4840-4845.

[130] Moine, L.; Deleuze, H.; Maillard, B. *Tetrahedron Lett.* **2003**, *44*, 7813-7816.

[131] Cetinkaya, S.; Khosravi, E.; Thompson, R. *J. Mol. Catal. A Chem.* **2006**, *254*, 138-144.

[132] Fern´andez-Trillo, F.; van Hest, J. C. M.; Thies, J. C.; Michon, T.; Weberskirch, R.; Cameron, N. R. *Adv. Mater.* **2009**, *21*, 55-59.

[133] Okay, O. *Prog. Polym. Sci.* **2000**, *25*, 711.

[134] Seidl, J.; Malinsky, J.; Dusek, K.; Heitz, W. *Adv. Polym. Sci.* **1967**, *5*, 113.

[135] Dusek, K.; Haward, In: E. N.; Editor. *Developments in polymerization, Applied Science, London* **1982**, *3*,143.

[136] Haupke, K.; Schwachula, G. *Plaste und Kautschuck* **1985**, *2*, 48.

[137] Sing, K. S. W.; Everett, D.H.; Haul R. A. W.; Moscou L.; Pierotti R. A.; Rouquerol, J.; Siemieniewska, T. *Pure Appl. Chem.* **1985.** *57*, 603.

[138] Sherrington, D.C.; Hodge, P. *Syntheses and separations using functional polymers Wiley, New York,* **1989**.

[139] Jacobelli, H.; Bartholin, M.; Guyot, A. *J. Appl. Polym. Sci.* **1979**, *23*, 927.

[140] Cheng, C.M.; Micale, F. J.; Vanderhoff, J. W.; El-Aasser, M. S. *J. Coll. Interf. Sci.* **1992**, *150*, 549.

[141] Williams, J. M.; Wrobleski, D. A.; *Langmuir* **1988**, *4*, 656.

[142] Williams, J. M.; Gray, A. J.; Wilkerson, M. H. *Langmuir* **1990**, *6*, 437.

[143] Hainey, P.; Huxham, I. M.; Rowatt, B.; Sherrington, D. C.; Tetley. L.; *Macromol.* **1991**, *24*, 117.

[144] Barbetta, A.; Cameron, N. R. *Macromol.* **2004**, *37*, 3188.

[145] Zhang, H.; Cooper, A. I.; *Chem. Mater.* **2002**, *14*, 4017.

[146] Sergienko, Y.; Tai, H.; Narkis, M.; Silverstein, M. S.; *J. Appl. Polym. Sci.* **2004**, *94*, 2233.

[147] DesMarias, T.A.; Stone, K. J.; Dyer, J.C.; Hird, B.; Goldman, S. A.; Peace, M. R. *PCT Patent 9621680 A1* **1996**.

[148] Hainey, P.; Huxham, I. M.; Rowatt, B.; Sherrington, D. C.; Tetley, *Macromolecules* **1991**, *24*, 117-121.

[149] Cameron, N. R.; Barbetta, A.; *J. Mater. Chem.* **2000**, *10*, 2466-2472.

[150] Barbetta, A.; Cameron, N. R. *Macromolecules* **2004**, *37*, 3188-3201.

[151] Barbetta, A.; Cameron, N. R. *Macromolecules* **2004**, *37*, 3202-3213.

[152] Richez, A.; Deleuze, H.; Vedrenne, P.; Collier, R. *J. Appl. Polymer Sci.* **2005**, *96*, 2053-2063.

[153] Jerabek, K.; Pulko, I.; Soukupova, K.; Stefanec, D.; Krajnc, P. *Macromolecules* **2008**, *41*, 3543-3546.

[154] Schwab, M. G.; Senkovska, I.; Rose, M.; Klein, N.; Koch, M.; Pahnke, J.; Jonschker, G.; Schmitz, B.; Hirscherd, M.; Kaskel, S. *Soft Matter* **2009**, *5*, 1055-1059.

[155] Zhang, L.; Tang, Y. J.; Zhong, C. F.; Luo, X. A.; Zhang, H. Q. *Nucl. Instr. Meth. Phys. Res. A Accel. Spectrom Detect. Assoc. Equip.* **2002,** *480*, 242-245.

[156] Small, P. W.; Sherrington, D. C. *J. Chem. Soc. Chem. Commun.* **1989**, 1589-1591

[157] Schoo, H. F. M.; Challa, G.; Rowatt, B.; Sherrington, D. C. *React Polym* **1992**, *16*,125-136.

[158] Ruckenstein, E.; Hong, L. *Chem. Mater.* **1992**, *4*, 122-127.

[159] Hitchen, D. A. *EP 365327*, **1993**.

[160] Ruckenstein, E.; Wang, X. B. *Biotechnol Bioeng.* **1994**, *44*, 79-86.

[161] Ruckenstein, E.; Wang, X. *Biotechnol Bioeng.* **1993**, *42*, 821-828.

[162] Krajnc, P.; Leber, N.; Stefanec, D.; Kontrec, S.; Podgornik, A. *J. Chromatogr. A* **2005**,*1065*, 69-73.

[163] Junkar, I.; Koloini, T.; Krajnc, P.; Nemec, D.; Podgornik, A.; Strancar, A. *J. Chromatogr. A* **2007**, *1144*, 48-54.

[164] Benicewicz, B. C.; Jarvinen, G. D.; Kathios, D. J.; Jorgensen, B. S. *J Radioanal. Nucl. Chem.* **1998**, *235*, 31-35.

[165] Wakeman, R. J.; Bhumgara, Z. G.; Akay, G. *Chem. Eng. J* **1998**, *70*, 133-141.

[166] Ottens, M.; Leene, G.; Beenackers, A.; Cameron, N.; Sherrington, D. C. *Ind Eng. Chem. Res.* **2000**, *39*, 259-266.

[167] Krajnc, P.; Leber, N.; Brown, J. F.; Cameron, N. R. *React Funct. Polym.* **2006**, *66*, 81-91.

[168] Krajnc, P.; Stefanec, D.; Brown, J. F.; Cameron, N. R. *J. Polym. Sci. A Polym. Chem.* **2005**, *43*, 296-303.

[169] Brown, J. F.; Krajnc, P.; Cameron, N. R. *Ind. Eng. Chem. Res.* **2005**, *44*, 8565-8572.

[170] Pierre, S. J.; Thies, J. C.; Dureault, A.; Cameron, N. R.; van Hest, J. C. M.; Carette, N.; Michon, T.; Weberskirch, R. *Adv. Mater.* **2006**, *18*, 1822-1826.

[171] Chemin, A.; Mercier, A.; Deleuze, H.; Maillard, B.; Mondain-Monval, O. *J. Chem. Soc. Perkin Trans* **2001**, *1*, 366-370.

[172] Mercier, A.; Deleuze, H.; Maillard, B.; Mondain-Monval, O. *Adv. Synth. Catal.* **2002**, *344*, 33-36.

[173] Zhang, H.; Cooper, A. I. *Adv. Mater.* **2007**, 19, 2439-2444.

[174] Sergienko, A. Y.; Tai, H. W.; Narkis, M.; Silverstein, M. S. *J. Appl. Polym. Sci.* **2002**, *84*, 2018–2027.

[175] Su, F.; Bray, C. L.; Tan, B.; Cooper, A. I. *Adv. Mater.* **2008**, *20*, 2663-2666.

[176] Hayman, M. W.; Smith, K. H.; Cameron, N. R.; Przyborski, S. A. *Biochem. Biophys. Res. Commun.* **2004**, *314*, 483.

[177] Akay, G.; Birch, M. A.; Bokhari, M. A. *Biomaterials* **2004**, *25*, 3991.

[178] Bokhari, M. A.; Akay, G.; Zhang, S. G.; Birch, M. A.; *Biomaterials* **2005**, *26*, 5198.

[179] Barbetta A.; Dentini, M. E.; Zannoni, M.; De Stefano, M. E. *Langmuir* **2005**, *21*, 12333.

[180] Christenson, E. M.; Soofi, W.; Holm, J. L.; Cameron, N. R.; Mikos, A. G.; *Biomacromolecules* **2007**, 8 , 3806.

[181] Lumelsky, Y.; Silverstein, M. S. *Macromolecules* **2009**, *42*, 1627.

[182] Gan, L. M.; Lian, N.; Chew, C. H.; Li, G. Z. *Langmuir* **1994**, 10, 2197.

[183] Xu, X. J.; Chew, C. H.; Siow, K. S.; Wong, M. K.; Gan, L. M. *Langmuir* **1999**, *15*, 8067.

[184] Stoffer, J. O.; Bone, T. *J. Polym. Sci. A Polym. Chem.* **1980**, *18*, 2641.

[185] Atik, S. S.; Thomas, J. K. *J. Am. Chem. Soc.* **1981**, *103*, 4279.

[186] Haque, E.; Qutubuddin, S. *J. Polym. Sci. C Polym. Lett.* **1988**, *26*, 429.

[187] Menger, F. M.; Tsuno, T.; Hammond, G. S. *J. Am. Chem. Soc.* **1990**, *112*, 1263.

[188] Gan, L. M., Chew, C. H. *J. Dispers. Sci. Technol.* **1984**, *5*, 179.

CHAPTER - II

Aims and Objectives

2.1 Aims and objectives

The objective of this thesis was focused on the study of polymers synthesized using high internal phase emulsion methodology in the form of monoliths. The purpose to use this methodology was to synthesize polymers having different functional groups having high pore volume and interconnected pore structure. Porous polymers synthesized using conventional synthesis methods have pores distributed in irregular patterns within the polymer matrix, while HIPE method has the advantage of formation of interconnected pores. The work emphasized to synthesize polyHIPEs to study their properties and potential use as porous polymeric supports. Polymers were synthesized using monomers having different functional constituents like acrylates, methacrylates, styrene, acrylonitrile and crosslinker such as divinylbenzene.

Experiments were designed to prepare the polyHIPEs based on acrylate monomers like ethylhexyl acrylate, ethylhexyl methacrylate and ethylene glycol dimethacrylate. The effects of different reaction parameters like initiator concentration, inhibitor concentration, salt type and concentration and porogen were evaluated. The effect of these parameters on polyHIPE morphology and the mechanical properties was evaluated. Stability of HIPE was evaluated at different time intervals. The yield stress values of the acrylate-based polyHIPEs were affected profoundly by using different water-soluble initiators. An attempt to generate the kinetic profile of the HIPE polymerization was made. The effect of initiator as well as inhibitor type and concentration on the rate profile was evaluated. The generated kinetic data at various initiator and inhibitor concentration at different temperatures was modeled using a

phenomenological model. The results obtained were in good agreement with the experimental data.

Experiments were designed to study the effect of reaction variables on the formation and stability of styrene based HIPE emulsions as well as morphology of the polyHIPEs formed. Surfactant type is an important parameter in designing the architecture of HIPE polymers. The first step was to study the effect of different surfactants on HIPE formation and stability. It is well known that stable water in oil emulsions are formed using nonionic surfactants and high ratios of aqueous discontinuous phase. The task of the present work was to check the feasibility of the use of ionic surfactant in comparison with nonionic surfactant to form stable water in oil HIPEs in case of styrene and divinyl benzene monomers. The effect of low ratios of discontinuous water phase with respect to oil phase in comparison with higher ratios on HIPE formation, stability and morphology of the polymers was studied. The pores generated after HIPE polymerization become unique due to their dimensions and structure. The use of these pores was employed to study the viability of the polymers as supports to incorporate inorganic particles inside the polymer matrix. Protocols were established to incorporate cadmium sulphide particles in the poly (styrene-divinylbenzene) matrix. Studies were carried out to correlate the strategies to incorporate CdS particles in the polyHIPE matrix.

It is well known that hydrophobic monomers can easily form water in oil HIPEs. Experiments were done to study HIPE methodology wherein one of the monomer is hydrophilic in nature. HIPE emulsion, stability and morphology based on use of acrylonitrile monomer along with divinylbenzene as crosslinker was studied. The effect

of variance in reaction parameters on the emulsion and polymer characteristics was studied. The effect of use of porogens on the surface area of the polymer was studied. The nitrile functionality present in the poly (acrylonitrile-divinyl benzene) matrix was post modified into amidoxime functionality that can be used as metal chelants. The synthesized porous poly (acrylonitrile-divinylbenzene) monoliths were tested for their efficiency for chromium adsorption. The effect of variation in synthesis parameters on the efficiency as supports for adsorption was studied.

CHAPTER - III

Synthesis, characterization and polymerization kinetics of acrylate based polyHIPEs

3.1 Introduction

Macroemulsions can be applied as templates for porous polymers if sufficiently stable to allow for the polymerization of the monomer phase. To prepare monolithic materials with an interconnected cellular structure, an emulsion with a sufficiently high volume ratio of internal phase is essential. Emulsions, where the volume fraction of the internal phase exceeds the volume fraction of most densely packed equal spheres (74.05%) are termed as high internal phase emulsions (HIPEs) and materials produced from their polymerization as polyHIPEs. There is growing interest in such materials due to their specific, hierarchically porous structure and their application in various fields.

Polymerization of these water-in-oil (W/O) HIPEs results in extremely porous (up to 90% pore volume) hydrophobic polymers in monolithic form. They form readily by slowly adding water to a stirred solution of oil phase having monomers and surfactant of low HLB value. The aqueous internal or discontinuous phase consists of small droplets having size of approximately 10 μm. Polymerization occurs around emulsion droplets, which creates voids in the final material. The void fraction is very high and can reach levels upto 0.99. Complete removal of the aqueous phase after polymerization leaves behind monolithic polyHIPE polymer with interconnected cellular structures and an overall low bulk density. Varying the composition such as monomers, amount of crosslinker, surfactant and oil : water ratio can control morphological features of the resulting porous materials such as void diameter and interconnectivity of the pores. Use of either a precipitating porogen or a solvating porogen in the monomer oil phase, a secondary pore structure can be generated within the cell ‘walls’ of the polyHIPE

polymers. The transition from discrete emulsion droplets to interconnected cells was observed to occur around the gel-point of the polymerizing system. This would suggest that the formation of holes between neighbouring cells is due to the contraction of thin monomeric films on conversion of monomer to polymer, as a result of the entropic forces and conformational restrictions of the latter. Macroporous crosslinked polymers are effective efficient materials for many separation processes and therefore they have wide applications. Addition of porogens in the oil phase was found to generate macroporous polymers. Polymers having high crosslinker concentration are mechanically more stable and provide larger pore structures. Structuring solvents, non-solvents or linear polymers acts as porogens during polymerization.

Soft and rubbery materials can be produced from hydrophobic long chain functional monomers. Present work deals with studies of two types of systems having different combinations of long chain acrylates. The systems are as (i) 2-ethylhexyl acrylate (EHA), 2-ethylhexyl methacrylate (EHMA) and ethylene glycol dimethacrylate (EGDMA) and (ii) 2-ethylhexyl acrylate (EHA) and ethylene glycol dimethacrylate (EGDMA). An attempt was made (i) to study the effect of variation in composition on the properties of HIPEs and polyHIPEs (emulsion stability, polymer morphology and mechanical properties) and (ii) to study the kinetics of HIPE polymerization and develop a phenomenological model to predict the rate parameters of HIPE polymerization using the generated kinetics data. The compositional variations used for morphological studies were initiator type and concentration, stabilizer type, surfactant concentration, porogens and water soluble polymers. Polymerization kinetics data was generated using different initiator concentrations, different pH, inhibitor concentration and temperature.

3.2 Synthesis and characterization of acrylate polyHIPEs

3.2.1 Experimental

3.2.1.1 *Materials*

2-Ethylhexyl acrylate (EHA), 2-ethylhexyl methacrylate (EHMA), ethylene glycol dimethacrylate (EGDMA), di(hydrogenated tallow alkyl)dimethyl ammonium chloride(Arquad 2HT-75) and 1- Eicosanol (from Aldrich); sorbitan monooleate-Span 80, sodium peroxy disulphate (NaPS), ammonium peroxydisulphate (APS) and potassium peroxy disulphate (KPS) (from Loba Chemie); decanol, 1-hexadecanol, calcium chloride ($CaCl_2$) and sodium chloride (NaCl) (from Merck) were used as received. De-ionized water was collected from Millipore unit. The HLB values of Span 80 and Arquad 2HT-75 are 4.3 and 13.0 respectively.

3.2.1.2 *Preparation of polyHIPEs*

A range of polyHIPE monoliths of two different monomer compositions were prepared by polymerization of HIPEs. A combination of two surfactants nonionic and ionic was used for HIPE preparation. Span 80 and Arquad HT-75 were chosen as surfactants for HIPE formation. Experiments were carried out for the preparation of polyHIPE monoliths with variation in reaction parameters. The synthesis details are tabulated in Tables 3.1 to 3.5. A general procedure for polyHIPE preparation is as follows.

3.2.1.3 *Procedure*

The requisite amount of oil phase comprising of monomers and surfactant was taken in a 50 mL plastic container. The aqueous discontinuous phase was prepared by dissolving calcium chloride (4 wt%) in the requisite quantity of deionized water. The aqueous phase was transferred to a double walled jacketed dropping funnel having a temperature of 65^{o}C which is controlled by a constant temperature circulating water bath. The aqueous phase was then added slowly to the oil phase under a constant stirring having speed of 1400 rotation per minute. HIPE formation took place gradually until the complete addition of aqueous phase at the same rate. After complete addition of aqueous phase the initiator sodium peroxydisulphate (0.05 wt% dissolved in 1 mL water) was added to the HIPE formed and the reaction mixture was mixed thoroughly for 1 min (1 mL water was inclusive of total water used). The formed emulsions were polymerized at 65^{o}C by keeping them in a constant temperature water bath. The polymerization was continued for a period of 8 hours.

After the polymerization was over, the polyHIPE monolith was cut in the form of discs of 15 mm diameter and 5 mm thickness dimension. The discs were then washed several times with water to remove the $CaCl_2$ present in the monolith. The monolithic discs were dried in the air oven at 60^{o}C.

The polyHIPEs prepared were labeled as PH3A and PH2A. PH3A series polyHIPEs prepared using three monomers viz. EHA, EHMA and EGDMA and PH2A represents polyHIPEs prepared using two monomers viz. EHA and EGDMA.

Table 3.1 Synthesis of PH3A and PH2A monoliths varying the persulphate type and concentration.

Polymer Code	NaPS Wt%	APS Wt%	KPS Wt%
PH3A-1, PH2A-1	0.05	-	-
PH3A-2, PH2A-2	0.20	-	-
PH3A-3, PH2A-3	-	0.05	-
PH3A-4, PH2A-4	-	0.20	-
PH3A-5, PH2A-5	-	-	0.05
PH3A-6, PH2A-6	-	-	0.20

[PH3A- polyHIPE using EHA, EHMA and EGDMA and PH2A-polyHIPE using EHA and EGDMA]

PH3A: 2-Ethylhexyl acrylate (EHA) = 0.74 g (0.0040 mol); 2-ethylhexyl methacrylate (EHMA) = 0.76 g (0.0038 mol); ethylene glycol dimethacrylate (EGDMA) = 0.35 g (0.0018 mol); water = 54 mL (oil : water ratio = 1: 27); $CaCl_2$ = 2.16 g (4 wt.% on aqueous); Span-80 = 0.13 g (6.5% on oil phase); Arquad 2HT-75 = 0.016 (0.8% on oil phase); NaPS = KPS = APS = 0.027 g (0.05 wt% on aqueous) and 0.108 g (0.2 wt% on aqueous); Temperature = 65ºC; stirring speed =1400 rotation per minute.

PH2A: 2-Ethylhexyl acrylate (EHA) = 0.721 g (0.0078 mol); ethylene glycol dimethacrylate (EGDMA) = 0.215 g (0.0022 mol); water = 48 mL (oil: water ratio = 1: 24), $CaCl_2$ = 1.92 g (4 wt.% based on aqueous phase), Span-80 = 6.94% based on oil phase; Arquad 2HT-75 = 0.85% based on oil phase; NaPS = KPS = APS = 0.024 g (0.05 wt% on aqueous) and 0.096 g (0.2 wt% on aqueous); Temperature = 65ºC; Stirring speed =700 rotation per minute.

(APS = ammonium peroxydisulphate; NaPS = Sodium peroxydisulphate; KPS = Potassium peroxydisulphate)

Table 3.2 Synthesis of PH3A polyHIPE monoliths using different salts and salt concentration

Polymer Code	Initiator NaPS conc. (Wt %)	$CaCl_2$ Wt%	NaCl Wt%
PH3A-1	0.05	4	-
PH3A-8.1/ PH3A-8.2	0.05/0.20	-	1
PH3A-9.1/ PH3A-9.2	0.05/0.20	-	2
PH3A-10.1/ PH3A-10.2	0.05/0.20	-	3
PH3A-11.1/ PH3A-11.2	0.05/0.20	-	4
PH3A-12.1/ PH3A-12.2	0.05/0.20	-	5
PH3A-13.1/ PH3A-13.2	0.05/0.20	-	6

2-Ethylhexyl acrylate (EHA)= 0.74 g (0.0040 mol), 2-ethylhexyl methacrylate (EHMA)=0.76 g (0.0038 mol); ethylene glycol dimethacrylate (EGDM)=0.35 g (0.0018 mol); water = 54 mL (oil : water ratio= 1: 27), $CaCl_2$ = 2.16 g (4 wt.% on aqueous phase); NaCl = 1, 2, 3, 4, 5 and 6 wt% on aqueous phase; Span-80 = 0.13 g (6.5%); Arquad 2HT-75 =

0.016 (0.8%); NaPS - sodium peroxydisulphate =0.027 g (0.05 wt% on aqueous phase) and 0.108 g (0.2 wt% on aqueous phase); Temperature = 65ºC; Stirring speed =1400 rotation per minute.

Table 3.3 Synthesis of PH2A polyHIPE monoliths using octanol, decanol and hexadecanol as porogens with decrease in surfactant concentration

Polymer Code	Total surfactant conc. (Wt%)	Total surfactant conc. (Wt%)	Porogen-Octanol (Wt%)	Porogen-decanol (Wt%)	Porogen-hexadecanol (Wt%)
PH2A-1	7.3	-	-	-	-
PH2A-7	-	2.2	10	-	-
PH2A-8	-	2.2	50	-	-
PH2A-9	-	2.2	300	-	-
PH2A-10	-	2.2	-	10	-
PH2A-11	-	2.2	-	50	-
PH2A-12	-	2.2	-	300	-
PH2A-13	-	2.2	-	-	10
PH2A-14	-	2.2	-	-	50
PH2A-15	-	2.2	-	-	300

PH2A: 2-Ethylhexyl acrylate (EHA) = 0.721 g (0.0078 mol); ethylene glycol dimethacrylate (EGDMA) = 0.215 g (0.0022 mol); water = 48 mL (oil: water ratio = 1: 24), $CaCl_2$ = 1.92 g (4 wt.% based on aqueous phase), Span-80 = 6.94% based on oil phase; Arquad 2HT-75 = 0.85% based on oil phase; NaPS = 0.024 g (0.05 wt% on aqueous) and 0.096 g (0.2 wt% on aqueous); Temperature = 65ºC; Stirring speed =700 rotation per minute.

Table 3.4 Synthesis of PH3A polyHIPE monoliths using decanol, hexadecanol and 1-eicosanol as porogens with decrease in surfactant concentration

Polymer Code	Total surfactant conc. (Wt%)	Total surfactant conc. (Wt%)	Porogen-Decanol (Wt%)	Porogen-hexadecanol (Wt%)	Porogen-Decanol (W%)
PH3A-1	7.3	-	-	-	-
PH3A-14	-	2.2	5	-	-
PH3A-15	-	2.2	10	-	-
PH3A-16	-	2.2	300	-	-
PH3A-17	-	2.2	-	1	-
PH3A-18	-	2.2	-	10	-
PH3A-19	-	2.2	-	300	-
PH3A-20	-	2.2	-	-	1
PH3A-21	-	2.2	-	-	5
PH3A-22	-	2.2	-	-	20

PH3A- 2-Ethylhexyl acrylate (EHA)= 0.74 g (0.0040 mol), 2-ethylhexyl methacrylate (EHMA)=0.76 g (0.0038 mol); ethylene glycol dimethacrylate (EGDM)=0.35 g (0.0018 mol; Water = 54 mL (oil : water ratio= 1: 27), $CaCl_2$ = 2.16 g (4 wt.%), Span-80) = 0.13 g (6.5%), 0.0782 g (3.91%) and 0.0392 g (1.96%) ; Arquad 2HT-75 = 0.016 g (0.8%), 0.0096 g (0.48%) and 0.0048 g (0.24%) ; NaPS = Sodium peroxydisulphate = 0.027 g (0.05 wt% on aqueous phase); Temperature = 65ºC; Stirring speed =1400 rotation per minute.

Table 3.5 Synthesis of PH3A polyHIPE monoliths in presence of water soluble polymers.

Polymer Code	Water soluble polymer (Wt%)		Salt (Wt%)		Yield stress (psi)
	Gum Acacia Guar Gum	Sodium Alginate	$CaCl_2$	NaCl	
PH3A-23	0.1	-	4		1.070
PH3A-24	0.2	-	4		0.865
PH3A-25	0.3	-	4		0.668
PH3A-26	0.5	-	4		0.525
PH3A-27	-	0.1		1	1.140
PH3A-28	-	0.1		2	1.243
PH3A-29	-	0.1		3	1.208
PH3A-30	-	0.1		5	1.139
PH3A-31	-	0.3		1	0.760
PH3A-32	-	0.3		2	0.804
PH3A-33	-	0.3		3	0.834

PH3A- 2-Ethylhexyl acrylate (EHA)= 0.74 g (0.0040 mol), 2-ethylhexyl methacrylate (EHMA)=0.76 g (0.0038 mol); ethylene glycol dimethacrylate (EGDM)=0.35 g (0.0018 mol; Water = 54 mL (oil : water ratio= 1: 27), $CaCl_2$ = 2.16 g (4 wt.%), Span-80) = 0.13 g (6.5%),; Arquad 2HT-75 = 0.016 g (0.8%),; NaPS - Sodium peroxydisulphate = 0.027 g (0.05 wt% on aqueous phase); Temperature = 65ºC; Stirring speed =1400 rotation per minute.

3.2.2 Characterization

The morphology of the HIPE emulsions formed were studied using optical microscopy. The polyHIPEs formed were studied for their morphology and mechanical properties.

3.2.2.1 *Emulsion study - optical microscopy*

The HIPE emulsion before polymerization was characterized for its formation and structure elucidation by an OLYMPUS polarized optical microscope at a magnification of 50X. The microphotographs were recorded using OLYMPUS digital camera.

3.2.2.2 *Monolith morphology - scanning electron microscopy (SEM)*

The surface morphologies of the polyHIPE prepared was studied using a Lieca Stereoscan 440 scanning electron microscope at different magnifications. The energy of analysis was 20 keV.

3.2.2.3 *Mechanical properties - RSA-III DMA*

Stress-strain behaviour and the yield stress of the polymers was evaluated using RSA-III dynamic mechanical analyzer from TA instruments. Yield stress was determined using the multiple extension mode with compression rate of 0.1%/sec upto 60% compression. Average yield stress value was evaluated for each composition.

3.2.3 Results and discussion

Due to several physicochemical processes, which occur during polyHIPE preparation, the resulting material's morphology is rather unique and has a hierarchical pore distribution. The materials have spherical pores that have roughly the same diameter as the droplets of the precursor HIPE. This is governed by the thermodynamics of the polymer gel phase separation from the continuous phase and the delicate equilibrium of the emulsion phase separation versus droplet stabilization.

From the studies, it was found that internal phase volume ratio played a role in HIPE formation but the initiator type, surfactant concentration and porogens in fact played an important role in designing of porous architecture within the polymer matrix. Formation of porous structure depends on the initial droplet formation which is further dependent on the HLB value of the nonionic surfactant.

3.2.3.1 *HIPE stability studies*

Several acrylate based HIPEs were prepared using different compositions. Time dependent stability of the emulsion formed in case of PH3A composition (Oil Phase: EHA, EHMA and EGDMA and 1:27 oil : water ratio) was studied. The emulsion stability was checked by observing the HIPE formed under optical microscope at different time intervals of 10 min, 1, 20, 25, 42 and 52 h as shown in Figure 3.1. It was observed that the emulsion formed for PH3A-1 composition was quite stable even after 52 h.

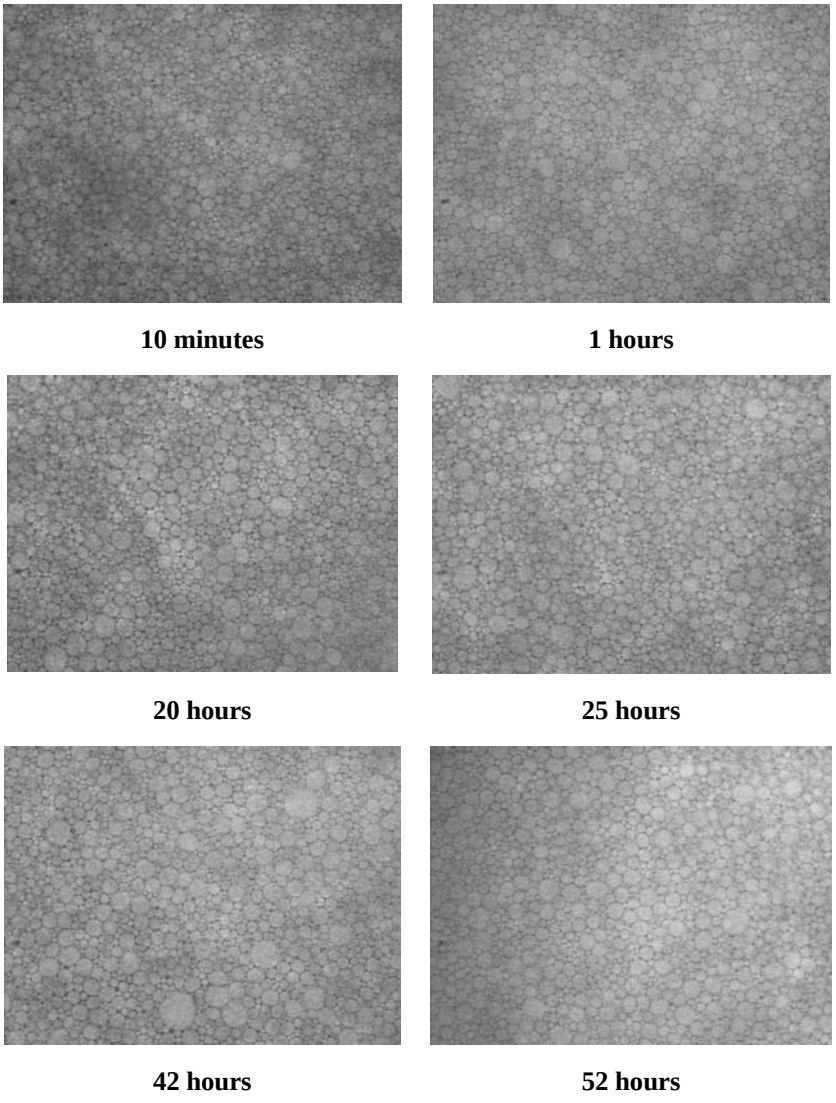

Figure 3.1 : Effect of time on the stability of PH3A HIPE emulsion

3.2.3.2 *Effect of initiator type*

The initiator is generally either oil or water-soluble or a combination of both. In case of an oil-soluble initiator, the initiator is dissolved in the monomeric phase prior to emulsification. In case of water-soluble initiator, it is dissolved to be a part of aqueous discontinuous phase followed by formation of free radicals at elevated temperatures.

The effect of different types of persulphate initiators and their concentration on polyHIPEs were studied. The initiators employed in the present investigation were ammonium peroxydisulphate (APS), sodium peroxydisulphate (NaPS) and potassium peroxydisulphate (KPS). Emulsions were prepared using 0.05 wt% and 0.2 wt% of NaPS, APS and KPS for two different monomeric compositions of PH3A and PH2A. At the dissociation temperature of the initiator, the free radicals generated in the aqueous phase travels across the water phase and diffuse into the oil phase to initiate polymerization of the monomers. Figure 3.2 depicts the morphology of PH3A monoliths synthesized using different persulphate initiators having a concentration of 0.05 wt% with respect to aqueous discontinuous phase. From the SEM data it was observed that the cell size is in the range of 2-20 μm having an average size of 10-12 μm. In case of polymers synthesized using APS and KPS as initiators it was observed that the cell wall was thick as compared to polymers synthesized using NaPS. This was reflected in yield stress values of the polyHIPEs. The yield stress values observed were 1.249, 1.315 and 1.323 psi for polymers synthesized using NaPS, KPS and APS initiators respectively.

Figure 3.3 depicts the morphology of PH3A monoliths synthesized using different persulphate initiators having a concentration of 0.20 wt% with respect to aqueous discontinuous phase. Similar trend was observed in the morphology and as well as yield stress values. The yield stress values observed were 1.351, 1.496 and 1.476 psi for polymers synthesized using NaPS, KPS and APS initiators respectively. It was observed that with an increase in initiator concentration the yield stress value also increased for all the three type of persulphates. Increase in initiator concentration leads to enhancement in rate of polymerization of the monomers giving rigidity to the polymer structure.

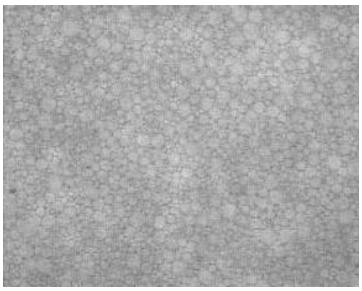

Optical microscopy of HIPE before initiator addition (50X)

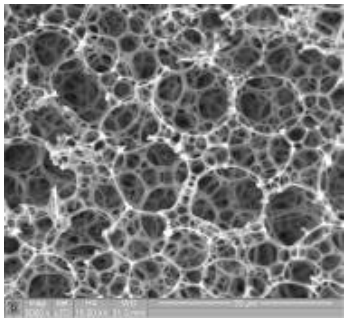

NaPS

Yield Stress – 1.249

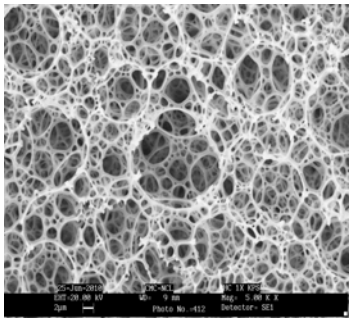

KPS

Yield Stress – 1.315

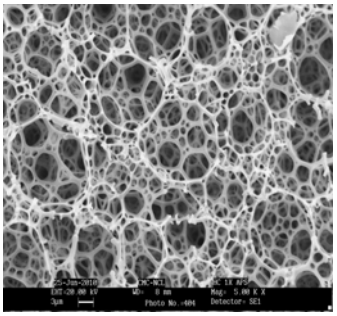

APS

Yield Stress – 1.323

5000X

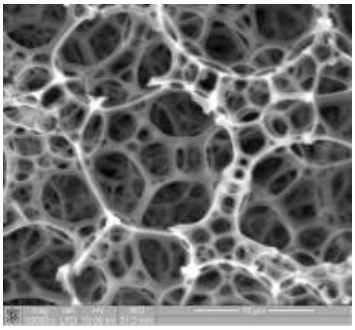

NaPS

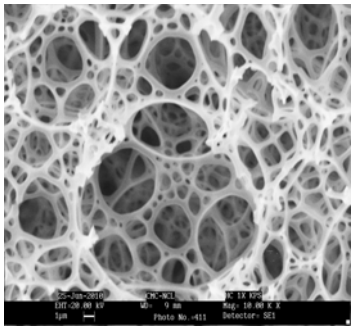

KPS

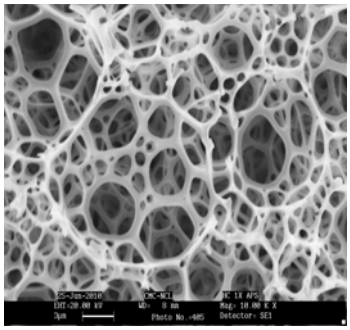

APS

10 KX

Figure 3.2 : Effect of initiator type on morphology and yield stress values of PH3A monoliths using 0.05 wt% initiator concentration

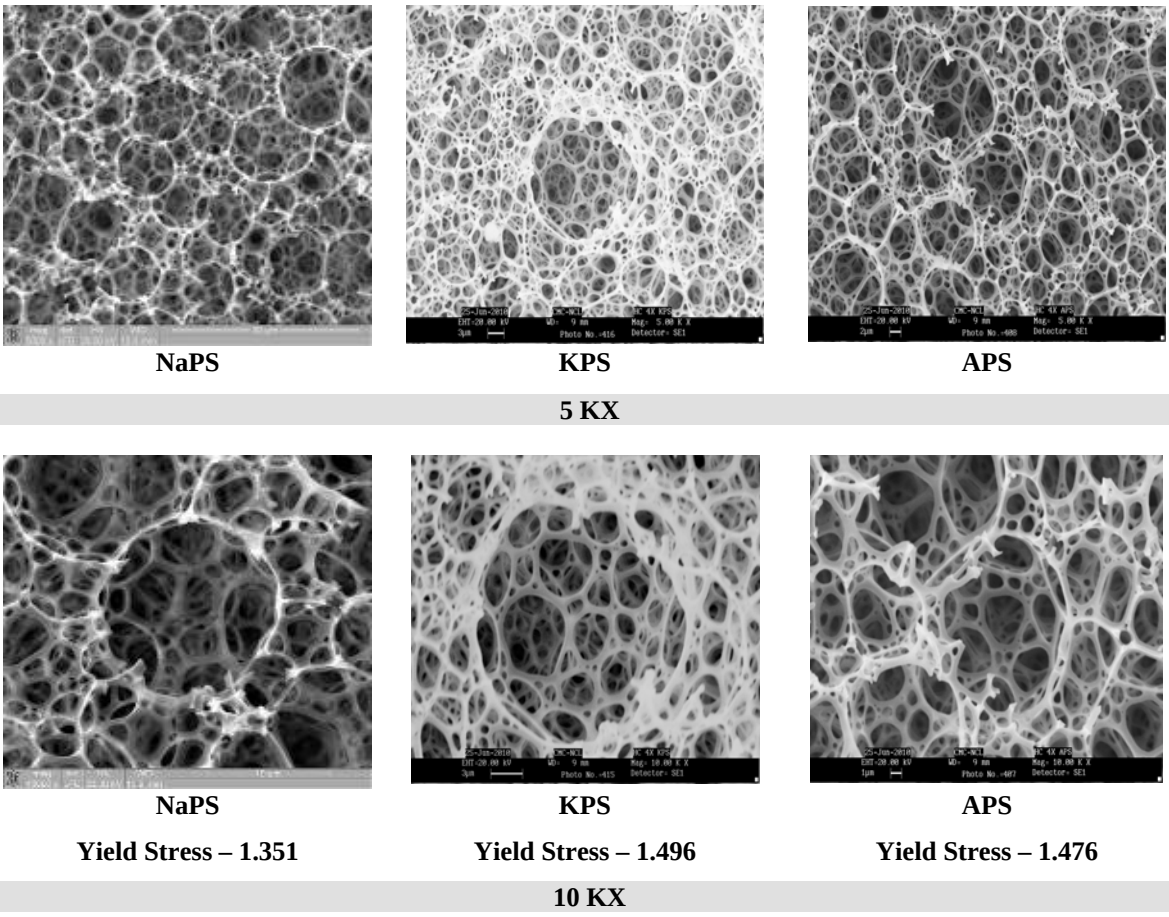

Figure 3.3 : Effect of initiator type on morphology and yield stress values of PH3A monoliths using 0.2 wt% initiator concentration

Figure 3.4 shows the effect of initiator type on the morphology and the yield stress values of the monoliths synthesized for PH2A composition. No significant change in morphology was observed in case of NaPS, KPS and APS. The yield stress values observed were 0.566, 0.589 and 0.587 psi for polymers synthesized using NaPS, KPS and APS initiators having 0.05 wt% initiator concentration respectively. For polymers synthesized using 0.2 wt% initiator concentration, the yield stress values were 0.580, 0.593 and 0.640 respectively for NaPS, KPS and APS. The yield stress values were on the lower side in comparison with to the PH3A monoliths. PH2A monoliths comprised of

only two monomers viz EHA and EGDMA while PH3A monoliths comprised of three monomers viz EHA, EHMA and EGDMA.

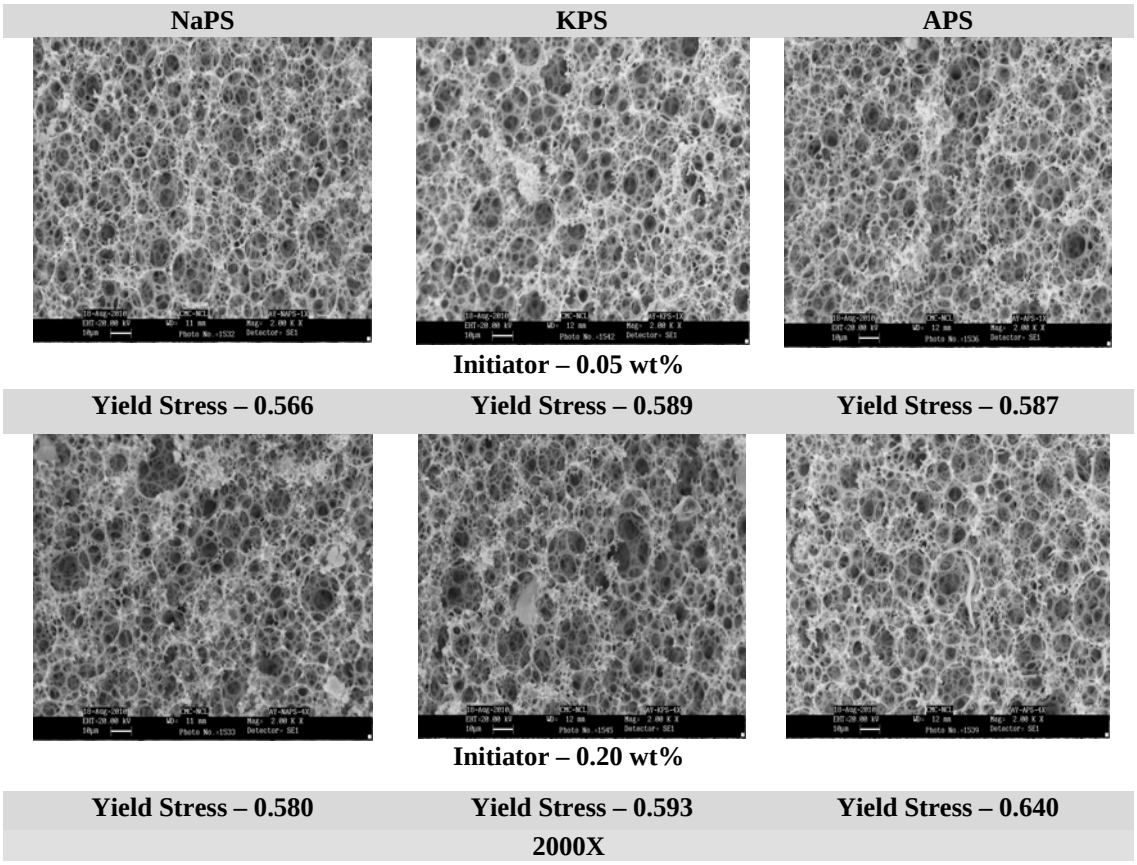

Figure 3.4 : Comparison of effect of initiator type on morphology of PH2A monoliths using 0.05 wt% and 0.2 wt% initiator concentration

3.2.3.3 *Effect of salt type and concentration*

Monoliths were synthesized using sodium chloride (NaCl) as an electrolyte instead of calcium chloride ($CaCl_2$) dissolved in aqueous phase. NaCl was used at different concentrations viz. 1, 2, 3, 4 and 6 wt% based on aqueous phase. The synthesis details are tabulated in Table 3.2. The effect of NaCl concentration on morphology of HIPE emulsions is collated in Figure 3.5. No significant change in the stability of the HIPE emulsion formed was observed but an effect in yield stress values were observed.

Figure 3.6 depicts SEM images and yield stress values of the PH3A monoliths synthesized with variation in NaCl concentrations using 0.05 wt% initiator concentration. Maximum yield stress value of 1.538 psi was observed for polyHIPEs synthesized using 1 wt% NaCl and it was subsequently reduced with an increase in NaCl concentration.

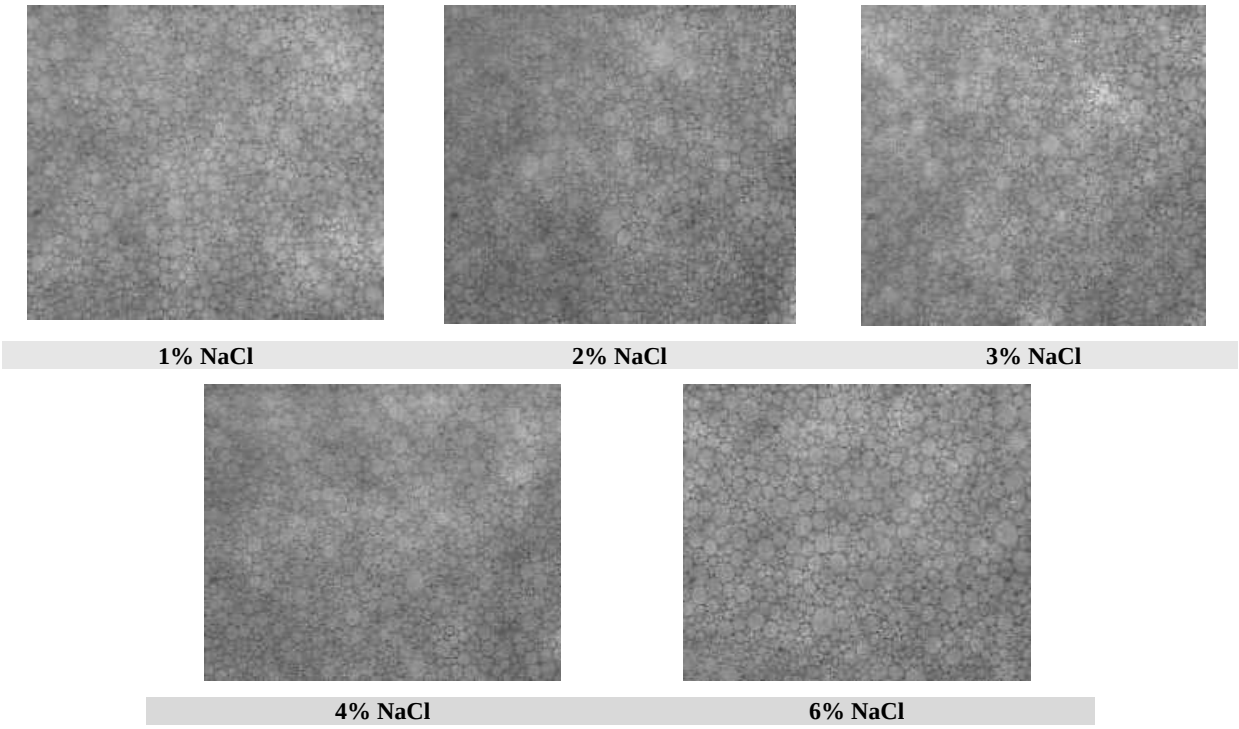

Figure 3.5 : Effect of NaCl concentration on the PH3A emulsion morphology

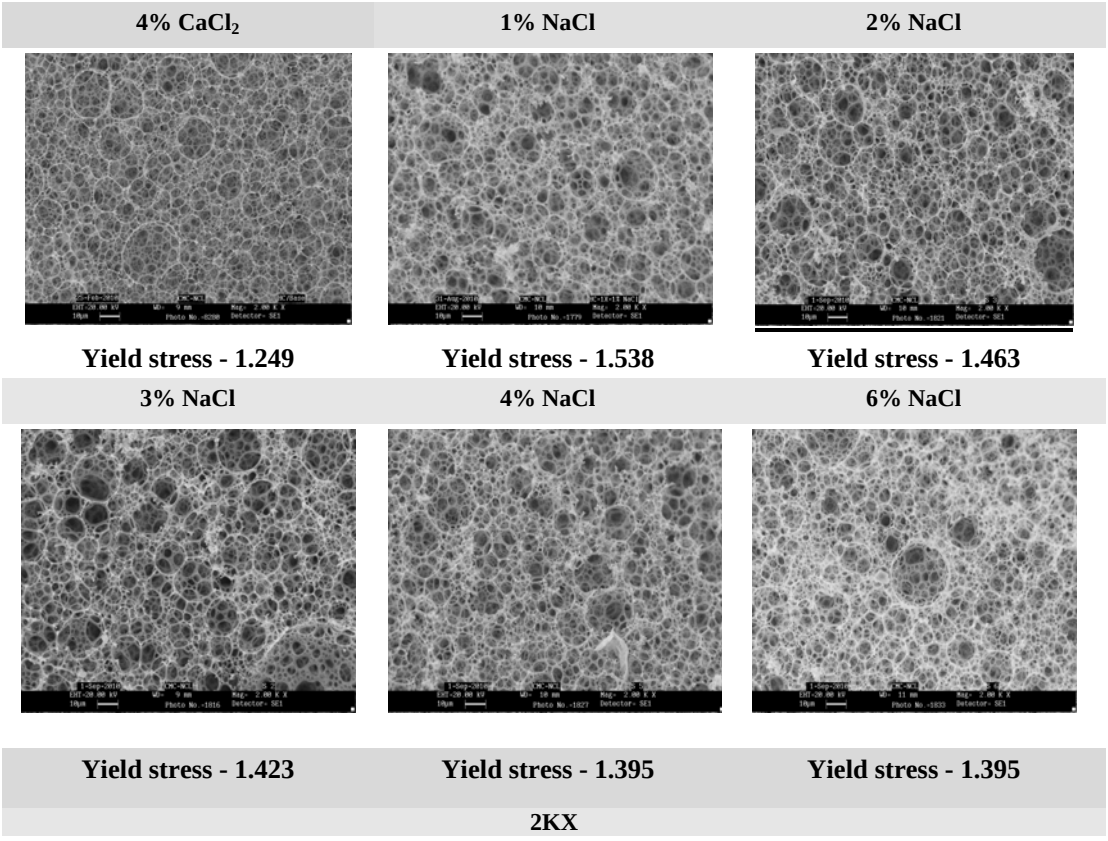

Figure 3.6 : Effect of NaCl concentration on the morphology and yield stress value of the PH3A monoliths using 0.05 wt% initiator

Figure 3.7 shows the effect of NaCl concentration on the morphology of the PH3A monoliths using 0.2 wt% NaPS. Similar trend in the morphology and yield stress values was observed. Maximum yield stress of 1.499 was observed for polyHIPEs synthesized using 1% NaCl. At lower concentration the stabilizing effect of NaCl is less, its association with ionic surfactant also decreases hence the monolith formed is little bit stiff which leads to an increase in yield stress value. The yield stress value decreases and reaches equilibrium at higher NaCl concentrations.

[4% $CaCl_2$]	1% NaCl	2% NaCl
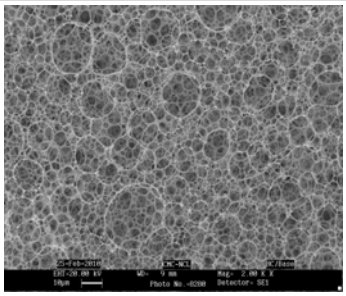	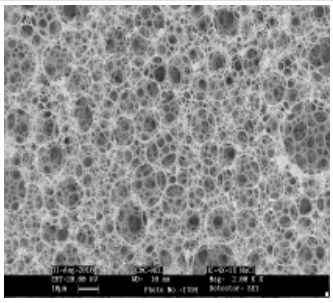	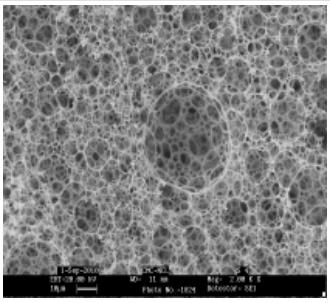
Yield stress – 1.249	**Yield stress – 1.499**	**Yield stress – 1.435**
3% NaCl	**4% NaCl**	**6% NaCl**
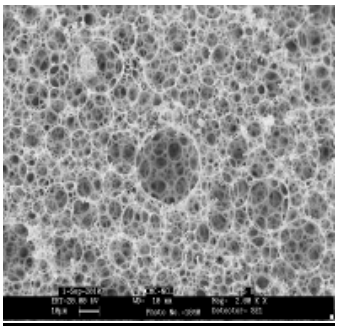	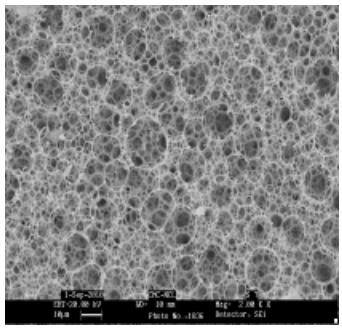	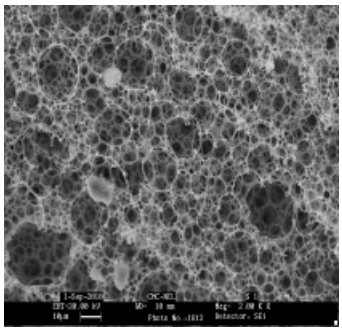
Yield stress – 1.401	**Yield stress – 1.401**	**Yield stress – 1.320**
	2KX	

Figure 3.7 : Effect of NaCl concentration on the morphology and yield stress value of PH3A monoliths using 0.20 wt% initiator

3.2.3.4 *Effect of porogen*

The effect of different long chain organic porogenic solvents viz. octanol (C_8), decanol (C_{10}), hexadecanol (C_{16}) and 1-Eicosanol (C_{20}) on the morphology and yield stress values of the polymers formed was studied. The HIPE emulsion stability in case of polymers synthesized with and without octanol as porogen and two different surfactant concentrations 2.2 wt% and 4.4 wt% was studied. In case of both the surfactant concentrations, emulsions prepared in absence of porogen were stable enough having uniform morphology. Two different concentrations of octanol (1 and 10% of surfactant

concentration) were employed to form HIPEs. As the porogen concentration increased the uniform morphology of HIPE was disturbed leading to unstability. The effect was prominently observed in case of lower surfactant concentration i.e. 2.2 wt% and higher octanol concentration i.e. 10%. All these parameter variations and their effect on the HIPE emulsion stability confirms the fact that HIPE stability depends on the hydrophobicity of the oil phase and its interaction with the aqueous phase.

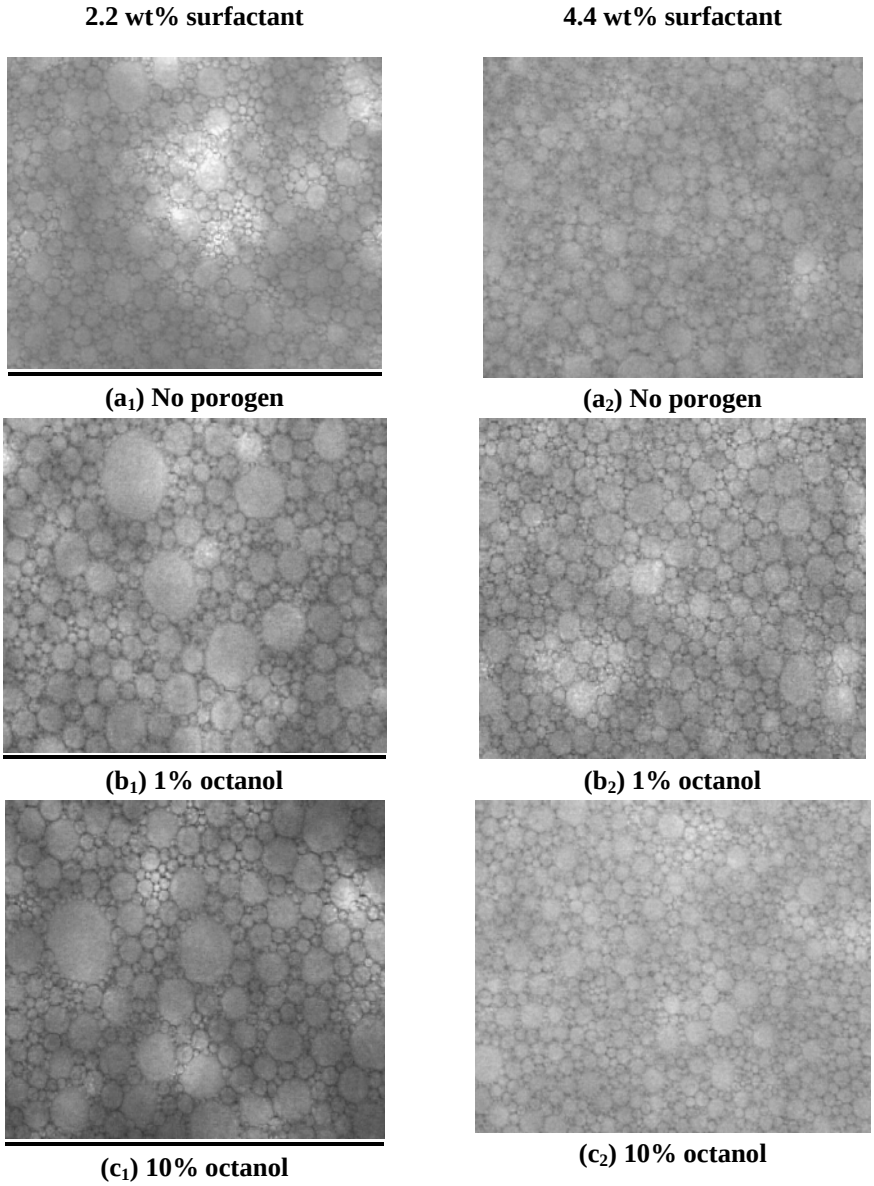

Figure 3.8 : Emulsion stability studies in presence of octanol as porogen.

Figure 3.9 shows the effect of octanol concentration on the morphology of the resulting PH2A polyHIPEs. Porogen concentrations used were 10 %, 50% and 300%. From Figure 3.6, it was observed that as the octanol concentration was increased the emulsion gets destabilized and the occluded cells were formed. This is due to the fact that the emulsion stability depends on the hydrophobicity and hydrophilicity at the interface. In the case where higher concentrations of octanol was used, resulted to a HLB change at the interface and the water droplets were coalesced that lead to formation of large occluded cells in the final polymer. Figure 3.10 shows the SEM images of PH2A polyHIPEs synthesized using octanol, decanol and hexadecanol as porogen keeping the same concentration. (10 %). It was observed that as the alcohol chain length increased the uniformity in cell size and continuous porous structure also increased.

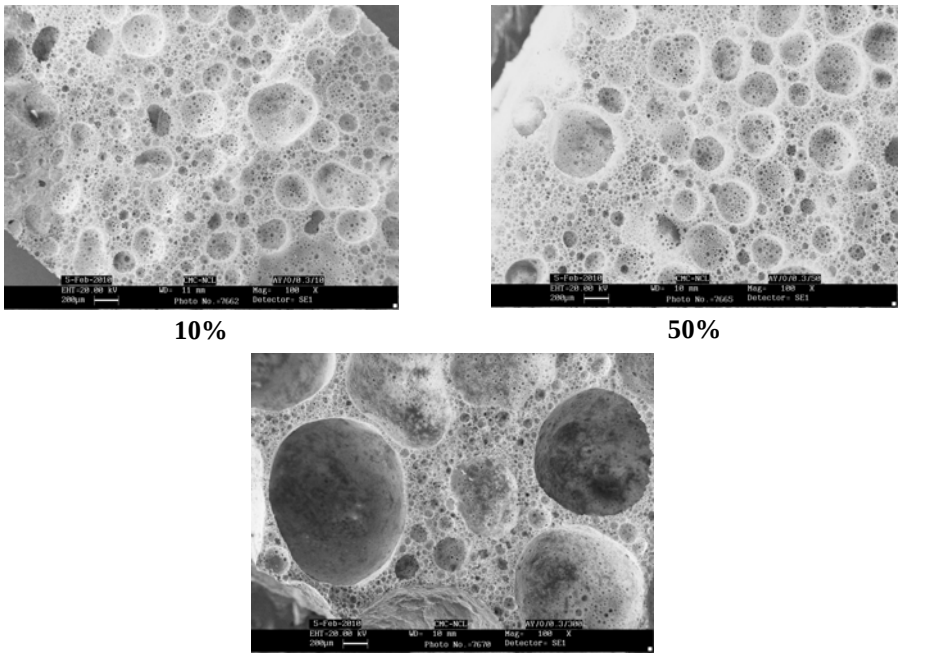

10% **50%**

300 %

100X

Figure 3.9 : Effect of octanol concentration on the morphology of PH2A polyHIPEs

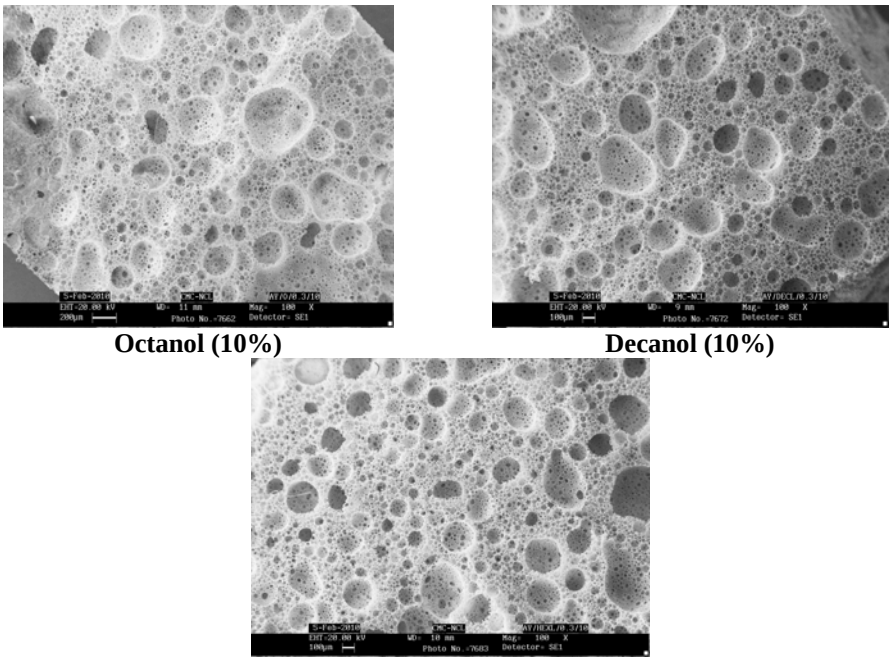

Octanol (10%) **Decanol (10%)**

Hexadecanol (10%)

100X

Figure 3.10 : Effect of porogen type on the morphology of PH2A polyHIPEs

Experiments were done to study effect of higher concentration of porogens i.e 50 and 300 wt% of octanol and decanol on synthesis of PH2A series polymers. Figures 3.11 and 3.12 show their morphological behavior. It was observed that higher concentration of porogen leads to formation of occluded pores. Presence of porogen in the oil phase leads to change in the hydrophobicity of the oil phase that reflects in arrangement of closely packed structure formation.

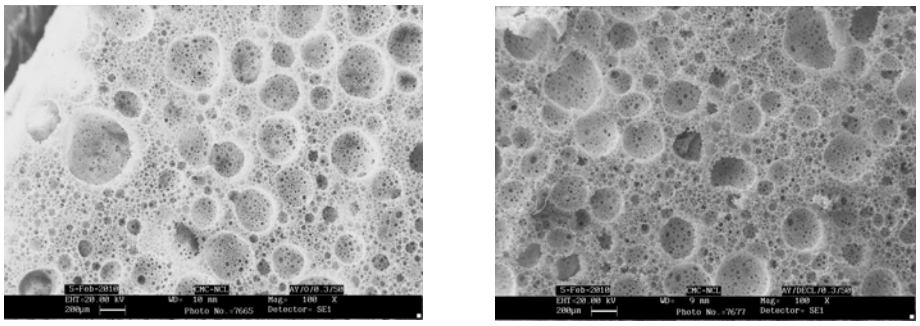

100X

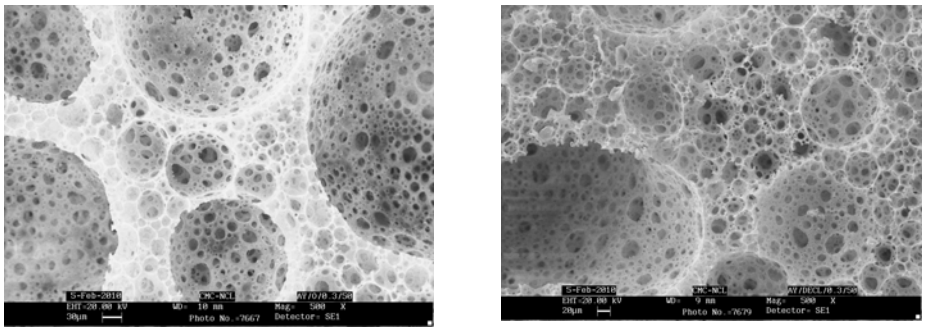

500X

Octanol (50%) **Decanol (50%)**

Figure 3.11 : Effect of octanol and decanol using 50 wt% concentration on the morphology of PH2A polyHIPEs

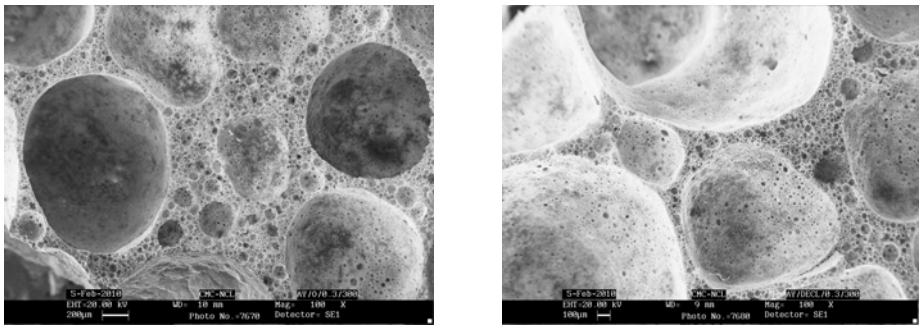

100X

Octanol (300%) **Decanol (300%)**

Figure 3.12 : Effect of octanol and decanol using 300 wt% concentration on the morphology of PH2A polyHIPEs

The effect of porogen type and concentration on PH3A series monoliths was also studied. The SEM images are shown in Figures 3.13 to 3.15. As the concentration of porogen increased, the occlusion of pores also increased giving rise to secondary pore structure. This can be attributed to the phase separation phenomenon during polymerization and change in hydrophobic-hydrophilic levels during the HIPE formation. In case of polyHIPEs synthesized using hexadecanol using 300 wt% concentration, the occlusion phenomena is predominantly observed hence leads to the formation of larger closed cells as compared to the polyHIPEs where octanol and decanol were used. Long chain alcohols like eicosanol also generate formation of larger voids.

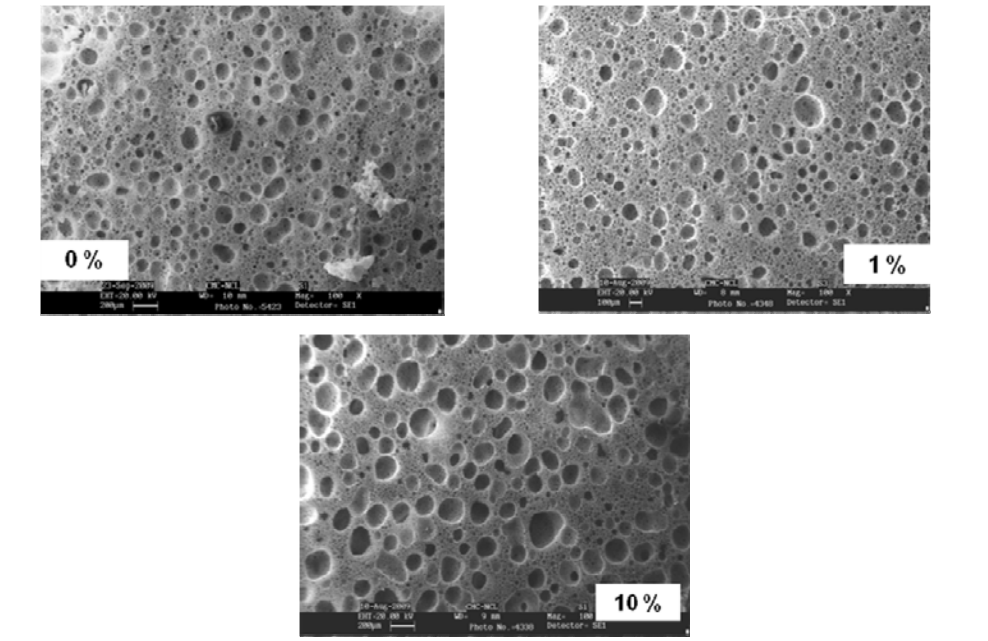

Figure 3.13 : Effect of hexadecanol using 1 and 10 wt% concentration on the morphology of PH3A monoliths.

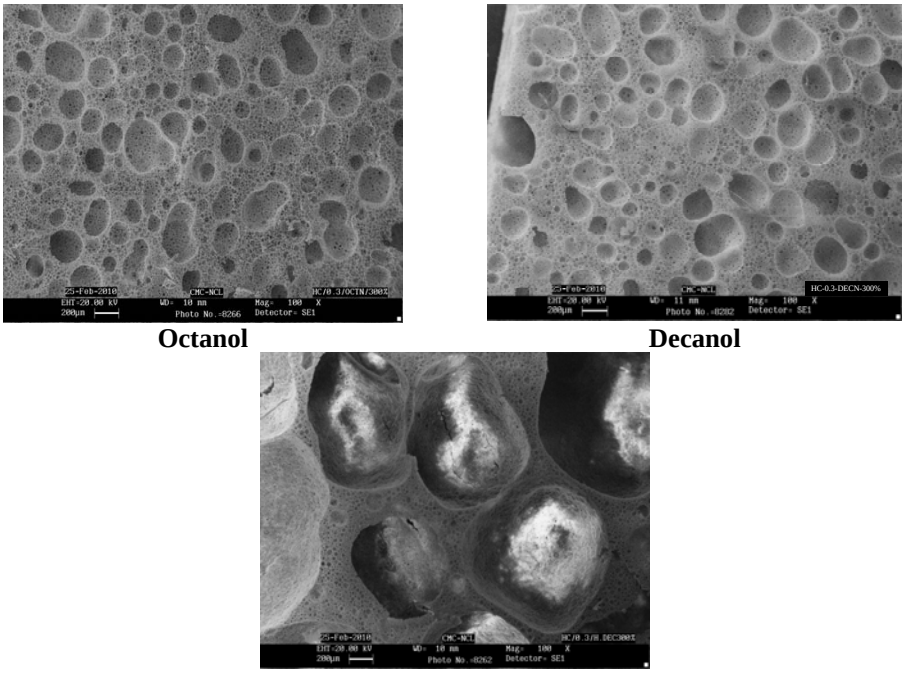

Figure 3.14 : Effect of type of porogen using 300% concentration on the morphology of PH3A monoliths

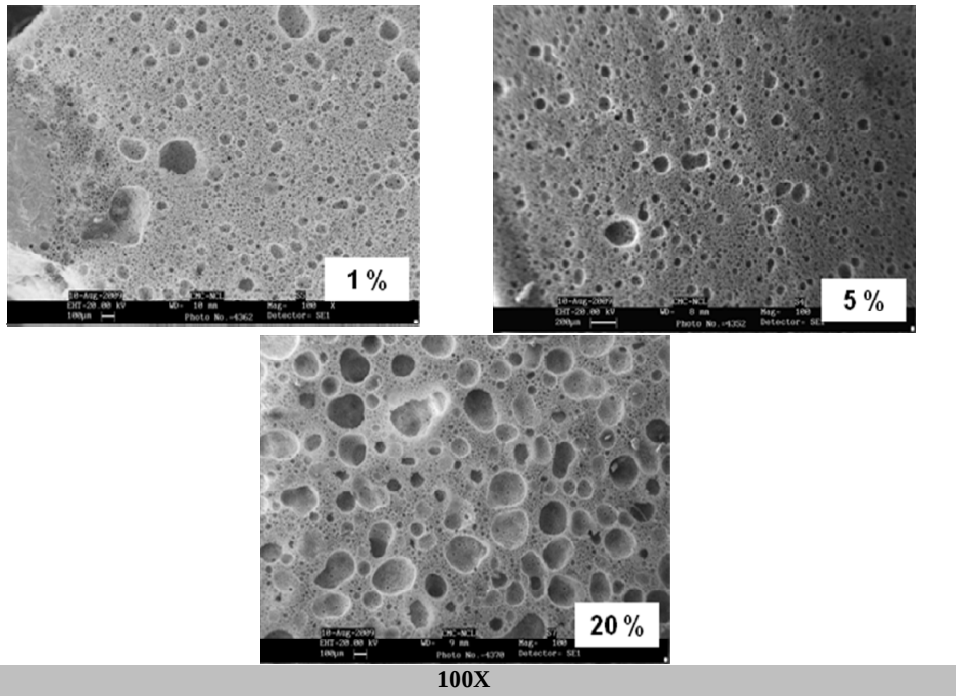

Figure 3.15 : Effect of 1-eicosanol as porogen using 1, 5 and 20 wt% concentration on the morphology of PH3A monoliths

3.2.3.5 *Effect of water soluble polymers*

Water soluble polymers like guargum and sodium alginate are highly viscous linear polymers. Their effect on the morphology and mechanical properties of PH3A polyHIPEs were evaluated. Figure 3.16 depicts the SEM images of PH3A polyHIPEs synthesized using various concentrations of guargum. It was observed that as the concentration of guargum was increased, the occlusion increased. At higher concentration of guargum, the viscosity of the emulsion also increased reducing the stability of the emulsion. Guargum present in aqueous phase interacts with the oil phase which affects the HLB of the system leading to destabilization. Guargum present in the polyHIPE increasing the softness of the polymer which is reflected in the yield stress values which decreased linearly with increase in guargum concentration as shown in Figure 3.17. It was observed that the yield stress value decreased from 1.070 psi to 0.525 psi indicating polymer having elasticity.

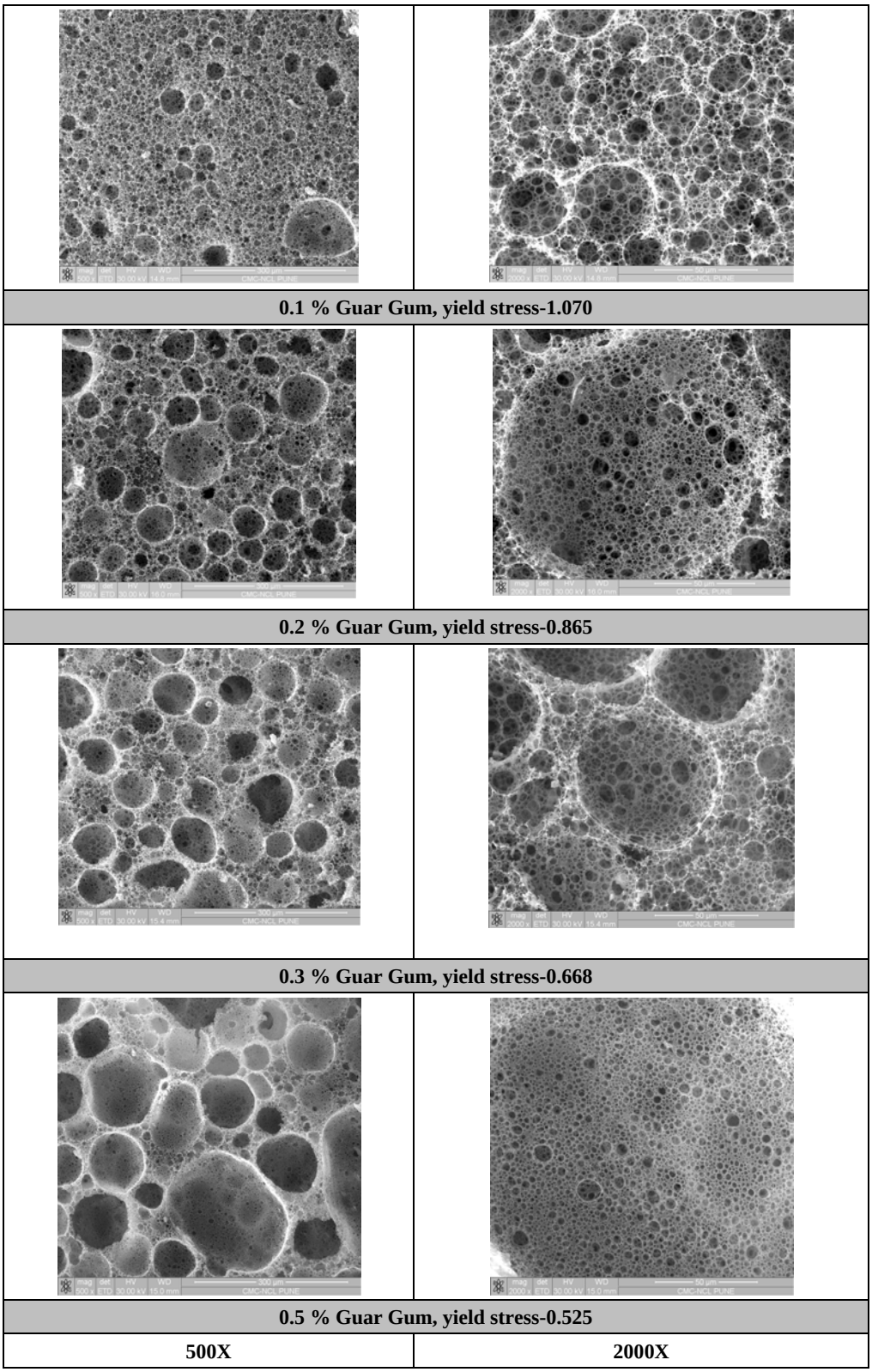

Figure 3.16: Effect of guar gum concentration on the morphology and yield stress value of PH3A polyHIPEs using 0.05 wt% initiator and 4 wt% $CaCl_2$ as salt electrolyte

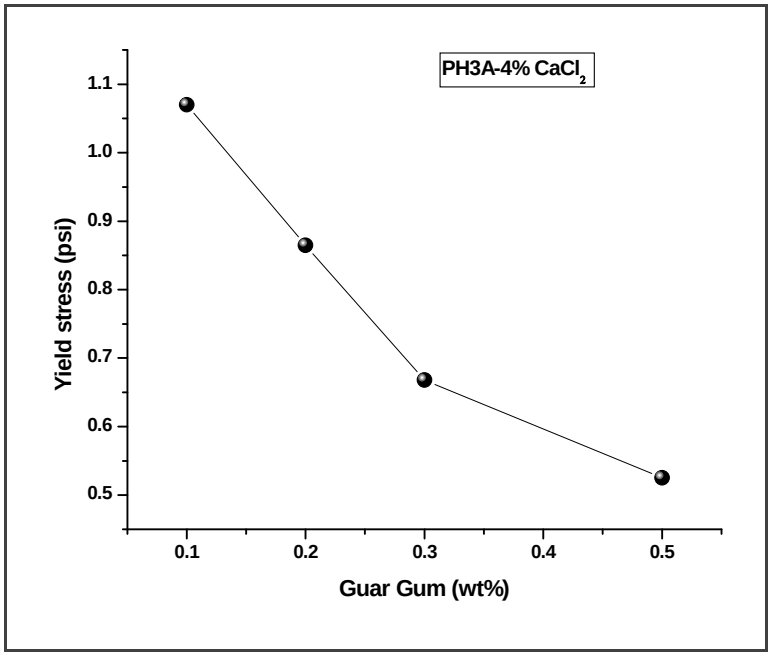

Figure 3.17: Effect of guar gum concentration on the yield stress value of PH3A polyHIPEs using 0.05 wt% initiator and 4 wt% $CaCl_2$ as salt electrolyte

Figures 3.18 and 3.19 show the effect on morphology of PH3A polyHIPEs synthesized using 0.1 and 0.3 wt% of sodium alginate respectively with variation in sodium chloride concentration. Increase in NaCl concentration leads to increase in association with sodium alginate polymer leading to enhancement in stability of the HIPE formed giving rise to a uniform interconnected pore structure. Lower yield stress values were observed in case of polymers synthesised using 0.3 wt % sodium alginate in comparison to that of polymers synthesized using 0.1 wt % sodium alginate.

Polymers synthesized in presence of water soluble polymers were highly soft and elastic in nature that can be utilized in fluid absorption materials.

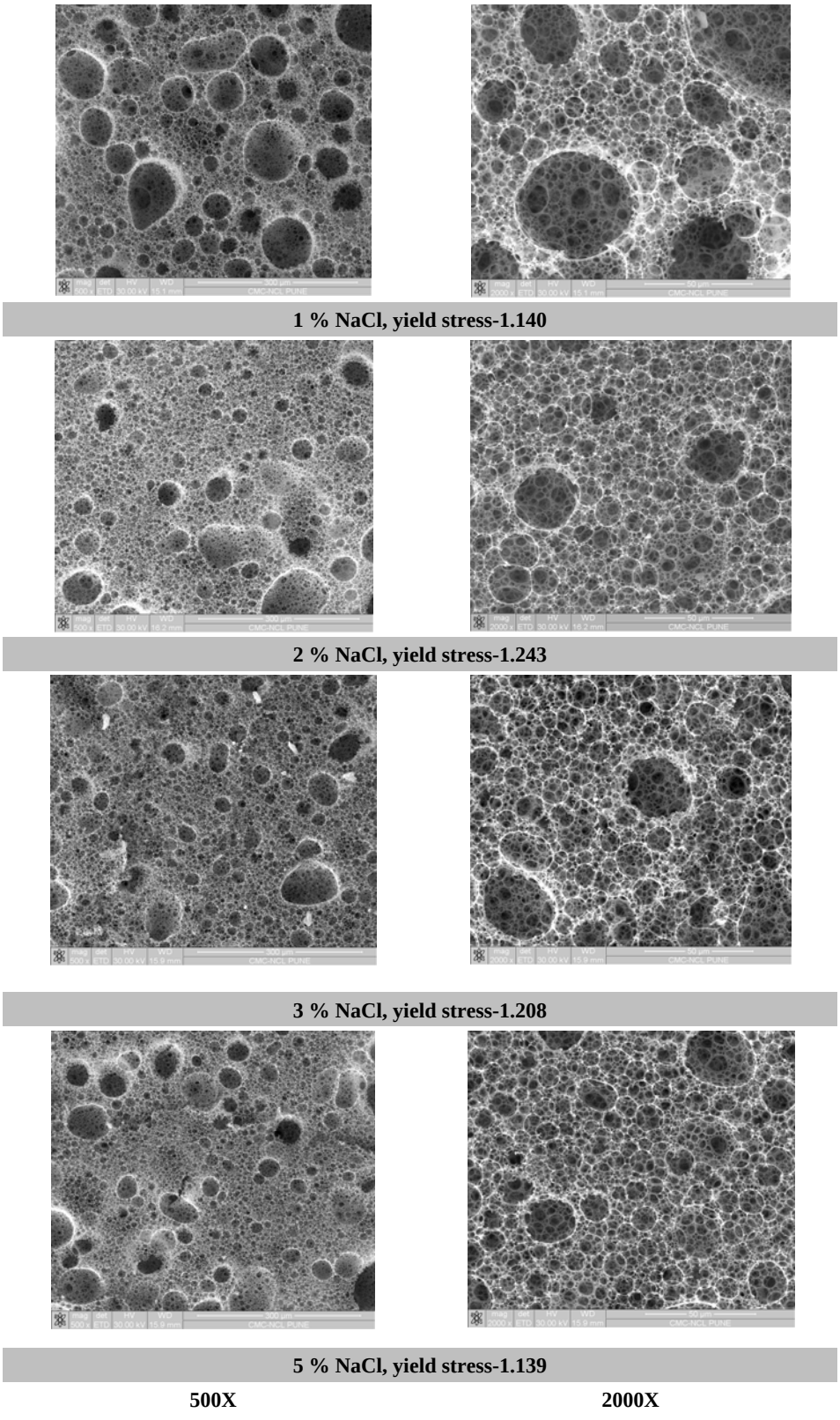

Figure 3.18: Effect of NaCl concentration on the morphology and yield stress value of PH3A polyHIPE using 0.1% wt% sodium alginate

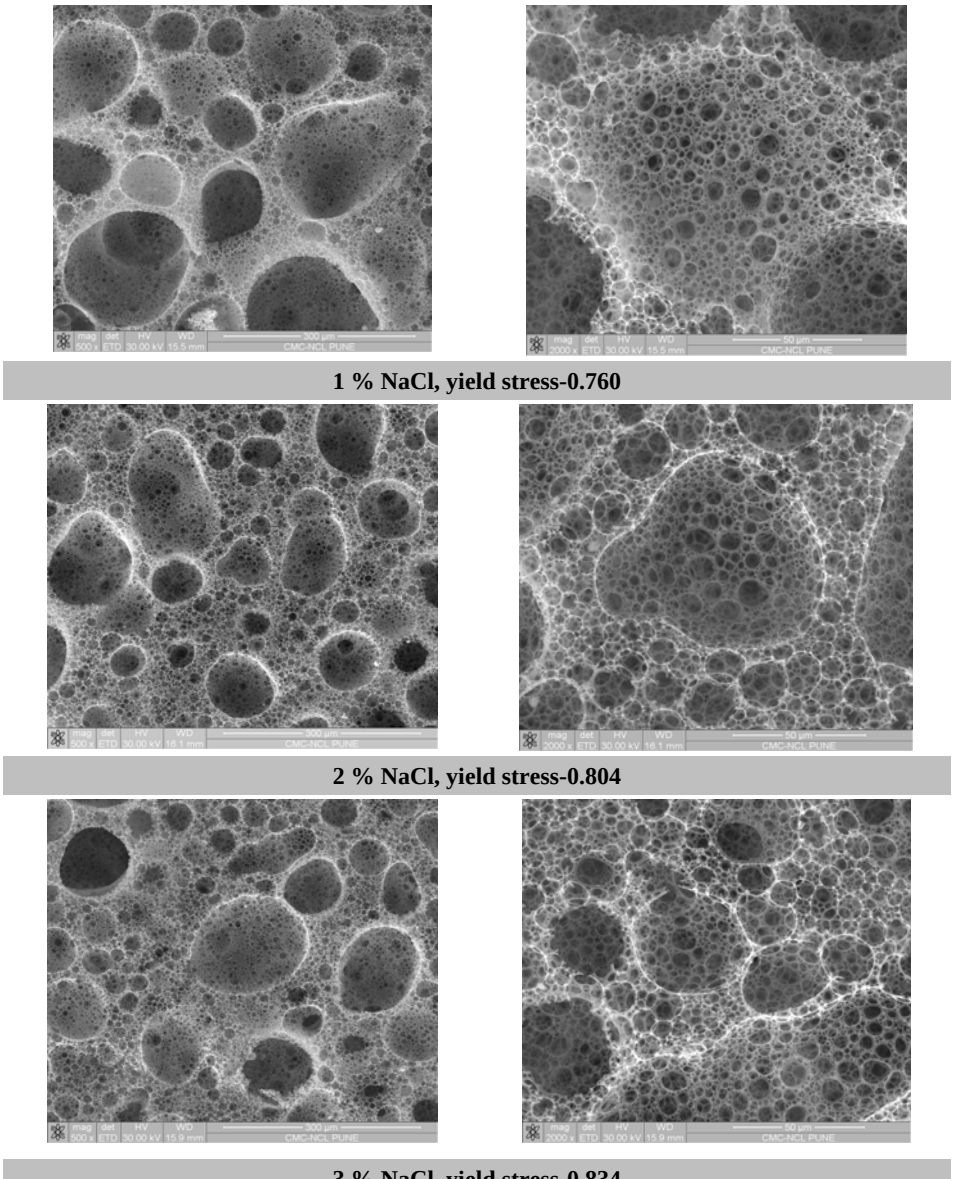

Figure 3.19: Effect of NaCl concentration on the morphology and yield stress value of PH3A polyHIPE using 0.3 wt% sodium alginate

3.2.4 Conclusion

The effect of comonomer type plays an important role in the polyHIPE properties as it significantly contributes to the differentiation in hydrophobic hydrophilic nature of the oil phase affecting the HIPE emulsion stability. Each factor such as initiator type and concentration, salt type and concentration, porogen type and concentration, presence of water soluble monomer in aqueous discontinuous phase plays an important role in designing the architecture of the porous polyHIPE. These preliminary studies help to understand the complexity of HIPE methodology. Increase in salt concentration and presence of water soluble polymers in the aqueous discontinuous phase leads to the formation of soft and elastic polymers. The yield stress of the polymer can be varied with an interplay in composition of the HIPE constituents. For all the polymers synthesized in this study the yield stress was observed in the range of 0.525-1.538 psi depending on the parameter varied.

3.3 Polymerization kinetics of acrylate based polyHIPEs

3.3.1 Introduction

Chain growth polymerization using free radical initiation is ideal for synthesis of novel polyHIPE materials. Step growth polymerization that can involve monomers with hydrophilic end groups is more problematic for HIPE formation. This especially is the case where water is by-product of the reaction can react with one of the components or can render one of the components inactive. In addition, many step growth polymerization reactions occur at temperatures above 100^{o}C, temperatures that are not practical for HIPEs containing an aqueous phase.

3.3.2 Free radical polymerization

Free radical polymerization is one of the most studied chemical processes which is carried out on a large industrial scale and counts the world production of polymers in the range of 100 million tons per year (~50% of all synthetic polymers). Free radical polymerization has been known as far back as the 1950s when the basic theory and comprehension of radical polymerization was established.[1-5] It included the thorough understanding of the mechanism of the process, encompassing the chemistry and kinetics of the elementary reactions involved, with the determination of the corresponding absolute rate constants, the structure, and concentrations of the growing species, as well as a correlation of the structure of the involved reagents and their reactivities.

Polymerizable monomers under radical polymerization include styrene and its substitution products, dienes, mono and disubstituted ethylene derivatives, such as vinyl

acetate, acrylonitrile, acrylates, (meth)acrylates, (meth)acrylamides, vinyl chloride, and a variety of halogenated alkenes. The essential polymerization step is a repetitive free radical addition to the monomer double bonds, forming chains of carbon atoms constructed of units (CH_2-CHR) or (CH_2- CRR′) linked together predominantly head-to tail (the substituted carbon atom is denoted as the head).

3.3.2.1 *Initiation*

The initiation process constitutes the first reaction step in free radical polymerization, leading to the generation of (primary) radicals. The kinetics of the initiation process, i.e. its rate and effectiveness are of fundamental importance in both theoretical studies and commercial applications. Commercial procedures mainly rely on the formation of primary radicals via thermal decomposition processes using azo- and peroxy type compounds. Investigative kinetic studies are to a large extent carried out using photo initiators, which decompose upon irradiation with UV or visible light.

$$Initiator \xrightarrow[h\nu,\Delta]{k_d} I_1^{\bullet} + I_2^{\bullet} \tag{1}$$

The measurable decrease of the initiator concentration [I] in a polymerizing system with time is given by

$$-\frac{d[I]}{dt} = k_d[I] \tag{2}$$

Integration of equation 2 leads to equation 3, an expression which describes the decreasing initiator concentration as a function of time.

$$[I] = [I]_0 e^{-kdt} \tag{3}$$

However, the rate of the formation of initiating primary radicals is of greater interest in kinetic studies. The rate of generation of radicals that are capable of initiating the polymerization process R_d, is described via the following general first-order rate law:

$$R_d = \frac{d[I]}{dt} = -\frac{2fd[I]}{dt} = 2fk_d[I] \quad (4)$$

where, k_d corresponds to the rate coefficient of initiator decomposition and f denotes the initiator efficiency. It should be noted that in the case of photo initiation, k_d is a composite of various variables. In order to initiate the polymerization process via reaction with a monomer unit, the generated primary radicals, $I_1^{\bullet}$ and $I_2^{\bullet}$, have to leave the solvent cage that surrounds them. The ability of the primary radicals to leave the solvent cage unreacted and to start the polymerization process is quantified by the initiator efficiency *f,* with theoretical values between zero and unity. Not all generated primary free radicals initiate polymer growth. Shortly after decomposition, the free radicals are very close to each other and recombination can occur. In addition, they can also react in alternative ways before they can react with a monomer unit. An efficiency of zero corresponds to no initiation taking place, whereas $f = 1$ indicates that every generated primary radical escapes the solvent cage and subsequently initiates polymerization. Typical values of '*f*' are between 0.5 and 0.8, depending on the viscosity of the reaction medium indicating that the escaping process is diffusion controlled.

The rate of initiation, R_i, is given by equation 5.

$$R_i = \frac{d[R_1^{\bullet}]}{dt} = -\frac{d[I_1^{\bullet}]}{dt} - \frac{d[I_2^{\bullet}]}{dt} = k(1)_i[M][I_1^{\bullet}] + k(2)_i[M][I_2^{\bullet}] \quad (5)$$

Because $[I_1^{\bullet}] = [I_2^{\bullet}] = [I^{\bullet}]/2$, the rate coefficient of initiation, k_i, is a composite of the individual rate coefficients of initiation for the initiator fragments $I_1^{\bullet}$ and $I_2^{\bullet}$.

$$R_i = k_i[M][I^{\bullet}] \tag{6}$$

3.3.2.1.1 *Thermal initiation*

Thermally decomposing initiators (mainly) fall into two classes: azo- and peroxy-type molecules. The general structures of azo- and peroxy-initiators are represented by **1** and **2** respectively.

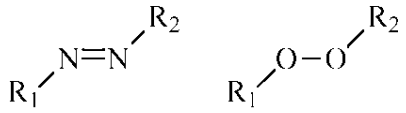

1 **2**

An important quantity of a thermal initiator is its *half-life* $t^{1/2}$. The half-life is the time period during which half of the initiator molecules initially present is decomposed. There are initiators available for virtually any desired decomposition rate in a given solvent (or monomer) at a given temperature. Initiators are often characterized by the temperature at which their half-life is 10 h. These temperatures range from 20 to 120^{o}C, depending on the structure of the initiator. The basic features of thermal initiation systems are discussed as follows.

Azoinitiators

Azoinitiators are widely used class of thermally decomposing initiators. Most of the azoinitiators generate two identical radical species upon fragmentation. The most common azoinitiators are 2,2′-azobisisobutyronitrile (AIBN), dimethyl 2,2′-

azobisisobutyrate, 1,1′-azobis(1-cyclohexanecarbonitrile) and 2,2′-azobis-2,4-dimethylvaleronitrile. Both the delocalization of the free electron in the generated radical[6,7] and the steric demand of the leaving radical[8] significantly affect the decomposition rate coefficient k_d: the more the free electron in the resulting radical is delocalized and the bulkier the leaving radical, the larger is k_d. The choice of the solvent, however, has comparatively little effect on the rate of azoinitiator decomposition.

Peroxide based initiators

The use of peroxides as thermally decomposing initiators is especially in an industrial context more widely spread than the use of azoinitiators.[9,10] Peroxy compounds range from alkyl, acyl and peresters to inorganic peroxides.[11] The most employed peroxides are di-*tert*-butyl peroxide, benzoyl peroxide, di-*tert*-butyl peroxalate, cumene hydroperoxide and di-*n*-propyl peroxydicarbonate. The rate of peroxide decomposition is strongly dependent on the structure of the molecule in question. The rate of decomposition for diacyl peroxides and peresters increases when going from aryl to primary alkyl to secondary alkyl to tertiary alkyl substituents.[12] Because of the strong dependence of the rate of decomposition on the peroxide structure, a wide variety of decomposition rates exists for a given temperature. The general guideline is that dialkyl peroxides and hydroperoxides are mostly used at elevated temperatures, whereas dialkyl peroxydicarbonate are best suited for lower temperatures.

3.3.2.1.2 *Photoinitiation*

An attractive alternative to thermally decomposing initiators are photoinitiators that decay upon irradiation with UV or visible light.[13-17] The use of photoinitiators is (in

most cases) restricted to applications involving accurate kinetic measurements, whereas their usage in industrial processes is very limited because of the technical problems associated with the uniform irradiation of large reaction volumes. Some exceptions are applications involving coatings and surface polymerizations. The main advantage of photoinitiators used in polymerizing systems is the possibility to define exact start and end points of the polymerization process via the duration of the irradiation period. In addition, the rate of (most) photoinitiator decomposition is almost independent of the reaction temperature, but depends strongly on the (UV) light intensity. An ideal photoinitiator for a specific polymerization may be defined via the following criteria: (i) the photoinitiator should decompose upon irradiation with the (UV) light source; eg. absorption should coincide with the radiation wavelength. The monomer(s) used in the specific polymerization process should not absorb light at the selected wavelength, (ii) the efficiency of the initiator should be high, preferably close to one; ie, all radicals generated should start growing chains. (iii) at best, there should be only one type of free radical species that is formed upon laser irradiation.

3.3.2.1.3 *Redox initiation*

Redox initiating systems are very often used especially in aqueous media. However, the redox initiation can also be carried out in organic media. These systems consist of a reducing and oxidizing agent.[18-19] Redox initiators very often form only one radical (example, classic Fenton system of ferrous salts and hydrogen peroxide or other peroxides) which, by eliminating cage termination, increases initiation efficiency:

$$Fe^{2+} + RO\text{-}OR \rightarrow Fe^{3+} + RO^{-} + RO^{\bullet}$$

Commercially important is also the use of ceric salts, which can reduce alcohols to alkoxy radicals and enable grafting from cellulose and other surfaces with OH groups. Some redox systems provide two radicals such as persulfates with thiosulfates and metabisulfates:

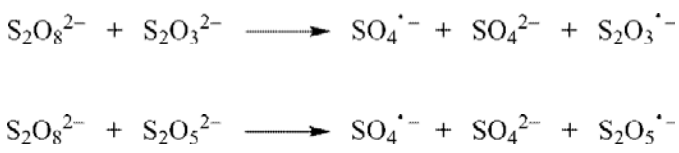

The electrostatic repulsion between radical anions also reduces the probability of cage termination. Transition metals in redox initiation usually act as reducing agents but may also act as oxidants:

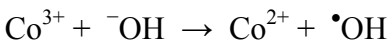

3.3.2.1.4 *Other methods of initiation*

Apart from the above-mentioned methods of initiating free radical polymerizations, there are several more alternatives, which can be selected from if required for the specific application. These techniques include (*i*) ionizing irradiation, (*ii*) plasma initiation, (*iii*) electroinitiation and (*iv)* ultrasonic initiation.

3.3.2.2. *Initiator efficiency*

A prerequisite for primary radical/monomer reactions is the successful escape of the generated radicals from their solvent cage. If the formed radicals remain inside the cage, they may undergo reactions with themselves. Potential in-cage reactions are the main reason for initiator efficiencies, *f*, being below unity ($0.3 < f < 0.8$, typically).[20] In cage reactions include radical recombination or disproportionation. If the initiator is

regenerated by an in-cage reaction, the initiator efficiency is not affected, but the rate of initiator decomposition is reduced. The importance of reactions within the solvent cage strongly depends on the rate of diffusion of the generated radicals away from each other. Therefore, both the size and the reactivity of the primary radicals as well as the medium's microviscosity determine the initiator efficiency. As increasing monomer-to-polymer conversion goes hand in hand with a large increase in system viscosity, the likelihood of in-cage reaction will increase with monomer conversion.[21,22] The species generated by reactions within the solvent cage can be reactive under the polymerization conditions or they may have detrimental effects on the polymer properties the fragmentation of AIBN can react to yield methacrylonitrile, which undergoes copolymerization and will be incorporated in the final polymer.[23,24]

The efficiency of peroxide initiators is affected by the mode of their fragmentation. Concerted decomposition results in an alkoxy and in an acyloxy radical, whose recombination will not affect the initiator efficiency.[25] Such processes have also been termed 'cage-return' reactions. However, concerted two-bond scission yields alkyl and alkoxy radicals, which when coupled inside the cage lead to a lower f value. Experimental investigations into the initiator efficiency can be carried out via radical trapping techniques,[26] infrared spectroscopy[27] and product or polymer end-group analysis via NMR.[21] Measurements of the temperature dependency of the initiator efficiency are extremely scarce; however, it has been found that in the AIBN-initiated bulk free radical polymerization of styrene at 100 MPa, f increases by approximately a factor of 1.5 when going from 40 to 80^{o}C.[27] The same study indicated that the initiator efficiency decreases when the reaction pressure is increased (f decreases by close to one third when going

from ambient pressure to 200 MPa bar at 70°C). As mentioned earlier, initiation efficiency is much higher in the redox process since in many systems only one radical is generated.

3.3.2.3 *Propagation*

The propagation step in free radical polymerization has been in the center of scientific interest because of the advent of novel methods for the accurate determination of propagation rate coefficients. The addition of a macro radical to a monomer unit can be described via the following rate law expression:

$$-\frac{d[M]}{dt} = \sum_i k_p^i [R_i^\bullet][M] \qquad (7)$$

with k_p^i being the propagation rate coefficient of a macro radical with chain length i, R_i, [M] the monomer concentration and [R_i] the free radical concentration. It is generally accepted that the propagation reaction is chemically controlled up to high monomer conversions, ie high viscosities of the reaction medium. This implies that the propagation rate coefficient is independent of monomer conversions up to 80%. The chemical control of the propagation step is impressively demonstrated when comparing the average collision frequency of 1012 s^{-1} in the liquid phase at room temperature[28] to the frequency of successful propagation reactions (typically close to 103 s^{-1}). These numbers indicate that (approximately) only every 109th collision leads to a successful addition of a monomer unit to a macro radical. The propagation rate coefficient carries the index I (representing the chain length of the growing chain), because it is beyond doubt that k_p is a chain-length-dependent rate coefficient. This is especially true for the

first few addition steps, which proceed at a markedly increased rate compared to long-chain propagation. In the case of methyl methacrylate, for example, the first propagation step at 60°C is approximately 16 times faster than the long-chain propagation.[29-34] The difference in the polymerization of monosubstituted monomers may be smaller.[35] Nevertheless, recent evidence points toward a chain length dependence of the product of k_p and the monomer concentration [M], up to chain lengths of hundreds of monomer units.[36-39]

It is thus quite possible that the apparent chain length dependence of k_p reflects a structuring of the monomer concentration at the propagating chain end. For most free radical polymerizations, the propagation step is fast and exothermic. The thermodynamics of free radical polymerization propagation have been reviewed by a few authors including Busfield,[40] Sawada,[41] and Allen and Patrick.[42] Heats of free radical polymerization have been commonly determined from calorimetric data using standard thermochemical techniques. Entropies of polymerization are more scarce. It should be noted that the addition of radicals to vinyl monomers is at least in principle a reversible process.

3.3.2.3.1 *Monomer structure and reactivity*

The absolute value of the propagation rate coefficient is governed by the nature of the monomer unit and the reactivity of the propagating radical. Both entropic and electronic factors influence the absolute value of the propagation rate coefficient and its activation parameters, E_A and A. It is important to note that the reactivity of the propagating radical and the reactivity of the monomer units correlate reciprocally. For

example, methacrylates are several times more reactive then acrylates but polyacrylate radicals are significantly more reactive than poly(methacrylate) radicals. For polymerization and chain growth to take place, it is mandatory that the free macro radical lives long enough to survive the above mentioned ineffective collisions. The addition of the monomer in a propagation reaction has to take place before any possible decomposition reaction or other side reaction. For example, acetone cannot be polymerized at ambient reaction conditions besides thermodynamic reasons, which make the polymerization unfavorable, because the associated free radicals quickly decompose into methyl free radicals and a ketone. The substituent that is introduced into the ethene molecule to facilitate polymerization via activation of the double bond and stabilization of the propagating radical, respectively, has also the effect of adding steric hindrance to the propagation step. A mechanistic model has been proposed for the propagation of sterically hindered monomers.[43] In such a model, the propagating radical and the monomer attain the maximum overlap of the π-electrons and the unpaired electron at a certain angle between the C_α C_β bonds of the monomer and the propagating radical. If the propagation reaction is sterically hindered, the bond formation is energetically not suppressed, but the probability that the radical and the monomer approach each other such that bond formation can occur is decreased.

It is thus evident that it is close to impossible to completely separate enthalpic from entropic effects. While electronic effects should be reflected in the activation energy E_A, steric effects are associated with the pre-exponential factor A. When going from methyl methacrylate to dimethyl itaconate,[44] a substantial decrease in the pre-exponential factor of about one order of magnitude is observed. This decrease is due to the sterically

more demanding nature of the propagating dimethyl itaconate radical. When going from methyl methacrylate to ethyl α-hydroxy methacrylate, the pre-exponential factor remains unchanged, but the activation energy is reduced due to the electronic effect of the additional β-oxygen atom. This illustrates the effect of different contributions (ie steric and electronic) to the activation parameters using different monomers.

3.3.2.4 *Rate of polymerization*

The chain nature of the process resides in the propagation step in which large numbers of monomer molecules are converted to polymer for each initiating radical produced in the first step. In order to obtain a kinetic expression for the rate of polymerization, it is necessary to assume that k_p and k_t are independent of the size of the radical. Very small radicals are more reactive than propagating radicals, but this effect is not important because the effect of size vanishes at the dimer or trimer size [Gridnev and Ittel, 1996; Kerr, 1973]. The rate of monomer disappearance, which is synonymous with the rate of polymerization, is given by,

$$-\frac{d[M]}{dt} = R_i + R_p \tag{8}$$

where R_i and R_p are the rates of initiation and propagation, respectively. However, the number of monomer molecules reacting in the initiation step is far less than the number in the propagation step for a process producing high polymer. To a very close approximation the former can be neglected and the polymerization rate is given simply by the rate of propagation

$$-\frac{d[M]}{dt} = R_p \tag{9}$$

The rate of propagation, and therefore the rate of polymerization, is the sum of many individual propagation steps. Since the rate constants for all the propagation steps are the same, one can express the polymerization rate by

$$R_p = k_p[M^\bullet][M] \tag{10}$$

where [M] is the monomer concentration and [M$^\bullet$] is the total concentration of all chain radicals, that is, all radicals of size $M_1^\bullet$ and larger.

A radical chain polymerization is started when the initiator begins to decompose according to Eq. 10, and the concentration of radicals in the system [M$^\bullet$], increase from zero. The rate of termination or disappearance of radicals, being proportional to [M$^\bullet$]^2, is thus zero in the beginning and increase with respect to time till at some stage it equals the rate of radical generation.

3.3.2.5 *Inhibition*

The addition of certain substances suppresses the polymerization of monomers. These substances act by reacting with the initiating and propagating radicals and converting them to either non-radical species or radicals of reactivity too low to undergo propagation. Such polymerization suppressors are classified according to their effectiveness. Inhibitors stop every radical, and polymerization is completely halted until they are consumed. Retarders are less efficient and stop only a portion of the radicals. The difference between inhibitors and retarders is simply one of degree and not kind.

Polymerization is completely stopped by benzoquinone, a typical inhibitor, during an induction or inhibition period. At the end of this period, when the benzoquinone has been consumed, polymerization proceeds at the same rate as in the absence of inhibitor. It is initially an inhibitor but is apparently converted to a product that acts as a retarder after the inhibition period. This latter behavior is not at all uncommon. Inhibition and retardation are usually the cause of the irreproducible polymerization rates observed with insufficiently purified monomers. Impurities present in the monomer may act as inhibitors or retarders. On the other hand, inhibitors are invariably added to commercial monomers to prevent premature thermal polymerization during storage and shipment. These inhibitors are usually removed prior to polymerization or, alternatively, an appropriate excess of initiator may be used to compensate for their presence.

3.3.3 Experimental

Time-conversion study of high internal phase emulsion polymerization was studied for different acrylate based polyHIPEs. Preliminary efforts were focused to carry out kinetic experiments and to collect data for polymer conversion by monitoring the unreacted monomer by gas chromatography. Data was generated at different time intervals in initial and the propagation steps. Polymerization kinetics experiments were carried out for both PH3AK and PH2AK polyHIPEs. The details of the experiments are tabulated in Tables 3.6.

3.3.3.1 *Materials*

2-Ethylhexyl acrylate (EHA), 2-ethylhexyl methacrylate (EHMA), ethylene glycol dimethacrylate (EGDMA), di(hydrogenated tallow alkyl)dimethyl ammonium chloride(Arquad 2HT-75) (from Aldrich); sorbitan monooleate-Span 80, sodium peroxy disulphate (NaPS), calcium chloride ($CaCl_2$) (from Loba Chemie), butyl acrylate (BA) (S.d. fine Chemicals), LR grade cyclohexane (Rankem Ltd.). De-ionized water was collected from Millipore unit.

3.3.3.2 *Procedure*

The requisite amount of oil phase comprising of monomers and surfactant was taken in a glass reactor and kept in a water bath (kept at the polymerization temperature i.e. 65^{o}C) equipped with the overhead stirrer. The aqueous discontinuous phase was prepared by dissolving calcium chloride (4 wt%) in the requisite quantity of deionized water. The aqueous phase was transferred to a double walled jacketed dropping funnel having a temperature of 65^{o}C which is controlled by a constant temperature circulating

water bath. The aqueous phase was then added slowly to the oil phase under a constant stirring speed of 1400 rotation per minute. HIPE emulsion was formed gradually and continued to form until the complete addition of aqueous phase at the same rate. After complete addition of aqueous phase the initiator sodium peroxydisulphate (0.05 wt% dissolved in 1 mL water) was added to the HIPE formed and the stopwatch was started to measure the reaction time (1 mL water was inclusive of total water used). Then the reaction mixture was mixed thoroughly for one minute and there after the reactor was removed, capped and rapidly shifted to constant temperature water bath (kept at the 65^{o}C) for polymerization for predefined time.

3.3.3.3 *Monomer Extraction*

After predetermined time was over, the polymerization reaction mass was quenched in liquid nitrogen to stop the polymerization at the predefined time. The polymer properly crushed with the help of a glass rod, homogenized and kept for 5 minutes (to ensure freezing of reaction mass). Further to avoid post polymerization, monomethyl ether hydroquinone (MEHQ) in 1 mL acetone was added to the reactor (twice the moles of initiator used). To the reactor, 100mL of cyclohexane containing the internal standard was added for exhaustive monomer extraction. The reactor was then kept for 10 minutes in a water bath at room temperature. Slowly the frozen mass started melting and the unreacted monomers are exhaustively dissolved in cyclohexane. The reaction mass was then mixed thoroughly and kept for extraction for 48 hours. After 48 hrs, the reactors were sonicated for about 10 min. Sonication helps to extract the trace amount of monomers trapped in the porous polymer particles. Then 5mL of the upper aliquot of cyclohexane layer was decanted and 1-2 g of anhydrous magnesium sulphate

(dried in a furnace at 400^{o}C) was added, stirred and then kept undisturbed for half an hour to settle magnesium sulphate down till a clear solution was obtained. This clear solution was transferred to GC vial and was subjected to GC analysis.

Likewise simultaneously, multiple HIPEs were prepared in different glass reactors and polymerized for different time intervals (for example; 2, 4, 6….30 min) to generate data for polymer conversion at different time intervals as shown in the Table 3.7.

Table 3.6 Synthesis of PH2AK and PH3AK using various parameters

Polymer Code	NaPS Wt%	Redox	pH	MEHQ mol%	Phenothiazine mol%
PH3AK-1, PH2AK-1	0.05	-	-	-	-
PH3AK-2	0.125	-	-	-	-
PH3AK-3, PH2AK-2	0.20				
PH3AK-3, PH2AK-3	-		-	-	-
PH3AK-4, PH2AK-4	-		-	-	-
PH3AK-5	0.20	-	2.0	-	-
PH3AK-6	0.20	-	4.0	-	-
PH3AK-1	0.20	-	7.5	-	-
PH3AK-2	0.20	-	8.5	-	-
PH3AK-3, PH2AK-3	0.20	-	-	1	-
PH3AK-4, PH2AK-4	0.20	-	-	2	-
PH3AK-5, PH2AK-5	0.20	-	-	3	-
PH3AK-6, PH2AK-6	0.20	-	-	4	-
PH3AK-1, PH2AK-1	0.20	-	-	-	1
PH3AK-2, PH2AK-2	0.20	-	-	-	2
PH3AK-3, PH2AK-3	0.20	-	-	-	3
PH3AK-4, PH2AK-4	0.20	-	-	-	4

PH3AK: 2-Ethylhexyl acrylate (EHA) = 0.74 g (0.0040 mol); 2-ethylhexyl methacrylate (EHMA) = 0.76 g (0.0038 mol); ethylene glycol dimethacrylate (EGDMA) = 0.35 g (0.0018 mol); water = 50 mL (oil : water ratio = 1: 25); $CaCl_2$ = 2.0 g (4 wt.% on aqueous); Span-80 = 0.13 g (6.5% on oil phase); Arquad 2HT-75 = 0.016 (0.8% on oil phase); NaPS = KPS = APS = 0.025 g (0.05 wt% on aqueous) and 0.1 g (0.2 wt% on aqueous); Temperature = 65ºC; stirring speed =1400 rotation per minute.

PH2AK: 2-Ethylhexyl acrylate (EHA) = 0.721 g (0.0078 mol); ethylene glycol dimethacrylate (EGDMA) = 0.215 g (0.0022 mol); water = 40 mL (oil: water ratio = 1: 20), $CaCl_2$ = 1.6 g (4 wt.% based on aqueous phase), Span-80 = 6.94% based on oil phase; Arquad 2HT-75 = 0.85% based on oil phase; Temperature = 65ºC; Stirring speed = 700 rotation per minute.

3.3.4 Characterization

3.3.4.1 *Gas chromatography - Monomer estimation*

A GC chromatograph (GC-14 B, Shimadzu Corporation, Kyoto, Japan) was used for monomer measurement. Hydrogen gas and "UHP" grade nitrogen gas were purchased from Inox, Mumbai. Zero air used for FID flame ignition was supplied from Air Generator (Domnik Hunter, USA). Data acquisition and processing was carried out on Shimadzu C-R7A plus Chromatopac Software. The weighing of standards and synthetic samples were done on digital balance (Mettler Toledo AG 245).

GC analysis protocol for monomers EHA, EHMA and EGDMA

The GC analysis protocol established are as follows.

Preparation of internal standard solution: Butyl acrylate (BA) was used as an internal standard and its solution of 2378 ppm concentration was made in cyclohexane. 2.378 g of butyl acrylate (BA) was accurately weighed and dissolved in 1 L cyclohexane.

GC analysis

The upper cyclohexane layer that contains the extracted monomers form the reaction mass was decanted (5mL) in a glass vial and 1-2 g of anhydrous magnesium sulphate (dried in a furnace at 400^{o}C) was added. The solution was stirred and then kept undisturbed for half an hour to settle magnesium sulphate down until a clear solution was obtained. This clear solution was transferred to GC vial and was injected as it is for GC analysis.

Operating conditions GC/FID

The GC separation was carried out on J&W Scientific, USA DB-1 column with a dimension of 100 m × 0.25 mm and a film thickness of 0.5 μm. UHP grade Nitrogen was used as the carrier gas at a constant pressure of 220 kPa. The GC oven temperature was maintained at 225 °C and the temperatures of injector and detector were set at 275 °C and 300°C, respectively. For FID system, the hydrogen and zero air pressures were kept at 60 and 50 kPa, respectively. The injection volume for each sample was 5 μL with a split ratio of 23:1.

Calibration

For generating calibration curves, five different compositions of EHA, EGDMA, and EHMA were prepared and to each composition, the same amount of internal standard (BA) was added. All the individual standard solutions were prepared in 25 ml volumetric flask. The contents in each flask were diluted up to the mark with 2378 ppm solution of internal standard (BA).

Quantification of GC curves

The individual standard solutions were injected into GC and response factors were calculated. GC chromatogram of the PH3AK sample extract shows total five peaks. The very first peak is due to cyclohexane, which appears at a retention time (RT) of 12.5 min. The second peak is that of butyl acrylate (RT- 13.5 min), third is of EHA (RT-945 to 948 sec), fourth is EGDMA (RT-993 sec) and fifth is of EHMA (RT-1008 to 1011 sec). The area of these peaks of interest was calculated by integrating the peaks by drawing a base line manually with the help of curser key. After integration of all peaks, the result

window shows the peak area and RT of the integrated peaks. The peak area of all the peaks mainly of butyl acrylate and all three monomers was noted down.

Calculation of residual monomer: The peak area was used to calculate amount of monomers present by using the formula:

$$Rf = \left(\frac{Conc.}{Area}\right)_{compound} \left(\frac{Area}{Conc.}\right)_{\text{int}\,ernals\,\text{tan}\,dard}$$

Rf is a response factor of the particular monomers and the values were as follows.

	EHA	**EGDMA**	**EHMA**
Rf values	0.78778	1.16008	0.75399

By putting all the known values, weight of monomer was calculated using the above formula. The value obtained was for 1000 mL of internal standard solution. So the corresponding value for 100 mL internal standard solution was calculated and this value obtained in milligram (mg) is the amount of monomer present. After the determination of unreacted monomers, subsequently the polymer conversion was determined from the unreacted monomer data as shown in Table 3.7 and 3.8.

3.3.5 Results and Discussion

High internal phase emulsions (HIPEs) of the combination of monomers ethylhexyl acrylate (EHA), ethylhexyl methacrylate (EHMA) and ethylene glycol dimethacrylate (EGDMA) were prepared. The two combinations of monomers viz. EHA and EGDMA (PH2AK) and EHA, EHMA and EGDMA (PH3AK) were studied in the present polymerization kinetics of HIPEs. Polymerization kinetics using bulk, solution and emulsion polymerizations are well known in the literature. But the polymerization kinetic of polyHIPEs has not been mentioned hitherto. Polymerization of HIPEs is generally carried out using free radical polymerization process hence the factors affecting or responsible in free radical polymerization kinetics of other polymerization methods hold good for HIPE polymerization kinetics as well. Polymerization kinetics data for both the systems viz. PH2AK and PH3AK was generated at various parameters. The data was generated by varying the parameters like initiator type and concentration, inhibitor type and concentration, pH and temperature as shown in Table 3.6.

3.3.5.1 *Effect of initiator type and concentration*

Polymerization kinetics of PH3AK and PH2AK polyHIPEs was carried using 0.05 wt% and 0.20 wt% sodium persulphate (NaPS) initiator. The typical kinetics data (polymer conversion data) obtained by GC analysis for PH3AK polyHIPE after is shown in Table 3.7 and 3.8. The effect of initiator concentration on polymerization rate of PH3AK and PH2AK using 0.05 and 0.20 wt% sodium persulphate is compared in Figures 3.20 and 3.21 respectively. In both the systems it was observed that, polymerization rate in case of 0.20 wt% initiator concentration is higher as compared to

0.05 wt% initiator. For doing the comparison of the rate, data for only EHA monomer was considered to avoid complexity in all the kinetics studies carried out for PH3AK and PH2AK polyHIPEs.

Table 3.7 Polymerization kinetics data for PH3AK polyHIPE using 0.05 wt% sodium persulphate (NaPS) concentration

Time	EHA		EGDMA		EHMA	
(min)	mg	% conv	mg	% conv	mg	% conv
0	334.0	0	149.6	0.0	343.2	0
2	331.9	0.62	148.2	0.9	341.8	0.40
4	332.1	0.56	147.1	1.7	343.2	0
6	328.8	1.55	148.4	0.8	339.6	1.048
8	326.1	2.36	144.0	3.7	335.1	2.36
10	325.5	2.54	135.2	9.6	327.5	4.57
12	318.4	4.67	126.8	15.2	316.5	7.77
14	305.4	8.56	110.4	26.2	298.6	12.99
16	281.1	15.83	102.2	31.7	269.4	21.50
18	268.9	19.49	89.6	40.1	253.8	26.048
20	243.8	27.00	74.9	49.9	222.6	35.13
22	273.2	18.20	86.9	41.9	252.1	26.54
24	262.1	21.52	75.7	49.4	235.8	31.29

Table 3.8 Polymerization kinetics data for PH3AK polyHIPE using 0.20 wt% sodium persulphate (NaPS) concentration

Time	EHA		EGDMA		EHMA	
(min)	mg	% conv	mg	% conv	mg	% conv
0	328.4	0.0	154.7	0.0	337.7	0.0
2	320.9	2.3	144.9	6.3	325.7	3.6
4	317.1	3.4	136.7	11.6	319.3	5.4
6	313.7	4.5	124.6	19.5	306.1	9.4
8	290.4	11.6	104.6	32.4	277.3	17.9
10	256.7	21.8	65.2	57.9	213.1	36.9
12	229.3	30.2	53.9	65.2	176.2	47.8
14	178.6	45.6	30.4	80.3	115.1	65.9
16	164.6	49.9	27	82.5	100.2	70.3
18	108.5	67.0	20.2	86.9	62.1	81.6
20	99.4	69.7	19.9	87.1	57.4	83.0
22	80.4	75.5	15.8	89.8	47.9	85.8
24	81.1	75.3	20.7	86.6	55.9	83.4
26	75.3	77.1	17.6	88.6	51.4	84.8
28	48.9	85.1	12.3	92.0	35.7	89.4
30	60.4	81.6	18.6	88.0	50	85.2

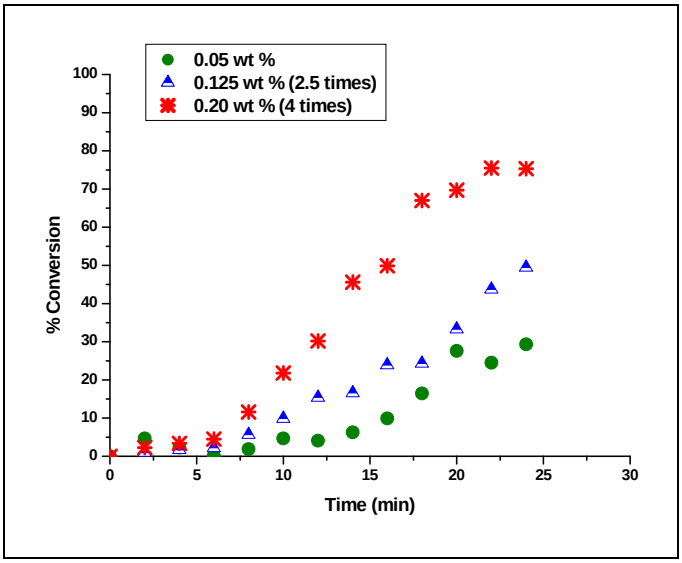

Figure 3.20 : Effect of initiator concentration (NaPS) on rate of polymerization of PH3AK polyHIPEs

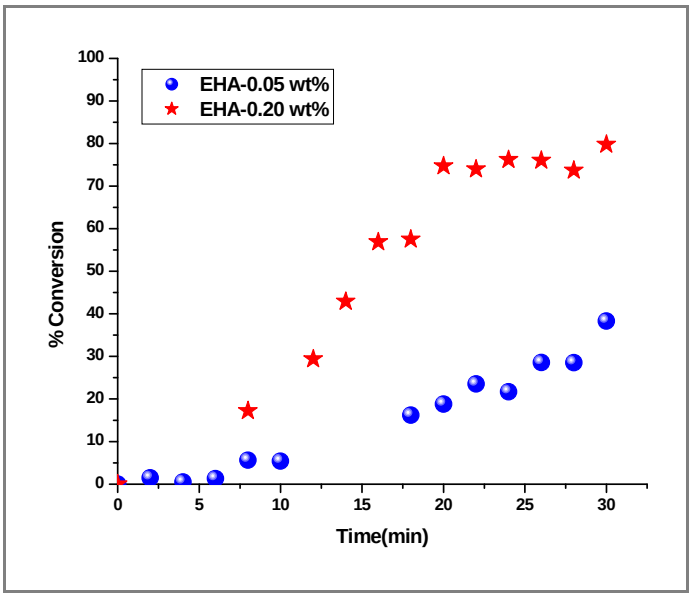

Figure 3.21 : Effect of initiator concentration (NaPS) on rate of polymerization of PH2AK polyHIPEs

The kinetics data was generated for PH2AK polyHIPEs using two redox-initiating systems. The redox initiators employed here were combination of NaPS: sodium bisulphite ($NaHSO_3$) and NaPS: sodium dithionite ($Na_2S_2O_4$). The redox system was used at 1:1 concentration. The effect of these two redox initiating system on rate of polymerization is as shown in Figure 3.22. From the data, it was observed that redox initiating system starts the polymerization faster and higher conversion of the polymer was achieved in approximately 10 min as compared to the system where 0.05 wt% NaPS was used as initiator.

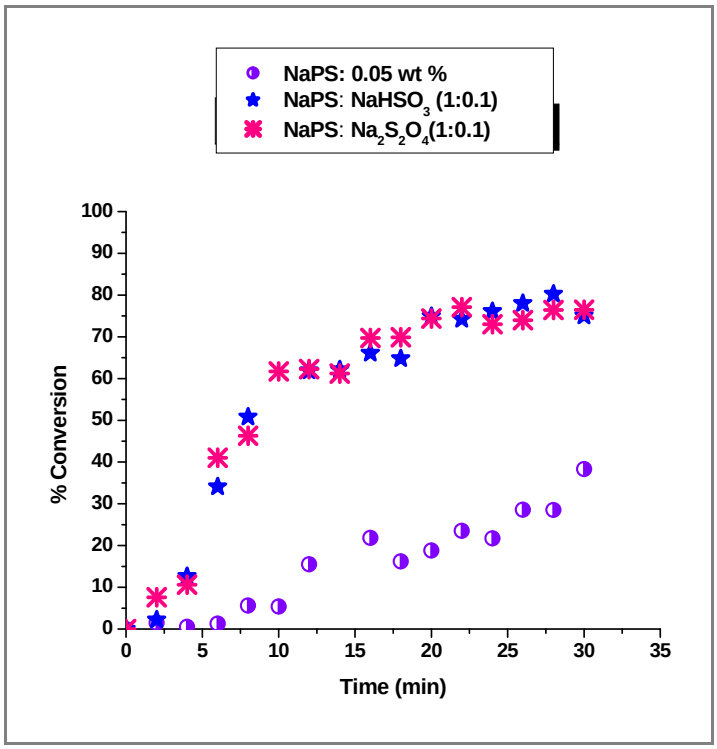

Figure 3. 22 : Effect of redox initiator on rate of polymerization of PH2AK polyHIPEs

3.3.5.2 *Effect of inhibitor type and concentration*

In the present investigation, two inhibitors were employed to see their effect on the rate of polymerization. The inhibitors employed were monomethyl ether hydroquinone (MEHQ) and phenothiazine (PTZ). Both the inhibitors were employed at different concentration levels viz, 1, 2, 3 and 4 mol% of NaPS used. Polymerization kinetics data was generated for both PH2AK and PH3AK polyHIPE synthesis using 0.2 wt% of NaPS and 1, 2, 3 and 4 mol% of MEHQ and PTZ as inhibitors. Figure 3.23 and 3.24 shows the effect of MEHQ concentration on the polymerization rate of PH3AK polymerization. The inhibition data was compared with the data where no inhibitor was used. At lower concentration of MEHQ, the effect is negligible but at higher concentration, i.e. 4.0 mol% the effect is predominantly observed. The dwell time (induction period) for 0 mol% inhibitor i.e., 7 min was shifted to 15 min in case where 4 mol% MEHQ was used. Hence, it was observed that lower concentration of MEHQ level hardly affects the rate of polymerization.

Figure 3.25 and 3.26 depicts the kinetics data generated using 0.2 wt% NaPS concentration and using phenothiazine (PTZ) as an inhibitor at 1, 2, 3 and 4 mol% concentration for PH3AK and PH2AK polyHIPEs respectively. The PTZ inhibition data was compared with data where no inhibitor was used. From the data, it was observed that phenothiazine acts as efficient inhibitor even at lower concentration. The effect on dwell time and rate is more in both PH3K and PH2K polymerizations. From Figure 3.27 it was observed that at 1 mol% concentration, phenothiazine was efficient inhibitor as compared to MEHQ inhibitor. This is due to the fact that MEHQ kills one radical per molecule while phenothiazine efficiently kills 4-5 radicals per molecule.

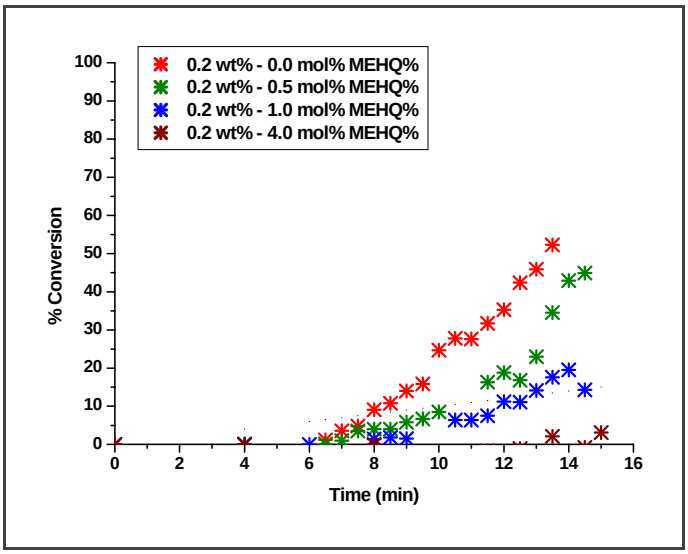

Figure 3.23 : Effect of MEHQ concentration on rate of polymerization of PH3AK polyHIPEs using 0.2 wt% initiator

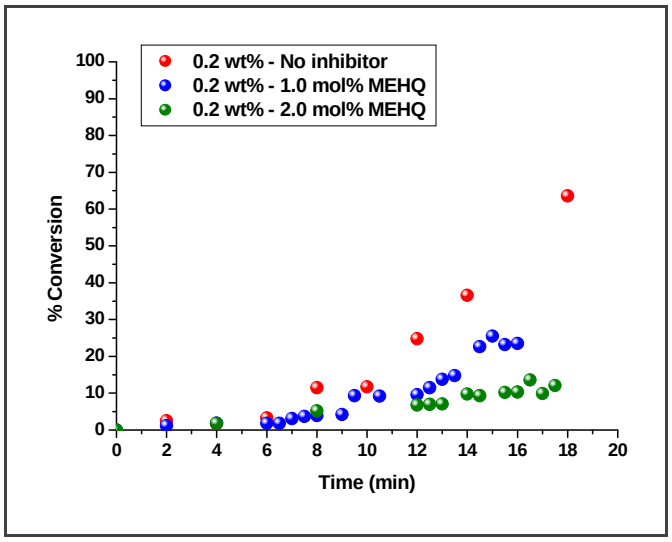

Figure 3.24 : Effect of MEHQ concentration (1 and 2 mol%) on rate of polymerization of PH3AK polyHIPEs using 0.2 wt% initiator

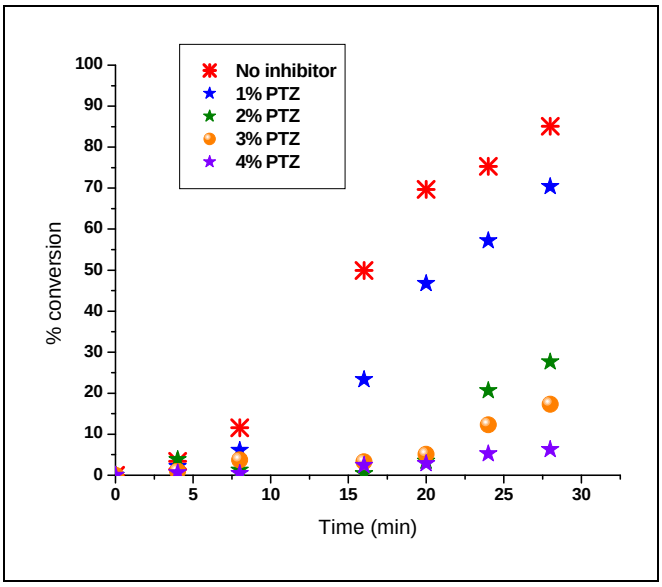

Figure 3.25 : Effect of Phenothiazine (inhibitor) concentration on rate of polymerization of PH3AK polyHIPEs

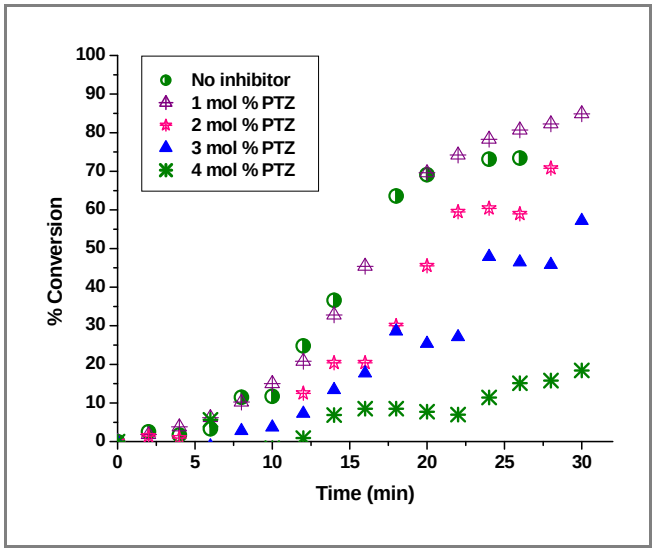

Figure 3.26 : Effect of Phenothiazine (inhibitor) concentration on rate of polymerization of PH2AK polyHIPEs

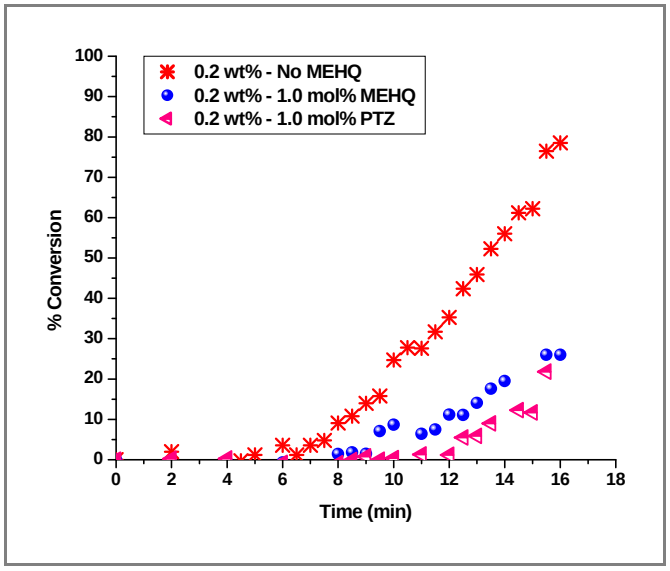

Figure 3. 27 : Effect of inhibitor type on the rate of polymerization of PH3AK polyHIPEs at 0.2 wt% initiator

3.3.5.3 *Effect of pH*

The influence of pH on the rate of HIPE polymerization of PH3AK system initiated by sodium persulphate (NaPS-0.2 wt%) was investigated. Polymerization kinetics data was generated for the PH3AK polyHIPEs by varying the pH of the system. Acrylic acid was used at 4 wt% based on oil phase. The kinetics data was generated at pH- 2.0, 4.0 , 7.5 and 8.5. Figure 3.28 shows the comparison of the kinetics data obtained at these four pH values. In case of normal emulsion polymerization, it is the well known fact that change in pH has effect on rate of polymerization, as due to pH, the interaction of the surfactant micelles changes and the rate is affected. But form the data obtained in case of HIPE polymerization by varying the pH, it is observed that change in pH has no effect on rate of polymerization. Since HIPE emulsion polymerization systems are very

complex, hence the conclusion could not be attributed to any factor which is involved in this phenomenon.

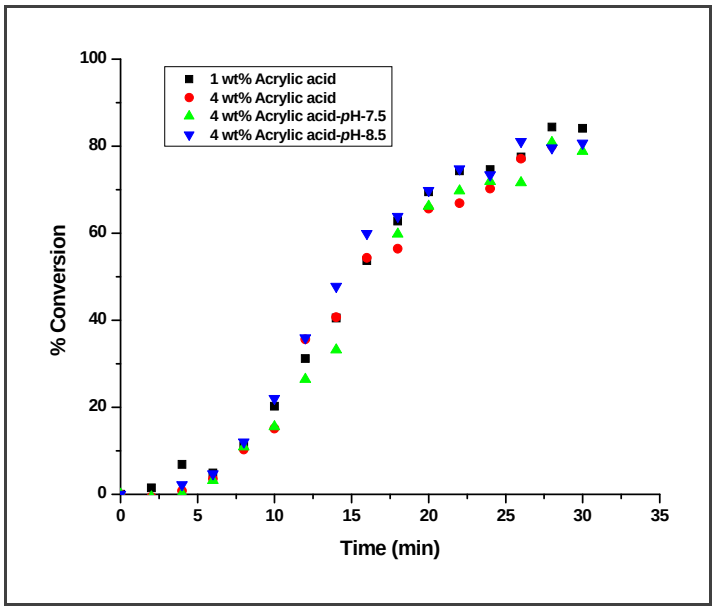

Figure 3.28 : Effect of pH on rate of polymerization of PH3AK polyHIPEs

3.3.5.4 *Effect of temperature*

Temperature has direct effect on the rate of polymerization. In case of HIPE polymerization also the rate of polymerization increases with an increase in temperature of the polymerization. Polymerization data was generated for PH3AK HIPEs at 65, 75 and 85^{o}C using 0.05 wt% sodium persulphate concentration. Figure 3.29 shows the prominent effect observed in the rate at higher temperatures.

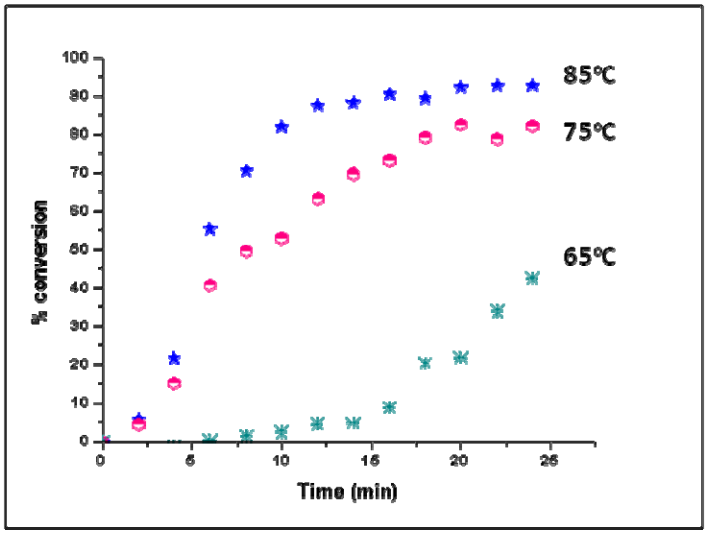

Figure 3. 29 : Effect of temperature on rate of polymerization of PH3AK polyHIPEs

3.3.6 Modeling of the kinetics data

3.3.6.1 Introduction

A comprehensive model to describe a complex chemical process usually consists of sets of differential and algebraic equations, containing multiple response variables, which are function of multiple input or design variables, and a potentially large number of parameters. As our understanding of chemical processes increases, the complexity of the models developed to describe them also increases. In most cases, the equations are nonlinear in the inputs and parameters and must be solved numerically. Various issues related to the different steps of parameter estimation have been addressed by various authors.[45-47] A series of benchmark papers have been critically evaluated k_p values and provided best fit Arrhenius parameters for styrene[48] and a series of methacrylates.[49] While also applied to other monomers, there have been significant difficulties in applying techniques to acrylates.

For a chemical reaction where substance A and B are reacting to produce C, the reaction rate has the form:

$$\text{Reaction: } A + B \rightarrow C$$

$$d[C]/dt = k(T)*[A]^m * [B]^n$$

k(T) is the reaction rate constant that depends on temperature. [C] is the concentration of substance C in moles per volume of solution. For order n, the rate coefficient has units of mol^{1-n} L^{n-1} s^{-1}. In statistics, regression analysis includes any

techniques for modeling and analyzing several variables, when the focus is on the relationship between a dependent variable and one or more independent variables.

Regression models involve the variables; (i) the unknown parameters denoted as β; this may be a scalar or a vector, (ii) the independent variables X and (iii) the dependent variable Y.

Linear regression: In linear regression, the model specification is that the dependent variable y_i is a linear combination of the parameters

Non Linear Regression analysis: When the model function is not linear in the parameters, the sum of squares must be minimized by an iterative procedure. In this, the best-fit curve is often assumed to be that which minimizes the sum of squared residuals. This is called ordinary least squares (OLS) approach.

Multiple regressions: A statistical technique allows us to predict someone's score on one variable based on their scores on several other variables. Regression diagnostics include R; it is the multiple correlation coefficients. It measures the degree of association (-1.0 to 1) between the criterion and the predictor variable taken simultaneously; R^2 is the coefficient of multiple determinations. It indicates the percentage of the variance in the criterion variable accounted for by the predictors taken together. Pearson's correlation coefficient is a measure of the correlation (linear dependence) between two variables X and Y, giving a value between +1 and −1 inclusive.

For the present kinetic studies, MATLAB was used for modeling, regression and simulation. The name MATLAB stands for MATrix LABoratory. MATLAB was written

originally to provide easy access to matrix software developed by the LINPACK (linear system package) and EISPACK (Eigen system package) projects. MATLAB is a high-performance language for technical computing. It integrates *computation*, *visualization*, and *programming* environment. Furthermore, MATLAB is a modern programming language environment: it has sophisticated *data structures*, contains built-in editing and *debugging tools*, and supports *object-oriented programming*. These factors make MATLAB an excellent tool for teaching and research. MATLAB has many advantages compared to conventional computer languages (e.g. C, FORTRAN) for solving technical problems. MATLAB is an interactive system whose basic data element is an *array* that does not require dimensioning. The software package has been commercially available since 1984 and is now considered as a standard tool at most universities and industries worldwide. It has powerful *built-in* routines that enable a very wide variety of computations. It also has easy to use graphics commands that make the visualization of results immediately available. Specific applications are collected in packages referred to as *toolbox*. There are toolboxes for signal processing, symbolic computation, control theory, simulation, optimization, and several other fields of applied science and engineering.

The Taylor methods in the preceding section have the desirable feature that the F.G.E. is of order $O(h^N)$, and N can be chosen large so that this error is small. However, the shortcomings of the Taylor methods are the a priori determination of N and the computation of the higher derivatives, which can be very complicated. Each Runge-Kutta method is derived from an appropriate Taylor method in such a way that the F.G.E. is of order $O(h^N)$. The Taylor methods have the desirable feature that the F.G.E is of the order

$O(h^N)$ and N can be chosen large so that a trade-off is made to perform several function evaluations at each step and eliminate the necessity to compute the higher derivatives. These methods can be constructed for any order N. The Runge-Kutta method of order N=4 is most popular. It is a good choice for common purposes because it is quite accurate, stable, and easy to program. A trade off is made to perform several function evaluations at each step and eliminate the necessity to compute the higher derivatives. These methods can be constructed for any order N. The Runge-Kutta method of order N=4 is most popular. It is a good choice for common purposes because it is quite accurate, stable and easy to program. Most authorities proclaim that it is not necessary to go to a higher-order method because the increased accuracy is offset by additional computational effort. If more accuracy is required, then either a smaller step size or an adaptive method should be used.

The Levenberg-Marquardt (LM) function from MATLAB was used for regression. The Levenberg-Marquardt (LM) algorithm is an iterative technique that locates the minimum of a multivariate function that is expressed as the sum of squares of non-linear real-valued functions. It is a standard technique for non-linear least-squares problems. LM can be thought of as a combination of steepest descent and the Gauss-Newton method. When the current solution is far from the correct one, the algorithm behaves like a steepest descent method: slow, but guaranteed to converge. When the current solution is far from the correct one, the algorithm behaves like a steepest descent method: slow, but guaranteed to converge. When the current solution is close to the correct solution, it becomes a Gauss-Newton method.

Least square regression analysis was used for estimating parameters. The term least squares describes a frequently used approach to solving over determined or inexactly specified systems of equations in an approximate sense. Instead of solving the equations exactly, we seek only to minimize the sum of the squares of the residuals. The least squares criterion has important statistical interpretations. If appropriate probabilistic assumptions about underlying error distributions are made, least squares produces what is known as the maximum-likelihood estimate of the parameters.

In numerical analysis, the Runge-Kutta methods are an important family of implicit and explicit iterative methods for the approximation of solutions of ordinary differential equations.

The common RK4 method is given by the following equations:

$$y_{n+1} = y_n + \frac{1}{6}(k_1 + 2k_2 + 2k_3 + k_4)$$
$$t_{n+1} = t_n + h$$

where y_{n+1} is the RK4 approximation of $y(t_{n+1})$, and

$$k_1 = hf(t_n, y_n)$$
$$k_2 = hf(t_n + \frac{1}{2}h, y_n + \frac{1}{2}k_1)$$
$$k_3 = hf(t_n + \frac{1}{2}h, y_n + \frac{1}{2}k_2)$$
$$k_4 = hf(t_n + h, y_n + k_3)$$

Thus, the next value (y_{n+1}) is determined by the present value (y_n) plus the weighted average of 4 deltas, where each delta is the product of the size of the interval ($h = \Delta t$) and an estimated slope: h (*slope*) = Δt (dy / dt) = Δy.

Averaging the four,

Delta= $1/6(k_1 + 2k_2 + 2k_3 + k_4)$;

The advantage of the RK4 method is obvious; no formulas for the higher derivatives need to be computed nor do they have to be in the program. The advantage of the RK4 method is obvious; no formulas for the higher derivatives need to be computed nor do they have to be in the program. It is not easy to determine the accuracy to which a Runge-Kutta solution has been computed. We could estimate the size of *y(4) (c)* and use formula (12). Another way is to repeat the algorithm using a smaller step size and compare results.

Arrhenius Equation: The Arrhenius equation gives "the dependence of the rate constant k of chemical reactions on the temperature *T* (in absolute temperature, such as Kelvin's or degrees Rankine) and activation energy E_a, as shown below

$k = A \exp(-E_a/RT)$, i.e.,

$\ln k = \ln A + ((-E_a/R)*1/T)$

where, k is in $mol1^{-n} \cdot L^{n-1} \cdot s^{-1}$, *A* is the pre-exponential factor or simply the prefactor and *R* is the Universal gas constant. (8.314 J/K mol)

3.3.6.2 Experimental

The kinetics data for modeling was generated for two monomer systems viz. EHA and EGDMA termed as PH2A-KM. To determine the activation energy and the rate constant, data was generated at three different temperatures viz 65, 75 and 85^oC. For each temperature the initiator and inhibitor concentrations were varied as shown in Table 3.9.

Table 3.9 Synthesis and generation of kinetics data for PH2A based polyHIPEs (PH2A-KM) for modeling studies

Polymer Code	NaPS Wt%	MEHQ mol% 65/75/85°C		MEHQ mol% 75°C	MEHQ mol% 85°C
PH2A-KM-1/17/33	0.05	0/0/0		0	0
PH2A-KM-2/18/34	0.05	1/1/1		1	1
PH2A-KM-3/19/35	0.05	2/2/-		2	-
PH2A-KM-4/20/36	0.05	3/3/-		3	-
PH2A-KM-5/21/37	0.05	4/-/-		-	-
PH2A-KM-6/22/38	0.10	0/0/0		0	0
PH2A-KM-7/23/39	0.10	1/1/1		1	1
PH2A-KM-8/24/39	0.10	2/2/2		2	2
PH2A-KM-9/25/40	0.10	3/3/3		-	3
PH2A-KM-10/26/41	0.10	4/4/4		4	4
PH2A-KM-11/27/42	0.20	0/0/0		0	0
PH2A-KM-12/28/43	0.20	-/1/1		1	1
PH2A-KM-13/29/44	0.20	2/-/2		-	2
PH2A-KM-14/30/45	0.20	3/3/3		3	3
PH2A-KM-15/31/46	0.20	4/4/-		4	-

3.3.6.3 Results and discussion

The data was joined based on temperature and modeled. Different model equations were used to model the data. The data for monomers (EHA, EGDMA), initiator and inhibitor was interpolated. Interpolation was done using curve fitting (constructing a function, which closely fits experimental data points). The nonlinear regression method by Levenberg-Marquardt, least square regression analysis was used for estimating kinetic parameters.

In this work an extensive experimental work involving synthesis of PH2A using thwo monomers (2-ethylhexyl acrylate; EHA and ethylene glycol dimethacrylate, EGDMA) and an initiator (sodium persulfate; NaPS) and an inhibitor (Monomethyl ether hydroquinone; MEHQ) was conducted. The experimental data comprised of results of variations in the concentrations of inhibitor and initiator. Variations in the reaction temperature were also studied. The experiments were carried out at three different temperatures viz; 65, 75 and 85^{o}C.

Model proposed

The phenomenological model was proposed to evaluate the rate parameters of the PH3A-KM kinetics data. The proposed model is as shown by equation 13.

$$r_p = -\frac{dc_m}{dt} = k_p \times (m_1)^a \times (Inhb)^b \times (Init)^c \times (m_2)^d \quad (13)$$

Where, r_p = Rate of Polymerization, moles/lit.min, k_p = Rate constant,min^{-1}

m_1 = Monomer Concentration 1(EHA), mol/ lit, Init = Initiator Concentration, mol/lit, Inhb = Inhibitor Concentration, mol/lit, m_2= Monomer Concentration 3(EGDMA), mol/lit. a, b, c and d are power terms of m_1, initiator, inhibitor, m_2 respectively. R is the correlation coefficient;

Value is the Sum of Squared Residuals.

1. rate of decrease of EHA = r1

At **65°C**

$$r_1 = -\frac{dc_{m1}}{dt} = k_{65} \times (m1)^{a1} \times (Inhb)^{b1} \times (Init)^{c1} \times (m2)^{d1} \quad (14)$$

At **75°C**

$$r_1 = -\frac{dc_{m1}}{dt} = k_{75} \times (m1)^{a1} \times (Inhb)^{b1} \times (Init)^{c1} \times (m2)^{d1} \quad (15)$$

At **85°C**

$$r_1 = -\frac{dc_{m1}}{dt} = k_{85} \times (m1)^{a1} \times (Inhb)^{b1} \times (Init)^{c1} \times (m2)^{d1} \quad (16)$$

Rate of initiation R_i is taken as

$$R_i = 2 \times f \times k_d \times I$$

R_i is the rate of initiator disappearance, mol lit^{-1} $min^{-1,}$ f is the initiator efficiency - 0.4 (initiator efficiency was considered as 0.4 because the parameter estimation results falls well in the range of 0.4), k_d is the initiator decomposition rate constant, which varies from 10^{-4}- 10^{-9} sec^{-1}.

$$I = I_o \times \exp(- k_d \times t)$$

I_o is the initial initiator concentration. mol/lit, t is the time in sec. Based on the temperature dependence assumption of k_d and its literature values, k_d was taken 10^{-6}, 10^{-5}, 10^{-4} for 65ºC,75ºC and 85ºC respectively. These values are taken according to the

literature reference and Arrhenius equation was evaluated. Figure 3.30 shows the Arrhenius plot for the evaluation of pre-exponential factor and activation energy.

Inhibition

Inhibitor, depending on the initiator and temperature.

$$Inhb = Inhb_0 - \frac{(R_i \times t)}{y}$$

Inhb = concentration of inhibitor. mol/lit, $Inhb_0$ = initial concentration of inhibitor mol/lit, R_i = rate of initiation. mol/lit.min, y = no. of molecules terminated, y = 1.

Rate of polymerization:

Experimental rate of polymerization i.e. dc_m/dt was calculated using the forward finite differences method as below:

$$\frac{dy_i}{dx} = \frac{1}{2 \times h} \times (-y_{i+2} + 4 \times y_{i+1} - 3 \times yi)$$

h (step size)= 0.5

The model was validated using MATLAB, fourth order Runge Kutta method was used to solve the ordinary differential equations as initial value problems.

-d[EHA]/dt=k*[EHA]^a*[EHMA]^b*[EGDMA]^c* [NaPS]^d*[MEHQ]^e

-d[EHMA]/dt = k*[EHA]^a *[EHMA]^b *[EGDMA]^c *[NaPS]^d*[MEHQ]^e

-d[EGDMA]/dt = k*[EHA]^a *[EHMA]^b *[EGDMA]^c *[NaPS]^d*[MEHQ]^e

$$d[NaPS]/dt = -K_d * [NaPS]_0 * \exp(-K_d * t)$$

$$d[MEHQ]/dt = -2*f*K_d*[NaPS]_0* \exp(-K_d * t)*(1- K_d*t)$$

Arrhenius Equation was used to plot rate constant values with temperature to find the Activation Energy values for the given process.

$$\ln k = \ln A+((-E_a/R)*1/T)$$

Table 3.10 Results of the modeling for EHA monomer at 65°C

Sr No.	Reaction temperature (°C)	Estimated Parameters
1	65	$k1_{65}$ = 8.9146e-05. a1 = 0.13415. b1 = -0.0249. c1 = 0.30813. d1 = 0.010325. e1 = -1.0807.
2	75	$k1_{75}$ = 1.41814e-04. a_1 = 0.13415. b_1 = -0.0249. c_1 = 0.30813. d_1 = 0.010325. e_1 = -1.0807.
3	85	$k1_{85}$ = 1.705e-04. a1 = 0.13415. b1 = -0.0249. c1 = 0.30813. d1 = 0.010325. e1 = -1.0807.

Table 3.10 shows the results of the parameters of the model equation at 65, 75 and 85°C. The modeled data was validated using Runge Kutta method. The experimental and modeled data are shown by green and red line respectively in Figure 3.30, 3.31 and 3.32 for EHA monomer at 65, 75 and 85°C.

R= 0.77 , Value = 3.43*10^-7;

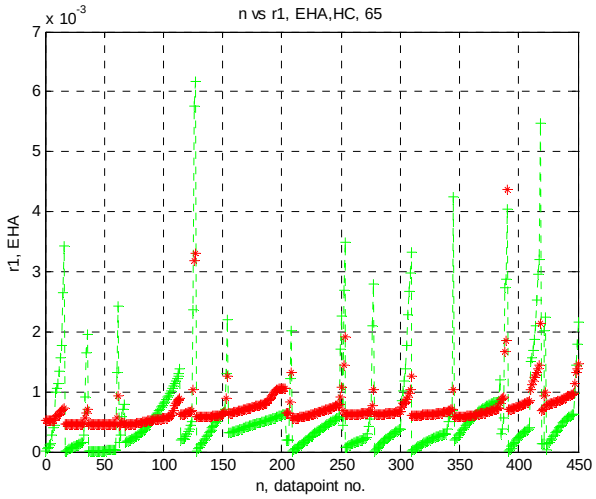

Figure 3.30: Verification of the experimental data by Runge Kutta method-EHA-65^{o}C

R= 0.89 , Value = 1.9182*10^-6;

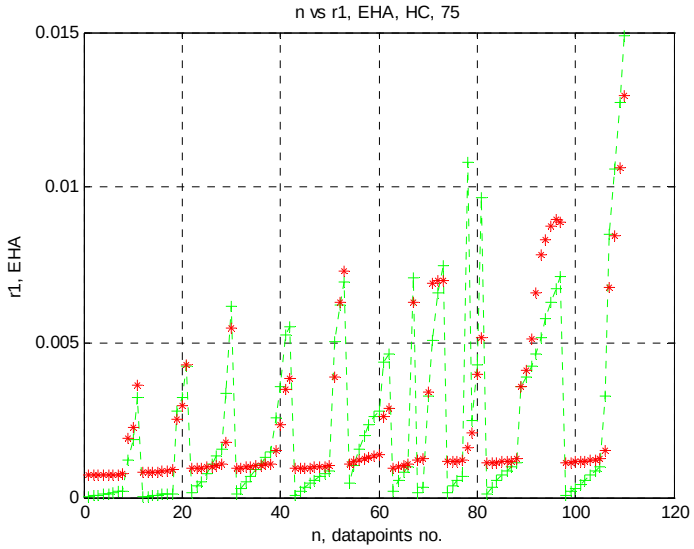

Figure 3.31: Verification of the experimental data by Runge Kutta method-EHA-75^{o}C

R= 0.6, Value = 1.78*10^-5;

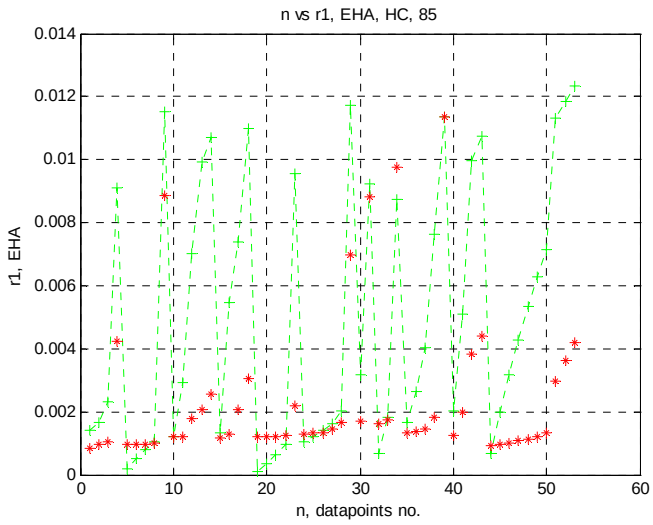

Figure 3.32 : Verification of the experimental data by Runge Kutta method-EHA-85^{o}C

From the data obtained Arrhenius plot was generated to evaluate activation energy of EHA monomer as shown in Figure 3.33.

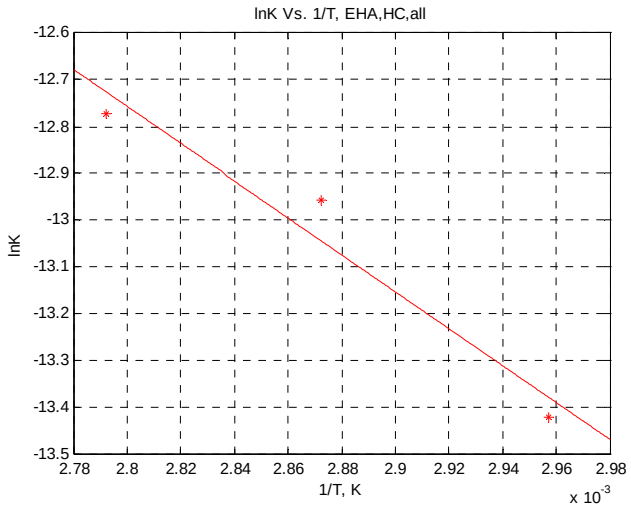

Figure 3.33 : Arrhenius plot for EHA monomer

Arrhenius plot- lnk vs. 1/T.

y = m*x + c

Coefficients: m = -3941.8, c = -1.7202, Norm of residuals = 0.1067

From the plot, Slope = -3941.8, Intercept = -1.7202

From Arrhenius equation,

The results obtained are,

(i) A= exp (-1.7202) = 0.17903 sec^{-1};

(ii) E_a = 32773.93843 J= 32.774 KJ.

E_a = 32773.93843*0.23890 cal= 7829.79 cal.

E_a = 7.83 kcal

The rate parameters and the activation energy were evaluated by using the modeling studies. The activation energy obtained for EHA monomer was 7829.79 cal or 32.77 KJ. The frequency factor determined was 0.17903 sec^{-1}. The above model studies can thus applied to various other reaction data generated using PH3AK type of polyHIPEs and by using phenothiazine as an inhibitor as well.

3.3.7 Conclusion

An attempt was made to investigate the effect of different parameters like initiator concentration, inhibitor concentration, pH and temperature on the rate high internal phase emulsion (HIPE) polymerization. To generate the polymerization kinetics, a synthesis method was established and kinetics data was generated. It was observed that like emulsion polymerization the rate increases with increase in initiator concentration and temperature. The inhibitor effect was also profoundly observed in case of MEHQ and phenothiazine.

An attempt was made to model the kinetics data by using a phenomenological modeled. Kinetics experiments using different initiator concentrations and inhibitor concentration were conducted at three different temperatures viz. 65, 75 and 85^{o}C. The phenomenological model was proposed to evaluate the rate parameters. Activation energy was calculated from the Arrhenius plot. The model was later validated by using Runge Kutta analysis method. The modeled data falls in close resemblance to the experimental data.

3.3.8 References

[1] Walling, C. *Free Radicals in Solution*, John Wiley & Sons, Inc., New York **1957**.

[2] Bamford, H.; Barb, W. G.; Jenkins, A. D.; Onyon, P. F. *The Kinetics of Vinyl Polymerization by Radical Mechanisms*, Academic Press, New York **1958**.

[3] Bagdasarian, H. S. *Theory of Radical Polymerization*, Izd. Akademii Nauk, Moscow **1959**.

[4] Moad, G.; Solomon, D. H. *The chemistry of Free Radical Polymerization*, Elsevier, Oxford, UK **1995**.

[5] Matyiaszewski, K.; Davis, T. P. *Handbook of Radical Polymerization*, Wiley-Interscience, Hoboken, N.J. 2002.

[6] Engel, P. S. *Chem. Rev*. **1980**, *80*, 99.

[7] Quinga, E. M. Y.; Mendenhall, G. D. *J. Org. Chem*. **1985**, *50*, 2836.

[8] Minamii, M.; Yamada, B.; Salamone, J. C. ed. *Polymeric Materials Encyclopedia*, CRC Press, Boca Raton, Fla. **1996**, p. 432.

[9] Callais, P. A.; Satas, D.; Tracton, A. A., eds., *Coatings Technology Handbook*, 2nd edn., Marcel Dekker, New York **2001**, p. 581.

[10] Sheppard, C. S. *Encycl. Polym. Sci. Eng*. **1987**, 11, 1.

[11] Moad, G.; Solomon, D. H. in Eastmond, G. C.; Ledwith, A.; Russo, S.; Sigwalt, P. eds. *Comprehensive Polymer Science*, Pergamon, London, **1989**, p.97.

[12] Moad, G.; Solomon, D. H. *The Chemistry of Free Radical Polymerization*, Pergamon, Oxford **1995**, p. 67.

[13] Fouassier, J. P. *J. Photopolym. Sci. Tec*. **1990**, *3*, 1.

[14] Fouassier, J. P. *Prog. Org. Coat*. **1990**, *18*, 229.

[15] Fouassier, J. P. *Recent Res. Dev. Photochem. Photobiol*. **2000**, *4*, 51.

[16] Yagci, Y. *Macomol. Symp*. **2000**, *161*, 19.

[17] Gruber, H. F. *Prog. Polym. Sci*. **1992**, *17*, 953.

[18] Sarac, A. S. *Prog. Polym. Sci.* **1999**, *24*, 1149.

[19] Bamford, C. H.; in Allen, G.; Agarwal S. L.; Russo, S. eds., *Comprehensive Polymer Science*, Vol. 3, Pergamon, Oxford, **1989**, p. 123.

[20] Odian, G. *Principles of Polymerization*, 3rd Edn. John Wiley & Sons, Inc., New York, **1991**, p.234.

[21] Moad, G.; Rizzardo E.; Solomon, D. H.; Johns, S. R.; Willing, R. I. *Makromol. Chem. Rapid Commun*. **1984**, *5*, 793.

[22] Achilias, D. S.; Kiparissides, C. *Macromolecules* **1992**, *25*, 3739.

[23] Moad, G.; Solomon, D. H.; Johns, S. R.; Willing, R. I. *Macromolecules* **1984**, *17*, 1094.

[24] Starnes, W. H. Jr.; Plitz, I. M.; Schilling, F. C.; Villacorta, G. M.; Park, G. S.; Saremi, A. H. *Macromolecules* **1984**, *17*, 2507.

[25] Buback, M.; Matyjaszewski, K. ed., *Controlled/Living Radical Polymerization* ACS Symposium Series 768, American Chemical Society, Washington, D.C., **2000**, p. 39.

[26] Matsumoto, A.; Mizuta, K. *Macromolecules* **1994**, *27*, 5863.

[27] Buback, M.; Huckestein, B.; Kuchta, F. D.; Russell, G. T.; Schmid, *Macromol. Chem. Phys*. **1994**, *195*, 2117.

[28] Samios, J.; Dorfmuller, T. *J. Chem. Phys*. **1982**, *76*, 5463.

[29] Gridnev, A. A.; Ittel, S. D. *Macromolecules* **1996**, *29*, 5864.

[30] Heuts, J. P. A.; Gilbert, R. G.; Radom, L. *Macromolecules* **1995**, *28*, 8771.

[31] Deady, M.;. Mau, A. W. H.; Moad, G.; Spurling, T. H. *Makromol. Chem.* 1993, 194, 1691.

[32] Zetterlund, P. B.; Busfield, W. K.; Jenkins, I. D. *Macromolecules* 1999, **32**, 8041.

[33] Shipp, D. A.; Smith, T. A.; Solomon, D. H.; Moad, G. *Macromol. Rapid Commun.* **1995**, *16*, 837.

[34] Moad, G.; Rizzardo, E.; Solomon, D. H.; Bechwith, A. L. J. *Polym. Bull.* **1993**, *29*, 1691.

[35] Zeterlund, P.; Busfield, W. K.; Jenkins, I. D. *Macromolecules* **1999**, *32*, 8041.

[36] Olaj, O. F.; Vana, P.; Kornherr, A.; Zifferer, G.; *Macromol. Rapid Commun.* **2000**, *19*, 913.

[37] Olaj, O. F.; Vana, P.; Zoder, M. *Macromolecules* **2002**, *35*, 1208.

[38] Zetterlund, P.B.; Busfield, W. K.; Jenkins, I. D. *Macromolecules* **2002**, *35*, 7232.

[39] Kajiwara, A.; Kamachi, M. *Polym. Prepr. (Am. Chem. Soc., Div. Polym. Chem.)* **2002***, 43,* 144.

[40] Busfield, W.K.; in Brandup, J.; Immergut, E. H. eds. Polymer Handbook, 3rd edn. John Wiley & Sons, Inc., New York, **1987**, p. 555.

[41] Sawada, H. *J. Macromol. Sci., C: Rev. Macromol. Chem.* **1969**, *3*, 313.

[42] Allen, P. E. M.; Patrick, C. R. *Kinetics and Mechanism of Polymerization Reactions* 1974, Ellis Horwood, Chichester, U.K.

[43] Azuma, H.; Katagiri, Y.; Yamabe, S. *J. Polym. Sci., Polym. Chem.* **1996**, *34*, 1407.

[44] Yee, L. H.; Coote, L. M.; Davis, T. P.; Chaplin, R.P. *J. Polym. Sci., Polym. Chem.* **2000**, *38*, 2192.

[45] Duever, T. A.; Penlidis, A. *Appl. Math. And Comp. Sci*. **1998**, *8*, 815.

[46] Bartus, "*Parameter Estimation in Dynamic Systems"*, PhD thesis, the University of Michigan, Michigan, USA, **1987**.

[47] Box, G. E. P.; Hunter, W. G.; MacGregor, J. F. Erjavec, J. *Technometrics* **1973**, 15, 33.

[48] Buback, M.; Gilbert, R. G.; Hutchinson, R. A.; Klumperman, B.; Kuchta, F. D.; Manders, B.G.; O'Driscoll, K. F.; Rusell G. T.; Schweer, J. *Macromol. Chem. Phys*. **1995**, *196*, 3267.

[49] Beuermann, S.; Buback, M. Davis, T. P.; Gilbert, R. G.; Hutchinson, R.A.; Olaj, O. F.; Rusell G. T.; Schweer, J. van Herk, A. M. *Macromol. Chem. Phys*. **1997**, *198*, 1545.

CHAPTER - IV

Synthesis and morphological studies of styrene based polyHIPEs

4.1 Introduction

Emulsion templating of high internal phase emulsions (HIPEs) was used to synthesize microcellular styrene-divinylbenzene (St-DVB) polyHIPE monoliths with open, interconnected porous structures. Styrene-divinylbenzene polyHIPEs have been subject of research extensively for many years. Different applications of these polyHIPEs have led researchers to look on various aspects of the synthesis of these polymers. PolyHIPEs prepared from these monomers are rigid and can be converted into various forms depending upon the usage. It is well known that polymers are used as templates to encapsulate inorganic particles inside the porous matrices. The size of the particles depends on the pore dimensions of the porous polymers. An attempt is being made to study the incorporation of cadmium sulphide (CdS) particles in the polymers synthesized using HIPE templating.

The present chapter deals with the effect of variation in composition and incorporation of inorganic particles on the stability of HIPE and morphology of the polyHIPEs synthesized. The St-DVB HIPE emulsions were stabilized using different type of surfactants. Experiments were conducted to prepare St-DVB HIPEs by varying crosslink density, type of surfactant and volume ratios of internal phase (oil : water ratios) and cured thermally. The details are as follows.

- *Synthesis and characterization of styrene-divinylbenzene polyHIPEs*

This part deals with studies of effect of variation in chemical composition like ratio of oil : aqueous phase, surfactant type and crosslink density on the morphology of polyHIPEs. The use of nonionic surfactants to form stable water in oil (W : O) emulsions

is well known. Non-ionic surfactants with high ratio of aqueous discontinuous phase are known to form stable HIPE. The present study emphasizes on the use of ionic surfactants. The feasibility of HIPE methodology on the polymer characteristics using low oil : water ratios using different surfactants was studied.

- *Incorporation of cadmium sulphide(CdS) particles in styrene-divinylbenzene polyHIPEs*

This part deals with studies of incorporation of inorganic particles like cadmium sulphide in poly(St-DVB) monoliths using two different strategies (insitu during HIPE formation and external incorporation after polymerization). The effect of incorporation of these particles on the morphology of the polymers was studied. The qualitative and quantitative presence of inorganic particles inside the poly(St-DVB) monolithic matrix was studied. The objective of this is to disperse CdS particles in the porous polymer matrix and see their effect on the morphology of the final polyHIPE.

4.2 Synthesis and characterization of St-DVB polyHIPEs

4.2.1 Experimental

4.2.1.1 *Materials*

Styrene (from Encore Chemicals), Divinylbenzene-80% and Di(hydrogenated tallow) dimethyl ammonium chloride (Arquad 2HT-75) (from Aldrich), Sorbitan monooleate (Span 80) and Sorbitan monolaurate (Span 20) and Sodium peroxydisulphate (from Loba Chemie), De-ionized water was collected from Millipore unit.

4.2.1.2 *Purification of monomer*

The monomer styrene was purified to remove the inhibitor present in it. Styrene was washed with 5 wt% aqueous NaOH solution to remove the inhibitor and then washed several times with water to ensure complete removal of NaOH.

4.2.1.3 *Procedure*

The requisite quantity of monomers and surfactant (oil phase) was weighed in a 100 mL plastic container. The aqueous phase i.e. water was added drop-wise to the oil phase under constant stirring speed of 1000 rotations per minute. Gradually with addition of water with continuous stirring HIPE was formed till complete addition of aqueous phase, followed by addition of sodium peroxydisulphate (initiator) dissolved in 1mL of water (1 mL water is the inclusive of total water used). The reaction mixture was mixed thoroughly for 1 min and then polymerized in a constant temperature water bath at 60^{o}C. The polymerization was carried out for 8 hours. After the polymerization was over, the polymeric monoliths were removed from the plastic container and cut into 5 mm thick discs. The discs were then punched into small discs having a diameter of 15 mm using a metallic punch. The discs were then dried at room temperature. The experimental details of variation in crosslink density, oil : water and surfactant type are tabulated in Tables 4.1 to 4.9 below.

Table 4.1 Synthesis of 50% cross-linked St-DVB polyHIPEs using Span 80 as surfactant

Polymer Code	Styrene g (mol)	Divinylbenzene g (mol)	oil : water ratio	Surface area (m^2/g)
SDN-1.1	1.123 ($10.79x10^{-3}$)	0.701 ($5.38x10^{-3}$)	1 : 1	2.00
SDN-1.2	1.123 ($10.79x10^{-3}$)	0.701 ($5.38x10^{-3}$)	1 : 2.5	2.34
SDN-1.3	1.123 ($10.79x10^{-3}$)	0.701 ($5.38x10^{-3}$)	1 : 5	3.30
SDN-1.4	1.123 ($10.79x10^{-3}$)	0.701 ($5.38x10^{-3}$)	1 : 10	3.95
SDN-1.5	1.123 ($10.79x10^{-3}$)	0.701 ($5.38x10^{-3}$)	1 :15	2.95
SDN-1.6	1.123 ($10.79x10^{-3}$)	0.701 ($5.38x10^{-3}$)	1 : 20	5.30
SDN-1.7	1.123 ($10.79x10^{-3}$)	0.701 ($5.38x10^{-3}$)	1 : 25	4.48

Span 80 = 20 wt % of oil phase, sodium peroxydisulphate = 1 mol % of oil phase, stirring speed = 1000 rpm, reaction temperature = 60°C

Table 4.2 Synthesis of 50% cross-linked St-DVB polyHIPEs using Span 20 as surfactant

Polymer Code	Styrene g (mol)	Divinyl benzene g (mol)	oil : water ratio	Surface area (m^2/g)
SDN-2.1	1.123 ($10.79x10^{-3}$)	0.701 ($5.38x10^{-3}$)	1 : 1	1.23
SDN-2.2	1.123 ($10.79x10^{-3}$)	0.701 ($5.38x10^{-3}$)	1 : 2.5	0.00
SDN-2.3	1.123 ($10.79x10^{-3}$)	0.701 ($5.38x10^{-3}$)	1 : 5	1.63
SDN-2.4	1.123 ($10.79x10^{-3}$)	0.701 ($5.38x10^{-3}$)	1 : 10	3.58
SDN-2.5	1.123 ($10.79x10^{-3}$)	0.701 ($5.38x10^{-3}$)	1 :15	9.32
SDN-2.6	1.123 ($10.79x10^{-3}$)	0.701 ($5.38x10^{-3}$)	1 : 20	13.02
SDN-2.7	1.123 ($10.79x10^{-3}$)	0.701 ($5.38x10^{-3}$)	1 : 25	9.96

Span 20 = 20 wt % of oil phase, sodium peroxydisulphate = 1 mol % of oil phase, stirring speed = 1000 rpm, reaction temperature = 60°C

Table 4.3 Synthesis of 50% cross-linked St-DVB polyHIPEs using Arquad 2HT-75 as surfactant

Polymer Code	Styrene g (mol)	Divinyl benzene g (mol)	oil : water ratio	Surface area (m^2/g)
SDN-3.1	1.123 ($10.79x10^{-3}$)	0.701 ($5.38x10^{-3}$)	1 : 1	1.58
SDN-3.2	1.123 ($10.79x10^{-3}$)	0.701 ($5.38x10^{-3}$)	1 : 2.5	0.00
SDN-3.3	1.123 ($10.79x10^{-3}$)	0.701 ($5.38x10^{-3}$)	1 : 5	0.00
SDN-3.4	1.123 ($10.79x10^{-3}$)	0.701 ($5.38x10^{-3}$)	1 : 10	0.31
SDN-3.5	1.123 ($10.79x10^{-3}$)	0.701 ($5.38x10^{-3}$)	1 :15	0.58
SDN-3.6	1.123 ($10.79x10^{-3}$)	0.701 ($5.38x10^{-3}$)	1 : 20	3.86
SDN-3.7	1.123 ($10.79x10^{-3}$)	0.701 ($5.38x10^{-3}$)	1 : 25	6.69

Arquad 2HT-75 = 20 wt % of oil phase, sodium peroxydisulphate = 1 mol % of oil phase, stirring speed = 1000 rpm, reaction temperature = 60°C

Table 4.4 Synthesis of 75% cross-linked St-DVB polyHIPEs using Span 80 as surfactant

Polymer Code	Styrene g (mol)	Divinyl benzene g (mol)	oil : water ratio	Surface area (m^2/g)
SDN-4.1	0.942 ($9.04x10^{-3}$)	0.883 ($6.78x10^{-3}$)	1 : 1	2.80
SDN-4.2	0.942 ($9.04x10^{-3}$)	0.883 ($6.78x10^{-3}$)	1 : 2.5	2.15
SDN-4.3	0.942 ($9.04x10^{-3}$)	0.883 ($6.78x10^{-3}$)	1 : 5	7.31
SDN-4.4	0.942 ($9.04x10^{-3}$)	0.883 ($6.78x10^{-3}$)	1 : 10	5.32
SDN-4.5	0.942 ($9.04x10^{-3}$)	0.883 ($6.78x10^{-3}$)	1 :15	9.38
SDN-4.6	0.942 ($9.04x10^{-3}$)	0.883 ($6.78x10^{-3}$)	1 : 20	2.30
SDN-4.7	0.942 ($9.04x10^{-3}$)	0.883 ($6.78x10^{-3}$)	1 : 25	4.87

Span 80 = 20 wt % of oil phase, sodium peroxydisulphate = 1 mol % of oil phase, stirring speed = 1000 rpm, reaction temperature = 60°C

Table 4.5 Synthesis of 75% cross-linked St-DVB polyHIPEs using Span 20 as surfactant

Polymer Code	Styrene g (mol)	Divinyl benzene g (mol)	oil : water ratio	Surface area (m^2/g)
SDN-5.1	0.942 ($9.04x10^{-3}$)	0.883 ($6.78x10^{-3}$)	1 : 1	6.75
SDN-5.2	0.942 ($9.04x10^{-3}$)	0.883 ($6.78x10^{-3}$)	1 : 2.5	4.57
SDN-5.3	0.942 ($9.04x10^{-3}$)	0.883 ($6.78x10^{-3}$)	1 : 5	3.34
SDN-5.4	0.942 ($9.04x10^{-3}$)	0.883 ($6.78x10^{-3}$)	1 : 10	7.70
SDN-5.5	0.942 ($9.04x10^{-3}$)	0.883 ($6.78x10^{-3}$)	1 :15	6.55
SDN-5.6	0.942 ($9.04x10^{-3}$)	0.883 ($6.78x10^{-3}$)	1 : 20	5.05
SDN-5.7	0.942 ($9.04x10^{-3}$)	0.883 ($6.78x10^{-3}$)	1 : 25	10.16

Span 20 = 20 wt % of oil phase, sodium peroxydisulphate = 1 mol % of oil phase, stirring speed = 1000 rpm, reaction temperature = 60°C

Table 4.6 Synthesis of 75% cross-linked St-DVB polyHIPEs using Arquad 2HT-75 as surfactant

Polymer Code	Styrene g (mol)	Divinyl benzene g (mol)	oil : water ratio	Surface area (m^2/g)
SDN-6.1	0.942 ($9.04x10^{-3}$)	0.883 ($6.78x10^{-3}$)	1 : 1	0.09
SDN-6.2	0.942 ($9.04x10^{-3}$)	0.883 ($6.78x10^{-3}$)	1 : 2.5	0.12
SDN-6.3	0.942 ($9.04x10^{-3}$)	0.883 ($6.78x10^{-3}$)	1 : 5	0
SDN-6.4	0.942 ($9.04x10^{-3}$)	0.883 ($6.78x10^{-3}$)	1 : 10	3.11
SDN-6.5	0.942 ($9.04x10^{-3}$)	0.883 ($6.78x10^{-3}$)	1 :15	3.19
SDN-6.6	0.942 ($9.04x10^{-3}$)	0.883 ($6.78x10^{-3}$)	1 : 20	3.14
SDN-6.7	0.942 ($9.04x10^{-3}$)	0.883 ($6.78x10^{-3}$)	1 : 25	3.62

Arquad 2HT-75 = 20 wt % of oil phase, sodium peroxydisulphate = 1 mol % of oil phase, stirring speed = 1000 rpm, reaction temperature = 60°C

Table 4.7 Synthesis of 100% cross-linked St-DVB polyHIPEs using Span 80 as surfactant

Polymer Code	Styrene g (mol)	Divinyl benzene g (mol)	oil : water ratio	Surface area (m^2/g)
SDN-7.1	0.812 ($7.79x10^{-3}$)	1.015 ($7.79x10^{-3}$)	1 : 1	0.94
SDN-7.2	0.812 ($7.79x10^{-3}$)	1.015 ($7.79x10^{-3}$)	1 : 2.5	8.24
SDN-7.3	0.812 ($7.79x10^{-3}$)	1.015 ($7.79x10^{-3}$)	1 : 5	7.23
SDN-7.4	0.812 ($7.79x10^{-3}$)	1.015 ($7.79x10^{-3}$)	1 : 10	1.89
SDN-7.5	0.812 ($7.79x10^{-3}$)	1.015 ($7.79x10^{-3}$)	1 :15	9.17
SDN-7.6	0.812 ($7.79x10^{-3}$)	1.015 ($7.79x10^{-3}$)	1 : 20	1.13
SDN-7.7	0.812 ($7.79x10^{-3}$)	1.015 ($7.79x10^{-3}$)	1 : 25	0.00

Span 80 = 20 wt % of oil phase, sodium peroxydisulphate = 1 mol % of oil phase, stirring speed = 1000 rpm, reaction temperature = 60^{o}C

Table 4.8 Synthesis of 100% cross-linked St-DVB polyHIPEs using Span 20 as surfactant

Polymer Code	Styrene g (mol)	Divinyl benzene g (mol)	oil : water ratio	Surface area (m^2/g)
SDN-8.1	0.812 ($7.79x10^{-3}$)	1.015 ($7.79x10^{-3}$)	1 : 1	0.00
SDN-8.2	0.812 ($7.79x10^{-3}$)	1.015 ($7.79x10^{-3}$)	1 : 2.5	0.00
SDN-8.3	0.812 ($7.79x10^{-3}$)	1.015 ($7.79x10^{-3}$)	1 : 5	0.00
SDN-8.4	0.812 ($7.79x10^{-3}$)	1.015 ($7.79x10^{-3}$)	1 : 10	0.00
SDN-8.5	0.812 ($7.79x10^{-3}$)	1.015 ($7.79x10^{-3}$)	1 :15	9.01
SDN-8.6	0.812 ($7.79x10^{-3}$)	1.015 ($7.79x10^{-3}$)	1 : 20	0.00
SDN-8.7	0.812 ($7.79x10^{-3}$)	1.015 ($7.79x10^{-3}$)	1 : 25	0.00

Span 20 = 20 wt % of oil phase, sodium peroxydisulphate = 1 mol % of oil phase, stirring speed = 1000 rpm, reaction temperature = 60^{o}C

Table 4.9 Synthesis of 100 % cross-linked St-DVB polyHIPEs using Arquad 2HT-75 as surfactant

Polymer Code	Styrene g (mol)	Divinyl benzene g (mol)	oil : water ratio	Surface area (m^2/g)
SDN-9.1	0.812 ($7.79x10^{-3}$)	1.015 ($7.79x10^{-3}$)	1 : 1	2.15
SDN-9.2	0.812 ($7.79x10^{-3}$)	1.015 ($7.79x10^{-3}$)	1 : 2.5	0.00
SDN-9.3	0.812 ($7.79x10^{-3}$)	1.015 ($7.79x10^{-3}$)	1 : 5	0.00
SDN-9.4	0.812 ($7.79x10^{-3}$)	1.015 ($7.79x10^{-3}$)	1 : 10	0.18
SDN-9.5	0.812 ($7.79x10^{-3}$)	1.015 ($7.79x10^{-3}$)	1 :15	0.62
SDN-9.6	0.812 ($7.79x10^{-3}$)	1.015 ($7.79x10^{-3}$)	1 : 20	3.30
SDN-9.7	0.812 ($7.79x10^{-3}$)	1.015 ($7.79x10^{-3}$)	1 : 25	7.67

Arquad 2HT-75 = 20 wt % of oil phase, sodium peroxydisulphate = 1 mol % of oil phase, stirring speed = 1000 rpm, reaction temperature = 60^oC

4.2.2 Characterization

The HIPE emulsions prepared were studied using optical microscopy and the polymerized (St-DVB) monoliths were characterized for morphology using SEM.

4.2.2.1 *Optical microscopy*

The HIPE emulsion before polymerization was characterized for its formation and structure elucidation by an OLYMPUS polarized optical microscope at a magnification of 50X. The images were recorded using OLYMPUS digital camera.

4.2.2.2 *Scanning electron microscopy (SEM)*

The morphologies of the polyHIPEs prepared were studied using a Lieca Stereoscan 440 scanning electron microscope at different magnifications. The energy of analysis was 20 keV.

4.2.2.3 *Surface area analysis-BET method*

Surface areas of the polymers were determined using NOVA 2000e surface area analyzer from Quantachrome. The analysis was done using pure nitrogen at a flow rate of 10 psi and the data was processed using Autosorb 1 software. The method used was Brunauer-Emmett-Teller method (BET). The samples were degassed for 3 hours at 60^{o}C and then analyzed.

4.2.3 Results and discussion

During polyHIPE preparation, many physicochemical processes occur and hence material's morphology is rather unique and has a hierarchical pore distribution. The materials have pores that have been shown to be roughly the same diameter as the droplets of the precursor HIPE. This is governed by the thermodynamics of polymer phase separation from the continuous phase and the delicate equilibrium of emulsion phase separation versus droplet stabilization. The polymerization of the monomer phase results in a continuous polymer domain droplet around the spherical pores thereby forming the skeleton of polyHIPE. These larger pores (typically 1 to 100 μm in diameter) can be considered the first level of polyHIPE porosity and result in the microcellular structure.

The effect of variation in composition on formation of St-DVB HIPE and morphology of subsequent polyHIPEs were studied. The details of the experiments carried out by varying oil: water ratios, crosslink density and surfactant type are tabulated in Tables 4.1 to 4.9. The water in oil (W/O) HIPEs were prepared using two different types of surfactants namely nonionic and ionic. In the nonionic category, sorbitan esters such as Span 80 and Span 20 were employed and the ionic surfactant chosen was Arquad 2HT-75. Surfactants have the tendency or ability to lower the interfacial tension between the oil and water phase, forming rigid interfacial film with rapid adsorption at the interface. Sorbitan monooleate (Span 80) comes under the class of unsaturated sorbitan monoesters while sorbitan monolaurate (Span 20) is saturated sorbitan monoester. Sorbitan fatty acid ester surfactants are known to be effective reducers of interfacial tension. The HLB value of Span 80 is 4.3 while that of Span 20 is 8.6. The short

hydrocarbon chain of sorbitan monolaurate and the double bonded hydrocarbon chain of sorbitan monooleate make these surfactants more polar than surfactants having longer hydrophobic chains. The hydrophilic lipophillic balance (HLB) represents the relative simultaneous attraction of an emulsifier for water and oil. Larger the size of the droplets that comprise the internal phase more readily the emulsion tends to coalesce. Arquad 2HT-75 is a di(hydrogenated tallow) dimethyl ammonium chloride. In all the cases it was observed that the surface area of the polymers obtained was too small in the range of 0 to 10 m^2/g. This is because in HIPE polymerization methodology, water having an average droplet size of 10 μm acts as discontinuous phase to obtain interconnected pore structure after polymerization.

The stability of the HIPE formed was studied using optical microscopy and the morphology of the polymerized HIPEs was studied using SEM. Figures 4.1- 4.14 depict the optical microscopy images and SEM micrographs of the HIPE emulsions and polymers respectively having 50 % crosslink density with variation in oil : water ratio and surfactant type. The effect of 1 : 1 (O : W) ratio with variation in surfactant type on the W/O emulsion stability and morphology of polymer is shown in Figure 4.1 (a) to (c) and Figure 4.2 (a) to (c) respectively. It was observed that for all the three different types of surfactants used at 1: 1 (O : W) ratio the emulsion was unstable. This confirms the fact that to form a stable HIPE, internal phase volume must be greater than 74%. Hence the quantity of aqueous discontinuous phase was insufficient to form a stable HIPE. Polymerization of these emulsions led to the formation of polymer having non-uniform distribution of pores failing to form interconnected polyHIPEs as observed in SEM images.

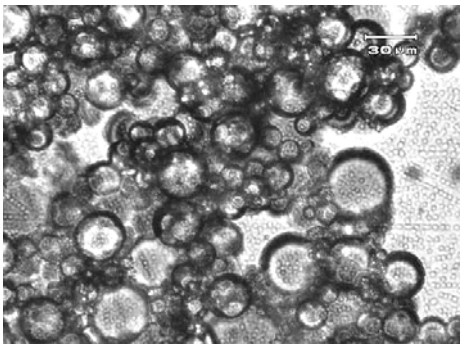

Figure 4.1 (a) : Span 80 (50 X)

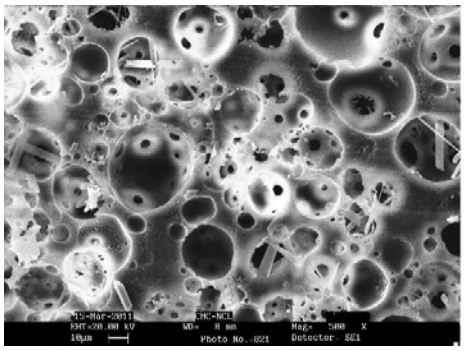

Figure 4.2 (a) : Span 80 (500 X)

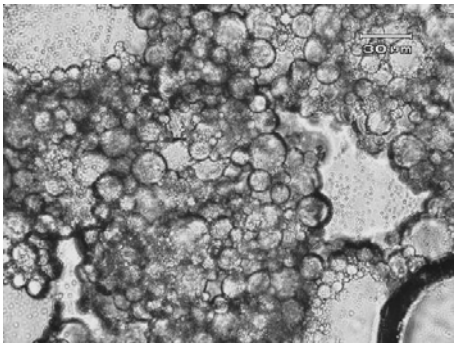

Figure 4.1 (b) : Span 20 (50 X)

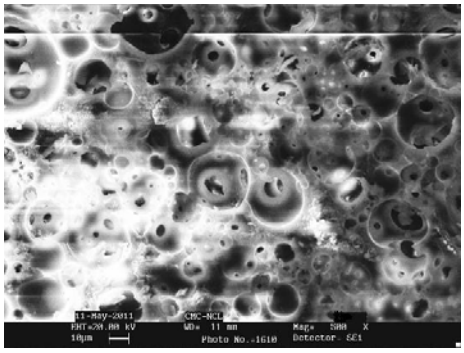

Figure 4.2 (b) : Span 20 (500 X)

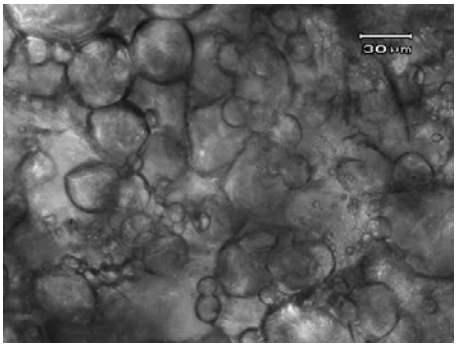

Figure 4.1 (c) : Arquad 2HT-75 (50 X)

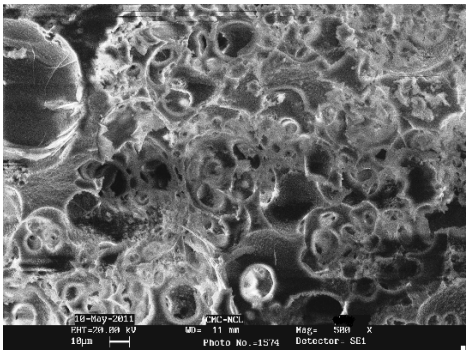

Figure 4.2 (c) : Arquad 2HT-75 (500 X)

Figure 4.1 : Optical microscopy images of HIPEs having 50% CLD and 1 : 1; oil : water ratio with surfactant variation

Figure 4.2 : SEM images of polyHIPEs having 50% CLD and 1 : 1; oil : water ratio with surfactant variation

The effect of 1 : 2.5 (O:W) ratio on the HIPE emulsion and pore morphology of the polymers is shown in Figure 4.3 (a-c) and 4.4 (a-c) respectively. From the optical microscopy images, it was observed that as the ratio of water was increased by 2.5 times that of the oil phase, the emulsion formed tends to organize itself to form a packed structure. In case of Span 80, the effect was more prominent as compared to Span 20 and Arquad 2HT-75. The HLB value difference between Span 80 and Span 20 makes Span 80 more hydrophobic as compared to Span 20. Arquad 2HT-75 being a cationic surfactant, the ions present on the surfactant does not allow it to form a stable HIPE at this water level. The SEM images of polymerized HIPEs show some formation of interconnected pores in case of Span 80 and slightly in Span 20 but not in the case of Arquad 2HT-75.

The effect of 1: 5 (O : W) ratio on the HIPE emulsion and pore morphology of the polymers is depicted in Figure 4.5 (a-c) and 4.6 (a-c) respectively. It was observed that in the case of non-ionic surfactants the emulsions tend to form more organized structure as compared to 1 : 1 and 1 : 2.5 (O : W) ratio. In case of Span 80, an increase in the formation of interconnected porous structure was observed while in case of Span 20 a mixed structure of closed and open interconnected pores was observed. In case of cationic surfactant, it was observed that the pore morphology was not uniform throughout the entire polymer and pores occur in cluster depending on the association between the surfactant and aqueous phase at molecular level.

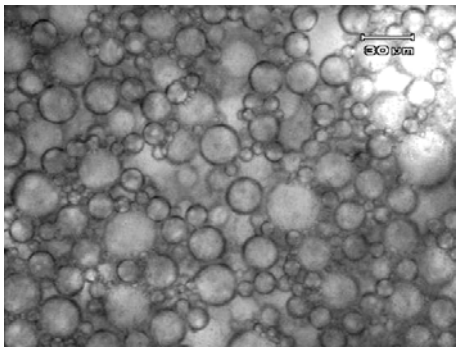

Figure 4.3 (a) : Span 80 as surfactant (50 X)

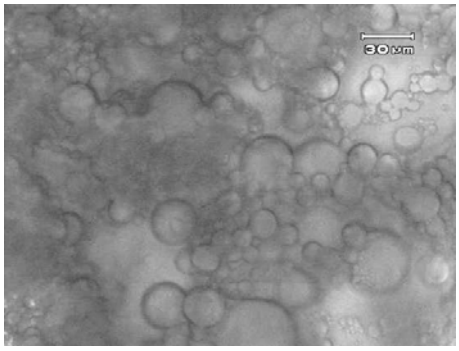

Figure 4.3 (b) : Span 20 as surfactant (50 X)

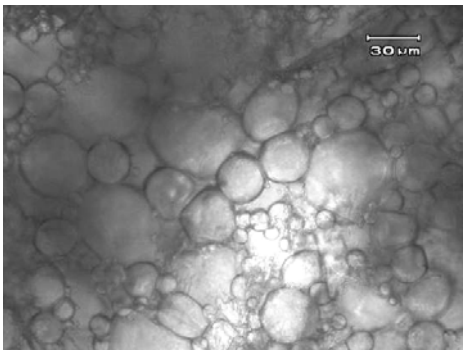

Figure 4.3 (c) : Arquad 2HT-75 as surfactant (50 X)

Figure 4.3 : Optical microscopy images of HIPEs having 50% CLD and 1 : 2.5; oil : water ratio with variation in surfactant type

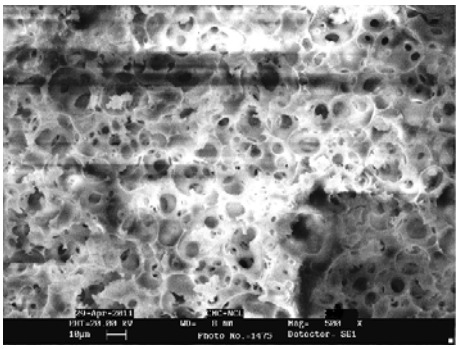

Figure 4.4 (a) : Span 80 as surfactant (500 X)

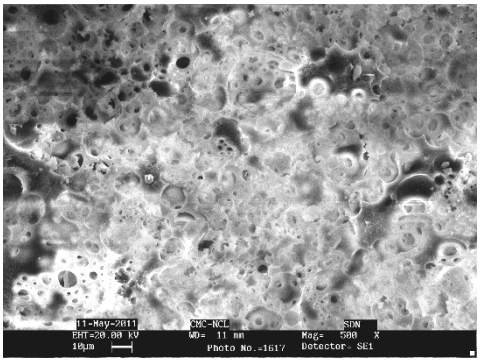

Figure 4.4 (b) : Span 20 as surfactant (500 X)

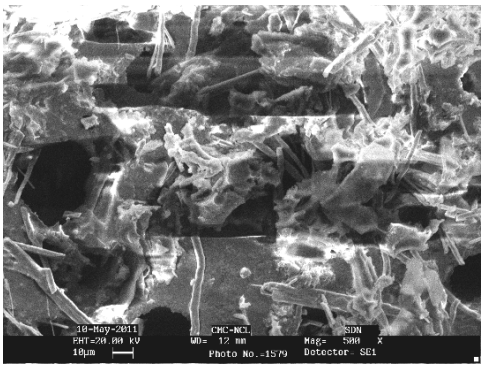

Figure 4.4 (c) : Arquad 2HT-75 as surfactant (500 X)

Figure 4.4 : SEM images of polyHIPEs having 50% CLD and 1 : 2.5; oil : water ratio with variation in surfactant type

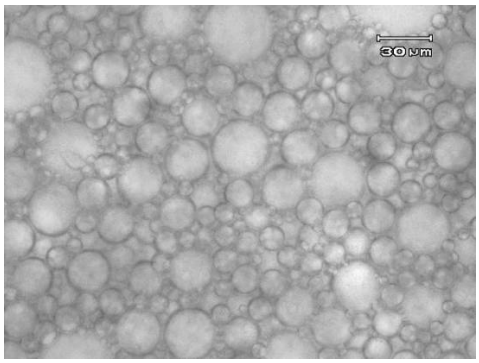

Figure 4.5 (a) : Span 80 as surfactant (50 X)

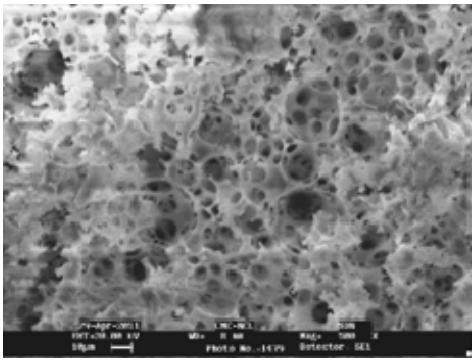

Figure 4.6 (a) : Span 80 as surfactant (500 X)

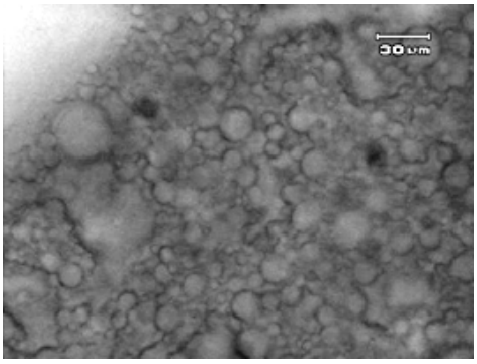

Figure 4.5 (b) : Span 20 as surfactant (50 X)

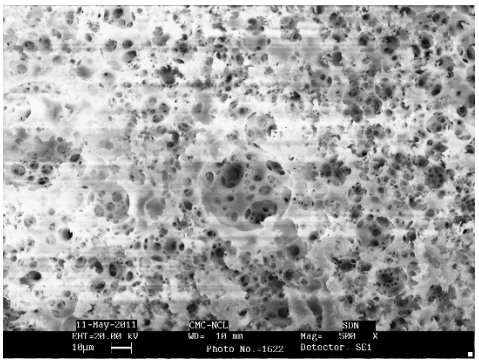

Figure 4. 6 (b) : Span 20 as surfactant (500 X)

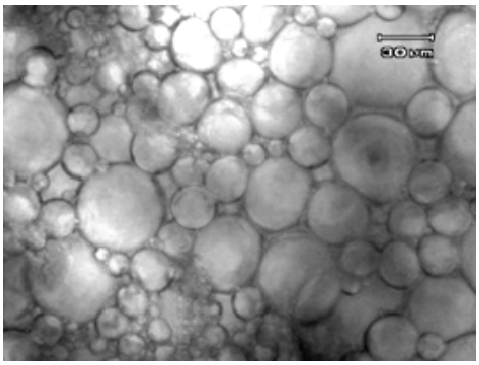

Figure 4.5 (c) : Arquad 2HT-75 as surfactant (50 X)

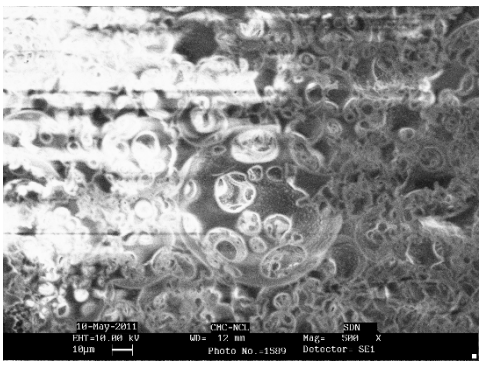

Figure 4.6(c) : Arquad 2HT-75 as surfactant (500 X)

Figure 4.5 : Optical microscopy of HIPEs having 50% CLD and 1 : 5; oil : water ratio with variation in surfactant type

Figure 4.6 : SEM images of polyHIPEs having 50% CLD and 1 : 5; oil : water ratio with variation in surfactant type

The effect of 1 : 10 (oil : water) ratio on the HIPE emulsion and pore morphology of the polymers is shown in Figures 4.7 (a-c) and 4.8 (a-c) respectively. The optical images and scanning electron microscopy results show that as the ratio of aqueous phase was increased, organized structure was being formed in the case of non-ionic surfactant as well as cationic surfactant. The pore structure formed in the case of cationic surfactant appeared to be closed and diffused.

The effect of 1: 15 (O: W) ratio on the HIPE emulsion and pore morphology of the polymers is shown in Figures 4.9 (a-c) and 4.10 (a-c) respectively. The optical micrographs and SEM results show that polyHIPEs formed prominently in the case of non-ionic surfactants as well as cationic surfactant at 1:15 O:W ratio. The pore structure formed in case of cationic surfactant was not exact but similar to that obtained using nonionic surfactant. It was also observed that as the water ratio increases in the case of Span 20 surfactant the structure becomes more compact and this may be attributed to the enhanced solubility interaction as the HLB value of Span 20 is 8.6.

The effect of 1 : 20 (O : W) ratio and 1 : 25 (O : W) ratio on the HIPE emulsion and pore morphology of the polymers is shown in Figures 4.11 (a-c), 4.12 (a-c), 4.13 (a-c) and 4.14 (a-c) respectively. It was observed in case of all the three surfactants with an increase in the ratio of aqueous discontinuous phase, a uniform interconnected structure was observed in the polymer.

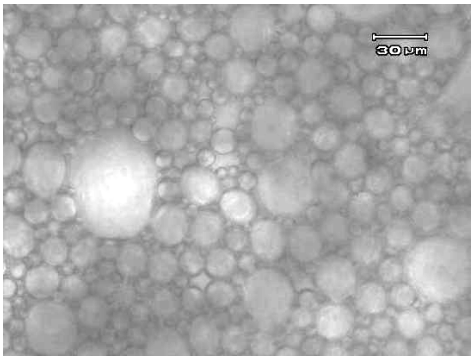

Figure 4.7 (a) : Span 80 as surfactant (50 X)

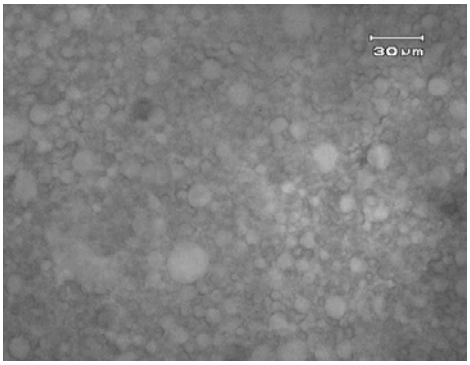

Figure 4.7 (b) : Span 20 as surfactant (50 X)

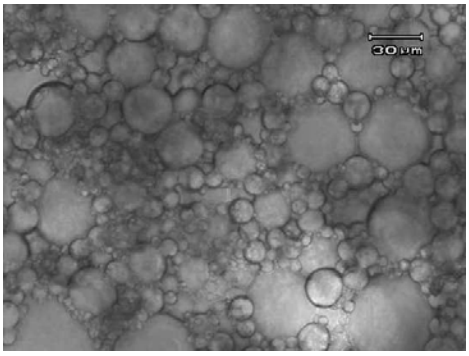

Figure 4.7 (c) : Arquad 2HT-75 as surfactant (50 X)

Figure 4.7 : Optical microscopy images of HIPEs having 50% CLD and 1 : 10; oil : water ratio with variation in surfactant type

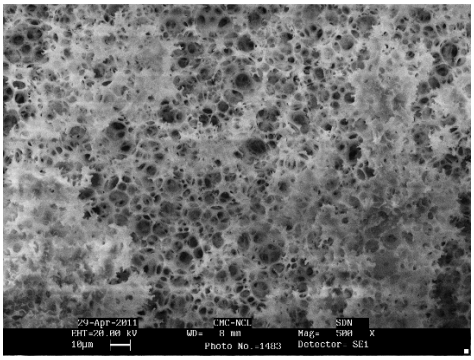

Figure 4.8 (a) : Span 80 as surfactant (500 X)

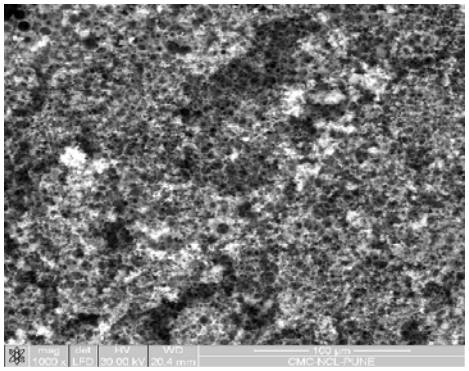

Figure 4.8 (b) : Span 20 as surfactant (500 X)

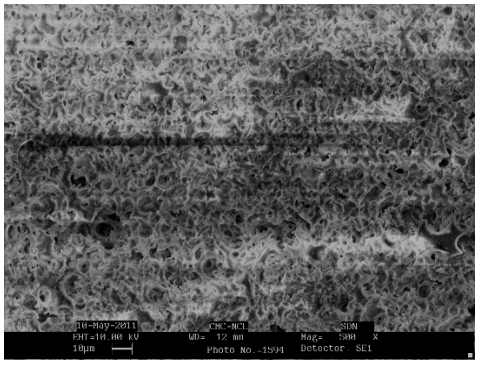

Figure 4.8 (c) : Arquad 2HT-75 as surfactant (500 X)

Figure 4.8 : SEM images of polyHIPEs having 50% CLD and 1 : 10; oil : water ratio with variation in surfactant type

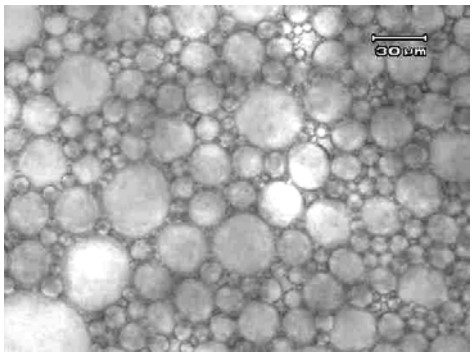

Figure 4.9 (a) : Span 80 as surfactant (50 X)

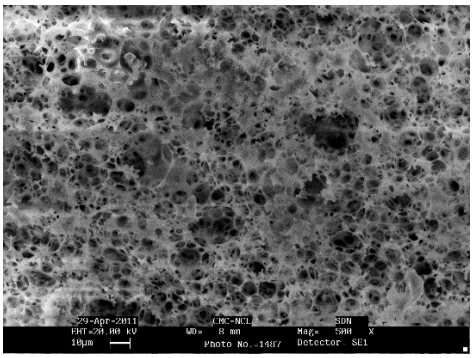

Figure 4.10 (a) : Span 80 as surfactant (500 X)

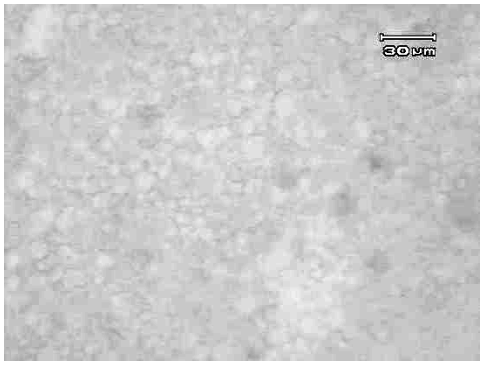

Figure 4. 9 (b) : Span 20 as surfactant (50 X)

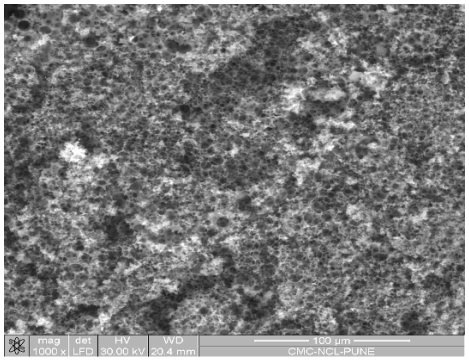

Figure 4.10 (b) : Span 20 as surfactant (1000 X)

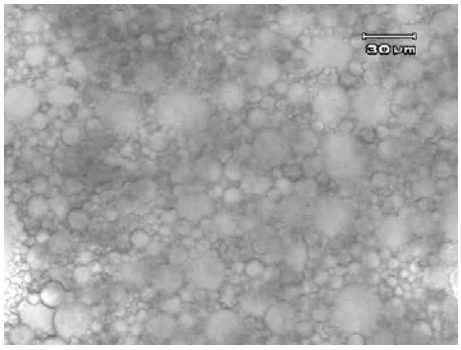

Figure 4.9 (c) : Arquad 2HT-75 as surfactant (50 X)

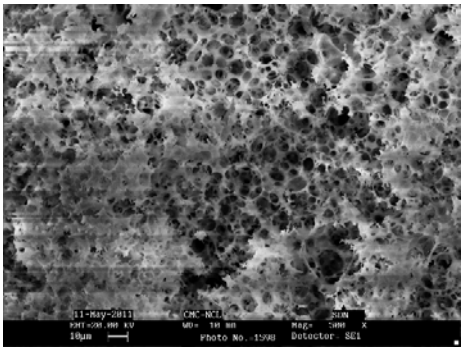

Figure 4.10 (c) : Arquad 2HT-75 as surfactant (500 X)

Figure 4.9 : Optical microscopy images of HIPEs having 50% CLD and 1 : 15; oil : water ratio with variation in surfactant type

Figure 4.10 : SEM images of polyHIPEs having 50% CLD and 1 : 15; oil : water ratio with variation in surfactant type

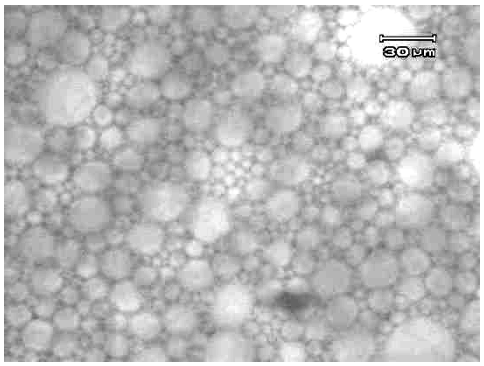

Figure 4.11 (a) : Span 80 as surfactant (50 X)

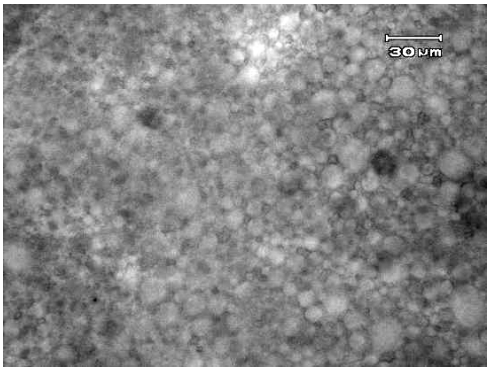

Figure 4.11 (b) : Span 20 as surfactant (50 X)

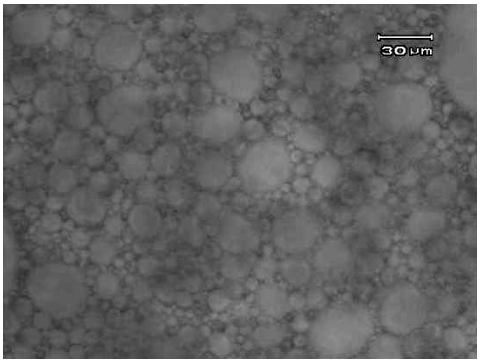

Figure 4.11 (c) : Arquad 2HT-75 as surfactant (50 X)

Figure 4.11 : Optical microscopy images of HIPEs having 50% CLD and 1 : 20; oil : water ratio with variation in surfactant type

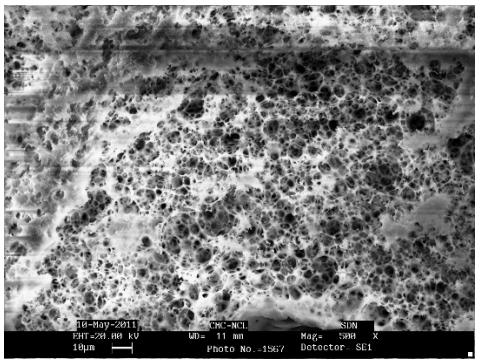

Figure 4.12 (a) : Span 80 as surfactant (500 X)

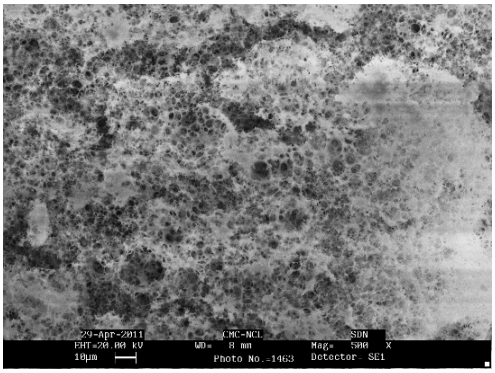

Figure 4.12 (b) : Span 20 as surfactant (500 X)

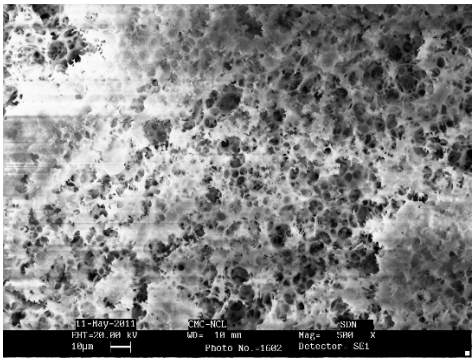

Figure 4.12 (c) : Arquad 2HT-75 as surfactant (500 X)

Figure 4.12 : SEM images of polyHIPEs having 50% CLD and 1 : 20; oil : water ratio with variation in surfactant type

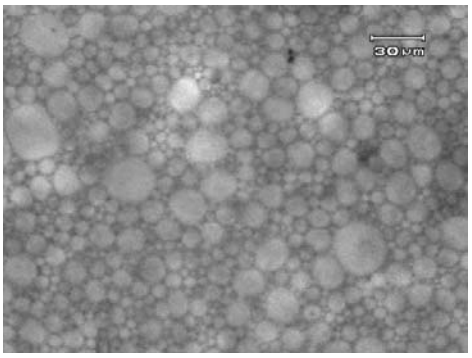

Figure 4.13 (a) : Span 80 as surfactant (50 X)

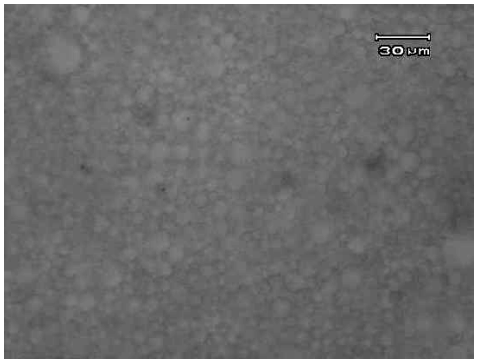

Figure 4.13 (b) : Span 20 as surfactant (50 X)

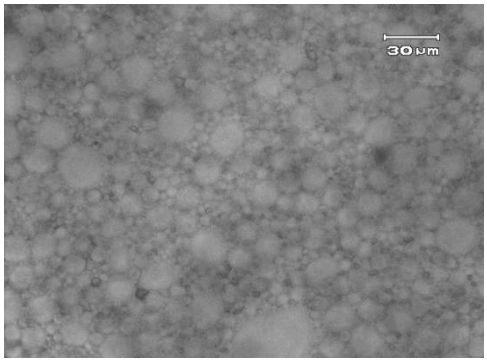

Figure 4.13 (c) : Arquad 2HT-75 as surfactant (50 X)

Figure 4.13 : Optical microscopy images of HIPEs having 50% CLD and 1 : 25; oil : water ratio with variation in surfactant type

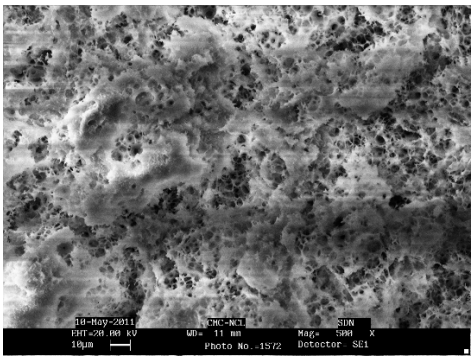

Figure 4.14 (a) : Span 80 as surfactant (500 X)

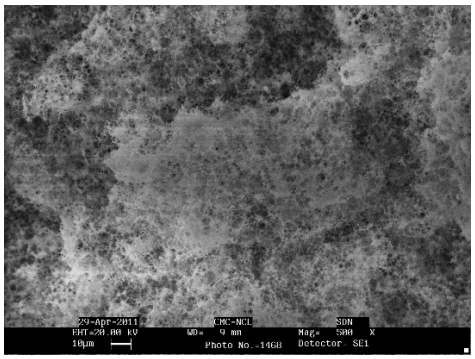

Figure 4.14 (b) : Span 20 as surfactant (500 X)

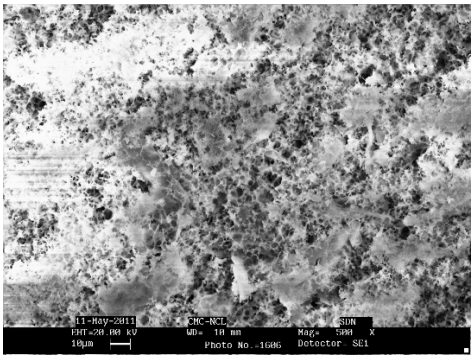

Figure 4.14 (c) : Arquad 2HT-75 as surfactant (500 X)

Figure 4.14 : SEM images of polyHIPEs having 50% CLD and 1 : 25; oil : water ratio with variation in surfactant type

Figures 4.15-4.28 depict the optical microscopy and SEM images of HIPE emulsions and polymers respectively having 75% crosslink density with variation in oil : water ratio and surfactant type. It was observed that there was not much difference in the structure with an increase in crosslink density. The trends of the effect of variance in oil : aqueous discontinuous phase is similar to that observed in case of 50% cross-linked polymers. There is difference in the size of the pores formed but trend in morphology of the polymers seemed to be the same.

The effect on morphology of 100% crosslinked polymers with variation in oil : water ratio using Span 80 as surfactant is shown in Figure 4.29 (a-f). It was observed that as the ratio of aqueous discontinuous phase increased the void size decreased. Figure 4.30 (a-f) and Figure 4.31 (a-f) show the SEM images of the polymers with variation in oil : water ratio using Span 20 and Arquad 2HT-75 as surfactant. In case of Span 20 same trend of variation in aqueous phase was observed as that in case of Span 80. In case of Arquad 2HT-75, no interconnecting pore structure was observed at lower oil : water ratios. The type of surfactant used determines the pore structure because the chemical structure of the surfactant plays an important role for the formation of uniform layer at the interface (interfacial tension). Span 20 and Arquad 2HT-75 surfactants are polar in nature as compared to Span 80. Therefore it indicates that to form a stable W/O HIPE, the oil phase should be more hydrophobic to achieve low interfacial tension. It was also observed that as the crosslink density increased the void size decreased due to an increase in hydrophobicity of the oil phase.

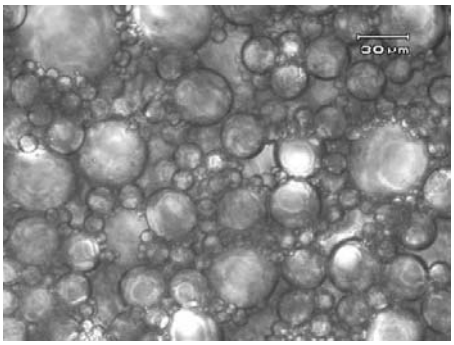

Figure 4.15 (a) : Span 80 as surfactant (50 X)

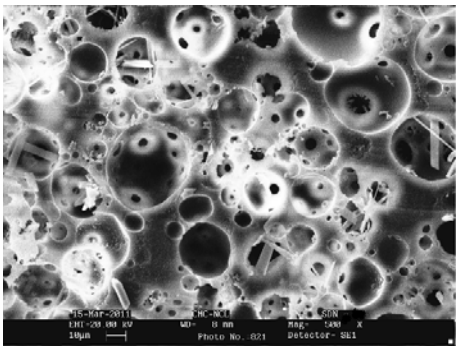

Figure 4.16 (a) : Span 80 as surfactant (500 X)

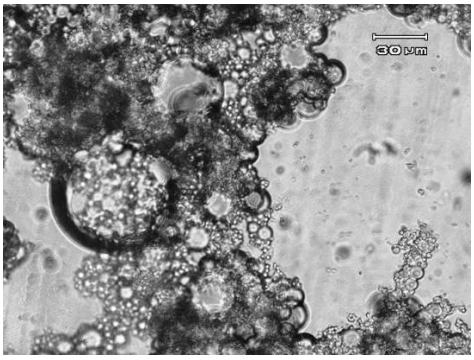

Figure 4.15 (b) : Span 20 as surfactant (50 X)

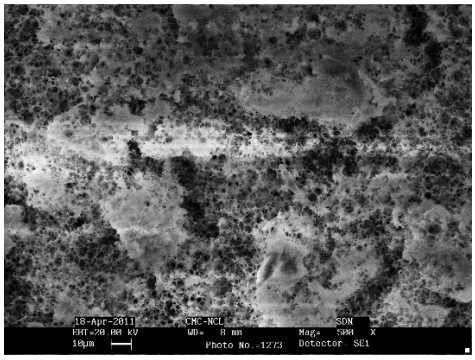

Figure 4.16 (b) : Span 20 as surfactant (500 X)

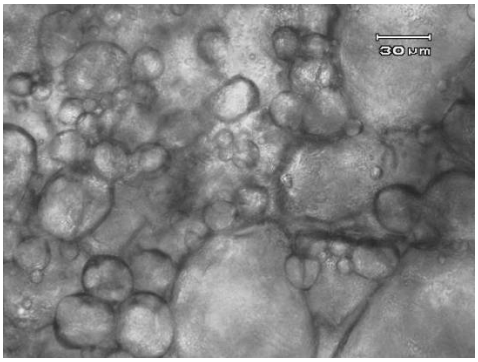

Figure 4.15 (c) : Arquad 2HT-75 as surfactant (50 X)

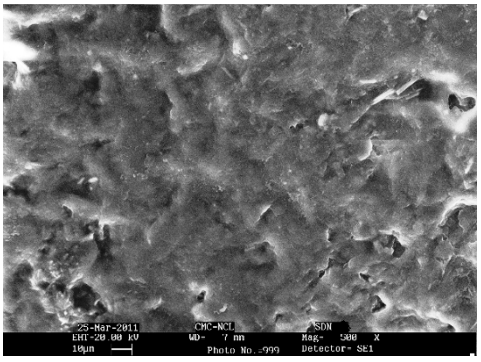

Figure 4.16 (c) : Arquad 2HT-75 as surfactant (500 X)

Figure 4.15 : Optical microscopy images of HIPEs having 75% CLD and 1 : 1; oil : water ratio with variation in surfactant type

Figure 4.16 : SEM images of polyHIPEs having 75% CLD and 1 : 1; oil : water ratio with variation in surfactant type

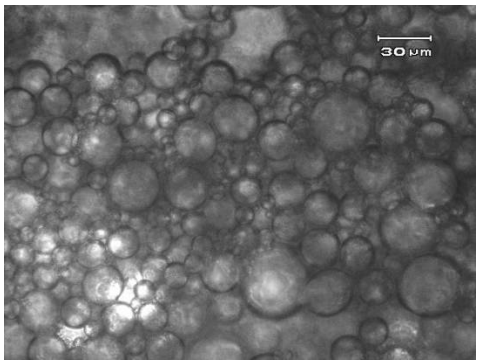

Figure 4.17 (a) : Span 80 as surfactant (50 X)

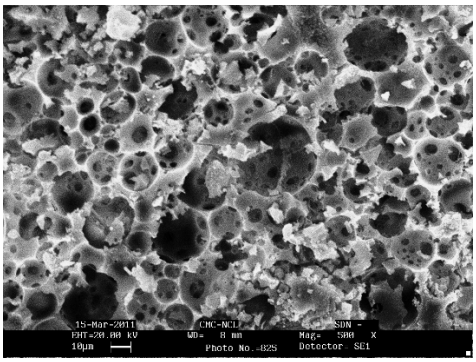

Figure 4.18 (a) : Span 80 as surfactant (500 X)

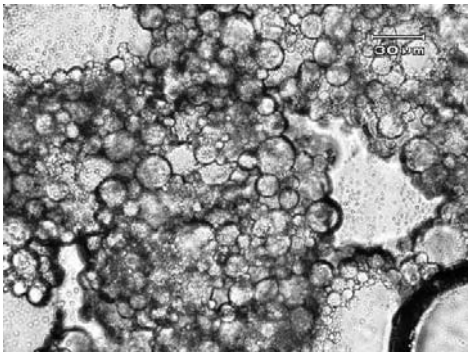

Figure 4.17 (b) : Span 20 as surfactant (50 X)

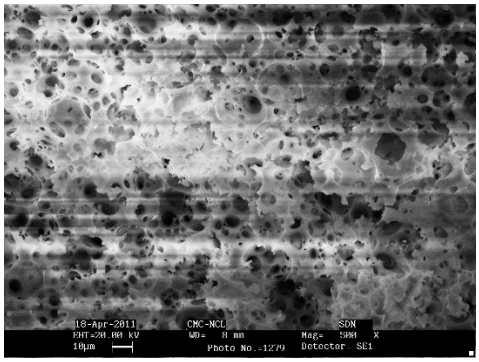

Figure 4.18 (b) : Span 20 as surfactant (500 X)

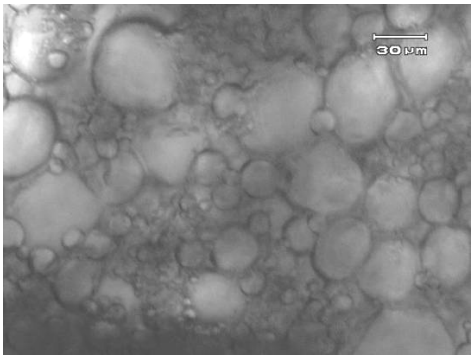

Figure 4.17 (c) : Arquad 2HT-75 as surfactant (50 X)

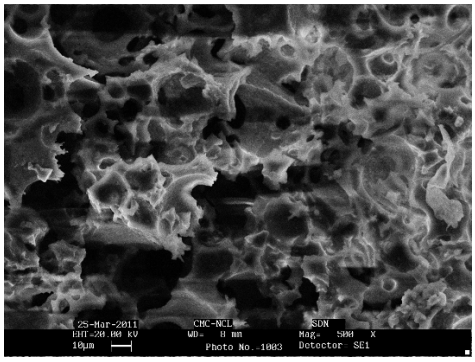

Figure 4.18 (c) : Arquad 2HT-75 as surfactant (500 X)

Figure 4.17 : Optical microscopy images of HIPEs having 75% CLD and 1 : 2.5; oil : water ratio with variation in surfactant type

Figure 4.18 : SEM images of polyHIPEs having 75% CLD and 1 : 2.5; oil : water ratio with variation in surfactant type

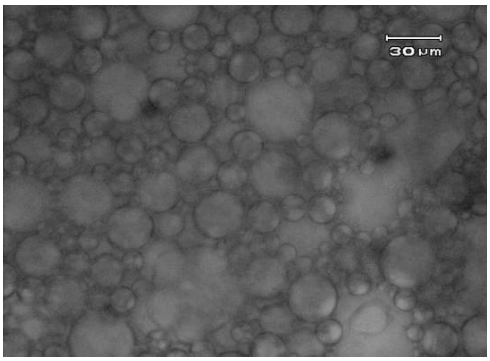

Figure 4.19 (a) : Span 80 as surfactant (50 X)

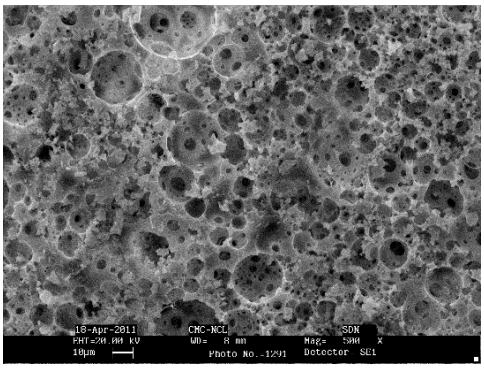

Figure 4.20 (a) : Span 80 as surfactant (500 X)

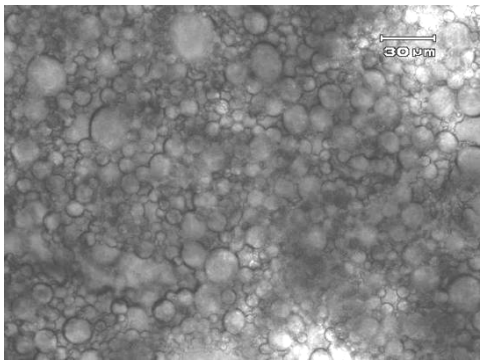

Figure 4.19 (b) : Span 20 as surfactant (50 X)

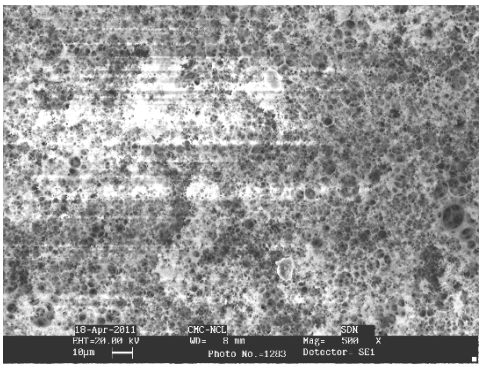

Figure 4.20 (b) : Span 20 as surfactant (500 X)

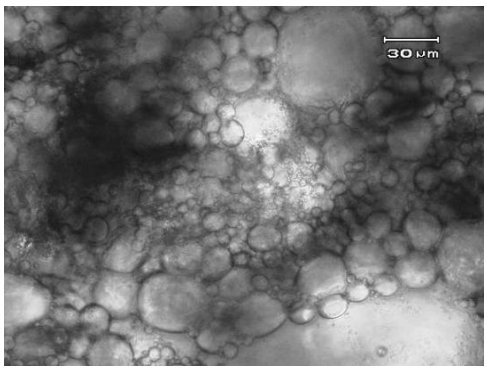

Figure 4.19 (c) : Arquad 2HT-75 as surfactant (50 X)

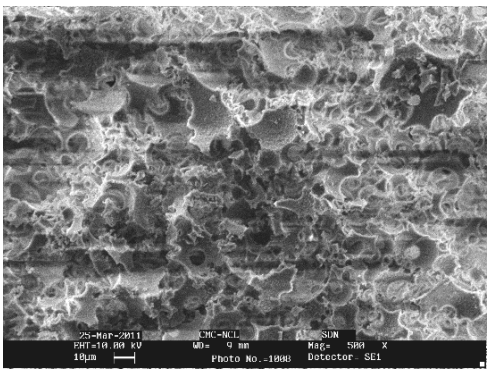

Figure 4.20 (c) : Arquad 2HT-75 as surfactant (500 X)

Figure 4.19 : Optical microscopy images of HIPEs having 75% CLD and 1 : 5; oil : water ratio with variation in surfactant type

Figure 4.20 : SEM images of polyHIPEs having 75% CLD and 1 : 5; oil : water ratio with variation in surfactant type

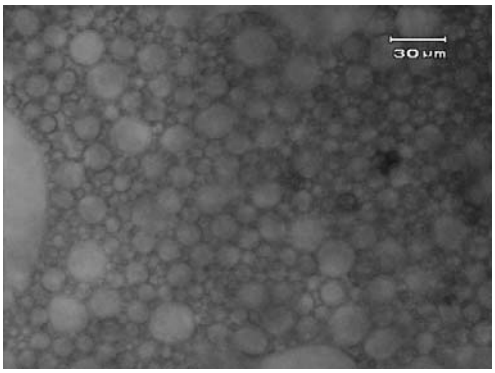

Figure 4.21 (a) : Span 80 as surfactant (50 X)

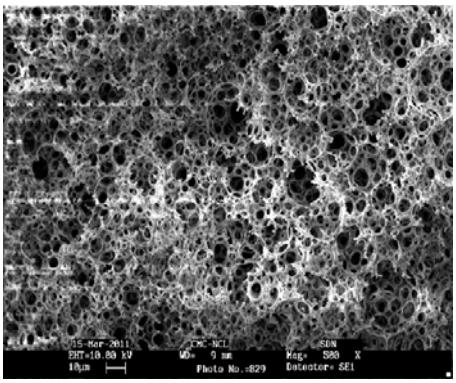

Figure 4.22 (a) : Span 80 as surfactant (500 X)

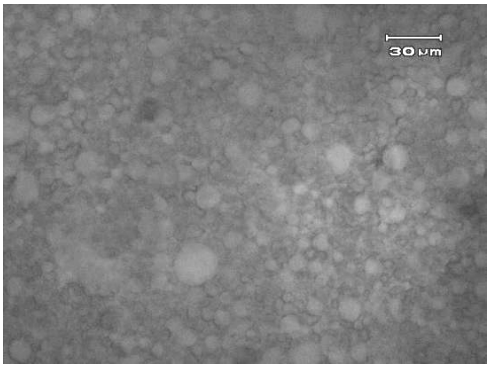

Figure 4.21 (b) : Span 20 as surfactant (50 X)

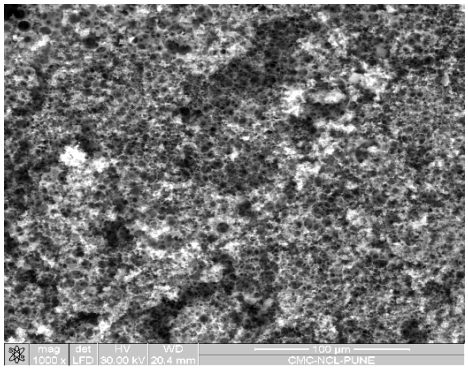

Figure 4.22 (b) : Span 20 as surfactant (1000 X)

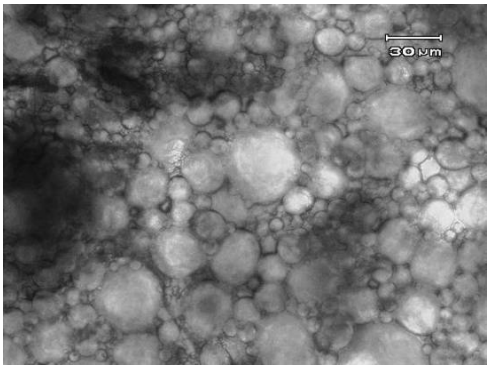

Figure 4.21 (c) : Arquad 2HT-75 as surfactant (50 X)

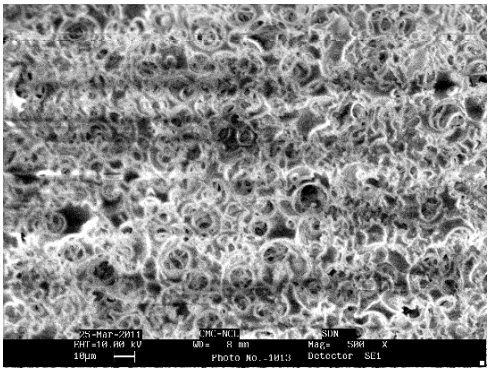

Figure 4.22 (c) : Arquad 2HT-75 as surfactant (500 X)

Figure 4.21 : Optical microscopy images of HIPEs having 75% CLD and 1 : 10; oil : water ratio with variation in surfactant type

Figure 4.22 : SEM images of polyHIPEs having 75% CLD and 1 : 10; oil : water ratio with variation in surfactant type

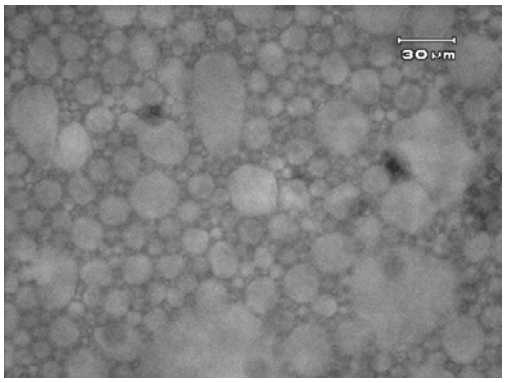

Figure 4.23 (a) : Span 80 as surfactant (50 X)

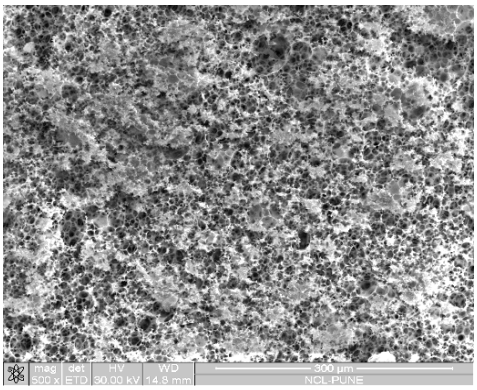

Figure 4.24 (a) : Span 80 as surfactant (500 X)

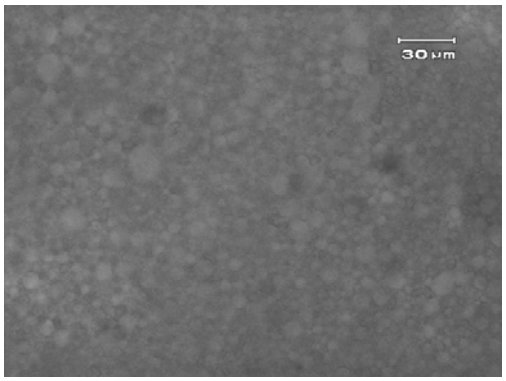

Figure 4.23 (b) : Span 20 as surfactant (50 X)

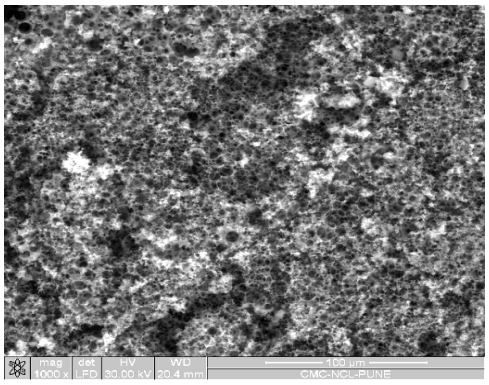

Figure 4.24 (b) : Span 20 as surfactant (1000 X)

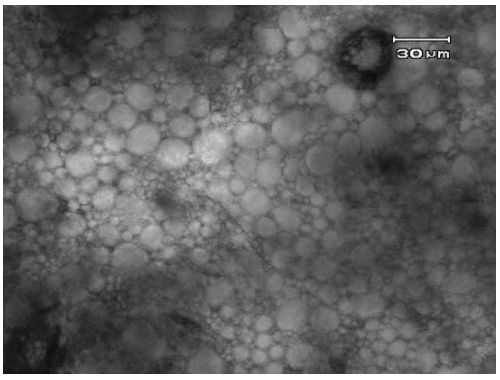

Figure 4.23 (c) : Arquad 2HT-75 as surfactant (50 X)

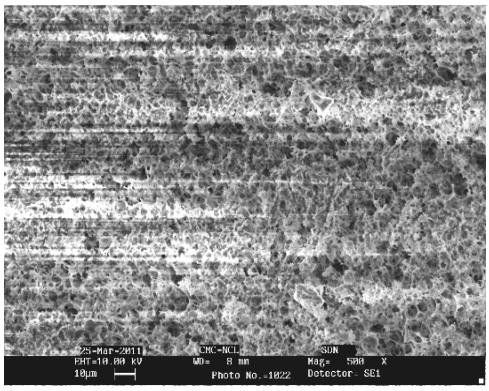

Figure 4.24 (c) : Arquad 2HT-75 as surfactant (500 X)

Figure 4.23 : Optical microscopy images of HIPEs having 75% CLD and 1 : 15 (oil : water) with variation in surfactant type

Figure 4.24 : SEM images of polyHIPEs having 75% CLD and 1 : 15; oil : water ratio with variation in surfactant type

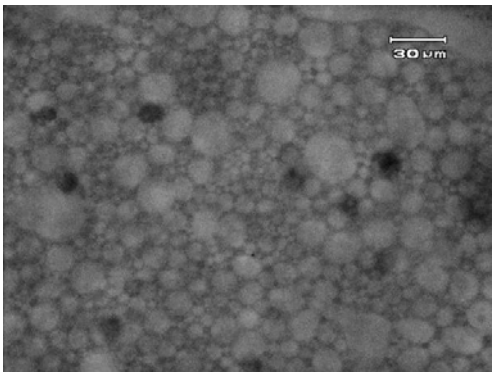

Figure 4.25 (a) : Span 80 as surfactant (50 X)

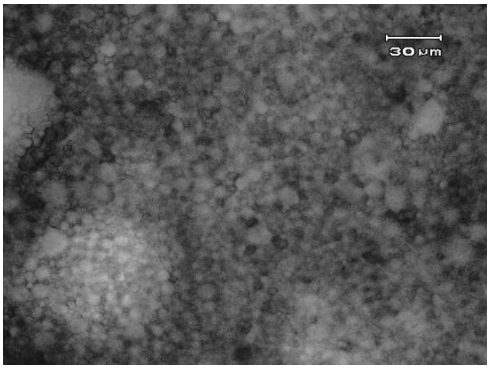

Figure 4.25 (b) : Span 20 as surfactant (50 X)

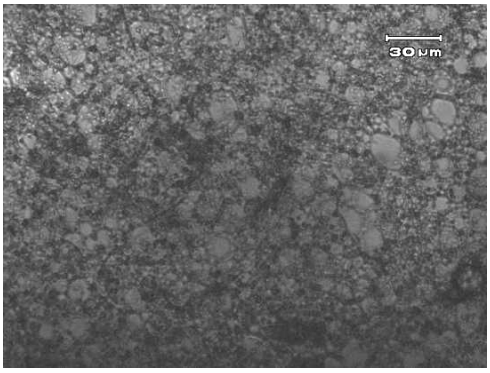

Figure 4.25 (c) : Arquad 2HT-75 as surfactant (50 X)

Figure 4.25 : Optical microscopy images of HIPEs having 75% CLD and 1 : 20; oil : water ratio with variation in surfactant type

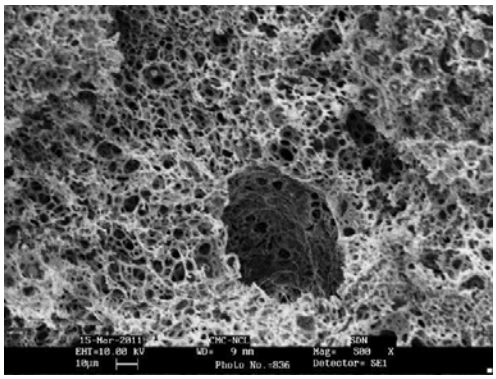

Figure 4.26 (a) : Span 80 as surfactant (500 X)

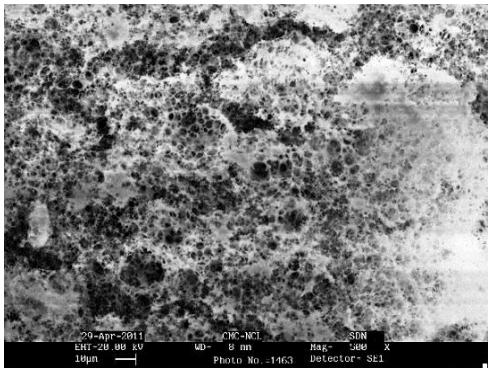

Figure 4.26 (b) : Span 20 as surfactant (500 X)

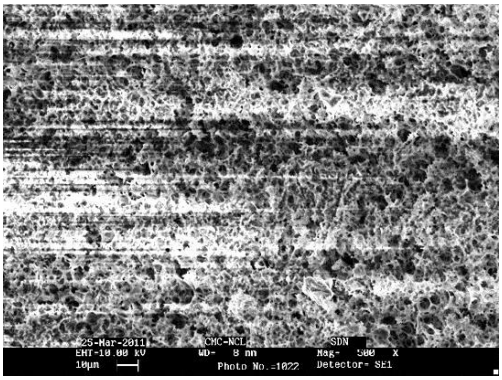

Figure 4.26 (c) : Arquad 2HT-75 as surfactant (500 X)

Figure 4.26 : SEM images of polyHIPEs having 75% CLD and 1 : 20; oil : water ratio with variation in surfactant type

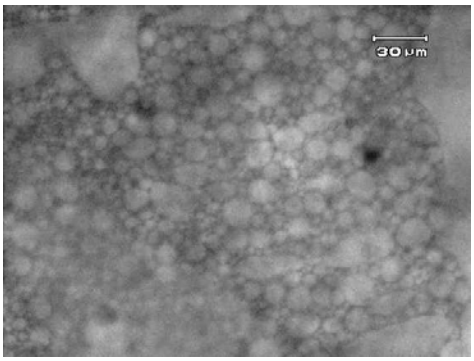

Figure 4.27 (a) : Span 80 as surfactant (50 X)

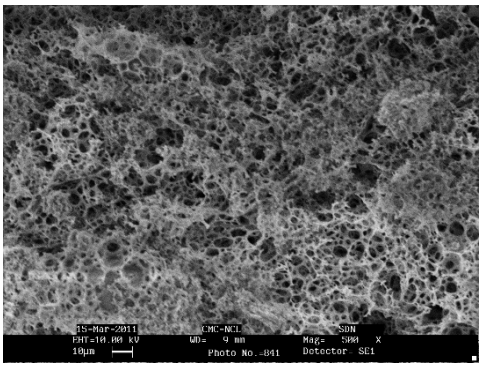

Figure 4.28 (a) : Span 80 as surfactant (500 X)

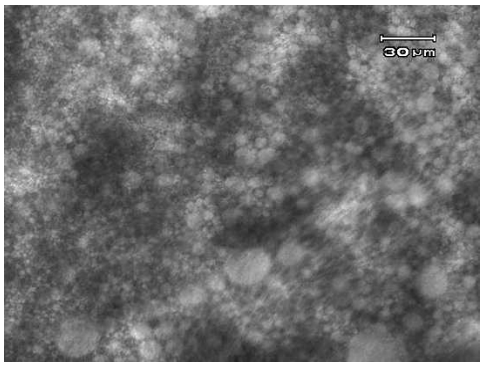

Figure 4.27 (b) : Span 20 as surfactant (50 X)

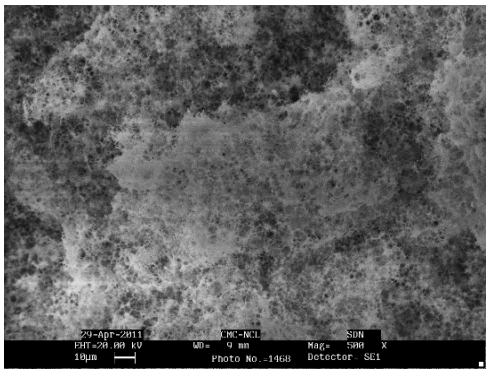

Figure 4.28 (b) : Span 20 as surfactant (500 X)

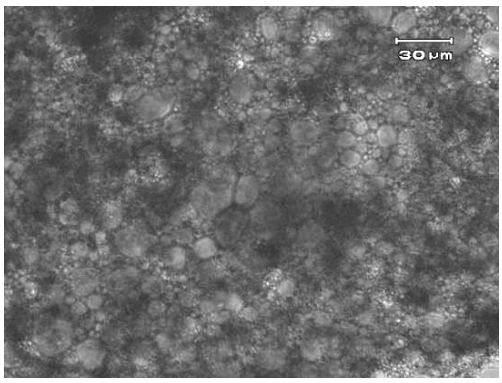

Figure 4.27 (c) : Arquad 2HT-75 as surfactant (50 X)

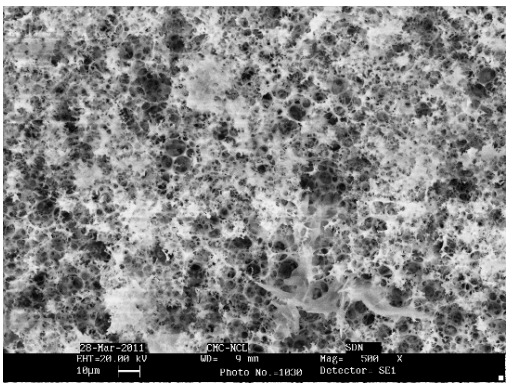

Figure 4.28 (c) : Arquad 2HT-75 as surfactant (500 X)

Figure 4.27 : Optical microscopy images of HIPEs having 75% CLD and 1 : 25; oil : water ratio with variation in surfactant type

Figure 4.28 : SEM images of polyHIPEs having 75% CLD and 1 : 25; oil : water ratio with variation in surfactant type

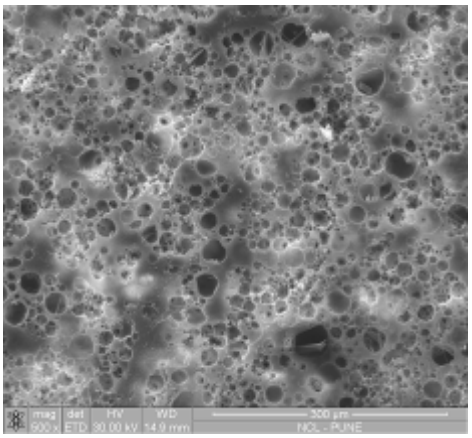

Figure 4.29 (a) : 1 : 1 (oil : water) (500 X)

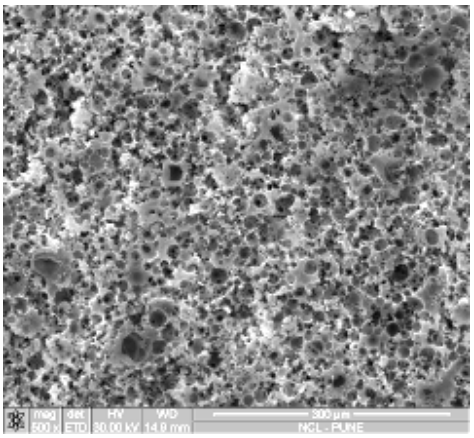

Figure 4.29 (b) : 1 : 2.5 (oil : water) (500 X)

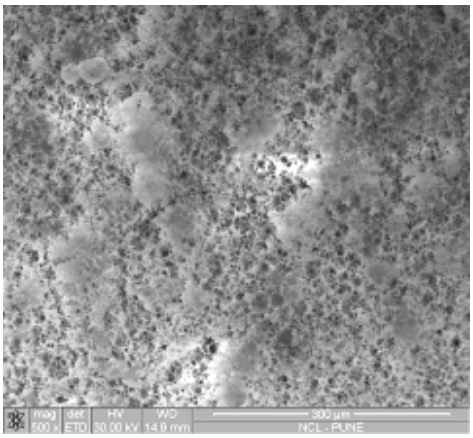

Figure 4.29 (c) : 1 : 5 (oil : water) (500 X)

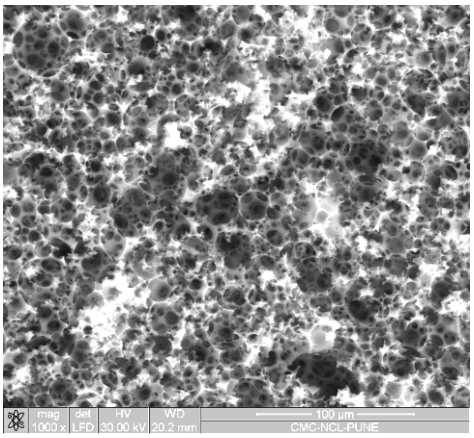

Figure 4.29 (d): 1 : 10 (oil : water) (1000 X)

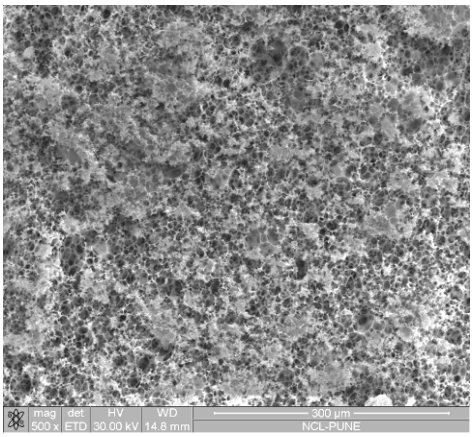

Figure 4.29 (e) : 1 : 15 (oil : water) (500 X)

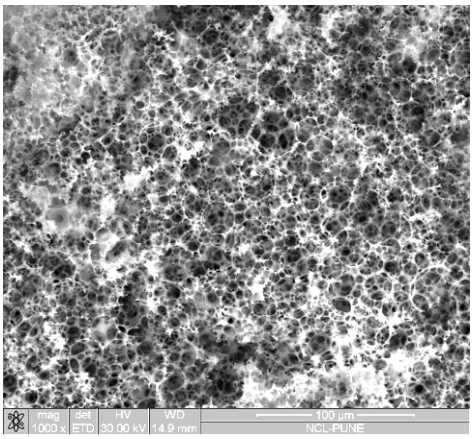

Figure 4.29 (f) : 1 : 20 (oil : water) (1000 X)

Fig 4.29 : SEM images of polyHIPEs having 100% CLD using Span 80 surfactant and variation in oil : water ratio

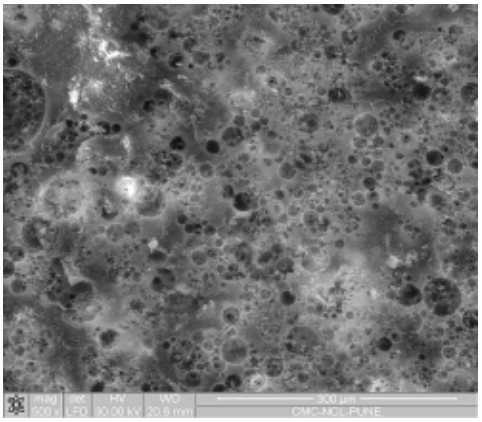

Figure 4.30 (a) : 1 : 1 (oil : water) (500 X)

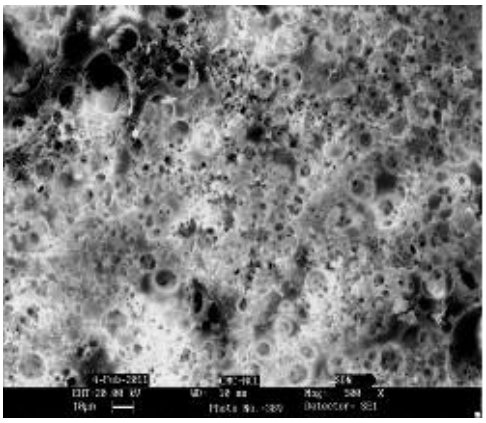

Figure 4.30 (b) : 1 : 2.5 (oil : water)

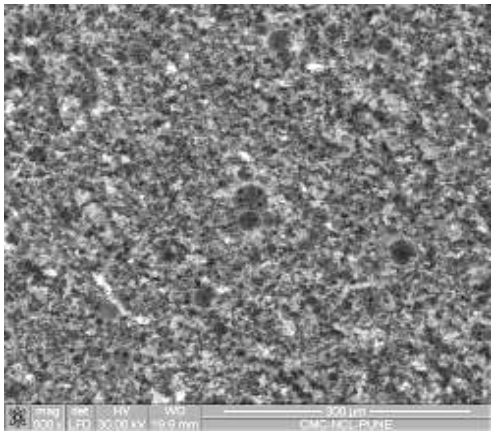

Figure 4.30 (c) : 1 : 5 (oil : water) (1000 X)

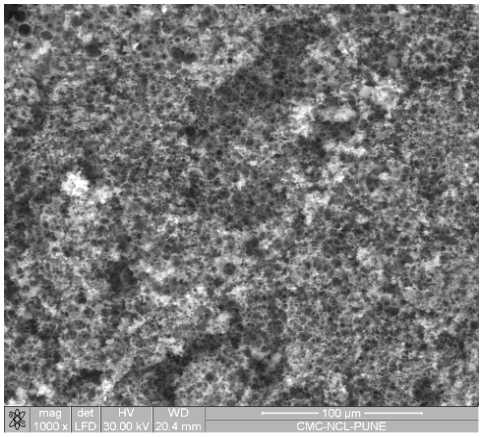

Figure 4.30 (d) : 1 : 10 (oil : water) (1000 X)

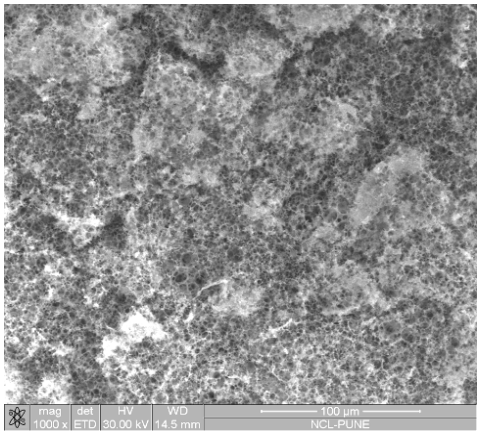

Figure 4.30 (e) : 1 : 15 (oil : water) (1000 X)

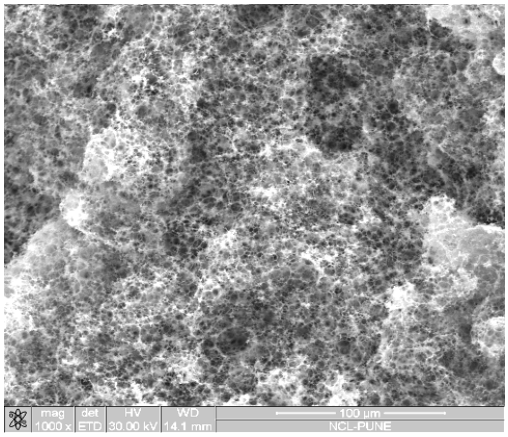

Figure 4.30 (f) : 1 : 20 (oil : water) (1000 X)

Fig 4.30 : SEM images of polyHIPEs having 100% CLD using Span 20 surfactant and variation in oil : water ratio

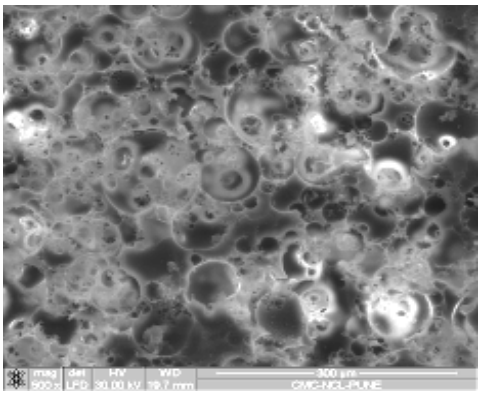

Figure 4.31 (a) : 1 : 1 (oil : water) (500 X)

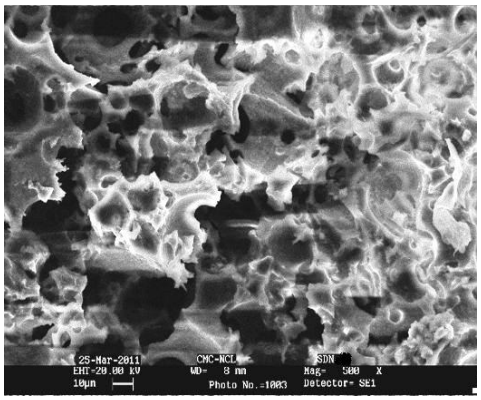

Figure 4.31 (b) : 1 : 2.5 (oil : water) (500 X)

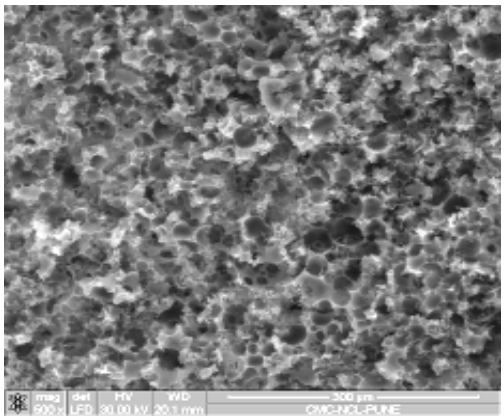

Figure 4.31 (c) : 1 : 5 (oil : water) (500 X)

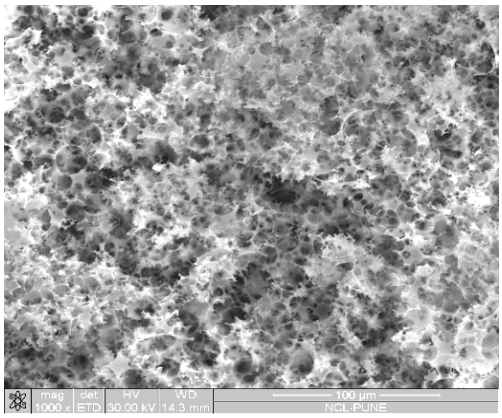

Figure 4.31 (d) : 1 : 10 (oil : water) (1000 X)

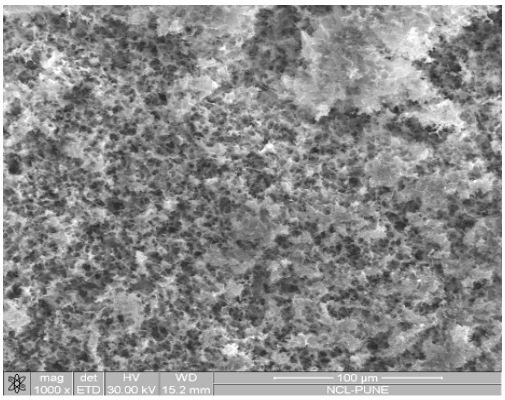

Figure 4.31 (e): 1 :15 (oil : water) (1000 X)

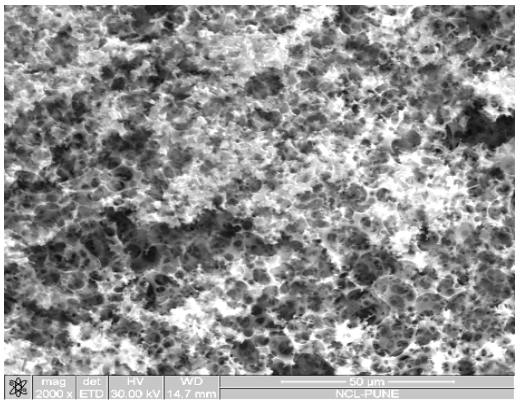

Figure 4.31 (f) : 1 : 20 (oil : water) (1000 X)

Fig 4.31 : SEM images of polyHIPEs having 100% CLD using Arquad 2HT-75 surfactant and variation in oil : water ratio

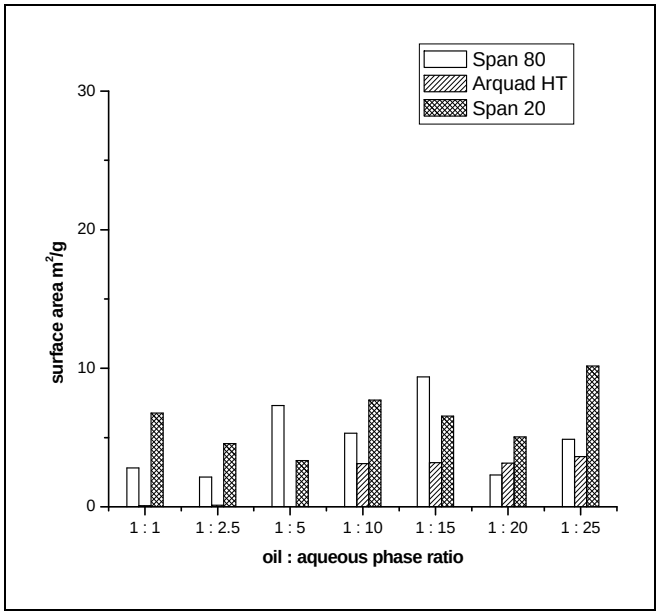

Figure 4.32 : Comparison of surface area in 75% cross-linked St-DVB polyHIPEs

Figure 4.32 shows a comparison of surface area for 75% crosslinked polymers with variation in oil : water and surfactant. The SEM data revealed that in case of cationic surfactant (Arquad 2HT-75), no porous structure was formed upto 1:1 to 1:5 (oil: water) ratio hence no surface area was observed. As the ratio of aqueous discontinuous phase increases, a uniform structure gives accountability to some small surface area that is observed in B.E.T nitrogen adsorption analysis. The analysis study confirm the fact that the type of surfactant and oil : water ratio are the key parameters in designing the pore structure and dimensions.

4.3 Incorporation of CdS particles in St-DVB polyHIPEs

This section deals with an attempt to study incorporation of cadmium sulphide (CdS) particles in porous monolithic St-DVB polyHIPE matrix, synthesized using high internal phase emulsion templating.

4.3.1 *Strategies*

The strategy used was to synthesize cadmium sulphide (CdS) from cadmium chloride ($CdCl_2$). Incorporation of cadmium sulphide particles in poly (styrene-divinylbenzene) discs was carried out in two steps:

4.3.1.1 *Incorporation of $CdCl_2$ within the polyHIPE matrix*

Poly (styrene-divinylbenzene) monoliths containing cadmium chloride using high internal phase emulsion methodology were prepared using two strategies:

a) *Before polymerization:* In-situ addition of cadmium chloride dissolved in aqueous discontinuous phase during HIPE formation.

b) *Post polymerization:* Imbibing cadmium chloride solution in the polyHIPE monolithic matrix after polymerization.

4.3.1.2 *Modification of cadmium chloride to cadmium sulphide*

Scheme 4.1 represents the modification strategy. Cadmium sulphide particles were synthesized from cadmium chloride embedded in polymer matrix by immersing the monolithic discs in 0.1 M sodium hydroxide solution to form cadmium hydroxide. Then the discs were immersed in 0.1 M sodium sulphide solution to convert cadmium

hydroxide to cadmium sulphide. The disc after the formation of cadmium sulphide is shown in Figure 4.33.

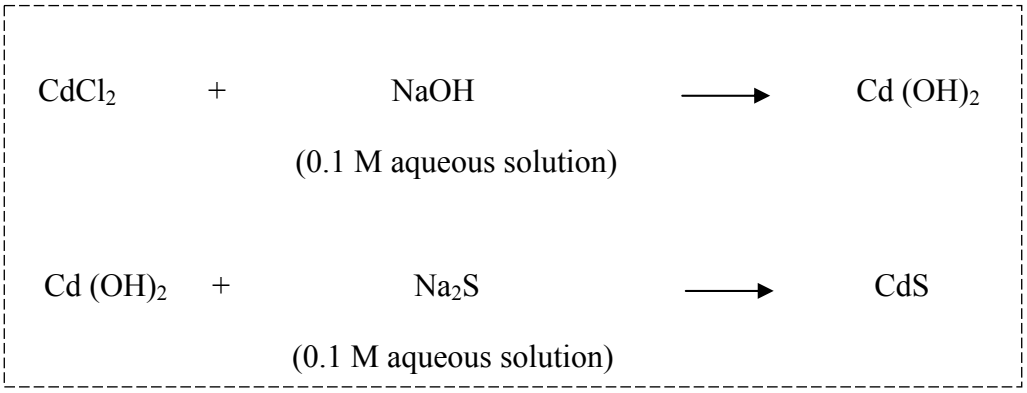

Scheme 4.1 : Synthesis of CdS particles from $CdCl_2$

Figure 4.33 : Pictorial representation of St-DVB polyHIPE containing cadmium sulphide (CdS) particles

4.3.2 Experimental

4.3.2.1 *Insitu incorporation*

Monoliths were prepared by polymerization of high internal phase emulsion in presence of cadmium chloride dissolved in aqueous discontinuous phase.

4.3.2.1.1 *Procedure*

St-DVB polyHIPE monoliths with 10% crosslink density were prepared. The oil phase comprised of requisite quantities of styrene, divinylbenzene and surfactant. The requisite amount of water with dissolved cadmium chloride was slowly added to the oil phase under stirring to form the high internal phase emulsion followed by addition of the initiator and polymerizing the HIPE emulsions at 60^{o}C to obtain porous polymeric monoliths. The monoliths were then cut in the form of 15 mm diameter and 5 mm thickness disc. The discs were then treated with 0.1 M NaOH solution to form cadmium hydroxide followed by treatment with 0.1 M sodium sulphide solution to form cadmium sulphide particles within the polymer matrix. The details of the synthesis are tabulated in Table 4.10.

Table 4.10 Synthesis of 10% cross-linked St-DVB polyHIPEs- insitu incorporation of cadmium chloride (1 : 15 ; oil : water ratio)

Polymer Code	Styrene (g) (mol)	Divinylbenzene (g) (mol)	$CdCl_2$ (%)
I 1-5	1.614 (0.0154)	0.201 ($1.54x10^{-3}$)	5
I 1- 10	1.614 (0.0154)	0.201 ($1.54x10^{-3}$)	10
I 1- 20	1.614 (0.0154)	0.201 ($1.54x10^{-3}$)	20

Span 80= 20 wt % of oil phase, sodium peroxydisulphate = 1 mol % of oil phase, stirring speed = 1000 rpm, Reaction temperature = $60^{o}C$

4.3.2.2 *External incorporation*

4.3.2.2.1 *Procedure*

Monoliths were prepared by polymerization of high internal phase emulsion with the same composition of the reactants as tabulated in 4.10 without cadmium chloride addition. The monolithic discs obtained after polymerization were then immersed in the requisite concentrated solution of cadmium chloride for a period of 2 hours. The discs were then treated with 0.1 M NaOH solution to form cadmium hydroxide followed by treatment with requisite concentration of sodium sulphide solution to form cadmium sulphide particles within the polymer matrix. Experiments were also carried out to study the effect of variance of oil : water ratio followed by external incorporation of cadmium sulphide particles. Tables 4.11 and 4.12 represent the synthesis details of external incorporation strategy.

Table 4.11 Incorporation of cadmium chloride in 10% cross-linked St-DVB polyHIPE monoliths using 1 : 15; oil : water ratio

Polymer Code	$CdCl_2$ (%)	Wt of pellet (g)	$CdCl_2$ (g)
E1-5	5	0.030	0.0015
E1-10	10	0.030	0.0030
E1-20	20	0.040	0.0080

Table 4.12 Incorporation of cadmium chloride onto 10% cross-linked St-DVB polyHIPE monoliths using 1 : 10; oil : water ratio

Polymer Code	% $CdCl_2$ (%)	Wt of pellet (g)	$CdCl_2$ (g)
E 2-5	5	0.060	0.0030
E 2-10	10	0.070	0.0070
E 2-20	20	0.080	0.0160

4.3.3 Characterization

The morphology of polymers was studied by SEM and the presence of cadmium sulphide or unconverted chloride was studied by Energy Dispersive X-ray (EDX) spectroscopy and X-ray Diffraction (XRD).

4.3.3.1 *EDX spectroscopy*

Elemental analysis of the synthesized polyHIPEs was noted using a Bruker EDX X-ray spectrometer, Quantax-200. The energy of analysis was done at 20 keV.

4.3.3.2 *X-ray diffraction (XRD)*

XRD analysis was carried out with the sample in the form of pellet using a Rigaku, Japan, XRD instrument. The scanning speed was 4 degrees per minute, with a radiation of CuK- J. The samples were scanned for 2θ values from 10^o to 80^o.

4.3.3.3 *Scanning electron microscopy (SEM)*

The morphologies of the polyHIPEs prepared were studied using a Lieca Stereoscan 440 scanning electron microscope at different magnifications. The energy of analysis was 20 keV.

4.3.4 Results and Discussion

Incorporation of CdS particles inside the porous polymer monolithic matrix synthesized using HIPE methodology was studied. The porous matrices used were St-DVB polyHIPEs having 10% crosslink density. The purpose of these studies was to explore the possibility to embed CdS particles and study their effect on the porous morphology of the resulting polyHIPEs. CdS particles were prepared by treating cadmium chloride ($CdCl_2$) with sodium hydroxide (NaOH) to form cadmium hydroxide ($Cd(OH)_2$) which was then treated with sodium sulphide (Na_2S) that led to formation of CdS. The first step in this process was to embed $CdCl_2$ in the polymeric matrix. For that two strategies were used; (a) insitu incorporation of $CdCl_2$ dissolved in aqueous discontinuous phase during HIPE formation or (b) imbibition of $CdCl_2$ solution in St-DVB polyHIPE monoliths after polymerization. Experiments were carried out to load 5, 10 and 20 wt% $CdCl_2$ with respect to the weight of polymer discs along with variation in oil : water ratio. The series I-1 represents the samples with insitu incorporation strategy

of $CdCl_2$ by dissolving it in the aqueous discontinuous phase (1 : 15; O : W ratio). The series E-1 (1 :15; O : W ratio) and E-2 (1 : 10; O : W ratio) represent the samples with exsitu incorporation strategy of $CdCl_2$ by dipping the polymeric discs in cadmium chloride solutions of requisite concentrations. Subsequently, $CdCl_2$ present in the polymer matrix was converted to CdS as mentioned previously in Scheme 4.1. The monolithic discs were characterized to study the effect of CdS particles on pore morphology by SEM, EDX for qualitative determination of CdS and XRD to study the crystal structure formation of CdS in the polymer matrix.

4.3.4.1 *Elemental analysis*

The EDX elemental data of insitu (I) series is tabulated in Table 4.13. It was observed that the EDX data follows the trend line with the experimental data that as the wt% loading of $CdCl_2$ was increased, an increase in the concentration of Cd and S was observed in EDX data.

Table 4.13 EDX data of polyHIPEs using insitu incorporation strategy

Polymer Code	C (wt %)	O (wt %)	Na (wt %)	S (wt %)	Cl (wt %)	Cd (wt %)
I 1-5	92.65	4.74	-	0.63	-	1.98
I 1-10	90.30	3.67	-	1.28	-	4.74
I 1-20	81.85	4.86	-	2.98	-	10.31

The EDX elemental data using external incorporation strategy of $CdCl_2$ (i.e. after polymerizing the HIPE to obtain monoliths followed by post treatment to convert the

cadmium chloride into cadmium sulphide) is tabulated in Tables 4.14 and 4.15, where polyHIPEs were synthesized by varying the O : W ratio 1 : 15 and 1 : 10 respectively.

Table 4.14 EDX data of polyHIPEs using external incorporation strategy (1 : 15; O : W ratio)

Polymer Code	C (wt %)	O (wt %)	Na (wt %)	S (wt %)	Cl (wt %)	Cd (wt %)
E1-5	81.23	2.76	0.22	0.54	5.90	9.36
E1-10	90.94	3.46	0.26	1.10	0.66	3.58
E1-20	58.18	5.19	0.86	4.22	3.78	27.78

Table 4.15 EDX data of polyHIPEs using external incorporation strategy (1 : 10; O : W ratio)

Polymer Code	C (wt %)	O (wt %)	Na (wt %)	S (wt %)	Cl (wt %)	Cd (wt %)
E 2-5	91.69	4.21	-	1.05	-	3.04
E 2-10	84.82	6.86	-	2.03	-	6.29
E 2-20	85.55	5.31	-	2.40	-	6.74

Figures 4.34 and 4.35 (a-c) show the EDX spectra for St-DVB polyHIPE and insitu $CdCl_2$ (I-1 series) for 5, 10 and 20 wt% loadings respectively. In case of St-DVB polyHIPE, only peak due to carbon was observed while in case of polyHIPEs containing CdS, peaks due to carbon, sulphur, cadmium and chlorine were observed. In case of insitu incorporation strategy, from the intensity of the peaks for Cd and S, it was confirmed that as the loading concentration of cadmium chloride was increased the

concentration of sulphur in the polymer matrix also increased. The values for wt% of S were 0.63, 1.28 and 2.98 and wt% of Cd were 1.98, 4.74 and 10.31 for 5, 10 and 20 wt% loadings respectively.

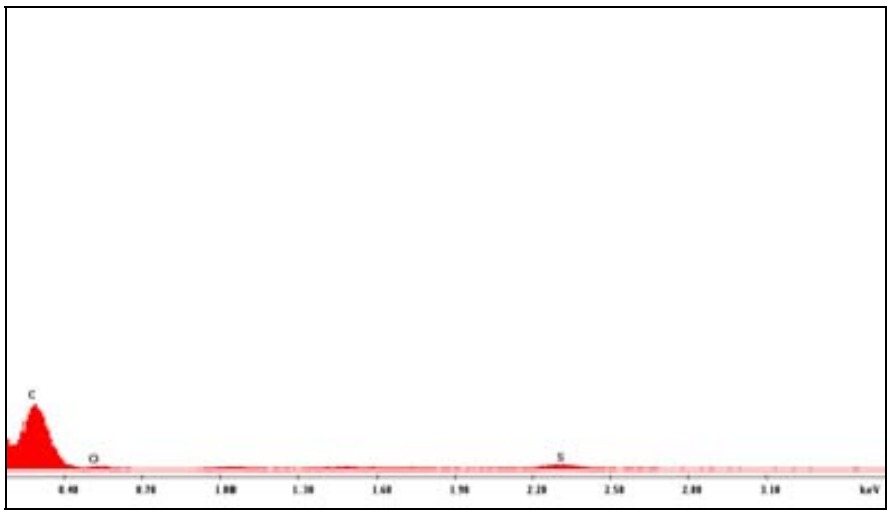

Figure 4.34 : EDX spectra of St-DVB polyHIPE

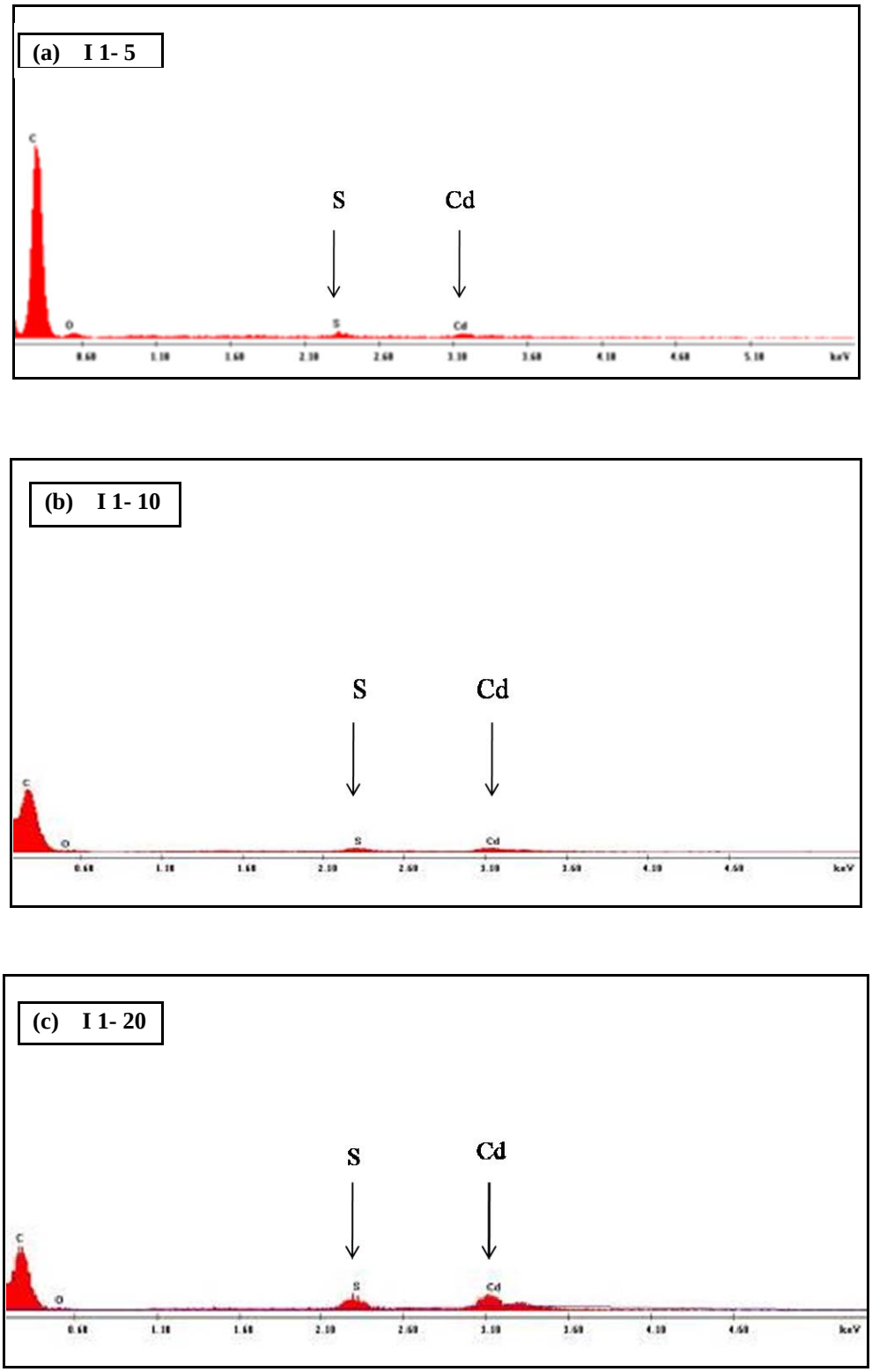

Figure 4.35 : EDX spectra of St-DVB polyHIPEs synthesized using insitu incorporation strategy using 1 : 15; oil : water ratio

The external incorporation of $CdCl_2$ inside the porous polymer matrix and subsequent conversion to CdS was also studied. Figure 4.36 (a-c) shows the EDX spectra for E-1 series polymers for 5, 10 and 20 wt % loadings respectively (oil : water ratio; 1 : 15). It was observed that along with peaks due to Cd and S, peaks due to chlorine were also observed. This indicated incomplete conversion of cadmium chloride to cadmium sulphide. The values for wt % of S were 0.54, 1.10 and 4.22 and wt% of Cd were 9.36, 3.58 and 27.78 for 5, 10 and 20 wt% loadings respectively. The presence of Cl peaks was also observed in all the cases indicating incomplete conversion of $CdCl_2$ to CdS, as diffusion of the reactants inside the pores becomes an important criteria.

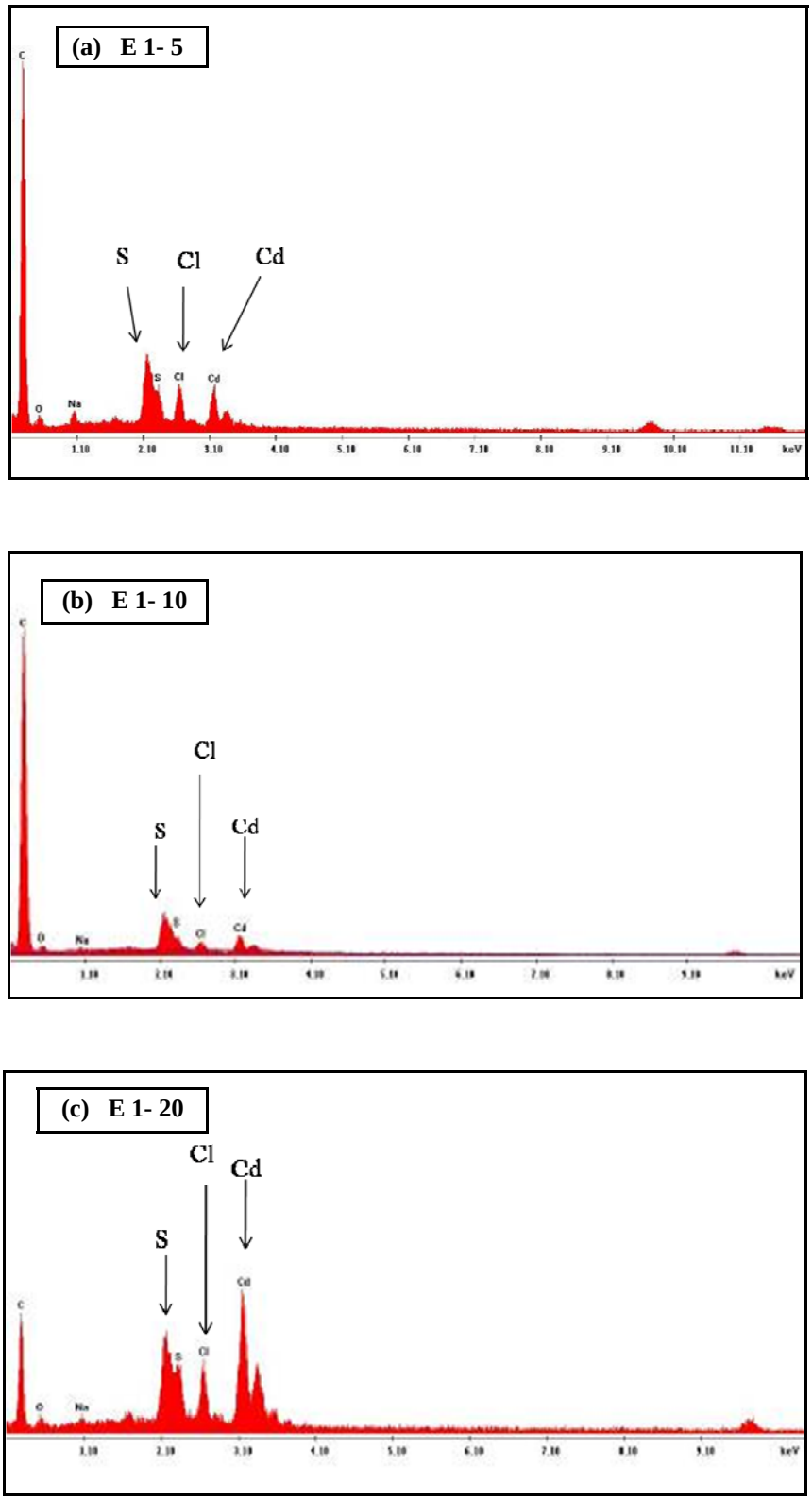

Figure 4.36 : EDX spectra of St-DVB polyHIPEs synthesized using external incorporation strategy using 1 : 15; oil : water ratio

Figure 4.37 (a-c) shows the EDX spectra for E-2 series polymers with 5, 10 and 20 wt % loadings respectively (1 : 10; O : W ratio). In this strategy, it was observed that along with cadmium and sulphur, peaks due to Cl were also observed but the concentration was negligible in comparison with that observed in E-1 series. This confirms that the diffusion of cadmium chloride into the voids present in the monolith becomes difficult, as an increase in ratio of water tends to form pores having small sizes as more water was incorporated during HIPE formation. Post treatment for conversion of chloride into sulphide also becomes difficult as it is related to ease in accessibility, pore dimensions and solvent diffusion capacity. The values of wt % of S was 1.05, 2.03 and 2.40 and wt% of Cd were 3.04, 6.29 and 6.75 for 5, 10 and 20 wt% loadings respectively.

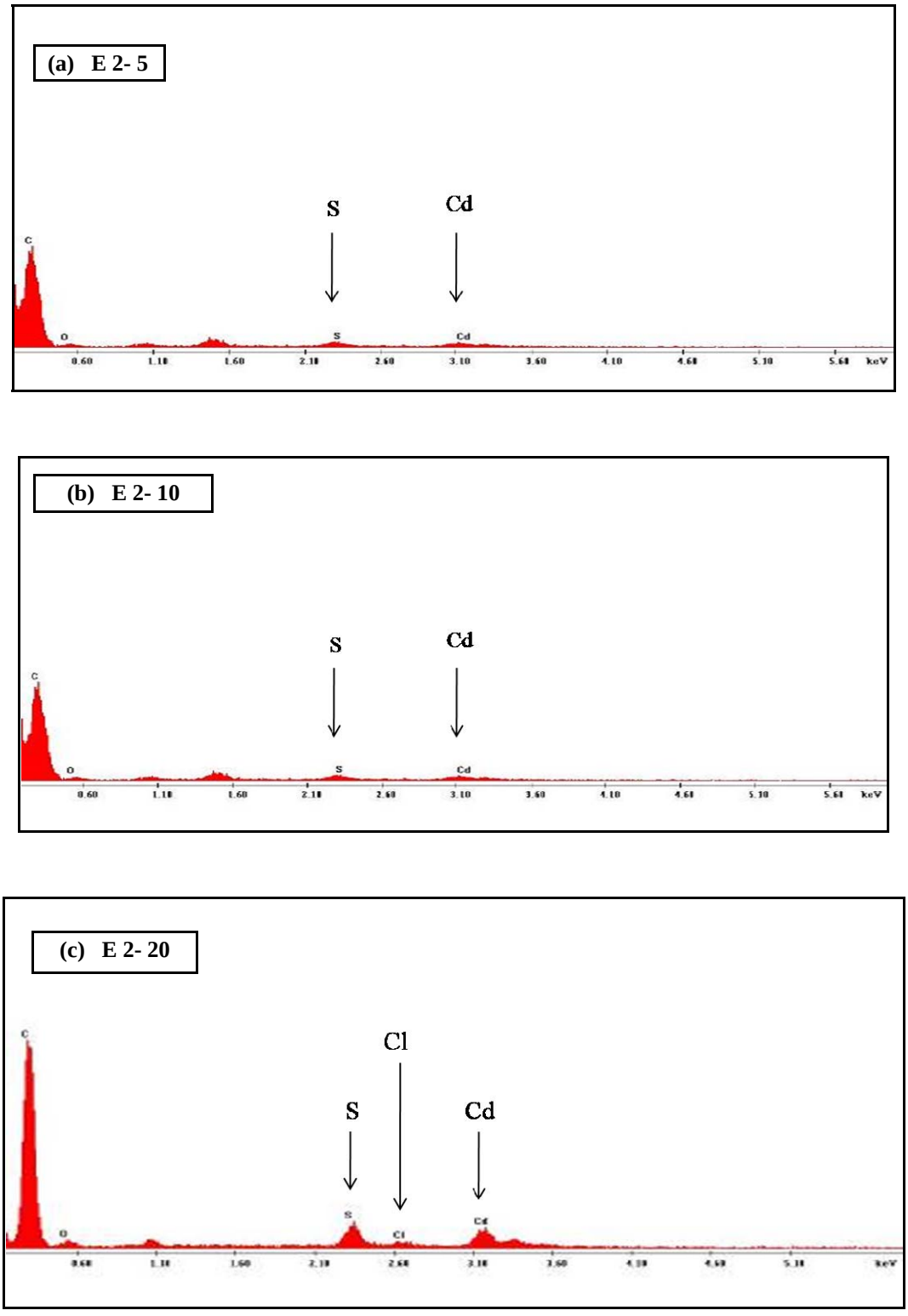

Figure 4.37 : EDX spectra of St-DVB polyHIPEs synthesized using external incorporation strategy using 1 : 10; oil : water ratio

EDX spectra confirmed the presence of Cl along with S in case of external incorporation strategy. Thus it can be concluded that insitu incorporation strategy is more suitable to obtain monoliths having maximum concentration of CdS particles. In external incorporation method, the ease in diffusion of the reactants for post modification inside the pores is minimized.

The comparison of elemental composition data of S and Cd using EDX analysis data for variation in initial loading of cadmium chloride as well as the method used for loading of cadmium chloride is shown in Figures 4.38 and 4.39 respectively. It was observed that in case of insitu imbibed cadmium chloride as the % loading was increased a linear increase in the wt. % of Cd and S ions was observed while no trend was observed in case of external incorporation strategy. A linear trend was not observed in the case of externally incorporated cadmium chloride in both the cases where 1: 10 (E-1) and 1: 15 (E-2) (oil: water) phase was used. This indicated that incorporation of uniform cadmium chloride after polymerization was difficult. The porosity, pore structure, wettability, water absorbing capacity of the polymer plays an important role for imbibition while in case of insitu incorporation strategy the cadmium chloride particles were well distributed under stirring in HIPE, prior to polymerization. It was also observed that as the ratio of oil : water changes the concentration of Cd and S ions also changes. This was because pore size and structure are dependent on the aqueous phase concentration.

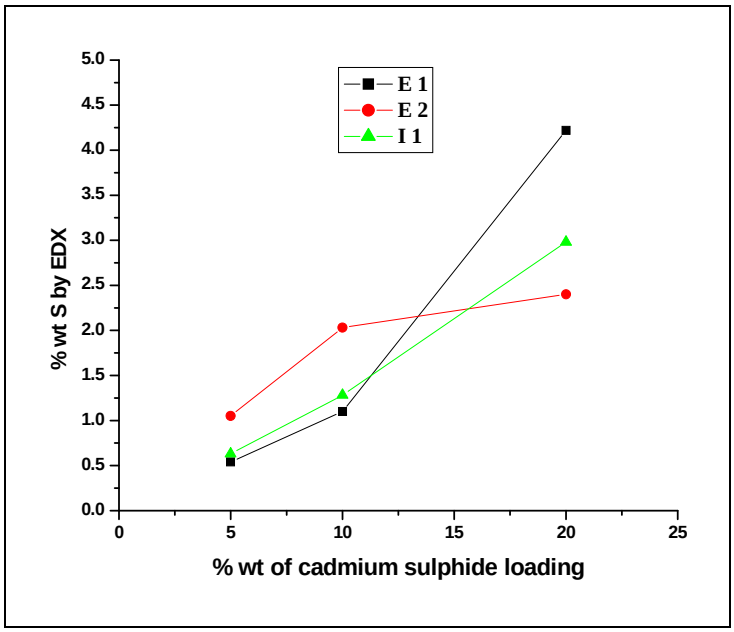

Figure 4.38: EDX data comparison of 'S' present in the polymer matrix

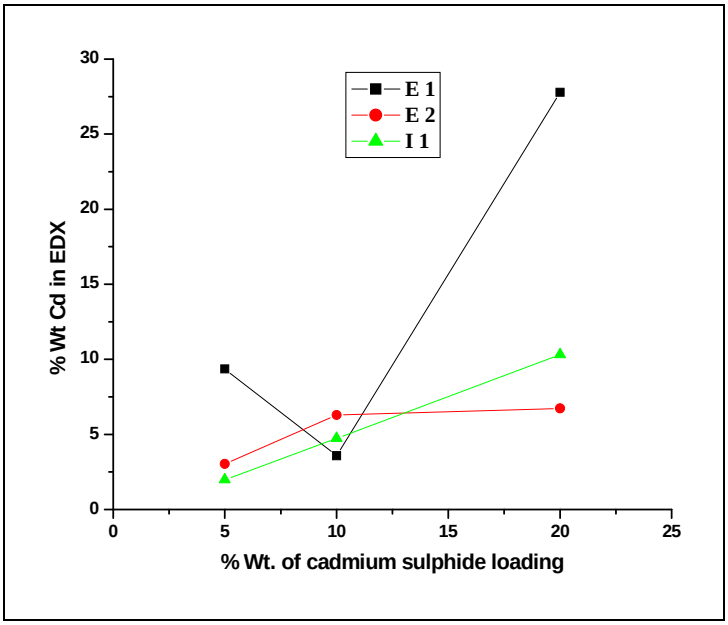

Figure 4.39: EDX data comparison of 'Cd' present in the polymer matrix

4.3.4.2 *Crystal structure studies*

X-ray diffraction spectroscopy was used to study the crystal structure formation of CdS. Figures 4.40- 4.42 show the comparison of the XRD data for all the strategies used for incorporation of CdS particles inside the St-DVB polyHIPE matrix using high internal phase emulsion methodology.

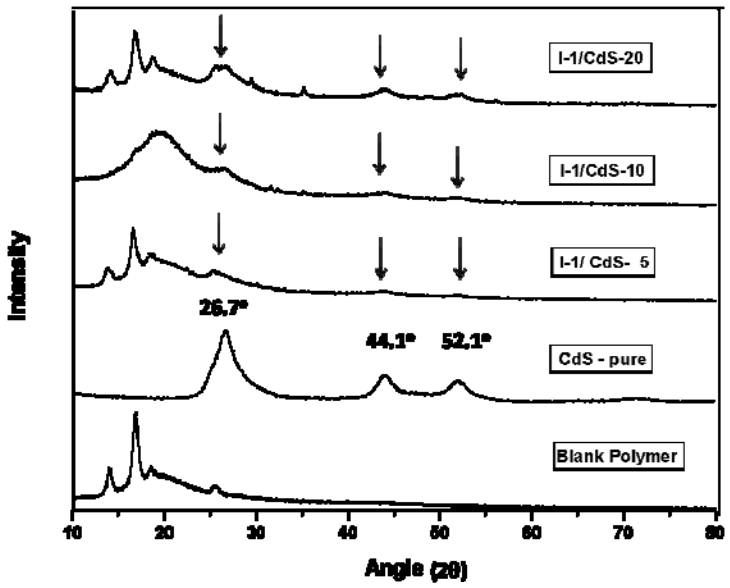

Figure 4.40: Comparison of XRD data of St-DVB polyHIPEs synthesized using external incorporation strategy with different wt% of CdS using 1 :15; oil : water ratio

Figure 4.40 shows comparison of XRD data of St-DVB polyHIPE, pure CdS and polyHIPEs synthesized using insitu incorporation strategy. The XRD pattern for pure cadmium sulphide shows prominent broad peaks at 2θ values of 26.7, 44.1 and 52.1 that can be indexed to scattering from 111, 220 and 311 crystal planes respectively of cubic CdS. For the St-DVB polyHIPE without any CdS loading peaks were observed at lower 2θ values that are due to the polymer matrix. It was observed that as the loading concentration increased the intensity of the CdS peaks at the respective 2θ angle also

increased. The XRD patterns confirmed the presence of CdS particles inside the polymer matrix. As the loading concentration was increased, some other peaks were also observed, indicating incomplete conversion of $CdCl_2$ to CdS. Figures 4.41 and 4.42 show XRD patterns for the polymer where external incorporation of cadmium chloride was done. Apart from the peaks attributed due to CdS few other small peaks were also observed. This can be due to incomplete conversion of $CdCl_2$ to CdS. After polymerization, the diffusion and uniform dispersion of cadmium chloride solution inside the porous polymer structure becomes an important criterion. It can be confirmed from the XRD patterns that CdS particles can be incorporated inside a porous polymer matrix synthesized using high internal phase emulsion HIPE methodology.

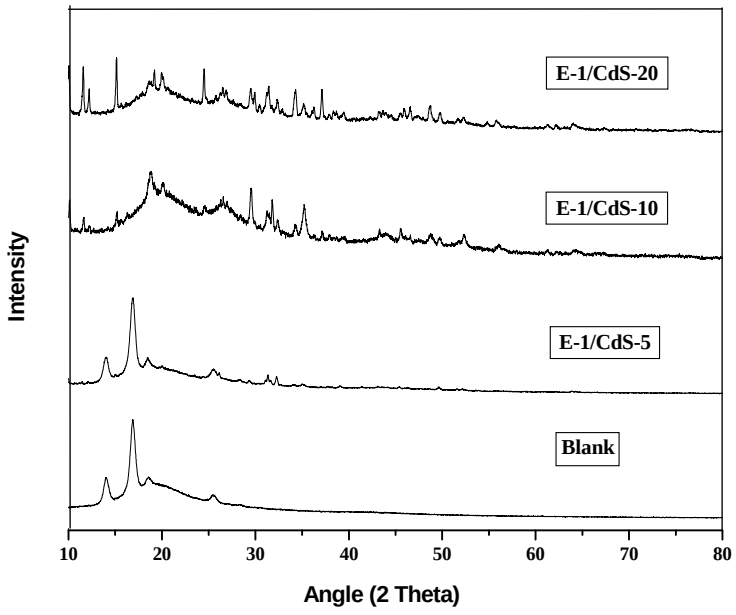

Figure 4.41: Comparison of XRD data of St-DVB polyHIPEs synthesized using external incorporation strategy with different wt% of CdS using 1 :15; oil : water ratio

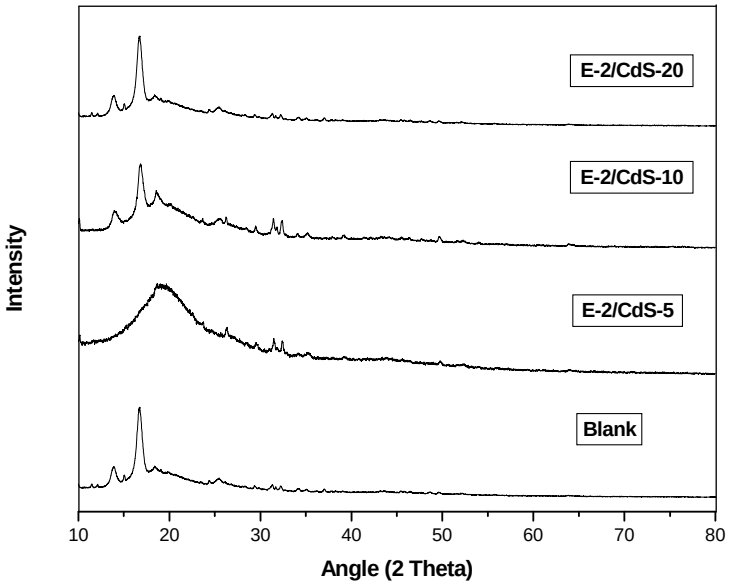

Figure 4.42: Comparison of XRD data of St-DVB polyHIPEs synthesized using external incorporation strategy with different wt% of CdS using 1 : 10; oil : water ratio

4.3.4.3 *Morphology studies*

The effect of presence of CdS particles on the polymer morphology was studied. The morphology of the polymers is shown in Figures 4.43-4.45 having 5, 10 and 20 wt % loadings of CdS respectively. Figure 4.43(a) shows the SEM image of St-DVB polyHIPE. In Figure 4.43(b), where the insitu incorporation strategy was used, it failed to maintain the interconnected pore structure of polyHIPE. The addition of salts to the aqueous phase affects the HIPE stability. The addition of particles led to the formation of closed pores. Figures 4.43(c) and 4.43(d) shows SEM micrographs of polymers wherein external incorporation strategy was used. In both the cases it was observed that clusters of cadmium sulphide were present inside the pores having interconnected morphology.

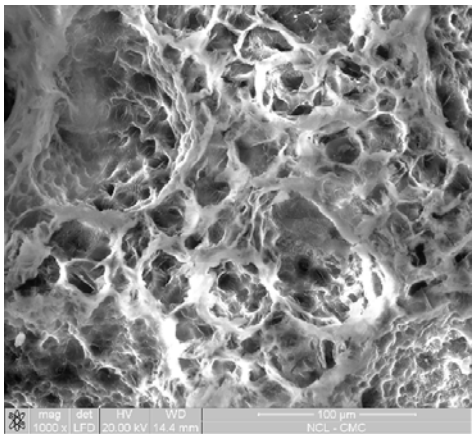

(a) SEM of St-DVB polyHIPE without any CdS loading (1000X)

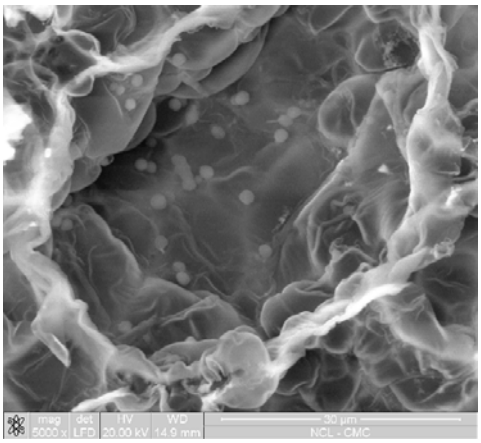

(b) Insitu incorporation strategy using 1 : 15; oil : water ratio (5000 X)

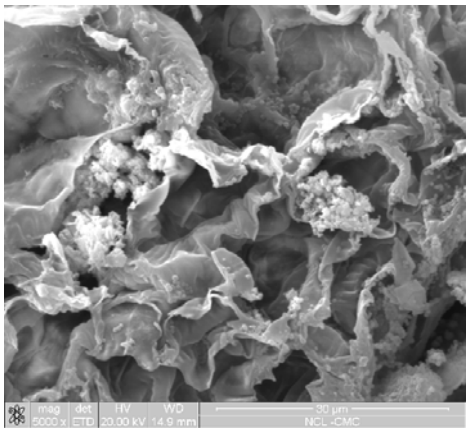

(c) External incorporation strategy using 1 : 15; oil : water (5000 X)

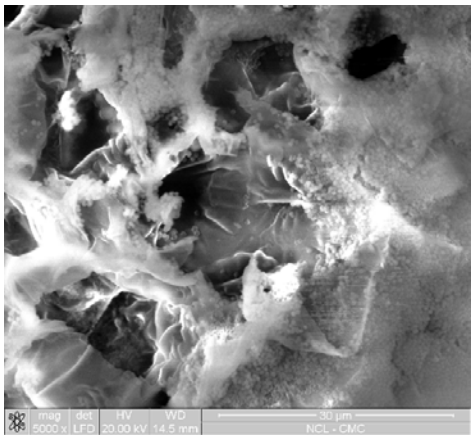

(d) External incorporation strategy using 1 : 10; oil : water (5000 X)

Figure 4.43: Comparison of SEM images of St-DVB polyHIPEs with 5 wt% loading

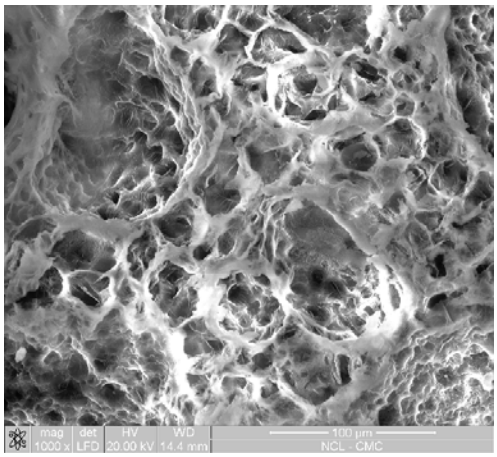

(a) SEM of St-DVB polyHIPE without any CdS loading (1000X)

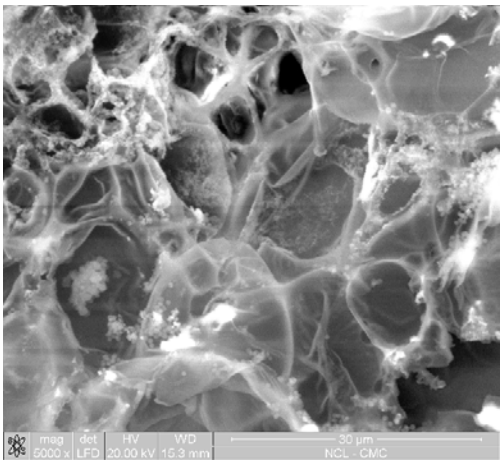

(b) Insitu incorporation strategy using 1 : 15; oil : water ratio (5000 X)

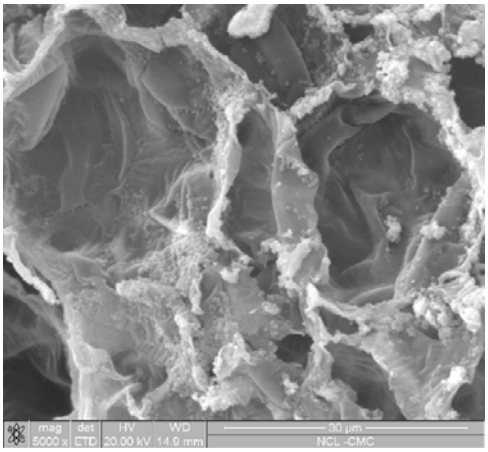

(c) External incorporation strategy using 1 : 15; oil : water (5000 X)

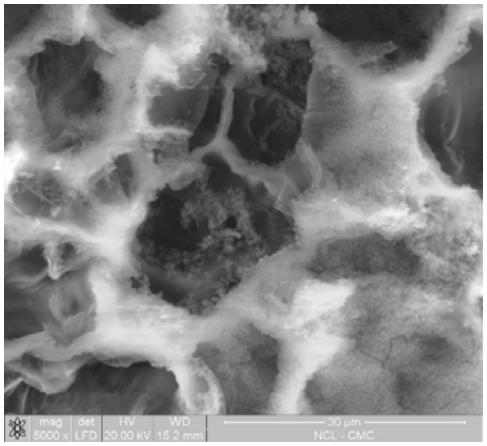

(d) External incorporation strategy using 1 : 10; oil : water (5000 X)

Figure 4.44: Comparison of SEM images of St-DVB polyHIPEs with 10 wt% loading

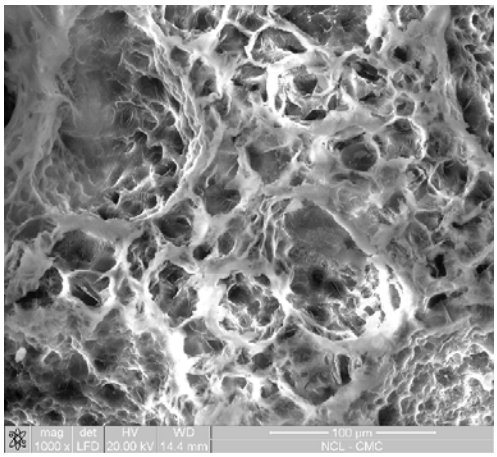

(a) SEM of St-DVB polyHIPE without any CdS loading (1000X)

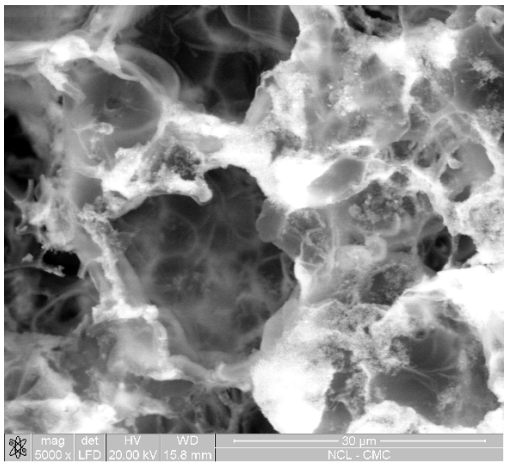

(b) Insitu incorporation strategy using 1 : 15; oil : water ratio (5000 X)

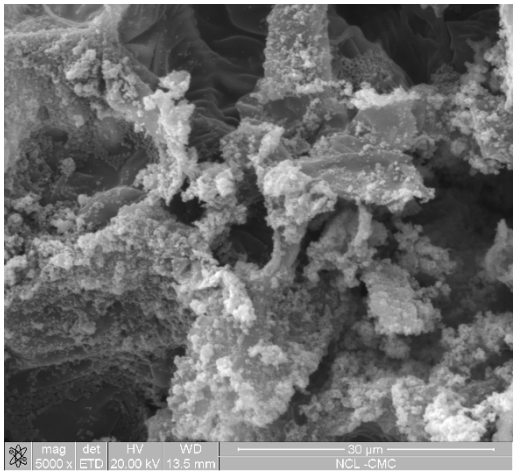

(c) External incorporation strategy using 1 : 15; oil : water (5000 X)

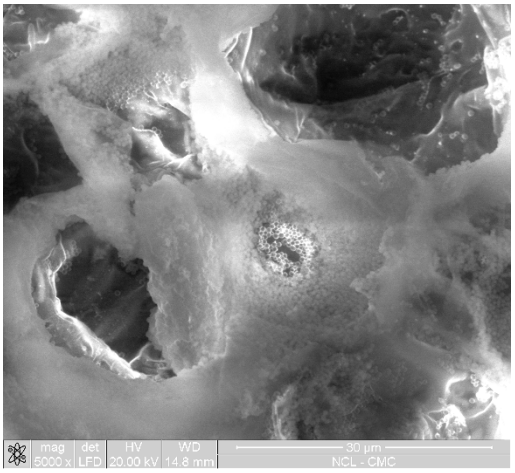

(d) External incorporation strategy using 1 : 10; oil : water (5000 X)

Figure 4.45: Comparison of SEM images of St-DVB polyHIPEs with 20 wt% loading

Figure 4.44 shows incorporation of 10 wt % loadings in I-1, E-1 and E-2 series. In case of I-1 as shown in 4.44 (b), there was some definite pore morphology observed with cadmium sulphide particles in the polymer matrix. As observed in Figure 4.45, for 20 wt% loading, the CdS particles were prominently seen. As the wt% loading of $CdCl_2$ was increased in insitu incorporation strategy, the interconnected morphology was observed.

In case of external incorporation strategy with 20% loading the incorporation of CdS was prominently observed in case of polymers synthesized using 1:15; oil : water ratio than that in case of polyHIPE synthesized using 1 : 10; oil : water ratio.

4.4 Conclusion

Highly porous styrene-divinylbenzene (St-DVB) polyHIPE were synthesized. The effect of use of ionic surfactants in comparison with non-ionic surfactants in HIPE formation and stability were studied. The type of surfactant and the ratio of the aqueous discontinuous phase play an important role in formation of a stable HIPE having a well-defined interconnected porous structure after polymerization. Low oil : aqueous phase ratios viz. 1 : 1/ 2.5/ 5 were insufficient to form a stable HIPE and generate an interconnected pore structure. Arquad 2HT-75, an ionic surfactant was employed to check its feasibility in formation of HIPEs. In case of ionic surfactants it was observed that at an oil : water ratios above 1 : 10, similar morphological structures were observed as that in case of non-ionic surfactants like Span 80 and Span 20. Arquad 2HT-75 being hydrophilic in nature, makes it less miscible in the oil phase. This leads to the formation of less stable emulsion and hence formation of closed pore structure. The surface area of the polymers obtained in all the cases was below 10 m^2/g. This is because the average droplet size of the water molecule is 10 μm and water acts as discontinuous phase to obtain interconnected pore structure after polymerization.

The effect of variation in crosslink density reveals that as the crosslink density increases, the oil phase becomes more hydrophobic leading to the formation of a stable

HIPE. SEM images confirmed the formation of uniform interconnected pore morphology with an increase in crosslink density.

Inorganic particles can be incorporated into the St-DVB polyHIPE matrix having interconnected pore structure. Incorporation of cadmium sulphide (CdS) particles inside the styrene-DVB polyHIPE matrix was achieved. Insitu incorporation strategy was found to have uniform distribution of particles over the entire polymer matrix as compared to external incorporation strategy. In the external incorporation strategy, the polymer properties such as void diameter, affinity for imbibing $CdCl_2$ solution and accessibility of the reactants for post conversion play an important role for complete conversion of cadmium chloride ($CdCl_2$) to cadmium sulphide (CdS).

In case of insitu incorporation strategy, the analysis data was linear with the increase in loading concentrations. In all the polymers containing CdS, the XRD pattern showed prominent broad peaks at 2θ values of 26.7, 44.1 and 52.1 that can be indexed to scattering from 111, 220 and 311 crystal planes of cubic CdS respectively. The morphology of the CdS containing polyHIPEs showed presence of CdS particles in the matrix. The CdS particles were prominently observed in the polymer matrix having higher concentration of $CdCl_2$.

CHAPTER - V

Synthesis, morphological studies and modification of acrylonitrile based polyHIPEs

5.1 Introduction

Crosslinked porous polymers of acrylonitrile (AN) and divinylbenzene (DVB), terpolymers of acrylonitrile, ethyl or butyl acrylate and DVB are interesting products that are used as sorbents and stationary phases for gas chromatography.[1-4] However, polyHIPEs of AN-DVB copolymer system has not been reported hitherto. The advantage of AN-DVB polyHIPE monoliths over the conventional beaded copolymers is to have uniform interconnected porous structure with high surface areas and pore volume that can be prepared in any desired forms and shapes (such as stationary columns). Chemical modification of these products with amines can be used in applications such as specific sorbents, anion-exchange resins and carriers for biologically active substances.[5-7] The reactive pendant nitrile group can be modified into different functional groups by nucleophilic addition and cycloaddition reactions. However, the degree of modification is low due to poor accessibility of the nitrile groups. The nitrile moiety on the polymer backbone can be modified by reacting it with hydroxylamine, hydrazine or ethanolamine to introduce amidoxime, amidazone or oxazoline groups respectively on the polymer backbone. Literature survey reveals that the amidoxime groups form stable complexes with different metal ions. Consequently, the polymers with the amidoxime groups can be successfully used for the preconcentration of trace metals from aqueous solutions as one of the important applications of these adsorbents is the recovery of heavy metals such as gallium, lead, and uranyl ion from sea water.[8] Waste-water quality is defined by physical, chemical or biological characteristics. Waste-water generally contains toxic inorganic and organic pollutants. Inorganic pollutants consist of mineral acids, inorganic salts, finely divided

metal, trace elements, cyanides, nutrients and organo-metallic compounds. Some of the trace elements play essential roles in biological processes. However at higher concentrations, they are toxic to biota as they disturb the biochemical processes and cause hazards. These elements include metals (Cd, Cr, Co, Cu, Zn, Pd, Hg, Ni, Ag) and metalloids (Se, As, Sb). Most of the trace elements are transition metals with variable oxidation states and coordination numbers.

Heavy metal pollution has become serious with the rapid increase in global industrial activities and it has accumulating characteristics in nature as it cannot be biodegraded. These heavy metals come from various industrial sources such as electroplating, metal finishing, textile, storage batteries, lead smelting, mining, plating, ceramic and glass industries. Lead, chromium, mercury, cadmium, arsenic and copper are the common contaminants in industrial pollutants. These metals cause various ailments such as dehydration, stomach ache, nausea, dizziness, lack of coordination in muscles, destruction of nervous systems in young children, lung irritation, eye irritation, skin rashes, vomiting, abdominal pain, lung insufficiency and liver damage. The separation or adsorption of these metal ions from an aqueous solution has been of considerable importance in different fields for solving waste-water problems, removing toxic metals from seawater, recovering raw materials etc. The separation of metals can be achieved by using macromolecular compounds containing functional groups such as amino, carboxyl, phosphoric, imidazoline, thioamido, amidoxime etc., which have complexing ability towards metals ions. Among them, amidoxime groups have high tendency to form strong complexes with a wide range of heavy metal ions such as lanthanides {La(III), Nd(III), Sm(III), Gd(III) and Tb(III)}, actinides {U(II)}, transition

metals {Ag(I), V(I), Cu(II), Pd(II), Au(III) and Fe(III)}, Cr(VI) and poor metals {Cd(II), Ga(III)}.

There is considerable interest in the treatment of polluted water generated by industrial processes. Various technologies have been developed over recent years and are now available for the removal of toxic metals from waste water, thereby preventing pollution of surface and ground water.[12] Chromium bearing waste water originates from a variety of industrial processes such as electroplating, dichromate, basic chrome sulphate manufacturing, tannery, anodizing, cutting tools, chrome mining etc. Many of these industrial processes usually produce a large volume of waste-water with a chromium concentration ranging from less than 1 ppm to 10 ppm. The two common oxidation states for chromium in natural water are Cr(III) and Cr(VI). Cr(III) is not a significant groundwater contaminant whereas Cr(VI) is approximately 100 times more toxic than Cr(III).[13]

In view of the toxic nature of Cr(VI), development of methods in order to establish their levels in the environment and industrial quality control are quite significant. Solid phase extraction has been explored for the pre-concentration of many metal ions.[14-17] A variety of adsorbents have been used for the preconcentration of chromium.[18-26] Literature survey of the preconcentration of Cr(VI) reveals that solid phase extraction is one of the most versatile methods. The major advantage of solid phase extraction is high selectivity and enrichment factor.

Much attention is paid to amidoxime chelating adsorbent in removing heavy toxic metals and/or selective recovering of precious metals from different sources

(sorption of uranium from seawater). Therefore it would be interesting to investigate the possibility of porous monoliths having amidoxime groups on the surface for adsorption and desorption of metal ions.

This chapter is divided into two parts as follows,

Part-A : Synthesis and characterization of AN-DVB polyHIPEs.

Part-B : Post modification of AN-DVB polymers and their evaluation as adsorbents for Cr(VI) metal ion.

Present work deals with the study of synthesis of AN-DVB polymeric monoliths using HIPE methodology using redox initiator, to generate porous polymers having high surface area and interconnecting pores. The effect of reaction parameters like nature of surfactant, surfactant concentration, ratio of aqueous (discontinuous) phase to oil (continuous) phase and the effect of porogen on HIPE formation, its stability and final porous morphology of the monoliths was studied.

The AN-DVB polymers synthesized were subjected to post modification reactions to convert the nitrile functionality to amide functionality followed by converting it to amidoxime functionality. The amidoxime modified monoliths were then tested for its efficiency as heterogeneous supports for the adsorption of Cr(VI) metal ion. The Cr(VI) metal ion was chosen because of its chelating properties and environmental significance. The adsorption of heavy metal ions onto conventional polyacrylonitrile-oxime polymers was reported previously. However, to our knowledge, the use of monolithic polyacylonitrile-oxime polymer synthesized using HIPE methodology for the adsorption of trace metal ions like Cr(VI) has not been reported.

5.2 Part A : Synthesis and characterization of AN-DVB polyHIPEs

5.2.1 Experimental

5.2.1.1 *Materials*

Acrylonitrile, Span 80, Span 85, Span 20, Tween 20, Tween 80, Brij 30, Brij 35, sodium peroxydisulphate (NaPS) and ascorbic acid (ASA) (from Loba Chemie), Divinylbenzene-80% (from Aldrich), heptane, toluene, chlorobenzene, chloroform (from Merck India), de-ionized water was collected from a Milli Q, Millipore unit.

5.2.1.2 *Procedure*

The oil phase comprising of requisite amount of monomers, surfactant and porogen was taken in a 100 mL plastic container. The weighed quantity of water that acts as discontinuous phase was added drop-wise to the oil phase under constant stirring speed (1400 rotations per minute) at room temperature. The HIPE was formed slowly and the addition was continued at the same rate until total water was incorporated. After complete addition of water, the redox initiator (NaPS : ascorbic acid; 1:0.5) dissolved in 1mL water each was added to the reactor (2 mL water is the inclusive of total water used) under stirring. There after the HIPE formed was kept for polymerization at 50^{o}C in constant temperature water bath. The polymerization was continued for a period of 8 h to ensure complete polymerization. The monoliths obtained after polymerization were then subjected to soxhlet extraction using methanol for 12 h, followed by drying at room temperature. The monoliths were then subsequently characterized for surface area and morphology. The details of the synthesis of various AN-DVB monoliths are tabulated as below.

Table 5.1 Synthesis of 100% cross-linked AN-DVB polyHIPEs using different oil : water ratios

Polymer Code	AN g (mol)	DVB g (mol)	Oil : Water Ratio
ANDVB-1.1	2.546 (0.0477)	6.247 (0.0477)	1 : 5
ANDVB-1.2	2.546 (0.0477)	6.247 (0.0477)	1 : 10
ANDVB-1.3	2.546 (0.0477)	6.247 (0.0477)	1 : 15
ANDVB-1.4	2.546 (0.0477)	6.247 (0.0477)	1 : 20

Span 80 = 20 wt % of oil phase, sodium peroxydisulphate (NaPS) = 0.00227 g (9.51 x 10^{-6} mol) 0.01 mol % of oil phase, ascorbic acid (ASA) = 0.00084 g (4.77 x 10^{-6} mol) 0.005 mol% of oil phase, stirring speed = 1400 rpm, reaction temperature = 50^{o}C

Table 5.2 Synthesis of 100% cross-linked AN-DVB polyHIPEs using different surfactant concentrations

Polymer Code	AN g (mol)	DVB g (mol)	Span 80 wt.% (g)
ANDVB-1.5	2.546 (0.0477)	6.247 (0.0477)	5 (0.4396)
ANDVB-1.6	2.546 (0.0477)	6.247 (0.0477)	10 (0.8793)
ANDVB-1.7	2.546 (0.0477)	6.247 (0.0477)	15 (1.3189)
ANDVB-1.8	2.546 (0.0477)	6.247 (0.0477)	20 (1.7586)
ANDVB-1.9	2.546 (0.0477)	6.247 (0.0477)	25 (2.1982)

Oil : Water ratio = 1:10, sodium peroxydisulphate (NaPS)= 0.00227 g (9.51 x 10^{-6} mol) 0.01 mol % of oil phase, ascorbic acid (ASA) = 0.00084 g (4.77 x 10^{-6} mol) 0.005 mol% of oil phase, stirring speed = 1400 rpm, reaction temperature = 50^{o}C

Table 5.3 Synthesis of 100% cross-linked AN-DVB polyHIPEs (1:10; oil : water ratio) using different porogens and porogen concentrations

Polymer Code	AN g (mol)	DVB g (mol)	Porogen	Monomer: porogen ratio
ANDVB-2.0	2.546 (0.0477)	6.247 (0.0477)	heptane	1:1
ANDVB-2.1	2.546 (0.0477)	6.247 (0.0477)	heptane	1:0.5
ANDVB-2.2	2.546 (0.0477)	6.247 (0.0477)	toluene	1:1
ANDVB-2.3	2.546 (0.0477)	6.247 (0.0477)	toluene	1:0.5
ANDVB-2.4	2.546 (0.0477)	6.247 (0.0477)	chlorobenzene	1:1
ANDVB-2.5	2.546 (0.0477)	6.247 (0.0477)	chlorobenzene	1:0.5
ANDVB-2.6	2.546 (0.0477)	6.247 (0.0477)	chloroform	1:1
ANDVB-2.7	2.546 (0.0477)	6.247 (0.0477)	chloroform	1:0.5

Span 80= 20 wt% of oil phase, oil: water= 1:10, sodium peroxydisulphate (NaPS)= 0.00227 g (9.51 x 10^{-6} mole) 0.01 mol % of oil phase, ascorbic acid (ASA) = 0.00084 g (4.77 x 10^{-6} mol) 0.005 mol% of oil phase, stirring speed = 1400 rpm, reaction temperature = 50^{o}C

Table 5.4 Synthesis of 100% cross-linked AN-DVB polyHIPEs (1:20; oil : water ratio) using different porogens and porogen concentrations

Polymer Code	AN g (mol)	DVB g (mol)	Porogen	Monomer: porogen ratio
ANDVB-2.8	2.546 (0.0477)	6.247 (0.0477)	toluene	1:1
ANDVB-2.9	2.546 (0.0477)	6.247 (0.0477)	chloroform	1:1
ANDVB-3.0	2.546 (0.0477)	6.247 (0.0477)	chloroform	1:0.5
ANDVB-3.1	2.546 (0.0477)	6.247 (0.0477)	toluene	1:0.5

Span 80= 20 wt%. of oil phase, oil: water= 1:20, sodium peroxydisulphate (NaPS)= 0.00227 g (9.51 x 10^{-6} mol) 0.01 mol % of oil phase, ascorbic acid (ASA) = 0.00084 g (4.77 x 10^{-6} mol) 0.005 mol% of oil phase, stirring speed = 1400 rpm, reaction temperature = 50^{o}C

5.2.2 Characterization

The stability of the HIPE emulsions formed was monitored using optical microscope. The subsequent AN-DVB polyHIPEs were characterized for morphology and surface area.

5.2.2.1 *Optical microscopy*

The HIPE emulsion before polymerization was characterized for its formation and structure elucidation by an OLYMPUS polarized optical microscope at magnification of 50X. The images were recorded using OLYMPUS digital camera.

5.2.2.2 *Scanning electron microscopy (SEM)*

The surface morphologies of the polyHIPE prepared was studied using a Lieca Stereoscan 440 scanning electron microscope at different magnifications. The energy of analyses was 20 keV.

5.2.2.3 *Surface area analysis-BET method*

Surface areas of the polymers were determined using NOVA 2000e surface area analyzer from Quantachrome. The analysis was done using pure nitrogen at a flow rate of 10 psi and the data was processed using Autosorb 1 software. The method used was Brunauer-Emmett-Teller method (BET). The samples were degassed for 3h at 60^{o}C and then analyzed.

5.2.3 Results and Discussion

The present study deals with use of high internal phase emulsion methodology to synthesize porous polymeric monoliths having acrylonitrile as core monomer and divinylbenzene as a crosslinker. The effect of variation in chemical composition on the emulsion stability and polymer properties was studied.

5.2.3.1 *Stability studies of AN-DVB HIPEs*

Acrylonitrile is hydrophilic in nature while divinylbenzene is hydrophobic in nature. It is well known that to form stable water in oil (W/O) HIPE emulsion, surfactant having low HLB in the range of 4-6 is used. In the present study, since one of the monomer is hydrophilic, surfactants having different HLB values were used to study their effect on HIPE formation and stability. Table 5.5 shows HIPE stability study using surfactants having different HLB values.

Table 5.5 Effect of surfactant type on stability of 100% cross-linked acrylonitrile-divinylbenzene HIPEs

HIPE Code	Surfactant	HLB value	Chemical composition of surfactant	HIPE Stability
1	Span 85	1.8	Sorbitan trioleate	Emulsion phase separate out
2	Span 80	4.3	Sorbitan mono oleate	Stable thick emulsion formed
3	Span 20	8.6	Sorbitan monolaurate	Stable thick emulsion formed
4	Tween 20	16.7	Poly oxyethylene (20) sorbitan monolaurate	Liquid like milky emulsion phase separates on standing
5	Tween 80	15.0	Poly oxyethylene (20) sorbitan monooleate	Milky liquid separates on standing
6	Brij 30	9.7	Poly oxyethylene (4) lauryl ether	Liquid like emulsion that separates on standing
7	Brij 35	16.9	Poly oxyethylene (23) lauryl ether	Liquid like emulsion that separates on standing

Oil phase = 100% CLD, AN = 2.534g (0.0477 mol), DVB = 6.222 g (0.0477 mol), Surfactant = 1.752 g (20 wt %), oil : water ratio = 1 : 20.

Three different types of non-ionic surfactants i.e. sorbitan esters (Span), polyoxyethylene ethers (Brij) and sorbitan polyoxyethylene fatty acid esters (Tween) were studied. Figure 5.1 depicts the pictorial representation of HIPE stability.

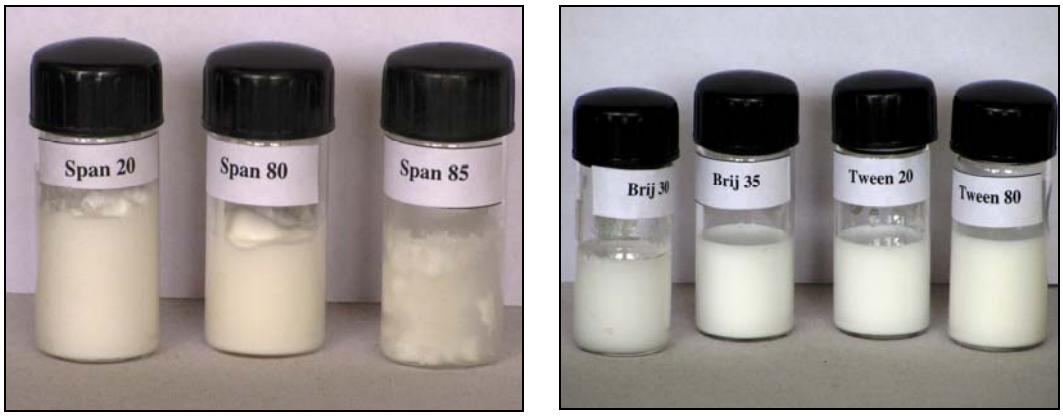

(a) **(b)**

Figure 5.1 Effect of surfactant type on AN-DVB HIPE stability
(a) Span series (b) Brij and Tween series

It was observed that in case of HIPE prepared using Span 85, emulsion phase separated during preparation. However, stable viscous emulsions were formed in case of Span 80 and Span 20 surfactants. The stability of HIPE is influenced both by chemical nature of continuous/discontinuous phase and surfactant. Span 85 is sorbitan trioleate having a HLB value of 1.8 and the structure reveals that three hydroxyl groups are modified with the ester moiety. While in the case of Span 80 and Span 20 only one hydroxyl group is esterified having high HLB values compared to Span 85. Span 80 is sorbitan monooleate with a HLB value of 4.3 with unsaturation while Span 20 is sorbitan monolaurate having a HLB value of 8.6. Sorbitan monolaurate has the shortest hydrophobic chain, which makes it most hydrophilic amongst the Span series surfactant studied here. Therefore viscous stable emulsion was formed where Span 80 and Span 20 were used as surfactants while in the case of Span 85 which was most hydrophobic no stable emulsion was formed. Brij and Tween type of surfactants were also studied to check its efficiency to form a stable HIPE using acrylonitrile and divinylbenzene monomers. A less viscous milky white emulsion was formed that separated in two layers

on standing in the case where Brij-30 and Brij 35 were used as surfactants. The use of high HLB value surfactants like Tween 20 and Tween 80 (HLB value of 16.7 and 15 respectively) also did not result in the formation of a stable HIPE on standing. Figure 5.2 depicts the optical micrographs (50X) of HIPE formed using different surfactants.

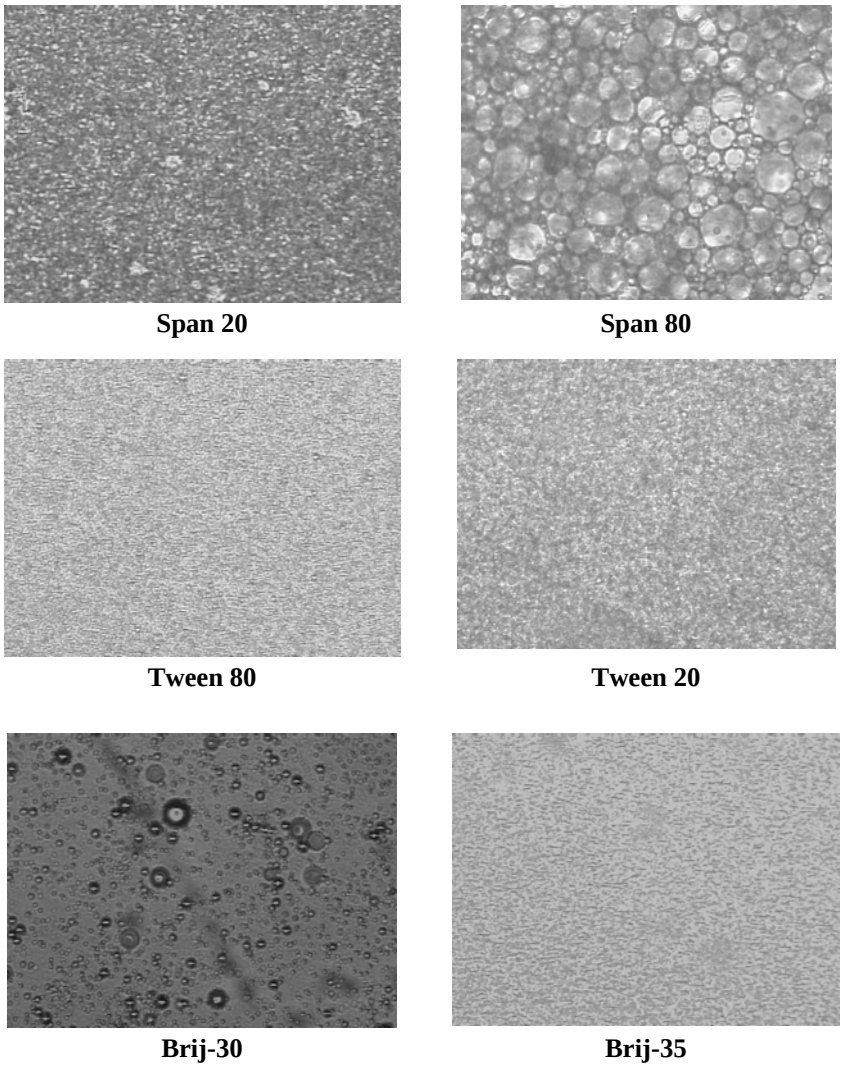

Figure 5.2 : Optical microscopy images (50X) of AN-DVB HIPEs (100% CLD) with variation in surfactant type

Very fine particles were observed in case where Brij and Tween surfactants were used as well as no uniform interconnected structure was formed. This could be because the HLB value being on the higher side, the surfactants are less soluble in the oil phase

and hence could not orient properly at the oil and water interface. This led to phase separation on standing. In case of Span 80 and Span 20 the HIPE was stable on standing having highly interconnected droplets.

Based on the preliminary data of stable emulsion formation Span 80 was chosen as the surfactant to study the effect of different reaction parameters such as crosslink density, oil : water ratio, surfactant concentration and porogen type and concentration on the surface area and pore morphology of AN-DVB polyHIPEs.

The stable HIPEs formed were polymerized to form a porous interconnected monolithic structure. A pair of redox initiating system consisting of sodium peroxydisulphate : ascorbic acid (1 : 0.5) was used to initiate the polymerization at 50^{o}C. The boiling point of acrylonitrile is 77^{o}C. Thermal initiators that are efficient above 70^{o}C like azobisisobutyronitrile (AIBN) and benzoyl peroxide (BPO) cannot be used as vaporization of acrylonitrile (carcinogen) would start above 70^{o}C. This would lead to reduction in concentration of the monomer in the oil phase which in turn will affect the stability of HIPE formed.

5.2.3.2 *Effect of crosslink density (CLD)*

Figures 5.3 and 5.4 depict the optical images of AN-DVB HIPE prepared with different crosslinker concentration using 1 : 10 and 1 : 20; oil : water ratios, respectively. It was observed that at lower crosslinker concentration, the stability of the HIPE formed is less as compared to that observed at higher crosslinker concentration. This is because the hydrophobicity of the oil phase is less at lower crosslink densities and it increases as the crosslink density increases.

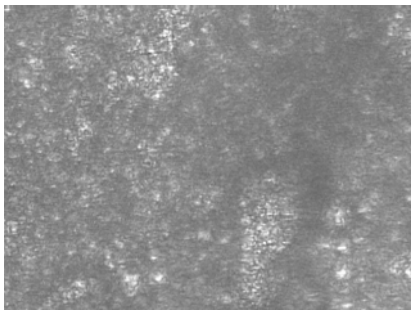

CLD- 5%

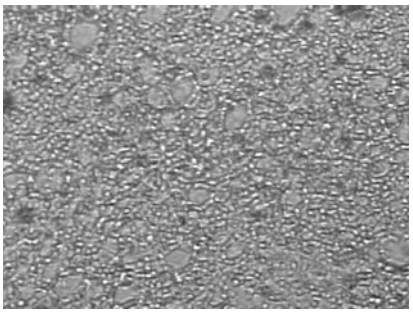

CLD- 10%

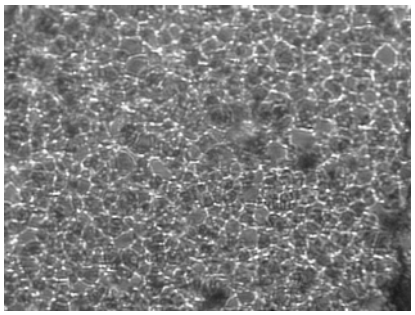

CLD- 15%

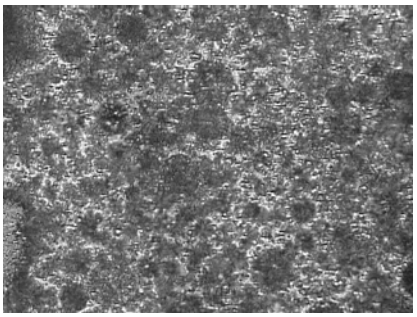

CLD- 20%

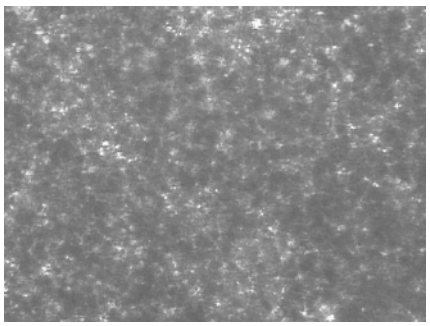

CLD- 25%

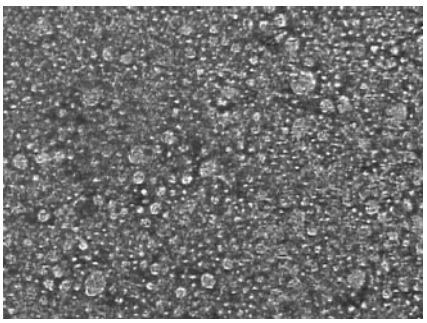

CLD- 50%

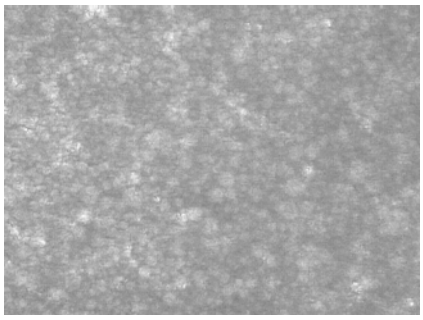

CLD- 75%

Figure 5.3 : Optical microscopy images of AN-DVB HIPE with variation in CLDs using 1 : 10; oil : water ratio

The hydrophilicity factor due to acrylonitrile causes the surfactant to solubilize to a less extent. This leads to destabilization of emulsion on standing and hence resulting in a non-uniform porous structure after polymerization. Similar trend was observed in HIPEs prepared using 1 : 20; oil : water ratio.

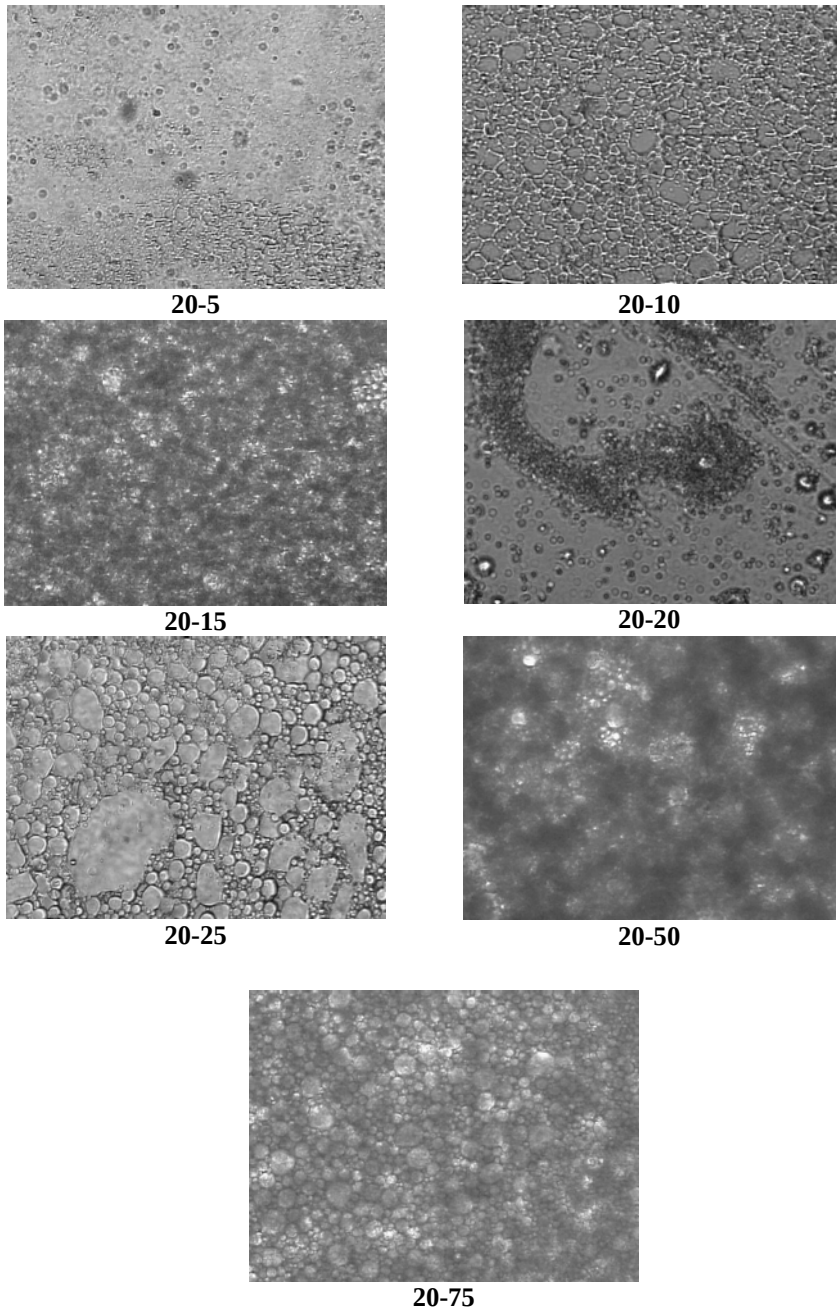

Figure 5.4 : Optical microscopy images of AN-DVB HIPE with variation in CLDs using 1:20; oil: water ratio

5.2.3.3 *Effect of oil : water ratio*

Table 5.6 shows the effect of oil : water ratio on the emulsion stability and surface area of the resulting polymers. Figure 5.5 shows the optical micrographs of the HIPE prepared at various oil : water ratios. No particular trend was observed in surface area values but optical micrographs show an increase in droplet size with an increase in ratio of the aqueous discontinuous phase. This observation is reverse of that is generally observed in the formation of W/O HIPEs. This can be attributed to the fact that acrylonitrile being hydrophilic in nature, its solubility in the discontinuous phase increases leading to coalescence of the droplets formed.

Table 5.6 Effect of variation in oil : water ratio on surface area of AN-DVB polyHIPEs

Polymer Code	Oil : water ratio	HIPE Stability	B.E.T surface area (m^2/g)
1.1	1 : 5	Stable emulsion formed	56.32
1.2	1 : 10	Stable emulsion formed	40.02
1.3	1 : 15	Stable emulsion formed	25.57
1.4	1 : 20	Stable emulsion formed	77.42

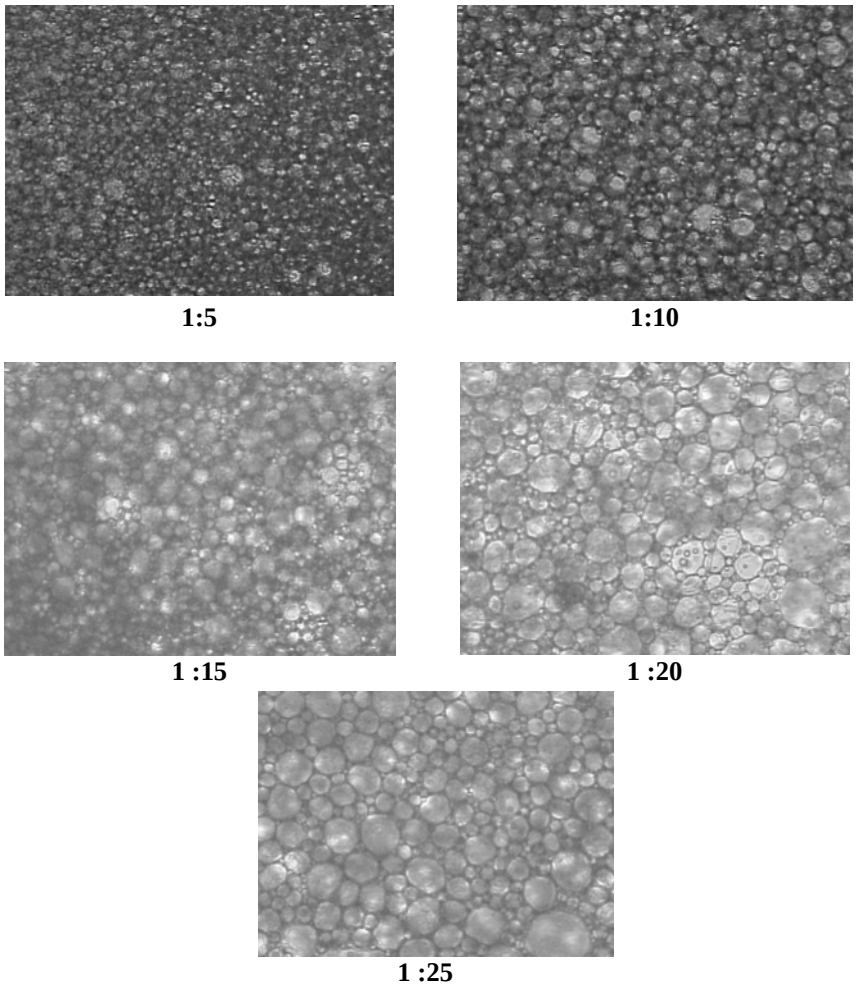

Figure 5.5 : Optical microscopy of AN-DVB HIPEs (100% CLD) at 1 : 5, 1 : 10, 1 : 15, 1 : 20 and 1 : 25; oil : water ratios

5.2.3.4 *Effect of surfactant concentration*

Table 5.7 shows the effect of surfactant concentration on the surface area of the polymers. It was observed that in case of polymers synthesized using 5 wt% Span 80 a very low surface area was obtained indicating presence of closed pores. As the surfactant concentration was increased, a considerable amount of surface area was observed. Increase in surfactant concentration leads to decrease in interfacial tension at the oil and water interface. More stable emulsion was formed at higher concentration of

surfactant leading to formation of compact structure. Figure 5.6 shows the formation of interconnected pore structure at higher surfactant concentration.

Table 5.7 Effect of surfactant concentration on surface area of AN-DVB polyHIPEs

Polymer Code	Wt % of Span 80	HIPE Stability	B.E.T surface area (m^2/g)
1.5	5	Stable emulsion formed	6.00
1.6	10	Stable emulsion formed	59.65
1.7	15	Stable emulsion formed	130.97
1.8	20	Stable emulsion formed	82.22
1.9	25	Stable emulsion formed	108..95

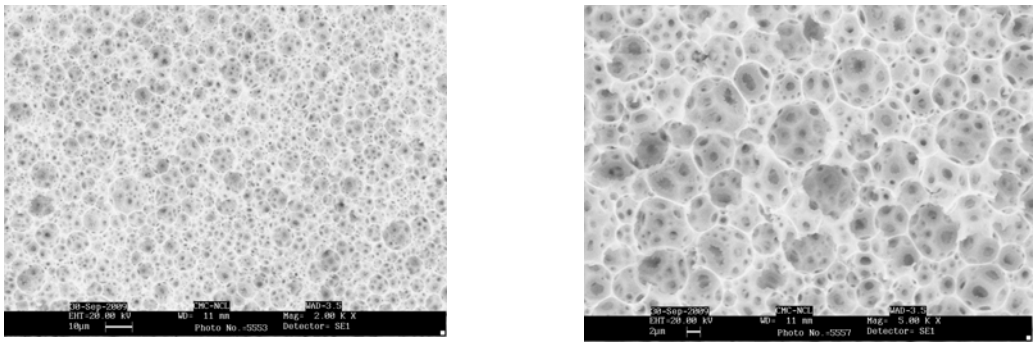

2000X **5000X**

Figure 5.6 : SEM images of AN-DVB monoliths using 25 wt% Span 80

5.2.3.5 *Effect of porogen*

The effect of porogen type and concentration on the surface area of the polymers is tabulated in Tables 5.8 and 5.9 respectively. The SEM images of the polymers synthesized using toluene and chloroform as porogen consisting of 1 : 10 and 1 : 20; oil : water ratios are shown in Figures 5.7 to 5.10. It was observed that the use of porogen led to considerable increase in surface area. In case where heptane was used as porogen the

surface area obtained was 150 and 162 m^2/g while in case of toluene the surface areas were 116 and 101 for 1:1 and 1:0.5 ratio of oil: porogen (1:10; O:W ratio). Heptane acts as a non solvent for the polymer while toluene acts as a solvent for the polymer. Hence the phase separation period of the polymer during polymerization is decided to form micropores or macropores reflecting in the surface area data. Maximum surface area of 329.74 m^2/g was observed in case of polymer synthesized using monomer and toluene in the ratio 1:1 and surface area of 206.75 m^2/g for 1:0.5 ratio (1:10; O:W ratio), respectively. The SEM images of these polymers are shown in Figures 5.7 and 5.8. Interconnected pore structure formation was also observed in presence of porogen.

Table. 5.8 Stability and surface area data of AN-DVB polyHIPEs with variation in porogen and porogen concentration with 1:10; O: W ratio

Polymer Code	Porogen	monomer : porogen ratio	HIPE Stability	B.E.T surface area m^2/g
2.0	heptane	1 : 1	Stable emulsion formed	150.00
2.1	heptane	1 : 0.5	Stable emulsion formed	162.07
2.2	toluene	1 : 1	Stable emulsion formed	116.5
2.3	toluene	1 : 0.5	Stable emulsion formed	101.77
2.4	chlorobenzene	1:1	Stable emulsion formed	81.96
2.5	chlorobenzene	1 : 0.5	Stable emulsion formed	108.37
2.6	chloroform	1:1	Stable emulsion formed	77.00
2.7	chloroform	1 : 0.5	Stable emulsion formed	56.28

Table 5.9 Stability and surface area data of AN-DVB polyHIPEs with variation in porogen and porogen concentration at 1:20; O:W ratio

Polymer Code	Porogen	monomer : porogen ratio	HIPE Stability	B.E.T surface area (m^2/g)
2.8	toluene	1 : 1	Stable emulsion formed	329.74
2.9	Chloroform	1 : 1	Stable emulsion formed	180.20
3.0	chloroform	1:0.5	Stable emulsion formed	150.70
3.1	toluene	1 : 0.5	Stable emulsion formed	206.75

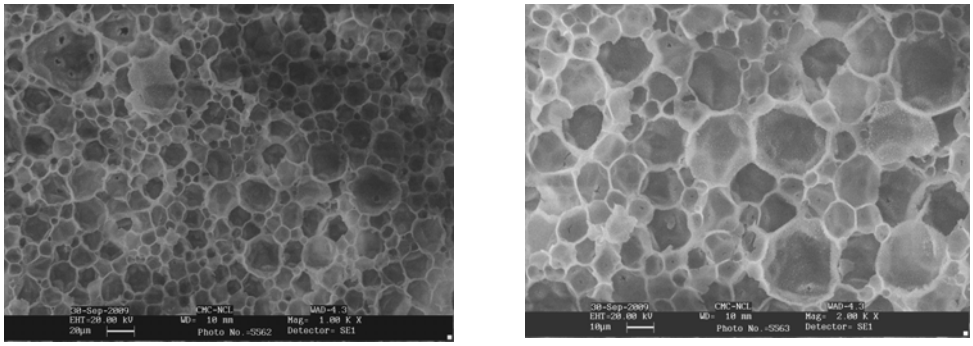

1000X 2000X

Figure 5.7 : SEM images of AN-DVB polyHIPEs using 1: 10; O : W ratio and toluene as a porogen (1: 1)

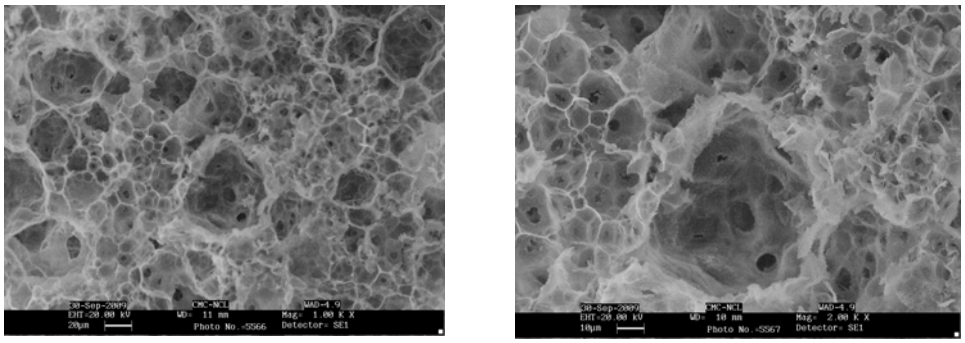

1000X 2000X

Figure 5.8 : SEM images of AN-DVB polyHIPEs using 1: 20; O :W ratio and toluene as a porogen (1: 1)

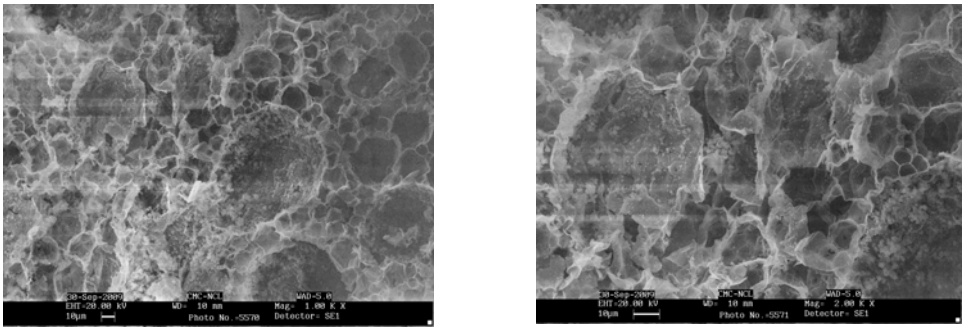

1000X 2000X

Figure 5.9 : SEM images of AN-DVB polyHIPEs using 1: 20; O : W ratio and chloroform as a porogen (1 : 1)

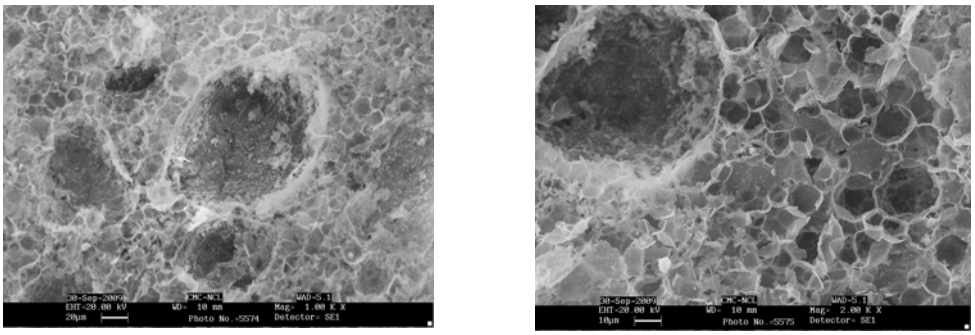

1000X 2000X

Figure 5.10 : SEM images of AN-DVB polyHIPEs using 1: 20; O : W ratio and chloroform as a porogen (1: 0.5)

5.3 Part-B: Post modification of AN-DVB polyHIPEs and evaluation as adsorbents for Cr(VI)

5.3.1 Experimental

5.3.1.1 *Materials*

Hydroxylamine hydrochloride (from Loba Chemie), sulfuric acid (95-98%), acetone (from Merck, India), potassium dichromate ($K_2Cr_2O_7$) (Loba Chemie), 1, 5-Diphenylcarbazide (DPC from Aldrich), water was deionized and purified with a Milli-Q water purification system (Millipore, USA).

Stock solution preparation:

(a) **Chromium (VI) stock solution:** 35.2 mg/mL Cr(VI) solution was prepared by dissolving requisite amount of potassium dichromate in 100 mL deionized water.

(b) **1,5-Diphenylcarbazide (DPC) solution**: 0.025% solution was prepared by dissolving 25 mg of DPC in 5 mL of acetone and 10 mL of 5M H_2SO_4, diluted to 100 mL with deionized water. The solution was kept in an amber-glass bottle.

5.3.2 Chemical modification of AN-DVB polyHIPEs

The reaction scheme for the modification of AN-DVB polymers is schematically represented in Scheme 5.1.

5.3.2.1 *Procedure*

1.5 g of poly(AN-DVB) monolith was taken in a 100 mL round bottom flask equipped with a water condenser. To the flask was added 2.0 g of hydroxylamine hydrochloride dissolved in 30 mL of methanol : water (5:1). 0.1 M NaOH solution was added to the reaction mixture to neutralize HCl of NH_2OH and was refluxed for the period of 24 h. The modified polymer was then filtered off and washed thoroughly with water followed by methanol and dried at 60^{o}C for 8 hours.

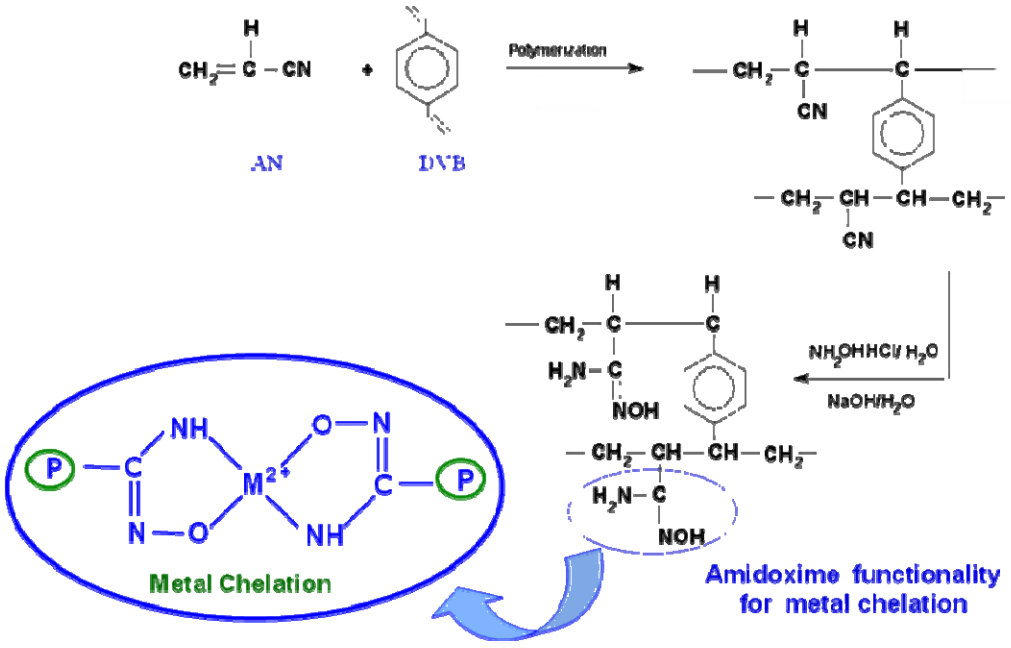

Scheme 5.1: Reaction scheme for modification of nitrile group to amidoxime

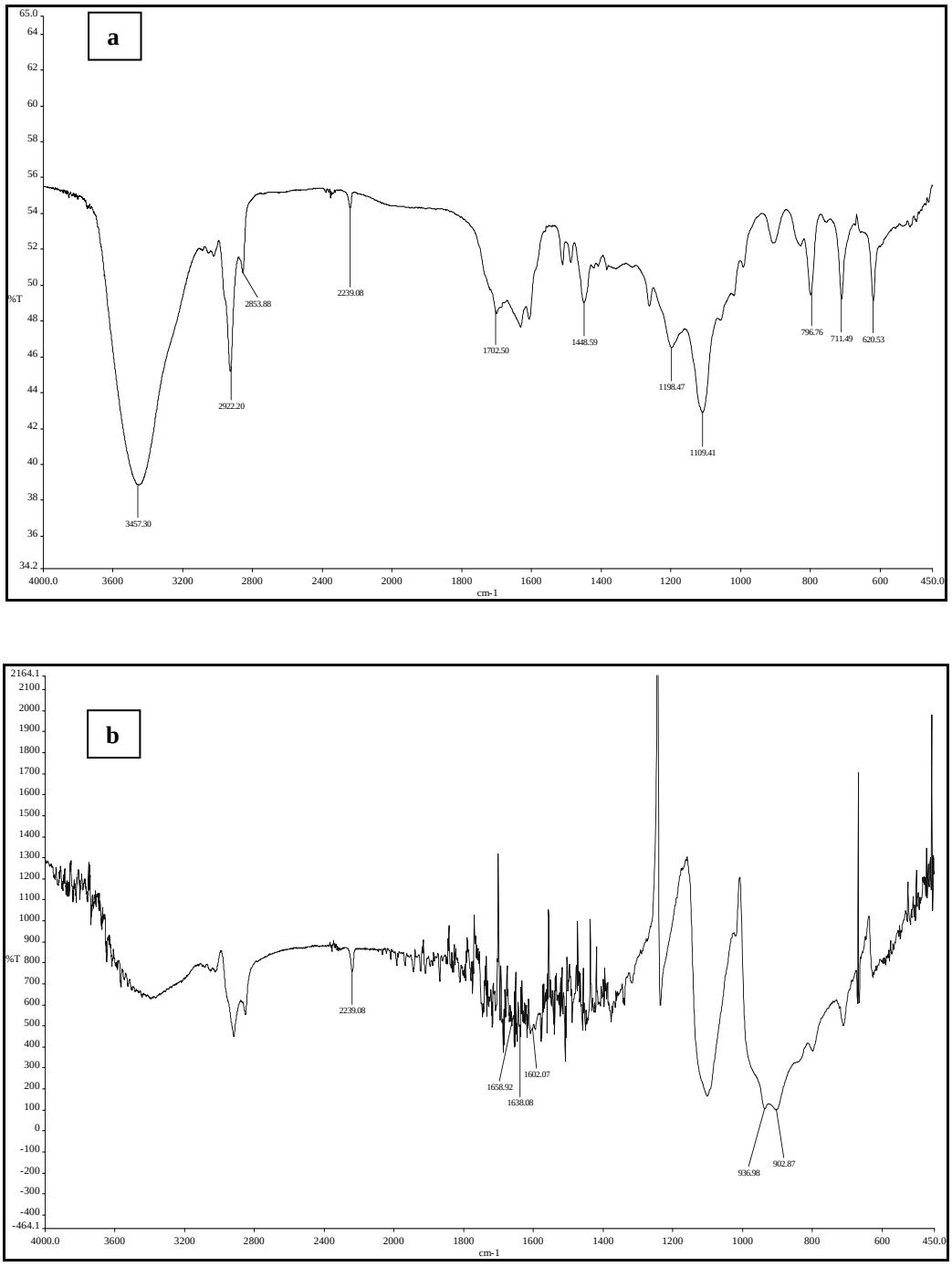

Figure 5.11 : FTIR spectra of (a) unmodified AN-DVB polyHIPE and (b) amidoxime modified AN-DVB polyHIPE

The unmodified and amidoxime modified AN-DVB monoliths were characterized by infrared spectroscopy to confirm the modification of nitrile group to amidoxime group. Figure 5.11(a) and (b) shows the IR spectra of the unmodified and modified polymers respectively. The peak at 2239 cm^{-1} observed is due to –C≡N stretching vibrations, which is the characteristic peak of the nitrile functionality. In the amidoxime modified polymer, the main characteristic absorption peaks observed at 1653 cm^{-1}, 1607 and 900-950 cm^{-1} are due to –C=N, $–NH_2$, and =N–O– groups respectively. The spectrum also shows presence of peak at 2239 cm^{-1}(–C≡N stretching) due to incomplete modification. This was because the polymer being porous, all the functional groups present within the polyHIPE monolithic matrix would not have been accessible for modifications. The diffusion of the reactants in to the porous matrices for modification also becomes difficult.

5.3.3 Evaluation as adsorbents for Cr(VI) metal ion

The amidoxime modified AN-DVB polyHIPEs were evaluated for their efficiency as heterogeneous supports for chromium (VI) adsorption.

5.3.3.1 *Procedure for Cr(VI) adsorption*

Batch method was used to investigate the adsorption studies of Cr(VI) on to amidoxime modified AN-DVB polyHIPEs. The effect of pH on Cr(VI) sorption was studied. 100 mg of polymer was immersed in 10 mL (17.6 ppm) of Cr(VI) stock solution at different pH. The mixture was stirred at room temperature for 24 h. The concentration of Cr(VI) ions in the effluent was determined spectrophotometrically using acidic solution of 1,5-diphenyl carbazide as complexing agent that leads to development of

purple color in presence of Cr(VI). After the addition of the reagent, the solutions were kept for 20 min and then the absorbance was recorded at a wavelength of 540 nm. Beer's law holds well in the concentration range 0.08-0.51 mg/mL based on preliminary studies.

Figure 5.12 shows the IR spectra of the Cr bound polymer. The peak at 550 cm^{-1} is for Cr-O bond and confirms the presence of Cr bound on the polymer matrix.

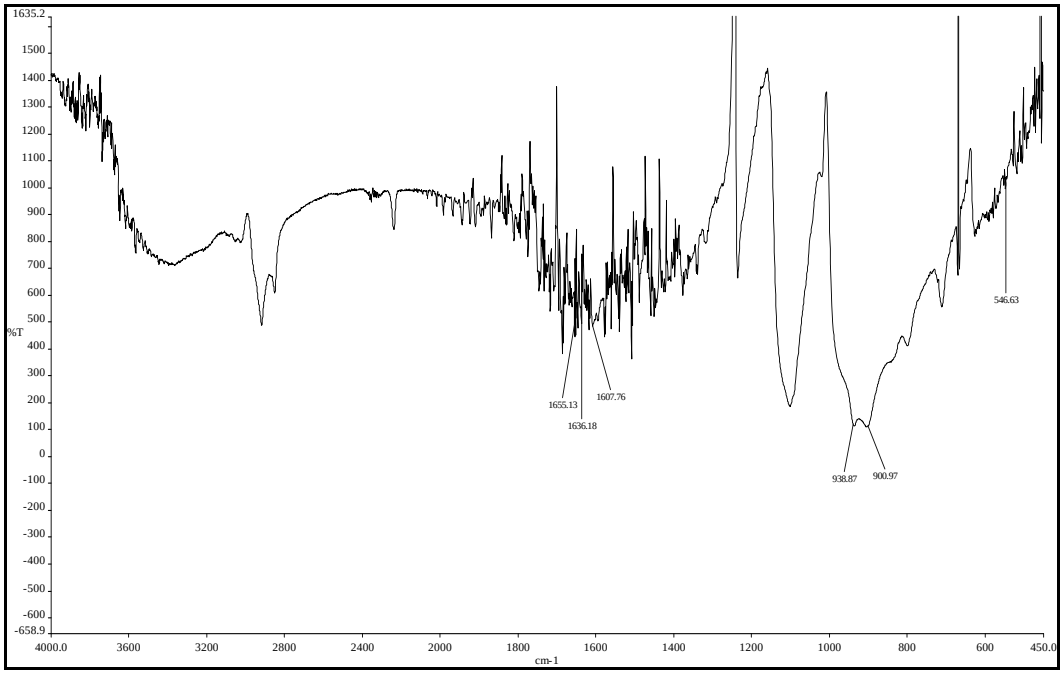

Figure 5.12 : FTIR spectra of Cr(VI) bound amidoxime modified AN-DVB polymer

5.3.3.2 *Effect of pH*

Tables 5.10 and 5.11 show the efficiency of the polymers synthesized using porogens in HIPE methodology for Cr(VI) adsorption capacity. The polymers synthesized using different porogens and ratios were evaluated for its adsorption efficiency at different pH.

Table 5.10 Adsorption studies of Cr(VI) on to amidoxime modified AN-DVB polyHIPEs synthesized using 1:10; oil : water ratio and 1 : 0.5; oil : porogen ratio

	Cr(VI) adsorption (%)			
Porogen → ***p*H ↓**	**Heptane (1:0.5)**	**Toluene (1:0.5)**	**Chlorobenzene (1:0.5)**	**Chloroform (1:0.5)**
2	91.6	99.8	66.8	91.5
3	51.3	79.6	22.2	35.4
4	31.6	57.4	21.0	22.1
6	31.8	43.1	20.1	20.2
8	30.8	31.8	20.0	19.9

Table 5.11 Adsorption studies of Cr(VI) on to amidoxime modified AN-DVB polyHIPEs synthesized using 1 : 20; oil : water ratio and 1 : 0.5; oil : porogen ratio

	Cr(VI) adsorption (%)	
Porogen → ***p*H ↓**	**Toluene (1:0.5)**	**Toluene (1:1)**
2	98.7	99.5
3	67.6	64.2
4	50.0	51.2
6	38.1	41.5
8	31.4	30.9

Figure 5.13 shows the comparison of % adsorption of Cr(VI) at different pH for the polymers synthesized with variation in porogen type having a ratio of 1 : 0.5 (oil : porogen ratio) and 1 : 10; oil : water ratio. Adsorption studies of Cr(VI) were studied in the pH range of 2-8. The experimental results revealed that the Cr(VI) adsorption on the

polymer was high (99.8%) at low pH (*p*H = 2). Cr(VI) exists in aqueous phase in different anionic forms such as chromate (CrO_4^{2-}), dichromate ($Cr_2O_7^{2-}$), or hydrogen chromate ($HCrO_4^-$). The dominant form of Cr(VI) at lower pH is $HCrO_4^-$. Increasing the pH shifts the concentration of $HCrO_4^-$ to other forms as CrO_4^{2-} and $Cr_2O_7^{2-}$.

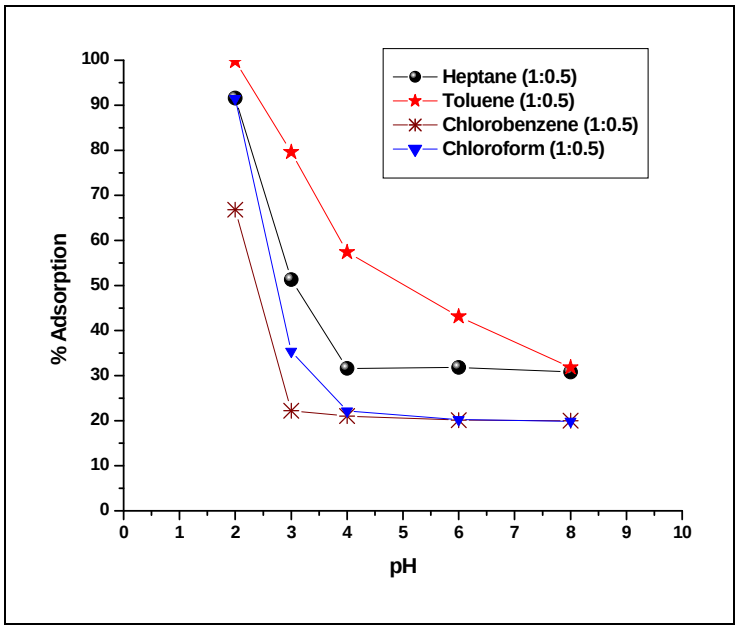

Figure 5.13 : Effect of pH on Cr(VI) adsorption on polyHIPEs using different porogens at 1:10; oil: water ratio

The porogen used were toluene, heptane, chloroform and chlorobenzene. In all the polymers maximum adsorption of Cr(VI) was observed at pH - 2. In case of heptane toluene and chloroform as porogens, the percentage Cr(VI) adsorption was 91.6, 99.8 and 91.5 respectively, while in case of chlorobenzene the adsorption was comparatively less up to 66.8%. The adsorption efficiency was found to decrease with increase in pH. At pH-3, the percentage Cr(VI) adsorption was 51.3, 79.6 and 35.42 for heptane, toluene and chloroform respectively while polyHIPEs synthesized using chlorobenzene had very poor adsorption efficiency of 22.2%. At pH- 4, 6 and 8 heptane showed steady adsorption efficiency of approximately 31%. The same trend was observed in case of

chlorobenzene and chloroform having an approximate value of 20%. But in case of toluene at *p*H - 4, 6 and 8 the percentage Cr(VI) adsorption values were, 57.4, 43.1 and 31.8 respectively. PolyHIPEs synthesized using toluene as a porogen, had maximum adsorption efficiency while in case of polyHIPEs synthesized using chlorobenzene it was the lowest. Porogens play an important role in deciding the surface area, pore dimensions and morphology. Therefore their effect was reflected in the adsorption behaviour studies.

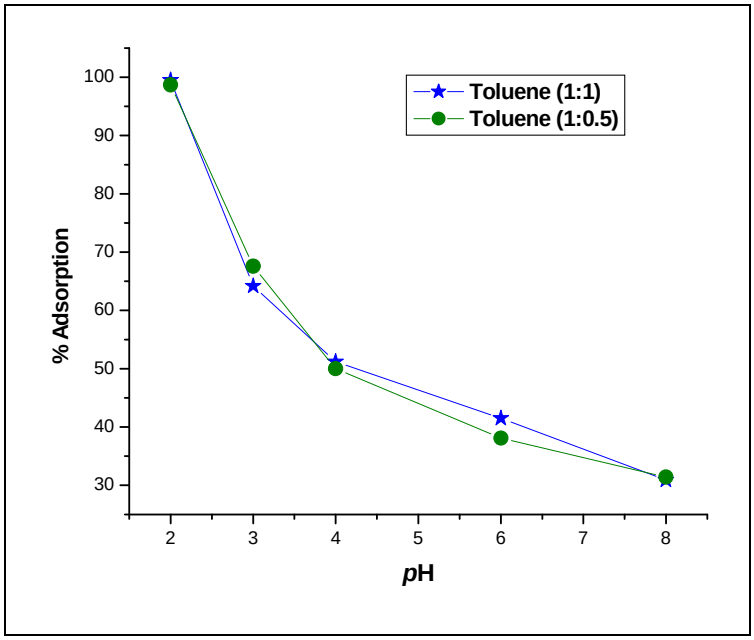

Figure 5.14 : Effect of pH on Cr(VI) adsorption on polyHIPEs using different porogens at 1: 20; oil : water ratio

Figure 5.14 depicts a comparison of polymers evaluated for Cr(VI) adsorption at different pH synthesized using toluene as porogen (1 : 0.5 and 1 : 1; oil : porogen ratio) and 1: 20; oil: aqueous phase ratio. The effect of oil : porogen ratio on the adsorption was studied. There was no considerable difference in the adsorption capacity in both the polymers under all pH conditions.

The decrease in the adsorption with increase in pH may be due to the decrease in electrostatic force of attraction between sorbent and sorbate ions. At lower pH, the percentage of Cr(VI) removal is high due to the high electrostatic force of attraction. The decrease in adsorption above pH- 4 is due to occupation of the adsorption sites by anionic species like CrO_4^{2-} and $Cr_2O_7^{2-}$, which retards the adsorption of such ions further towards the adsorbent surface. As the pH increases, the overall surface of amidoxime polymers became negative and thus adsorption decreases.

5.3.3.3 *Effect of contact time*

Based on the adsorption data in above section the polymer synthesized using toluene (1 : 0.5; oil : porogen ratio) and 1:10; oil : water ratio showed maximum adsorption and hence was selected for further studies. Time of contact is an important parameter in adsorption studies to achieve equilibrium to have maximum adsorption. Adsorption experiments were carried out by varying the contact time of the polymer with the Cr(VI) solution ranging from 45 to 270 minutes. The results are presented in Table 5.12 and the respective graph is shown in Figure 5.15. The results indicated that metal adsorption is dependent on contact time and increases with time. For the first 180 minutes, the percentage removal of Cr(VI) from aqueous solution increases rapidly and reaches a value of 89%, subsequently an equilibrium is achieved and the rate of increase in adsorption also decreases beyond 180 minutes up to 270 minutes accounting to 98% of adsorption of Cr(VI) from the standard solution. Once the equilibrium is achieved diffusion of the Cr(VI) solution on the polymer matrix is difficult since all the accessible sites and pores are being used off. The mechanism of solute transfer to the solid includes diffusion through the fluid film around the adsorbent particle and pores to the internal

adsorption sites. Initially the concentration gradient between the film and the solid surface is high and hence the transfer of solute onto the solid surface is faster. Therefore the optimum time for adsorption of Cr(VI) on modified polymer was chosen as 150 minutes for all batch studies

Table 5.12 Adsorption data of Cr(VI) with respect to time

Time (minutes)	Cr(VI) adsorption (%)
0	0
45	57.5
90	75
135	84.1
180	89.7
225	96.2
270	98.3

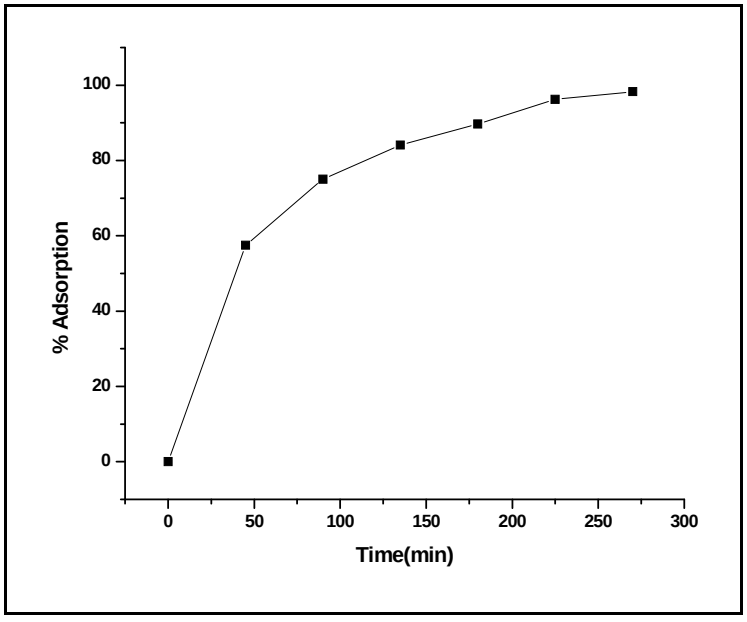

Figure 5.15 : Effect of contact time on Cr(VI) adsorption

5.3.3.4 *Effect of Cr(VI) concentration*

Adsorption efficiency of Cr(VI) is dependent on the concentration of Cr(VI) in aqueous solutions. The relative adsorption of Cr(VI) with respect to the amount of Cr(VI) in solution was studied. The Cr(VI) concentration was varied from 50 to 200 ppm. The effect of initial concentration on percentage removal of Cr(VI) is tabulated in Table 5.13 and the effect is depicted in Figure 5.16.

Table 5.13 Adsorption data of Cr(VI) with respect to Cr(VI) loading

Cr(VI) (mg)	Cr(VI) adsorbed (mg)
50	49.88
70	68.48
100	89.16
120	107.19
160	128.56
200	146.24

The percentage removal of Cr(VI) decreases with increase in initial Cr(VI) concentration. It may be due to an increase in the number of Cr(VI) ions for the fixed amount of adsorbent and the rate of adsorption is high due to the maximum amidoxime functional groups accessible. Due to adsorption a thick layer was formed and thus the capacity of the adsorbent gets exhausted resulting in control of uptake rate by the sorbate which is transported from the exterior to the interior sites of the adsorbent particles. The results indicate that the initial Cr(VI) ion concentration determines the

equilibrium concentration and hence the uptake rate of Cr(VI) ion and the kinetic characteristics.

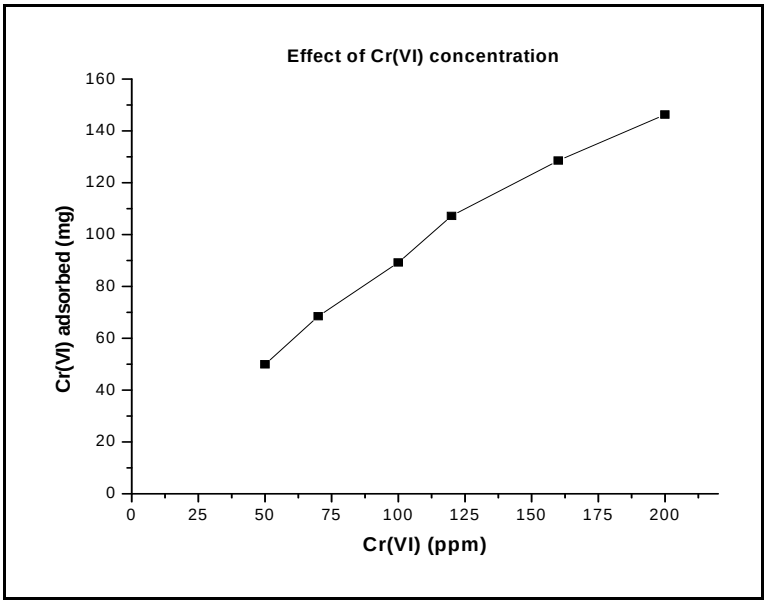

Figure 5.16 : Effect of Cr(VI) loading on adsorption

5.3.3.5 *Effect of adsorbent dose*

The effect of amount of polymer on adsorption capacity was studied. The modified polymer was taken at various amounts (50 to 250 mg) and was mixed with the metal ion solution and kept at room temperature for 24 hours. The adsorption capacities of polymer at different amounts were determined by keeping all other factors constants for example pH and temperature. The Cr(VI) adsorption (%) at different polymer quantity is shown in Table 5.14. The effect of amount of polymer (adsorbent) on the adsorption of Cr(VI) is shown in Figure 5.17.

Table 5.14 Adsorption data of Cr(VI) with respect to polymer dose

Modified PolyHIPE (mg)	Cr(VI) adsorption (%)
50	61.4
100	86.5
150	92.8
200	96.6
250	98.2

It was observed that percent removal of Cr(VI) increases with increase in weight of polymer due to the greater availability of functional groups present for binding with an increase in concentration of adsorbent. If the adsorbent amount is increased by keeping the Cr(VI) concentration constant the amount of Cr(VI) adsorbed per unit mass decreased due to availability of lower number of Cr(VI) ions per unit mass of adsorbent. For 35.2 ppm of Cr(VI) concentration at pH-2, optimum values of percentage adsorption and adsorbent amount were 98% and 250 mg respectively.

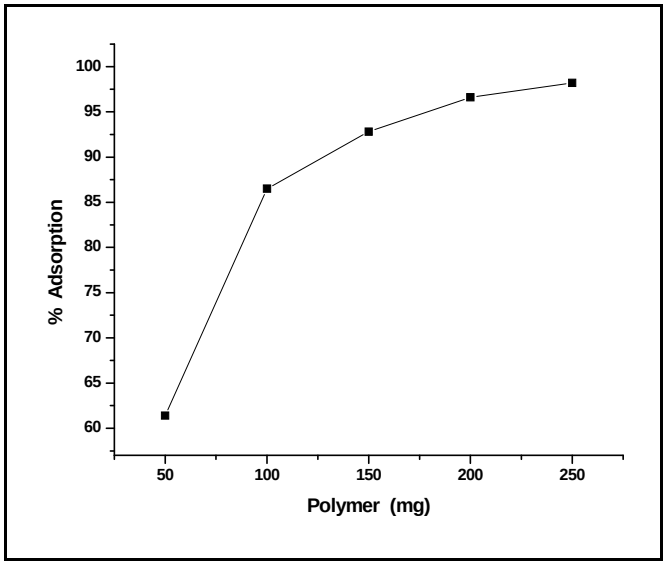

Figure 5.17 : Effect of polymer dose on C(VI) adsorption

5.4 Conclusions

Acrylonitrile containing crosslinked porous polymers were synthesized using high internal phase emulsion HIPE templating. The use of a hydrophilic monomer and hydrophobic crosslinker to form stable HIPE were studied. Several AN-DVB HIPE emulsions were prepared using various classes of nonionic surfactants i.e. sorbitan esters (Span), polyoxyethylene ethers (Brij) and sorbitan polyoxyethylene fatty acid esters (Tween). From optical microscopy and visual appearance of the HIPE emulsions, it was found that HIPEs prepared using Span 80 and Span 20 were stable and could be polymerized to obtain an interconnected porous morphology. In case of Span 85, no emulsion was formed at all. This can be attributed to the fact that the HLB value of Span 85 is very low (1.8) and hence it was less soluble in the oil phase. In case of Tween and Brij surfactants, emulsions were formed under stirring but phase separation was observed within few minutes.

The effect of reaction variants on the HIPE stability of 100% crosslinked acrylonitrile-divinyl benzene polymers like, crosslinker concentration, oil: water ratio, surfactant concentration and porogen were studied. It was observed that the hydrophilicity of acrylonitrile played an important role in formation of stable HIPE and interconnected pore structure formation on post polymerization, due to miscibility of the surfactant in the oil phase. The polymerization was carried out at 50^{o}C using redox initiating system (sodium peroxydisulphate: ascorbic acid (1:0.5)) to avoid vaporization of carcinogenic acrylonitrile as well as to maintain the feed concentration. An attempt was made to use porogens in synthesis of AN-DVB polymers using HIPE methodology to obtain polymers having high surface area. During polymerization, in presence of

porogen, phase separation is decided by the porogen type used which reflects in the pore dimensions formed and indirectly on the surface area of the polymer formed. Maximum surface area of 329.74 m^2/g obtained was in the case of polymer synthesized using toluene as a porogen (1:1) and oil : water ratio of 1:20.

The nitrile functionality present on the polymer backbone was post modified to amidoxime functionality. The modification was confirmed by IR spectroscopy showing the main characteristic peaks at 1653, 1607 and 900 -950 cm^{-1} for –C=N, $-NH_2$, and =N-O- groups respectively. The polymers synthesized using porogens were evaluated for its efficiency as a heterogeneous support for Cr(VI) metal ion adsorption. Studies were done at different pH (2, 4, 6, and 8). It was found that the adsorption of Cr(VI) was maximum at pH value of 2. Maximum adsorption efficiency of 99.8% was found in the case of polymer synthesized using toluene as a porogen (1:0.5) and 1 : 10; oil : water ratio.

5.5 References

[1] Wojaczynska, M.; Kolarz, B. N.; *J. Chromatogr*. **1980**, *196*, 75.

[2] Kolarz, B. N.; Wojaczynska, M.; Trochimczuk, A.; Luczynski, J.; *J. Chromatogr*. **1986**, *358*, 129.

[3] Riqueza, E. C.; Maria, L.C.S.; Aguiar, M. R. M. P.; Aguiar, A. P.; *Mater. Lett.* **2004**, *58*, 502.

[4] Riqueza, E. C.; Aguiar, A. P.; Maria, L.C.S.; and Aguiar, M. R. M. P.; *Polym. Bull.* **2002**, *48*, 407.

[5] Kolarz, B. N.; Lobarzewski, J.; Szewczuk, A.; Trochimczuk, A.; Wojaczyfiska, M.; Wierzchowski, *J. Polish Patent Appl. P-261505*, **1986**.

[6] Seidl, J. *Patent CS 169356*, **1976**.

[7] Seidl, J.; Matejcek, A.; Krajcar, A. *Patent CS 215740*, **1980**.

[8] Maria, L.C.S.; Amorim, M. C. V.; Aguiar, M. R. M. P.; Guimaraes, P. I. C.; Costa, M. A. S.; Aguiar, A. P.; Rezende, P. R.; Carvalho, M. S.; Barbosa, F. G.; Andrade, J. M. and Ribeiro, R. C. C.; *React. Funct. Polym.* **2001**, *49*, 133.

[9] Maria, L.C.S.; Amorim, M. C. V.; Aguiar, M. R. M. P.; Guimaraes, P. I. C.; Costa, M. A. S.; Aguiar, A. P.; Rezende, P. R.; Carvalho, M. S.; Barbosa, F. G.; Andrade, J. M. and Ribeiro, R. C. C.; *React. Funct. Polym.* **2001**, *49*, 133.

CHAPTER - VI

Summary and conclusions

6.1 Summary and Conclusions

The thesis has been divided into six chapters. Chapter 1 describes the current literature survey of synthesis of polymeric porous templates using high internal phase emulsion (HIPE) methodology. The detail introduction to HIPE and its physical properties, its formation has been explored. Synthesis of various types of polyHIPEs their structural properties and applications have been covered.

Study of morphological properties of acrylate based polyHIPEs have been investigated. The effect of comonomer type plays an important role in the polyHIPE properties as it significantly contributes to the differentiation in hydrophobic hydrophilic nature of the oil phase affecting the HIPE emulsion stability. Each factor such as initiator type and concentration, salt type and concentration, porogen type and concentration, presence of water soluble monomer in aqueous discontinuous phase plays an important role in designing the architecture of the porous polyHIPE. These preliminary studies help to understand the complexity of HIPE methodology. Increase in salt concentration and presence of water soluble polymers in the aqueous discontinuous phase leads to the formation of soft and elastic polymers. The yield stress of the polymer can be varied with an interplay in composition of the HIPE constituents. For all the polymers synthesized in this study the yield stress was observed in the range of 0.525-1.538 psi depending on the parameter varied.

An attempt was made to investigate the effect of different parameters like initiator concentration, inhibitor concentration, pH and temperature on the rate high internal phase emulsion (HIPE) polymerization. To generate the polymerization kinetics, a synthesis

method was established and kinetics data was generated. It was observed that like emulsion polymerization the rate increases with increase in initiator concentration and temperature. The inhibitor effect was also profoundly observed in case of MEHQ and phenothiazine.

An attempt was made to model the kinetics data by using a phenomenological model. Kinetics experiments using different initiator concentrations and inhibitor concentrations were conducted at three different temperatures viz. 65, 75 and 85^{o}C. The phenomenological model was proposed to evaluate the rate parameters. Activation energy was calculated from the Arrhenius plot. The model was later validated by using Runge Kutta analysis method. The modeled data falls in close resemblance to the experimental data.

As compared to nonionic surfactants to form a stable water in oil HIPE ionic surfactant as Arquad 2HT-75 can be used to generate poly(styrene-divinylbenzene) polymers at oil : water ratios above 1 : 15. Stable water in oil emulsions failed to form in case of nonionic as well as ionic surfactants at low oil : water ratios of 1 : 1 / 2.5 and 5 that was reflected in the morphology of the polymerized HIPEs. The pores generated in HIPE methodology can be used as templates for synthesis of cadmium sulphide particles. Poly (styrene-divinylbenzene) containing cadmium chloride monoliths using high internal phase emulsion methodology were prepared using two different strategies.

a) Before polymerization: In-situ addition of cadmium chloride dissolved in aqueous discontinuous phase during HIPE formation.

b) Post polymerization: Imbibing cadmium chloride solution inside the polymeric matrix synthesized using HIPE methodology.

The cadmium chloride was then converted into cadmium sulphide by treating it with sodium hydroxide followed by sodium sulphide.

Crystal structure was confirmed from X-ray Diffraction studies. XRD patterns showed prominent broad peaks at 2θ values of 26.7, 44.1 and 52.1 that can be indexed to scattering from 111, 220 and 311 crystal planes of cubic CdS respectively. The morphology of the CdS containing polyHIPEs showed presence of CdS particles in the matrix. Studies showed linearity in analysis data in case of insitu incorporation strategy in comparision with external incorporation strategy. Insitu incorporation strategy was found to have uniform distribution of particles over the entire polymer matrix as compared to external incorporation strategy. In the external incorporation strategy, the polymer properties such as void diameter, affinity for imbibing $CdCl_2$ solution, accessibility of the reactants for post conversion plays an important role for complete conversion of cadmium chloride ($CdCl_2$) to cadmium sulphide (CdS).

Functional group present in the polymer is the basic requirement for the polymer to be hydrophobic or hydrophilic in nature. Acrylonitrile containing crosslinked porous polymers were synthesized using high internal phase emulsion HIPE templating. Formation of a stable HIPE using a monomer having water affinity (acrylonitrile) and hydrophobic crosslinker (divinylbenzene) was studied. Several poly (AN-DVB) HIPE emulsions were prepared using various classes of nonionic surfactants i.e. sorbitan esters (Span), polyoxyethylene ethers (Brij) and sorbitan polyoxyethylene fatty acid esters

(Tween). From optical microscopy and visual appearance of the HIPE emulsions, it was found that HIPEs prepared using Span 80 and Span 20 were stable and could be polymerized to obtain an interconnected porous morphology. In case of Span 85 no emulsion was formed at all. This can be attributed to the fact that the HLB value of Span 85 is very low (1.8) and hence it was less soluble in the oil phase. In case of Tween and Brij surfactants emulsions were formed under stirring but on standing they phase separated.

The effect of reaction variants on the HIPE stability of 100% crosslinked acrylonitrile-divinyl benzene polymers like, crosslinker concentration, oil:water ratio, surfactant concentration and porogen were studied. It was observed that the hydrophilicity of acrylonitrile played an important role in formation of stable HIPE and interconnected pore structure formation post polymerization, due to miscibility of the surfactant in the oil phase. The polymerization was carried out at 50^{o}C using redox initiating system (sodium peroxydisulphate : ascorbic acid (1:0.5)) to avoid vaporization of carcinogenic acrylonitrile as well as to maintain the feed concentration. An attempt was made to use porogens in synthesis of AN-DVB polymers using HIPE methodology to obtain polymers having high surface area. During polymerization, in presence of porogen, phase separation is decided by the porogen type used which reflects in the pore dimensions formed and indirectly on the surface area of the polymer formed. Maximum surface area of 329.74 m^2/g obtained was in the case of polymer synthesized using toluene as a porogen (1:1) and oil : water ratio 1:20.

The nitrile functionality present on the polymer backbone was post modified to amidoxime functionality. The modification was confirmed by IR spectroscopy showing

the main characteristic peaks at 1653, 1607 and 900 -950 cm^{-1} for –C=N, -NH_2, and =N-O- groups respectively. The polymers synthesized using porogens were evaluated for its efficiency as a heterogeneous support for Cr(VI) metal ion adsorption. Studies were done at different pH-2, 4, 6, and 8. It was found that the adsorption of Cr(VI) was maximum at pH-2. Maximum adsorption efficiency of 99.8% was found in the case of polymer synthesized using toluene as a porogen (1 : 0.5) and 1 : 10 oil : water ratio.